

# **Wind Tunnel Aerodynamic Tests of Six Airfoils for Use on Small Wind Turbines**

**Period of Performance:  
October 31, 2002–January 31, 2003**

Michael S. Selig and Bryan D. McGranahan  
*University of Illinois at Urbana-Champaign  
Urbana, Illinois*



**NREL**

**National Renewable Energy Laboratory**  
1617 Cole Boulevard, Golden, Colorado 80401-3393  
303-275-3000 • [www.nrel.gov](http://www.nrel.gov)

Operated for the U.S. Department of Energy  
Office of Energy Efficiency and Renewable Energy  
by Midwest Research Institute • Battelle

Contract No. DE-AC36-99-GO10337

# Wind Tunnel Aerodynamic Tests of Six Airfoils for Use on Small Wind Turbines

**Period of Performance:  
October 31, 2002–January 31, 2003**

Michael S. Selig and Bryan D. McGranahan  
*University of Illinois at Urbana-Champaign  
Urbana, Illinois*

NREL Technical Monitor: Paul Migliore

Prepared under Subcontract No. XCX-2-32231-01



**NREL**

**National Renewable Energy Laboratory**  
1617 Cole Boulevard, Golden, Colorado 80401-3393  
303-275-3000 • [www.nrel.gov](http://www.nrel.gov)

Operated for the U.S. Department of Energy  
Office of Energy Efficiency and Renewable Energy  
by Midwest Research Institute • Battelle

Contract No. DE-AC36-99-GO10337

## NOTICE

This report was prepared as an account of work sponsored by an agency of the United States government. Neither the United States government nor any agency thereof, nor any of their employees, makes any warranty, express or implied, or assumes any legal liability or responsibility for the accuracy, completeness, or usefulness of any information, apparatus, product, or process disclosed, or represents that its use would not infringe privately owned rights. Reference herein to any specific commercial product, process, or service by trade name, trademark, manufacturer, or otherwise does not necessarily constitute or imply its endorsement, recommendation, or favoring by the United States government or any agency thereof. The views and opinions of authors expressed herein do not necessarily state or reflect those of the United States government or any agency thereof.

Available electronically at <http://www.osti.gov/bridge>

Available for a processing fee to U.S. Department of Energy and its contractors, in paper, from:

U.S. Department of Energy  
Office of Scientific and Technical Information  
P.O. Box 62  
Oak Ridge, TN 37831-0062  
phone: 865.576.8401  
fax: 865.576.5728  
email: <mailto:reports@adonis.osti.gov>

Available for sale to the public, in paper, from:

U.S. Department of Commerce  
National Technical Information Service  
5285 Port Royal Road  
Springfield, VA 22161  
phone: 800.553.6847  
fax: 703.605.6900  
email: [orders@ntis.fedworld.gov](mailto:orders@ntis.fedworld.gov)  
online ordering: <http://www.ntis.gov/ordering.htm>



---

# Contents

---

|   |             |
|---|-------------|
| FOREWORD . . . . .  | <i>iii</i>  |
| PREFACE . . . . .   | <i>vii</i>  |
| ACKNOWLEDGMENTS . . . . .   | <i>ix</i>   |
| LIST OF FIGURES . . . . .   | <i>xi</i>   |
| LIST OF TABLES . . . . .  | <i>xv</i>   |
| LIST OF SYMBOLS AND ACRONYMS . . . . .                            | <i>xvii</i> |
| <br>  |             |
| 1 AIRFOILS TESTED . . . . .                                       | 1           |
| <br>  |             |
| 2 WIND TUNNEL FACILITY AND MEASUREMENT TECHNIQUES . . . . .       | 3           |
| 2.1 EXPERIMENTAL FACILITY AND FLOW QUALITY MEASUREMENTS . . . . . | 3           |
| 2.1.1 TURBULENCE INTENSITY . . . . .                              | 6           |
| 2.1.2 FREESTREAM VELOCITY . . . . .                               | 8           |
| 2.1.3 FREESTREAM FLOW ANGULARITY . . . . .                        | 11          |
| 2.2 AIRFOIL MODELS . . . . .                                      | 14          |
| 2.3 PERFORMANCE DATA MEASUREMENT TECHNIQUES . . . . .             | 15          |
| 2.3.1 LIFT FORCE MEASUREMENT . . . . .                            | 17          |
| 2.3.2 DRAG FORCE MEASUREMENT . . . . .                            | 17          |
| 2.3.3 PITCHING MOMENT MEASUREMENT . . . . .                       | 19          |
| 2.4 DATA ACQUISITION AND REDUCTION . . . . .                      | 21          |
| 2.4.1 WIND-TUNNEL BOUNDARY CORRECTIONS . . . . .                  | 23          |
| 2.4.2 ADDITIONAL VELOCITY CORRECTIONS . . . . .                   | 24          |
| 2.4.3 CORRECTIONS TO MEASURED QUANTITIES . . . . .                | 24          |
| 2.5 CALIBRATIONS AND UNCERTAINTY ANALYSIS . . . . .               | 27          |
| <br>  |             |
| 3 DATA VALIDATION . . . . .                                       | 29          |
| 3.1 SURFACE OIL FLOW MEASUREMENTS . . . . .                       | 29          |
| 3.2 LIFT AND MOMENT DATA . . . . .                                | 33          |
| 3.3 DRAG POLARS . . . . .   | 35          |
| 3.4 SUMMARY . . . . .   | 37          |
| <br>  |             |
| 4 SUMMARY OF AIRFOIL DATA . . . . .                               | 39          |
| <br>  |             |
| 5 AIRFOIL PROFILES AND PERFORMANCE PLOTS . . . . .                | 47          |
| <br>  |             |
| REFERENCES . . . . .  | 105         |
| <br>  |             |
| APPENDIX A TABULATED AIRFOIL COORDINATES . . . . .                | 109         |
| APPENDIX B TABULATED POLAR DATA . . . . .                         | 113         |



---

## Foreword

---

The U.S. Department of Energy (DOE), working through its National Renewable Energy Laboratory (NREL), is engaged in a comprehensive research effort to improve our understanding of wind turbine aeroacoustics. The motivation for this effort is the desire to exploit the large expanse of low wind speed sites that tend to be close to U.S. load centers. Quiet wind turbines are an inducement to widespread deployment, so the goal of NREL's aeroacoustic research is to develop tools that the U.S. wind industry can use in developing and deploying highly efficient, quiet wind turbines at low wind speed sites. NREL's National Wind Technology Center (NWTC) is implementing a multifaceted approach that includes wind tunnel tests, field tests, and theoretical analyses in direct support of low wind speed turbine development by its industry partners. NWTC researchers are working hand in hand with engineers in industry to ensure that research findings are available to support ongoing design decisions. To that end, wind tunnel aerodynamic tests and aeroacoustic tests have been performed on six airfoils that are candidates for use on small wind turbines. Results are documented in two companion NREL reports:

*Wind Tunnel Aeroacoustic Tests of Six Airfoils for Use on Small Wind Turbines*,  
Stefan Oerlemans, Principal Investigator, the Netherlands National Aerospace  
Laboratory

*Wind Tunnel Aerodynamic Tests of Six Airfoils for Use on Small Wind Turbines*,  
Michael Selig, Principal Investigator, University of Illinois at Urbana-Champaign  
(UIUC)

These reports provide a valuable database for those who wish to evaluate the airfoils tested,<sup>†</sup> but inevitably, designers will want to investigate other airfoils that have not been tested. They must consider, however, that wind tunnel tests are expensive and sometimes difficult to schedule within the overall time frame of a project development plan. This dilemma begs the question, "Is it really necessary to conduct wind tunnel tests, or can we rely on theoretical predictions?"

Predicting the aeroacoustic emission spectra of a particular airfoil shape is extremely difficult, but predicting the aerodynamic characteristics of a particular airfoil shape is routine practice. Nevertheless, there is always some uncertainty about the accuracy of the predictions in comparison to the results of wind tunnel tests or field performance, and there are questions about the efficacy of the two principal airfoil analysis methods: the Eppler and XFOIL codes. To address these related issues, at least in part, a

---

<sup>†</sup> The extensive test data discussed in these reports are provided in electronic format on compact disks (CDs) included with the printed documents. The CDs may also be obtained by calling the NWTC library at 303-384-6963.

theoretical analysis was commissioned of the same airfoils tested in the wind tunnel. The results are documented in the following NREL report:

*Theoretical Aerodynamic Analyses of Six Airfoils for Use on Small Wind Turbines Using Eppler and XFOIL Codes,*

Dan M. Somers and Mark D. Maughmer, Principal Investigators, Airfoils, Incorporated

Possessing both theoretically predicted aerodynamic characteristics and wind tunnel test data for the same six airfoils provides an extraordinary opportunity to compare the performance, measured by energy capture, of wind turbine rotors designed with the different data. This will provide the insight needed to assist designers in deciding whether to pursue wind tunnel tests. Although some differences in the resulting blade planforms (chord and twist distributions) can be expected, a more important question relates to the difference in energy capture and its significance in driving the choices that need to be made during the preliminary design stage. These issues are addressed in a report that compares the differences in Eppler and XFOIL predictions to the UIUC wind tunnel tests and examines the planform and energy capture differences in resulting blade designs:

*Comparison of Optimized Aerodynamic Performance of Small Wind Turbine Rotors Designed with Theoretically Predicted versus Experimentally Measured Airfoil Characteristics,*

Michael Selig, Principal Investigator, University of Illinois at Urbana-Champaign (UIUC)

Another research effort undertaken in support of the U.S. wind turbine industry involves a series of aeroacoustic field tests conducted at the NWTC. Using well documented, consistently applied test procedures, noise spectra were measured for eight small wind turbine configurations. Test results provide valuable information to manufacturers as well as potential users of these turbines. To our knowledge, this is the first comprehensive database of noise data for small wind turbines. The results of this effort are documented in another NREL report:

*Aeroacoustic Field Tests of Eight Small Wind Turbines,*

J. van Dam and A. Huskey, Principal Investigators, NREL's National Wind Technology Center

Wind tunnel tests, field tests, and theoretical analyses provide useful information for development and validation of NREL's semi-empirical noise prediction code. This effort is described in the following NREL report:

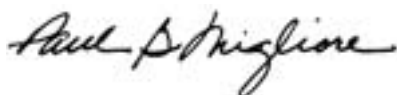
*Semi-Empirical Aeroacoustic Noise Prediction Code for Wind Turbines,*

Patrick Moriarty, Principal Investigator, NREL's National Wind Technology Center

The code will be continuously improved, but it may ultimately give way to more sophisticated, physics-based computational aeroacoustic codes also being developed by NREL

Each of the documents described above will be published as an NREL report. Undoubtedly, some results will also be presented in various journal articles or conference papers. All of the NREL reports will be available on NREL's web site at <http://www.nrel.gov/publications/>. Collectively, these reports represent a significant compendium of information on the aerodynamics and aeroacoustics of contemporary wind turbines. Therefore, NREL will also publish a CD-ROM containing these reports.

Clearly, this work represents a significant commitment of DOE resources as well as a significant commitment of personnel over an extended period. I am sure I express the sentiments of all the research participants in saying we sincerely hope the results of these efforts prove beneficial to the wind energy community.

A handwritten signature in cursive script, reading "Paul G. Migliore".

Paul G. Migliore  
NREL/NWTC Project Manager





---

## Preface

---

*Wind Tunnel Aerodynamic Tests of Six Airfoils for Use on Small Wind Turbines* represents the fourth installment in a series of volumes documenting the ongoing work of the University of Illinois at Urbana-Champaign Low-Speed Airfoil Tests program (UIUC LSATs). This particular volume deals with airfoils that are candidates for use on small wind turbines, which operate at low Reynolds numbers. The airfoil performance tests were conducted in November 2002; prior to this, flow quality tests were carried out over a two-month period from late June to late August 2002.

It is our intention for this report to follow closely the format of the previous volumes, making the current installment easy to navigate for those familiar with the series. Following along these lines, Chapter 1 presents the six airfoils tested and discusses the overall scope of the project. Chapter 2 gives an overview of the testing facility, including an extensive study of the flow quality of the UIUC low-speed subsonic wind tunnel. In addition, the descriptions of the LSATs measurement hardware given in the first three volumes is summarized in Chapter 2. Chapter 3 provides a comparison between UIUC LSATs data and data obtained by NASA Langley in the Low-Turbulence Pressure Tunnel (LTPT). Chapter 4 briefly discusses the performance of the airfoils, and Chapter 5 contains the corresponding performance plots, including pitching-moment data. Appendices A and B list tabulated airfoil coordinates and drag polars, respectively.

Finally, as a caveat, it is worth noting that in all of the LSATs test campaigns, only raw data are recorded and saved. These data are archival. On the other hand, the performance data can change over time as enhancements are made to the data reduction process. Thus, to compare these data with those of past test campaigns, it is important that comparisons only be made between data sets that are generated from archival raw data using the same version of the LSATs data reduction code.



---

## Acknowledgments

---

For our growing capability to test airfoils at low Reynolds numbers, we are indebted to several individuals, businesses, clubs, and organizations who collectively have contributed funds, wind tunnel models, and gifts that have helped to keep the UIUC LSATs program alive and thriving for many years. In supporting the foundations of this work, we are sincerely grateful to each of them, and their names are listed in past volumes. For this particular volume, we especially thank our technical monitor, Dr. Paul Migliore of the National Renewable Energy Laboratory. Without his support and encouragement, this volume of data would have not come into existence. Also, we thank Yvan Tinel, Tinel Technologies, for his skillful and meticulous work in making the six wind tunnel models presented in the study. Here at UIUC, we thank Dr. Andy P. Broeren and Biao Lu for their assistance in helping to take the tunnel flow quality data as presented in Chapter 3. Also, we owe a debt of gratitude to Benjamin A. Broughton for his dedication in helping to ensure the quality of the data acquisition and reduction methodology used to obtain the performance data, which form the central core of this work.



---

## List of Figures

---

|      |  |    |
|------|--|----|
| 1.1  | Airfoils tested during the UIUC Low-Speed Airfoil Tests (fall 2002)  | 1  |
| 2.1  | UIUC low-speed subsonic wind tunnel  | 4  |
| 2.2  | Photograph of wind-tunnel test section   | 5  |
| 2.3  | Photograph of wind-tunnel exit fan   | 5  |
| 2.4  | Experimental setup (Plexiglas <sup>®</sup> splitter plates and traverse enclosure box not shown for clarity)   | 6  |
| 2.5  | Turbulence intensity at tunnel centerline, empty test section and with rig in place  | 9  |
| 2.6  | Power spectrum comparison between empty tunnel and installed test apparatus cases for $Re = 350,000$   | 9  |
| 2.7  | Dynamic pressure variation across test section when empty  | 11 |
| 2.8  | Dynamic pressure variation across test section with the LSATs rig installed  | 12 |
| 2.9  | Illustration of the 7-hole probe used for flow angle measurements  | 13 |
| 2.10 | Pitch angle variation across test section with the LSATs rig installed   | 14 |
| 2.11 | Yaw angle variation across test section with the LSATs rig installed   | 15 |
| 2.12 | Combined pitch and yaw angle across test section with the LSATs rig installed  | 16 |
| 2.13 | LSATs lift beam balance assembly as viewed from the working side of the test section   | 17 |
| 2.14 | Control volume for the 2-D momentum deficit method to determine the profile drag   | 19 |
| 2.15 | Drag results for the E387 (E) airfoil depicting typical spanwise drag variations for the eight spanwise stations for $Re = 100,000, 200,000, 350,000,$ and $500,000$ | 20 |
| 2.16 | Moment measurement apparatus   | 21 |
| 2.17 | Drag polars for the E387 (C) with and without the necessary circulation correction (taken from Ref. 5)   | 25 |
| 2.18 | Velocity correction curve to account for boundary-layer growth between the splitter plates   | 26 |
| 3.1  | Representative upper-surface oil flow visualization on the E387 (E) airfoil  | 30 |
| 3.2  | Conceptual illustration of the relationship between the surface oil flow features and skin friction distribution in the region of a laminar separation bubble        | 31 |
| 3.3  | Comparison of major E387 (E) upper-surface flow features between UIUC and LTPT for $Re = 200,000$ and $300,000$  | 33 |

|      |  |    |
|------|--|----|
| 3.4  | Comparison between UIUC and LTPT E387 lift and moment coefficient data for $Re = 100,000, 200,000, 300,000,$ and $460,000$ . . . . . | 34 |
| 3.5  | Comparison between UIUC and LTPT E387 drag coefficient data for $Re = 100,000, 200,000, 300,000,$ and $460,000$ . . . . .            | 36 |
| 5.1  | Inviscid velocity distributions for the E387 . . . . .   | 50 |
| 5.2  | Comparison between the true and actual E387 (E) . . . . .  | 50 |
| 5.3  | Drag polar for the E387 (E) . . . . .  | 51 |
| 5.4  | Lift and moment characteristics for the E387 (E) . . . . .   | 52 |
| 5.5  | Drag polar for the E387 (E) with trip type F . . . . .   | 55 |
| 5.6  | Lift and moment characteristics for the E387 (E) with trip type F . . . . .  | 56 |
| 5.7  | Inviscid velocity distributions for the FX 63-137 . . . . .  | 58 |
| 5.8  | Comparison between the true and actual FX 63-137 (C) . . . . .   | 58 |
| 5.9  | Drag polar for the FX 63-137 (C) . . . . .   | 59 |
| 5.10 | Lift and moment characteristics for the FX 63-137 (C) . . . . .  | 60 |
| 5.11 | Drag polar for the FX 63-137 (C) with trip type F . . . . .  | 63 |
| 5.12 | Lift and moment characteristics for the FX 63-137 (C) with trip type F . . . . .   | 64 |
| 5.13 | Inviscid velocity distributions for the S822 . . . . .   | 68 |
| 5.14 | Comparison between the true and actual S822 (B) . . . . .  | 68 |
| 5.15 | Drag polar for the S822 (B) . . . . .  | 69 |
| 5.16 | Lift and moment characteristics for the S822 (B) . . . . .   | 70 |
| 5.17 | Drag polar for the S822 (B) with trip type F . . . . .   | 73 |
| 5.18 | Lift and moment characteristics for the S822 (B) with trip type F . . . . .  | 74 |
| 5.19 | Inviscid velocity distributions for the S834 . . . . .   | 78 |
| 5.20 | Comparison between the true and actual S834 . . . . .  | 78 |
| 5.21 | Drag polar for the S834 . . . . .  | 79 |
| 5.22 | Lift and moment characteristics for the S834 . . . . .   | 80 |
| 5.23 | Drag polar for the S834 with trip type F . . . . .   | 83 |
| 5.24 | Lift and moment characteristics for the S834 with trip type F . . . . .  | 84 |
| 5.25 | Inviscid velocity distributions for the SD2030 . . . . .   | 88 |
| 5.26 | Comparison between the true and actual SD2030 (B) . . . . .  | 88 |
| 5.27 | Drag polar for the SD2030 (B) . . . . .  | 89 |
| 5.28 | Lift and moment characteristics for the SD2030 (B) . . . . .   | 90 |
| 5.29 | Drag polar for the SD2030 (B) with trip type F . . . . .   | 92 |
| 5.30 | Lift and moment characteristics for the SD2030 (B) with trip type F . . . . .  | 93 |
| 5.31 | Inviscid velocity distributions for the SH3055 . . . . .   | 96 |
| 5.32 | Comparison between the true and actual SH3055 . . . . .  | 96 |
| 5.33 | Drag polar for the SH3055 . . . . .  | 97 |

5.34 Lift and moment characteristics for the SH3055 . . . . . 98  
5.35 Drag polar for the SH3055 with trip type F . . . . . 100  
5.36 Lift and moment characteristics for the SH3055 with trip type F . . . 101





---

## List of Tables

---

|     |  |    |
|-----|--|----|
| 2.1 | Turbulence Intensity Characteristics in Percent . . . . .          | 7  |
| 4.1 | Characteristics of the Airfoils Tested for Wind Turbines . . . . . | 39 |
| 4.2 | Wind Tunnel Model Characteristics . . . . .                        | 40 |
| 4.3 | Three-Dimensional Zigzag Trip Geometry . . . . .                   | 41 |
| 5.1 | Test Matrix and Run Number Index . . . . .                         | 48 |



---

## List of Symbols and Acronyms

---

|                   |   |
|-------------------|---|
| $A_{ts}$          | test section area   |
| $b$               | model span  |
| $c$               | airfoil chord   |
| $C_l$             | airfoil lift coefficient  |
| $C_{l,max}$       | maximum lift coefficient  |
| $\Delta C_{l,sc}$ | change in lift coefficient due to streamline curvature              |
| $C_{lu}$          | uncorrected lift coefficient  |
| $C_d$             | airfoil drag coefficient  |
| $C_{du}$          | uncorrected drag coefficient  |
| $C_m$             | same as $C_{m,c/4}$   |
| $C_{m,c/4}$       | airfoil pitching moment about the quarter-chord point               |
| $C_{mu}$          | uncorrected moment coefficient                                      |
| $d$               | drag per unit span  |
| $h_{ts}$          | test section height   |
| $K_1$             | wind-tunnel correction constant for solid blockage effects (0.74)   |
| $K_{vel}$         | ratio of upstream velocity to velocity at model quarter-chord point |
| $M_v$             | model volume  |
| $\Delta p$        | static pressure difference between upstream and downstream          |
| $P_{atm}$         | atmospheric pressure  |
| $P_0$             | total pressure  |
| $P_{0,1}$         | wake total pressure   |
| $P_{0,\infty}$    | freestream total pressure   |
| $P_s$             | static pressure   |
| $P_{s,1}$         | wake static pressure  |
| $P_{s,\infty}$    | freestream static pressure  |
| $\Delta P_0$      | total pressure difference between freestream and wake               |
| $q_\infty$        | freestream dynamic pressure   |
| $\Delta q_\infty$ | dynamic pressure difference between upstream and downstream         |
| $Q$               | dynamic pressure downstream   |
| $Q_u$             | dynamic pressure upstream   |
| $\Delta Q$        | dynamic pressure difference between upstream and downstream         |
| $R$               | ideal gas constant for air  |
| $Re$              | Reynolds number based on airfoil chord                              |
| $Re/l$            | Reynolds number per unit length                                     |
| $s$               | distance along airfoil surface                                      |
| $S$               | Sutherland's constant or wing area                                  |
| $T$               | temperature   |
| $T_0$             | reference temperature   |
| $u_1$             | streamwise velocity in wake   |
| $V$               | local velocity on airfoil surface                                   |

|                     |  |
|---------------------|--|
| $V_c$               | corrected velocity   |
| $V_u$               | uncorrected velocity   |
| $V_\infty$          | freestream velocity  |
| $x$                 | distance along airfoil chord                                       |
| $X$                 | spanwise direction in test section referenced to tunnel centerline |
| $y$                 | vertical distance  |
| $Y$                 | vertical direction in test section referenced to tunnel centerline |
| $\alpha$            | angle of attack  |
| $\alpha_{0l}$       | angle of attack for zero lift                                      |
| $\alpha_u$          | uncorrected angle of attack  |
| $\Delta\alpha_{sc}$ | change in angle of attack due to streamline curvature              |
| $\varepsilon_b$     | total blockage correction factor (solid and wake)                  |
| $\varepsilon_{sb}$  | solid blockage correction factor                                   |
| $\varepsilon_{wb}$  | wake blockage correction factor                                    |
| $\sigma$            | wind-tunnel correction parameter, $(\pi^2/48)(c/h)^2$              |
| $\mu$               | fluid viscosity  |
| $\mu_0$             | reference fluid viscosity  |
| $\Delta$            | an increment   |
| $\rho$              | fluid density  |
| HAWTs               | horizontal axis wind turbines                                      |
| HPF                 | high-pass filter   |
| LSATs               | Low-Speed Airfoil Tests  |
| LTPT                | Low-Turbulence Pressure Tunnel at NASA Langley Research Center     |
| UIUC                | University of Illinois at Urbana-Champaign                         |

---

# Chapter 1

## Airfoils Tested

---

This report documents the aerodynamic characteristics of six airfoils (shown in Fig. 1.1), which were also examined in a companion study dealing with their aeroacoustic properties.<sup>1</sup> These projects together were motivated by two intersecting factors. First, the U.S. Department of Energy, National Renewable Energy Laboratory (NREL), has initiated research into the aeroacoustics of wind turbines, which is an important design consideration when a potentially valuable wind resource and a population center coincide. Such an event—the confluence of wind technology and people—is increasingly probable as wind turbines become more efficient and better able to exploit lower wind speed sites, which are often found near U.S. load centers. Improving our understanding of the aeroacoustics will help designers exploit advances in noise mitigation design strategies. It is anticipated that having a reliable and self-consistent airfoil performance data set may be helpful in validating aeroacoustics prediction codes in support of such design activities. Second, small stand-alone wind turbines operating in close proximity to residential areas posed a noise concern. Given that aerodynamic efficiency increases with tip speed and hence wind turbine noise, advances in the development of small wind turbines can be envisioned using a suite of computational tools capable of predicting both the aeroacoustic characteristics and aerodynamic performance. Thus, an aerodynamic data set of representative wind turbine airfoils should help pave the way toward the development of design methodologies needed by the small wind turbine industry as it seeks to improve efficiency as well as acceptability.

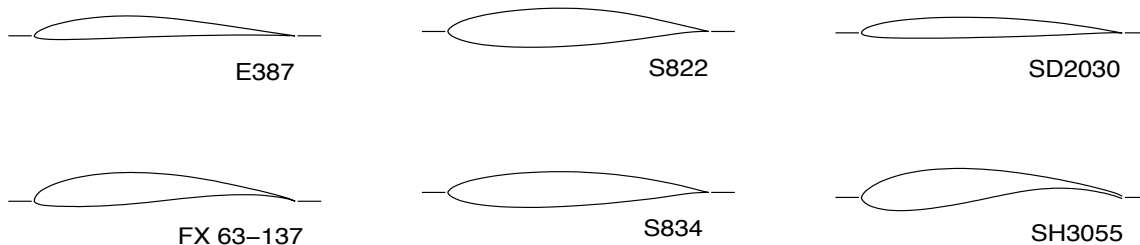


**Fig. 1.1** Airfoils tested during the UIUC Low-Speed Airfoil Tests (fall 2002).

Prior to testing the airfoils for their performance data, the authors carried out an extensive study of the wind tunnel flow quality. This precursor study included measurements of the freestream turbulence as well as variations in dynamic pressure and freestream flow angle across the center region of the test section. The results of these flow quality tests are presented in Chapter 2 along with an extensive discussion of the performance data-reduction procedure. Chapter 3 presents validation data on the E387 airfoil as compared with results from the Low-Turbulence Pressure Tunnel (LTPT) at NASA Langley. Chapter 4 includes a brief discussion of the airfoils and the associated performance data, which are graphically shown in Chapter 5. Appendices A and B include tabulated airfoil coordinates and performance data. Finally, it should be mentioned that this work is a continuation of a series of wind tunnel test campaigns documented in Refs. 2-5.

---

## Chapter 2

# Wind Tunnel Facility and Measurement Techniques

---

All experiments were performed in the UIUC Department of Aerospace Engineering, Subsonic Aerodynamics Laboratory. The low-speed subsonic wind tunnel has been in service at the University of Illinois at Urbana-Champaign since the early 1990's and has been used for all of the *Summary of Airfoil Data* volumes,<sup>3-5</sup> of which this is an example. Apart from documenting the wind-tunnel flow quality in considerable detail, this chapter also presents detailed descriptions of the wind tunnel facility, lift and drag measurement techniques, data acquisition equipment, and data reduction procedures that for the most part were first documented in Refs. 2-5.

## 2.1 Experimental Facility and Flow Quality Measurements

This research was conducted in the UIUC low-turbulence subsonic wind tunnel shown in Fig. 2.1. The wind tunnel is an open-return type with a 7.5:1 contraction ratio. The rectangular test section is nominally  $2.8 \times 4.0$  ft ( $0.853 \times 1.219$  m) in cross section and 8-ft (2.438-m) long. Over the length of the test section, the width increases by approximately 0.5 in. (1.27 cm) to account for boundary-layer growth along the tunnel sidewalls. Test-section speeds are variable up to 160 mph (71.53 m/s) via a 125-hp (93.25-kW) AC motor connected to a five-bladed fan. For a Reynolds number of 500,000 based on an airfoil chord of 1 ft (0.305 m), the resulting test-section speed is 80 ft/sec (24.38 m/s). Photographs of the test section and fan are presented in Figs. 2.2 and 2.3.

Since low Reynolds number airfoil performance is highly dependent on the behavior of the laminar boundary layer, low turbulence levels within the wind-tunnel test section are necessary to ensure that laminar flow does not prematurely transition to turbulent flow. In order to ensure good flow quality in the test section, the wind-tunnel settling chamber contains a 4-in. (10.16-cm) thick honeycomb in addition to four anti-turbulence screens, which can be partially removed for cleaning. The turbulence intensity has been measured to be less than 0.1%,<sup>6</sup> which is sufficient for low Reynolds number airfoil measurements. As presented later in this chapter, further testing of turbulence intensity levels has been conducted to examine the effects of having the LSATs measurement apparatus installed.



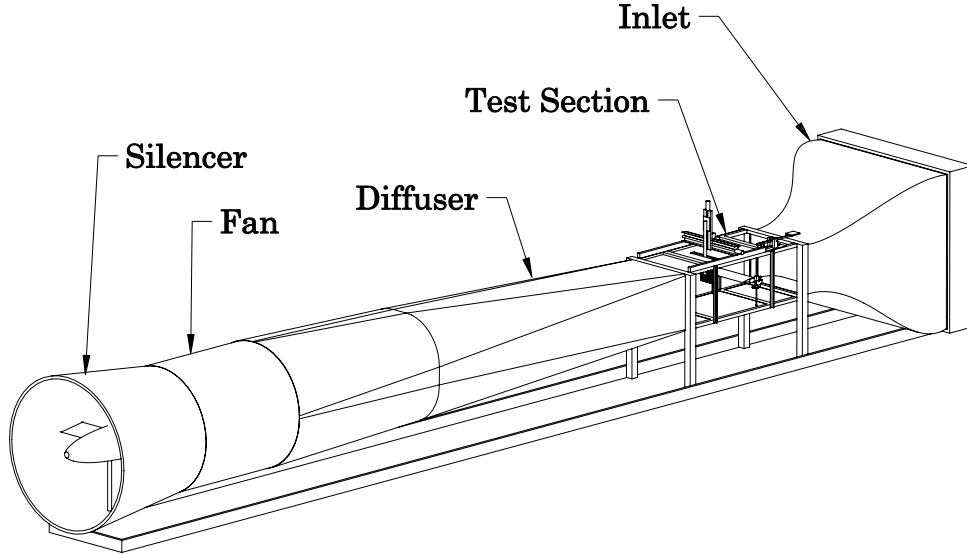


**Fig. 2.1** UIUC low-speed subsonic wind tunnel.

The experimental setup is depicted in Fig. 2.4. For the current tests, the 12-in. (0.305-m) chord, 33 5/8-in. (0.855-m) long airfoil models were mounted horizontally between two 3/8-in. (0.953-cm) thick, 6-ft (1.829-m) long Plexiglas<sup>®</sup> splitter plates to isolate the ends of the model from the tunnel side-wall boundary layers and the support hardware. For clarity, the Plexiglas splitter plates and the traverse enclosure box are not shown in Fig. 2.4. Gaps between the model and Plexiglas were nominally 0.05 in. (1.27 mm). The left-hand side of the model was free to pivot (far side of Fig. 2.4). At this location, the angle of attack was measured using a precision potentiometer. The right-hand side of the airfoil model was connected to the lift carriage through two steel wing rods that passed through the wing-rod fixture and were anchored to the model through two set screws. At this side, the airfoil model was free to move vertically on a precision ground shaft, but not free to rotate. The lift carriage was linked to a custom load beam, as described later in this chapter. Linear and spherical ball bearings within the lift carriage helped to minimize any frictional effects.

The two-axis traverse can be seen in Fig. 2.4, positioned above the wind-tunnel test section. Not shown is the pressure-sealed box that encloses the traverse system. The traverse was manufactured by LinTech and consists of horizontal and vertical screw-type linear positioning rails that operate in combination with two computer-controlled stepper motors. The rails are equipped with linear optical encoders that

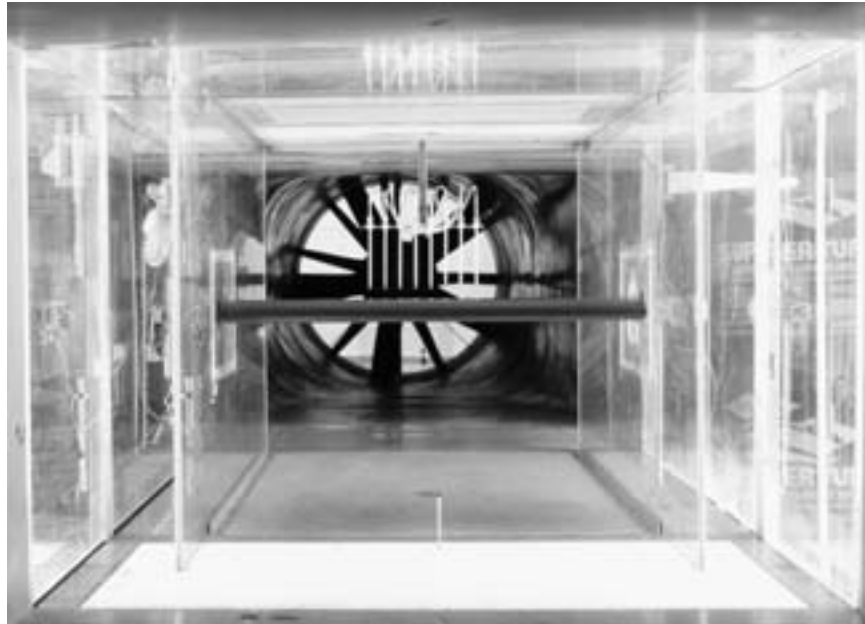


**Fig. 2.2** Photograph of wind-tunnel test section.



**Fig. 2.3** Photograph of wind-tunnel exit fan.

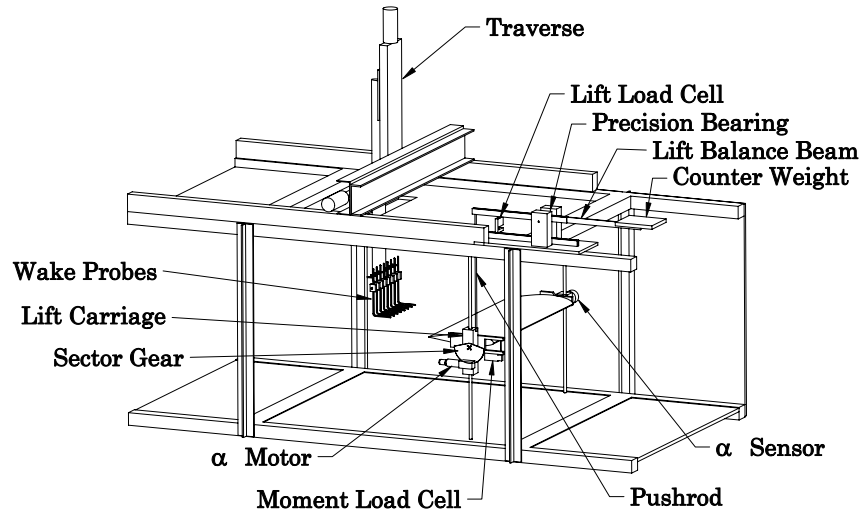


**Fig. 2.4** Experimental setup (Plexiglas<sup>®</sup> splitter plates and traverse enclosure box not shown for clarity).

supply a feedback signal to the motor controller allowing the traverse to operate with virtually no error. Attached to the traverse is a 3-ft (0.914-m) long boom that extends down into the wind tunnel test section to support the eight side-by-side wake pitot probes [spaced 1.5 in. (3.81-cm) apart in the spanwise direction].

### 2.1.1 Turbulence Intensity

As mentioned, the turbulence intensity of the UIUC low-speed wind tunnel was previously documented.<sup>6</sup> The measurements, however, were with an empty tunnel test section. It is of interest to examine what effect, if any, the splitter plates and other LSATs components have on the turbulence intensity.

The turbulence intensity was measured using hot-wire anemometry. In particular, the hot-wire system was a TSI Incorporated IFA 100 anemometer in conjunction with a TSI Model 1210-T1.5 hot-wire probe. The probe makes use of a 1.5 micron platinum-coated tungsten wire. The probe was mounted in the tunnel end-flow orientation with the wire perpendicular to the tunnel floor in order to measure the axial turbulence intensity. A PC equipped with a data acquisition card was used to log the signal from the anemometer. A Hewlett-Packard HP 35665A Dynamic Signal Analyzer, which performed an FFT (Fast Fourier Transform) analysis, was employed to allow the turbulence spectrum to be monitored over a broad range of frequencies.

The hot-wire probe was calibrated in the UIUC low-speed subsonic wind tunnel. The tunnel speed was set using static pressure probes inside the tunnel, and the corresponding (average) output of the anemometer was recorded. From these data, a curve fit was generated that was used to measure the fluctuating velocity with the hot-wire probe. Corrections were made to the signal to account for changes in temperature and density between the time the probe was calibrated and the time the measurements were made. A more detailed description of the methods used is found in Ref. 7.

**Table 2.1: Turbulence Intensity Characteristics in Percent**

| $Re$    | Configuration            | HPF Setting (Hz) | Turb. Intensity (%) |
|---------|--------------------------|------------------|---------------------|
| 100,000 | Tunnel Empty             | DC Coupled       | 0.1194              |
|         |                          | 0.1              | 0.0986              |
|         |                          | 3                | 0.0904              |
|         |                          | 10               | 0.0870              |
| 100,000 | Test Apparatus Installed | DC Coupled       | 0.1248              |
|         |                          | 0.1              | 0.1228              |
|         |                          | 3                | 0.1012              |
|         |                          | 10               | 0.0968              |
| 200,000 | Tunnel Empty             | DC Coupled       | 0.0944              |
|         |                          | 0.1              | 0.0834              |
|         |                          | 3                | 0.0736              |
|         |                          | 10               | 0.0722              |
| 200,000 | Test Apparatus Installed | DC Coupled       | 0.1418              |
|         |                          | 0.1              | 0.1458              |
|         |                          | 3                | 0.0800              |
|         |                          | 10               | 0.0772              |
| 350,000 | Tunnel Empty             | DC Coupled       | 0.0984              |
|         |                          | 0.1              | 0.0944              |
|         |                          | 3                | 0.0682              |
|         |                          | 10               | 0.0640              |
| 350,000 | Test Apparatus Installed | DC Coupled       | 0.1506              |
|         |                          | 0.1              | 0.1574              |
|         |                          | 3                | 0.0750              |
|         |                          | 10               | 0.0718              |
| 500,000 | Tunnel Empty             | DC Coupled       | 0.1016              |
|         |                          | 0.1              | 0.0930              |
|         |                          | 3                | 0.0690              |
|         |                          | 10               | 0.0644              |
| 500,000 | Test Apparatus Installed | DC Coupled       | 0.1580              |
|         |                          | 0.1              | 0.1957              |
|         |                          | 3                | 0.0842              |
|         |                          | 10               | 0.0754              |

The turbulence intensity was calculated from data using a total of 50,000 samples with a sample frequency of 10,000 Hz. Table 2.1 gives the resulting turbulence levels measured. The same information is also shown graphically in Fig. 2.5 for the case in which the tunnel was empty and that in which the full measurement apparatus was installed. As compared with the baseline empty tunnel, turbulence levels observed with the test apparatus installed are relatively unchanged at  $Re = 100,000$  but increase at higher Reynolds numbers. These effects all but disappear when the high-pass filter is set above 3 Hz. The main effect of the test rig appears to be added velocity fluctuations in the very low frequency range. Figure 2.6 shows the power spectra between 0 and 100 Hz for the  $Re = 350,000$  case both for the empty tunnel and for that with the test apparatus installed. Measurements were taken over a wide range of frequencies (up to 6,400 Hz), but in all cases the interesting features ranged between 0 and 100 Hz. Apart from the peaks in power at 56 and 79 Hz, the turbulent power spectrum is similar in magnitude for both configurations. It is only in the range from 0 to 25 Hz that there is a noticeable offset between the empty-tunnel test section and the installed-apparatus section.

### 2.1.2 Freestream Velocity

For proper force and moment measurements, it is important for the freestream velocity to be as uniform as possible in the test section. In ideal conditions, the freestream velocity is the same everywhere in the test section. In reality, there are small variations in the velocity caused by the presence of the tunnel walls and various effects such as flow turning the tight corner at the inlet of the tunnel.

The variation of velocity in the test section of the UIUC low-speed subsonic wind tunnel was obtained by comparing the dynamic pressure (directly related to velocity) at a pitot-static probe mounted near the entrance of the splitter plates with that measured by a downstream probe. The upstream probe was located at the centerline of the tunnel in the spanwise direction ( $X = 0$ ), 0.97 ft (0.296 m) below the centerline of the tunnel in the vertical direction [ $Y = -11.66$  in. (0.296 m)], and 1.323 ft (0.403 m) upstream of the quarter-chord location of the airfoil model when mounted in the test section. The downstream probe was traversed in the  $X$ - $Y$  plane perpendicular to the freestream and coincident with the quarter chord. Measurements were made both with the test section empty and with the LSATs test apparatus installed.

The measurement plane extended from 5.5 in. (13.97 cm) above the tunnel centerline to 14.5 in. (36.83 cm) below in the vertical direction  $Y$ , and from 10.5 in. (26.67 cm) to the left of the tunnel centerline to 10.5 in. (26.67 cm) to the right in the horizontal direction  $X$ . A grid spacing of 1 in. (2.54 cm) was used for the measurements, resulting in a total of 462 measurement points for each case tested.

Three differential-pressure transducers were used for the measurements. One transducer measured the upstream dynamic pressure  $Q_u$  by measuring the pressure

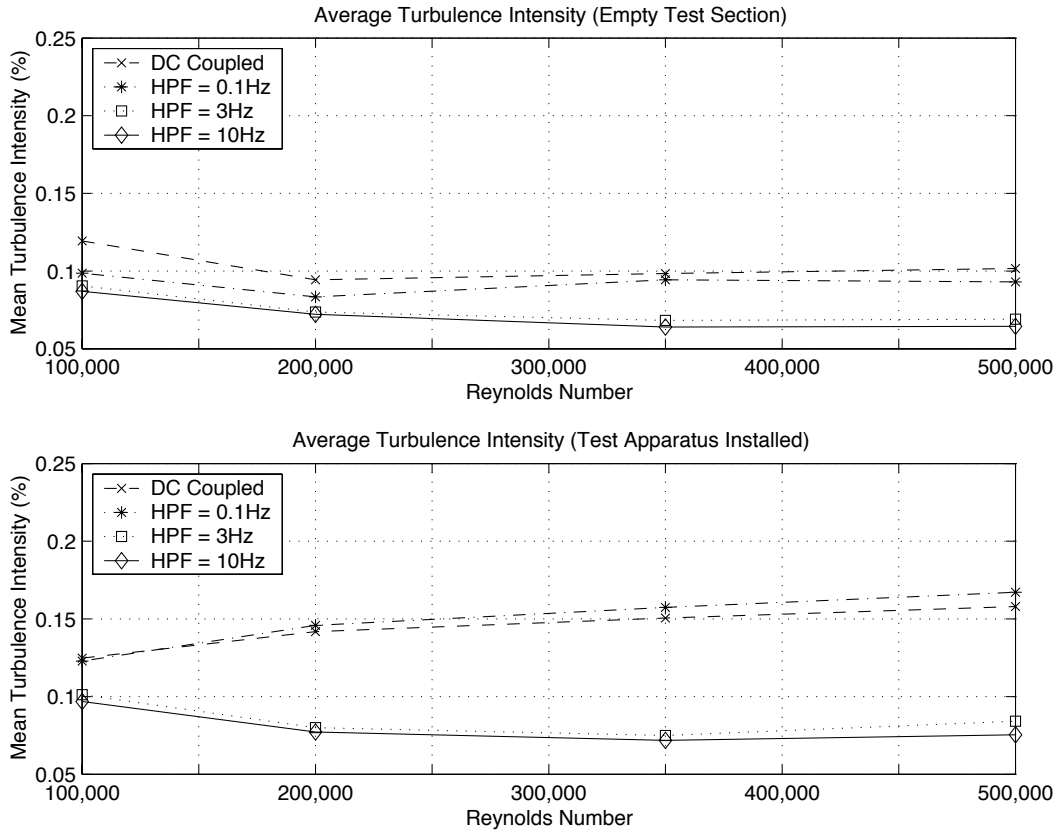


**Fig. 2.5** Turbulence intensity at tunnel centerline, empty test section and with rig in place.

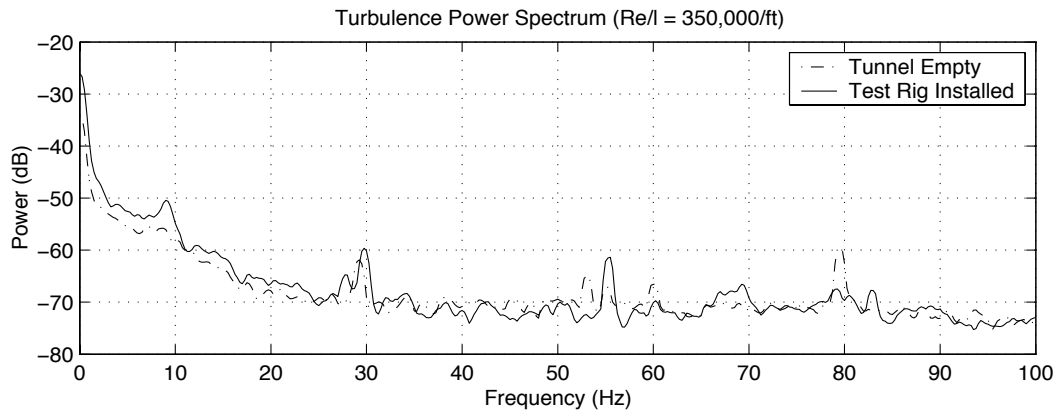


**Fig. 2.6** Power spectrum comparison between empty tunnel and installed test apparatus cases for  $Re = 350,000$ .

difference across the total pressure and static pressure ports of a pitot-static probe. A second pressure transducer was configured to measure the difference between the upstream and downstream total pressure  $\Delta P_0$ . A third transducer was configured to measure the difference between the upstream and downstream static pressure  $\Delta p$ . The change in dynamic pressure  $\Delta Q$  is just  $\Delta P_0 - \Delta p$ . Thus, the local dynamic pressure at each point is therefore

$$Q = Q_u + \Delta Q = Q_u + \Delta P_0 - \Delta p \quad (2.1)$$

For each Reynolds number tested, the tunnel speed was set using the upstream probe as the reference. Differences in temperature and ambient pressure were accounted for. The percent difference at each point was calculated according to

$$\Delta Q(\%) = \frac{Q - Q_u}{Q_u} \times 100\% \quad (2.2)$$

Figure 2.7 shows contours of  $\Delta Q$  for various Reynolds numbers plotted against its  $X$  and  $Y$  location for the case in which the wind tunnel was empty. For comparison, Fig. 2.8 shows  $\Delta Q$  plotted against its  $X$  and  $Y$  location with the LSATs test rig installed.

From Figs. 2.7 and 2.8, several observations can be made. First, for the empty test section case, there is a slight decrease in the test section flow speed at the location of the model relative to the upstream probe. When the LSATs rig is installed, there is instead an increase in the flow speed. It is likely that the velocity measured at the location of the model is higher than the upstream velocity because of the growth of the boundary layer along the splitter plates, ceiling and floor as well as the blockage that occurs between the splitter plates and the tunnel sidewalls. This percentage increase in the flow speed grows larger as the Reynolds number is reduced, which is consistent with the thicker wall boundary layers at lower Reynolds numbers. As discussed later, this rise in velocity is accounted for in the airfoil-performance data-reduction procedure. Second, over the region where the model is located, the net change in flow speed is observed to be relatively small. For instance, Fig. 2.8 shows that at  $Re/l = 200,000/\text{ft}$  ( $656,168/\text{m}$ ), the increase in the flow speed varies from approximately 1.4% to 1.8%, which is a relative difference of  $\pm 0.2\%$  in the working range of the test section. As stated in Ref. 8, it is desirable for the variation in dynamic pressure in the working range of the test section to be less than 0.5% from the mean, i.e.,  $\pm 0.5\%$ . The results show that the flow is well within the “rule of thumb.” A third observation is the existence of a slight asymmetry in the flow, noticeable mainly in the  $+X:-Y$  quadrant (bottom right corner in Figs. 2.7 and 2.8). The asymmetry is present with the tunnel empty and with the test rig in place; hence, it is unrelated to the LSATs rig. Moreover, the lines of constant  $Q$  are parallel to the tunnel floor at  $X = 0$  (centerline), so the effect is negligible with respect to the performance-measurement quantities in the center region of the test section.

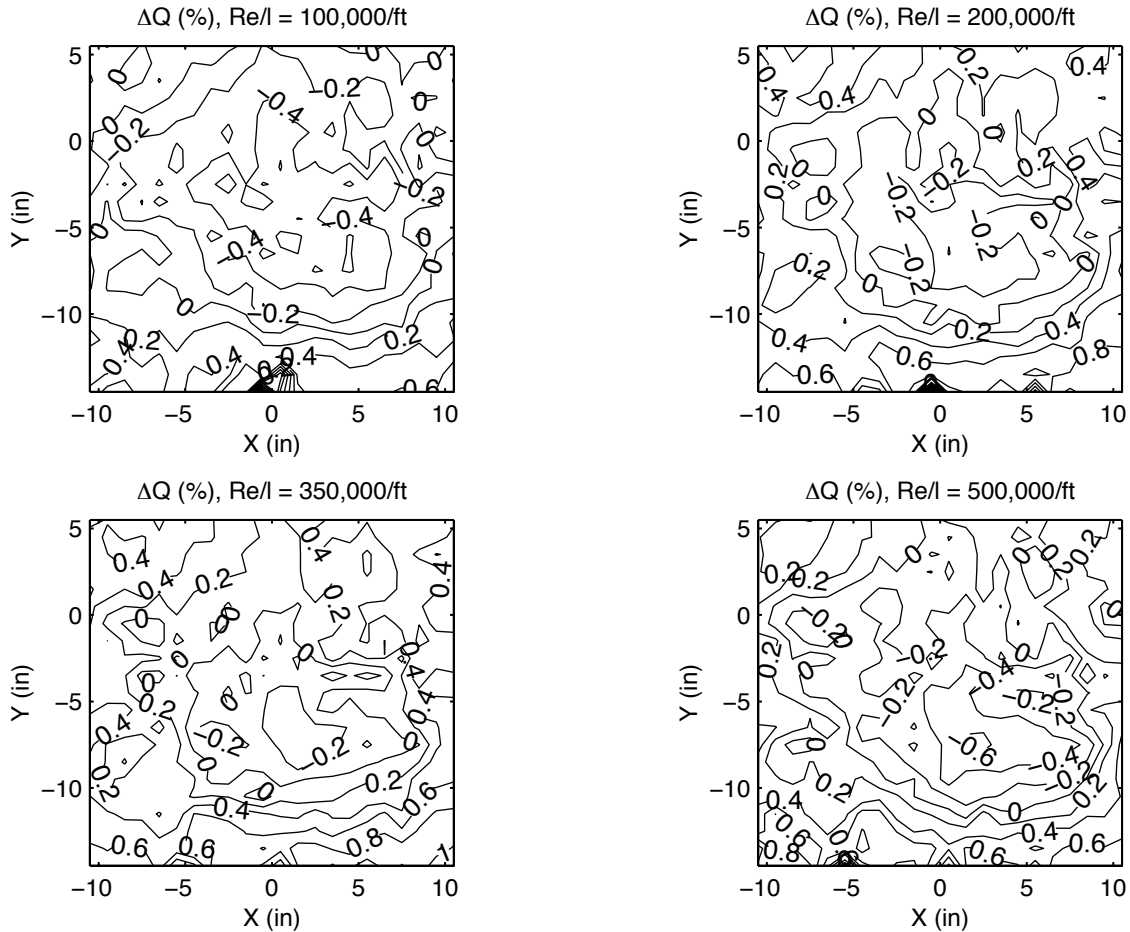


**Fig. 2.7** Dynamic pressure variation across test section when empty.

### 2.1.3 Freestream Flow Angularity

Just as it is important to have uniform flow velocity in the wind-tunnel test section, it is equally important to have the flow parallel to the axial direction.<sup>8</sup> For the most part, pitot-static probes are insensitive to flow angles in the range  $\pm 12$  deg, so a large flow angle is required to introduce an error in the dynamic pressure measurements. Similarly, large flow angles are required to introduce errors into total head measurements. Apart from pressure measurements, a small change in pitch angle contributes to a change in the effective angle of attack of the airfoil model; such an error can skew the lift and drag measurements when they are plotted versus the angle of attack.



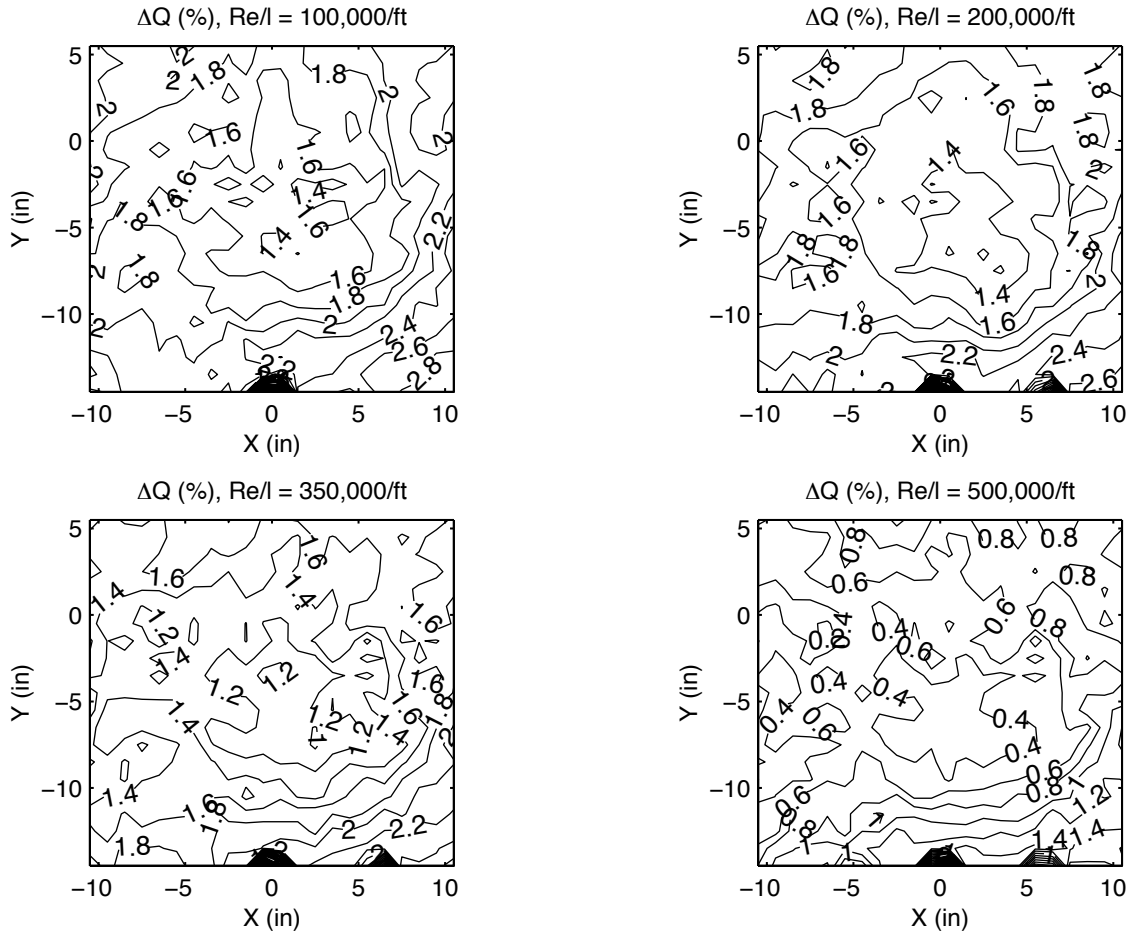


**Fig. 2.8** Dynamic pressure variation across test section with the LSATs rig installed.

The flow angularity in the test section of the UIUC low-speed subsonic wind tunnel was measured using an Aeroprobe Corporation Model S7TC317 7-hole probe. The probe has a total-head port located at the center, and six chamfered ports were equally spaced circumferentially around the center. Each port of the 7-hole probe was connected to the high-pressure side of an MKS Model 220CD 1-mm Hg pressure transducer. The reference side of each pressure transducer was left open to ambient pressure. The probe was mounted in the wind tunnel on a special two-beam sting attached to the computer-controlled LinTech traverse. The flow measurements were all taken with the LSATs test rig installed in the wind-tunnel test section, without the model. The probe was oriented as shown in Fig. 2.9. A more detailed description of the use of the 7-hole probe is found in Ref. 9.

The 7-hole probe was traversed in a plane perpendicular to the freestream flow over the range from  $X = \pm 6.5$  in. (16.51 cm) to  $Y = \pm 10$  in. (25.4 cm). The traverse was not extended to the edges of the test section, because of equipment

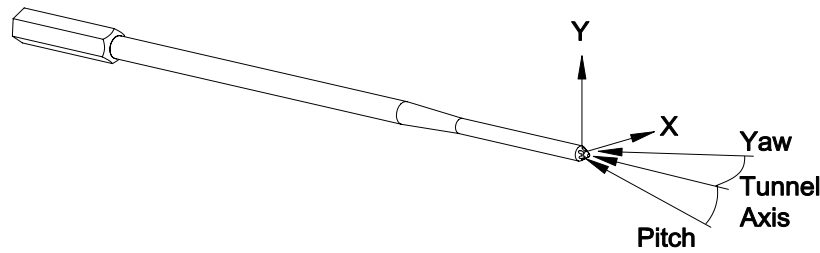


**Fig. 2.9** Illustration of the 7-hole probe used for flow angle measurements.

limitations. Traversing this central core was acceptable because one would expect to find the largest flow angle variation in the center of the test section rather than along the walls, where at a minimum the flow is parallel to the wall (yaw or pitch is thereby zero). A grid spacing of 1 in. (2.54 cm) was used, resulting in a grid of 252 sample locations for each case tested. The 7-hole probe tip was located approximately 1.5 chord lengths behind the quarter chord of the airfoil model. To set the tunnel speed, one pitot-static probe was located at  $X = 0$ ,  $Y = -11.66$  in. (29.62 cm). For redundancy, an additional probe was located at  $X = 5$  in. (12.7 cm),  $Y = -11.66$  in. (29.62 cm). Both pitot-static probes were mounted at the same streamwise location, 1.323 ft (3.36 cm) upstream of the location of the quarter chord of the airfoil model.

Calibration curves supplied by the manufacturer were used to determine the flow angle at each location. Three such curves were provided, each of which covers a particular angle of attack range, namely, 0 to 5 deg, 5 to 10 deg, or 10 to 15 deg. Because the flow angles measured never exceeded 1 deg, only the first curve was needed. Figures 2.10 through 2.12 show the measured flow angle at each point plotted against its  $X$  and  $Y$  coordinate.

The contour plots of flow angle in the test section show that pitch and yaw angles are smallest at  $Re = 500,000$ , becoming more pronounced at lower Reynolds numbers. Pitch angle, the more important angle for airfoil testing, is generally between 0 and 0.2 deg ( $\pm 0.1$  deg) across the working region of the test section where the airfoil model is located. According to Ref. 8, a flow angle variation of  $\pm 0.2$  deg is acceptable, but  $\pm 0.1$  deg or better is the preferred. The current measurements meet this latter desired level of flow quality.

It is worth noting that downstream of the pitot-static probes placed near the floor, relatively large flow angles were recorded locally. Flow angle perturbations due to probes near the wall, such as the dynamic pressure probes used to determine the flow speed during the airfoil tests, are of no concern because the corresponding flow is well below the working region of the test section where the model is located.

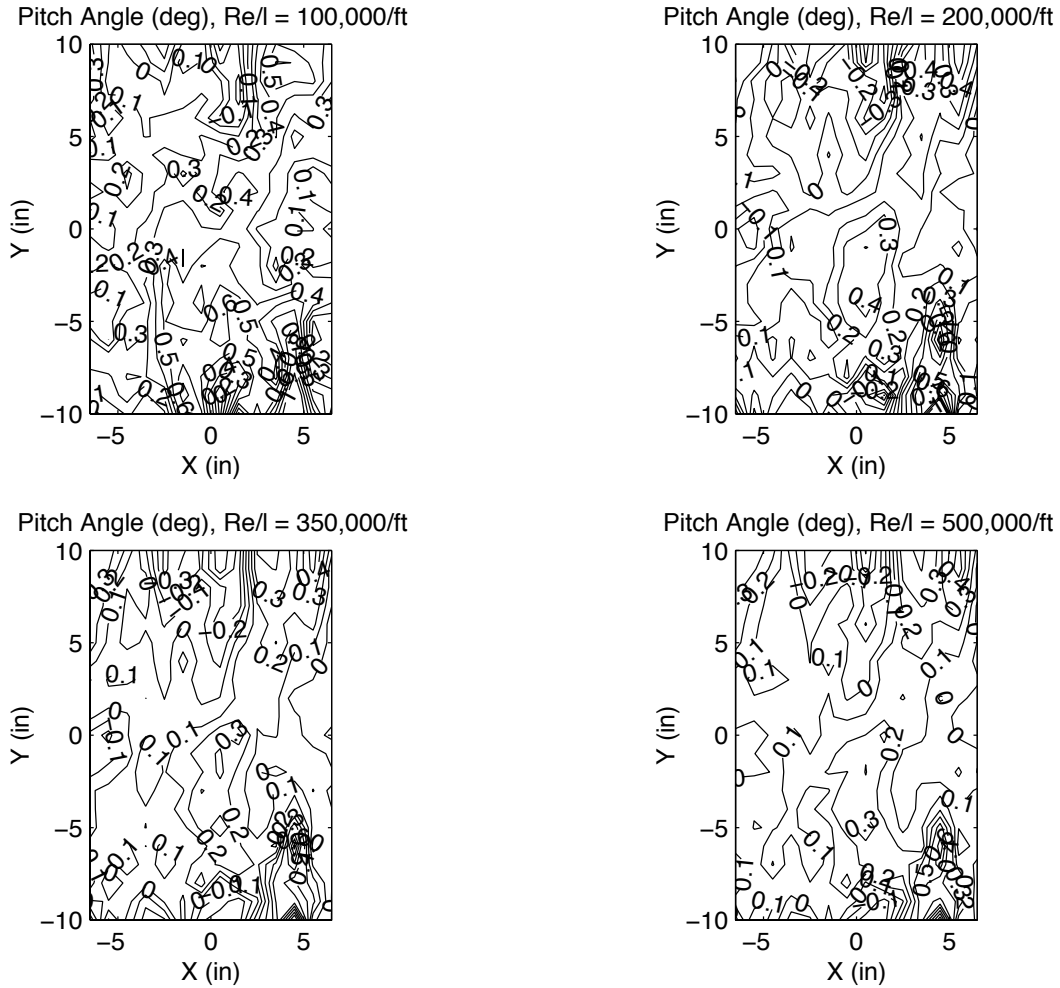
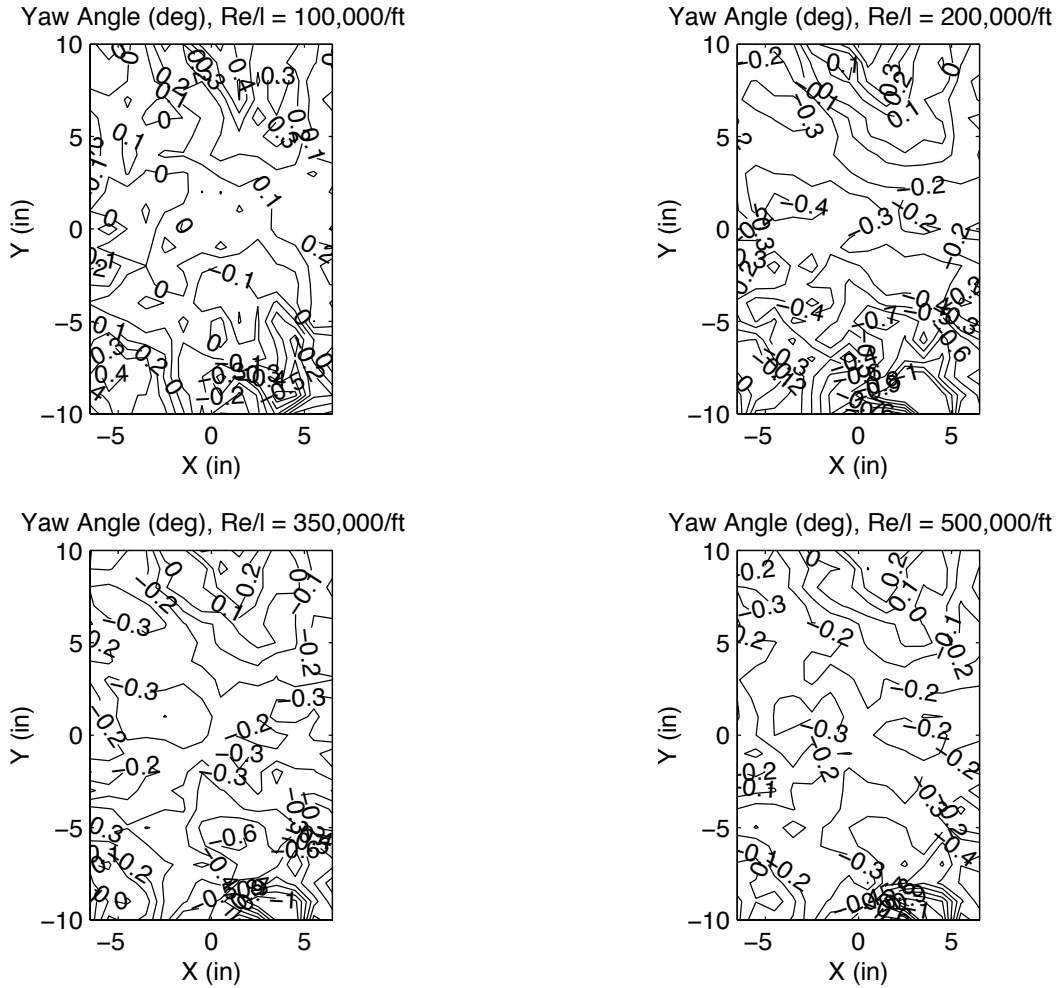


Fig. 2.10 Pitch angle variation across test section with the LSAT's rig installed.

## 2.2 Airfoil Models

In order to determine the accuracy of the wind-tunnel models, each model was digitized using a Brown & Sharpe coordinate measuring machine (CMM) to determine the actual airfoil shape. Approximately 80 points were taken around the airfoil. The spacing was more or less proportional to the local curvature. Near the leading and trailing edges the spacing was relatively small; over the airfoil midsection, it was as large as 0.7 in. (1.78 cm). All model coordinates were measured in the middle of the model.

Section profiles and model accuracy plots are presented in Chapter 5. The plots include the true airfoil as designed (solid line) compared with the “actual” digitized



**Fig. 2.11** Yaw angle variation across test section with the LSATs rig installed.

airfoil (dotted line). The model accuracy plots depict the differences between the true airfoil and actual airfoil coordinates for the upper surface (solid line) and lower surface (dotted line) of the airfoil. A displacement above or below the axis means that the model surface lies above or below the true, respectively.

## 2.3 Performance Data Measurement Techniques

As an overview to this section, the data acquisition process, which was largely choreographed by computer control, is briefly described. Two types of runs were performed: “lift runs” and “drag runs.” For the former, only lift and moment vs angle of attack data were taken for a fixed Reynolds number; for the latter, drag data were included. Lift runs were extended to high angle of attack and sometimes into stall; drag runs were set to take data nominally over the low drag range, which for this

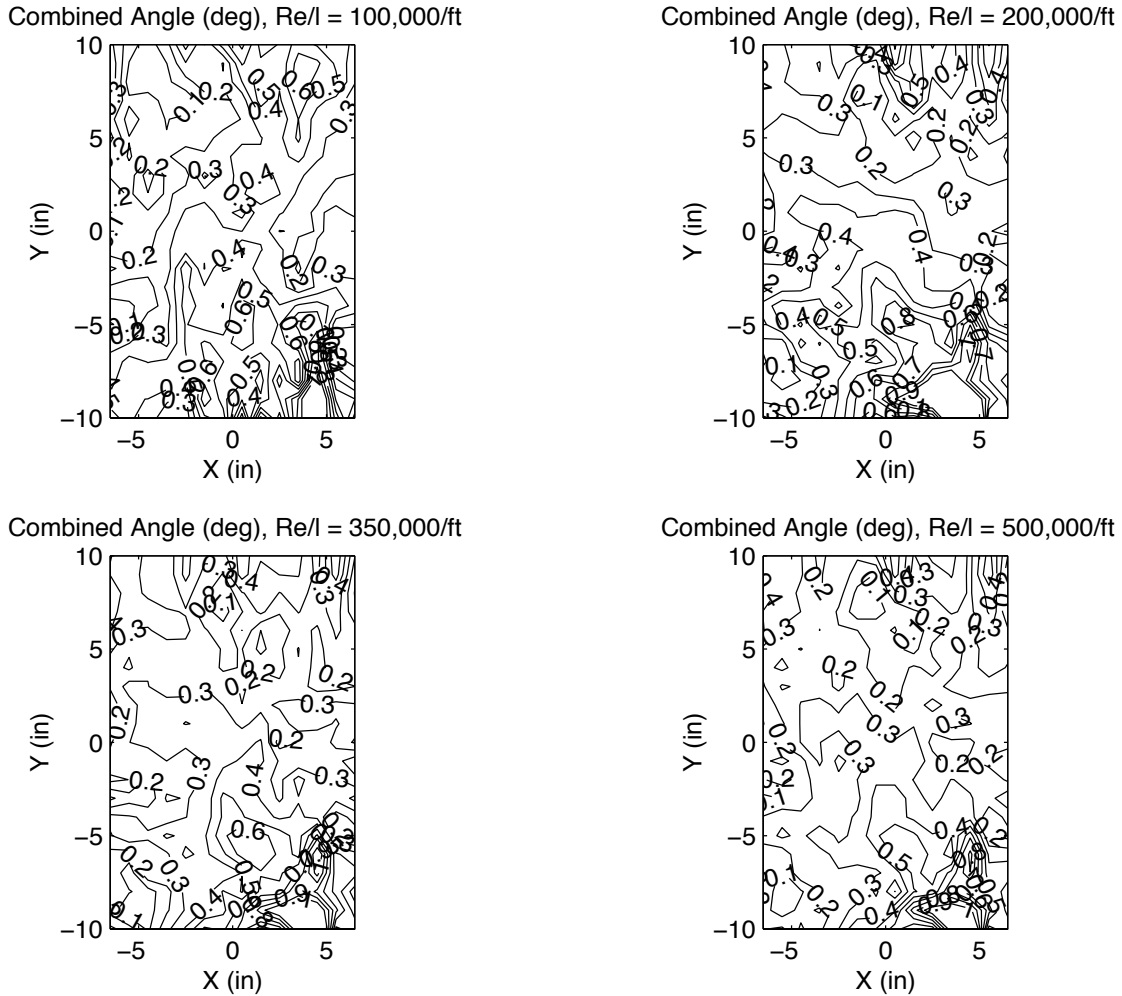


**Fig. 2.12** Combined pitch and yaw angle across test section with the LSAT's rig installed.

work was defined as  $C_d$  approximately less than 0.05. For lift runs, data were taken for both increasing and decreasing angles of attack to document any aerodynamic hysteresis present. For drag runs, data were taken only for increasing angles of attack. For each angle of attack, the tunnel speed was checked and, if necessary, adjustments were made to maintain a fixed Reynolds number. In general, acquiring data during a lift run was a relatively quick process compared with acquisition during a drag run. Since no wake measurements were taken during a lift run, it was possible, for instance, to cover a full angle of attack range from  $-10$  to  $20$  deg and back in  $1$  deg increments in approximately  $20$  min. For a drag run, however, the time could range from  $1$  to  $6$  hr, depending principally on the width of the wake and desired angle of attack range. Details pertaining to the lift, drag, and moment measurements are described in more detail in the following sections.

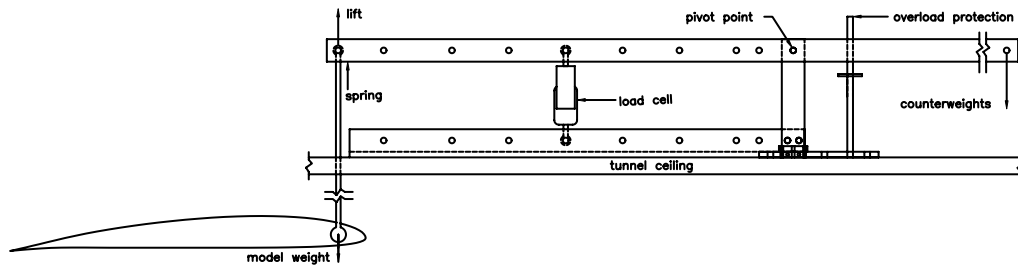


**Fig. 2.13** LSATs lift beam balance assembly as viewed from the working side of the test section.

### 2.3.1 Lift Force Measurement

Figure 2.13 depicts a schematic of the lift beam balance that was integrated into the test section and oriented according to Fig. 2.4. The lift apparatus consisted primarily of a fulcrum supported beam restrained in rotation by a strain-gauge load cell. The lift load acting through a pushrod was applied to the beam and transferred to the load cell via a lever arrangement, as shown. For correct operation of the lift balance, the load cell was required to be in tension. To ensure this outcome, spring tension on the lift side of the beam and counterweight on the opposite end were used, and the amount of each depended on the model weight as well as the range of loads expected. Moreover, the mix of spring tension and counterweight changed in going from a calibration to a performance data run.

Depending on the Reynolds number of the test and expected range in lift coefficient, one of three possible load cells (Interface Inc. Models SM-10, SM-25, and SM-50) was inserted into one of nine possible load cell attachment holes, allowing for a variation in the operational range of the lift beam balance. This approach offered the ability to measure the small forces present at the lower Reynolds numbers range ( $Re \approx 60,000$ ) while retaining the capability to handle the larger lift forces occurring at the higher Reynolds numbers ( $Re \approx 500,000$ ). The resulting lift measurements were repeatable to within 0.01% of the rated output of the particular load cell used. Calibrations were performed frequently to minimize the effects of drift.

### 2.3.2 Drag Force Measurement

While the lift force on airfoils at low Reynolds numbers can be obtained with acceptable accuracy through a lift balance, drag force is often considerably much lower than the lift. As a result, profile drag is often best obtained by the momentum method

instead of a force balance. For the current tests, the profile drag was determined through the method developed by Jones<sup>10</sup> (taken from Schlichting<sup>11</sup>).

After application of the two-dimensional momentum and continuity equations to a control volume shown in Fig. 2.14, the drag force per unit span can be calculated from

$$d = \rho \int_{-\infty}^{\infty} u_1(V_{\infty} - u_1)dy \quad (2.3)$$

Assuming that the location of the measurements is far enough behind the airfoil so that the static pressure has returned to upstream tunnel static pressure (i.e.,  $P_{s,1} = P_{s,\infty} = P_s$ ) and that the downstream flow outside the airfoil wake proceeds without losses (i.e., the total pressure remains constant along every streamline), the total pressure relationships from Bernoulli's equation are

$$P_s + \frac{1}{2}\rho u_1^2 = P_{0,1} \quad (2.4)$$

$$P_s + \frac{1}{2}\rho V_{\infty}^2 = P_{0,\infty} \quad (2.5)$$

Applying the above relationships to Eq. (2.3) and simplifying yields

$$d = 2 \int_{-\infty}^{\infty} \{ \sqrt{P_{0,1} - P_s} \sqrt{q_{\infty} - P_s} - (P_{0,1} - P_s) \} dy \quad (2.6)$$

$$P_{0,1} - P_s = P_{0,1} - P_s - P_{0,\infty} + P_{0,\infty} = q_{\infty} - \Delta P_0 \quad (2.7)$$

$$d = 2 \int_{-\infty}^{\infty} \sqrt{q_{\infty} - \Delta P_0} (\sqrt{q_{\infty}} - \sqrt{q_{\infty} - \Delta P_0}) dy \quad (2.8)$$

During the tests, to ensure that the wake had relaxed to tunnel static pressure, the wake measurements were performed 14.8 in (approximately 1.25 chord lengths) downstream of the trailing edge of the airfoil. Each vertical wake traverse consisted of between 20 and 80 total-head pressure measurements per probe (depending on wake thickness) with points nominally spaced 0.08 in. (2.03 mm) apart. No measurements were taken in stall owing to the size and unsteadiness of the wake.

Pressure measurements within the wake were made using MKS Baratron Model 220 variable-capacitance differential pressure transducers with a full-scale range of 1-mm Hg (0.02 psia), having a resolution of 0.01% of full-scale reading and an accuracy of 0.15% of reading. All of the transducers were factory calibrated prior to the tests.

In order to obtain an accurate value for the drag coefficient, wake profile measurements were taken at eight spanwise locations spaced 1.5 in. (3.81 cm) apart over the center 10.5 in. (26.67 cm) span of the model. The resulting eight drag coefficients were then averaged to obtain the drag at a given angle of attack. This average drag coefficient is presented in Chapter 5 and Appendix B. Figure 2.15 depicts a typical variation in the spanwise drag coefficient at Reynolds numbers from 100,000 to 500,000. For  $Re = 100,000$ , a component of the variation could be attributed to “scatter,” which is due partly to the unsteadiness in the wake and the difficulty in resolving such small pressure differences. At the higher  $Re$ 's, however, an intrinsic steady-state variation is present. For the interested reader, a thorough documentation of this phenomenon is presented in Refs. 12 and 13.

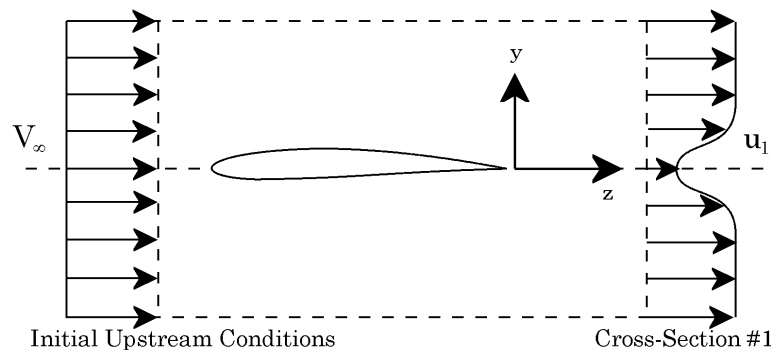


**Fig. 2.14** Control volume for the 2-D momentum deficit method to determine the profile drag.

### 2.3.3 Pitching Moment Measurement

Figure 2.16 shows a cut-away drawing of the system used to measure the moment produced by the airfoil model. A load cell (Interface Inc. Model MB-10) and connecting post served as a link between the free-member ‘A’ attached to the airfoil model and the fixed-member ‘B’ attached to the lift carriage. Because the load cell links the free and fixed members about a pivot point, it is subjected to any moment loads produced by the airfoil, thereby allowing the pitching moment of the airfoil to be measured. Also, in a manner similar to that employed on the lift balance, there are two sets of load cell attachment points, allowing for an expanded measurement range.

For some airfoils at high angle of attack and high Reynolds numbers, the unsteady loads and negligible damping led to flutter of the airfoil model. This unsafe flutter



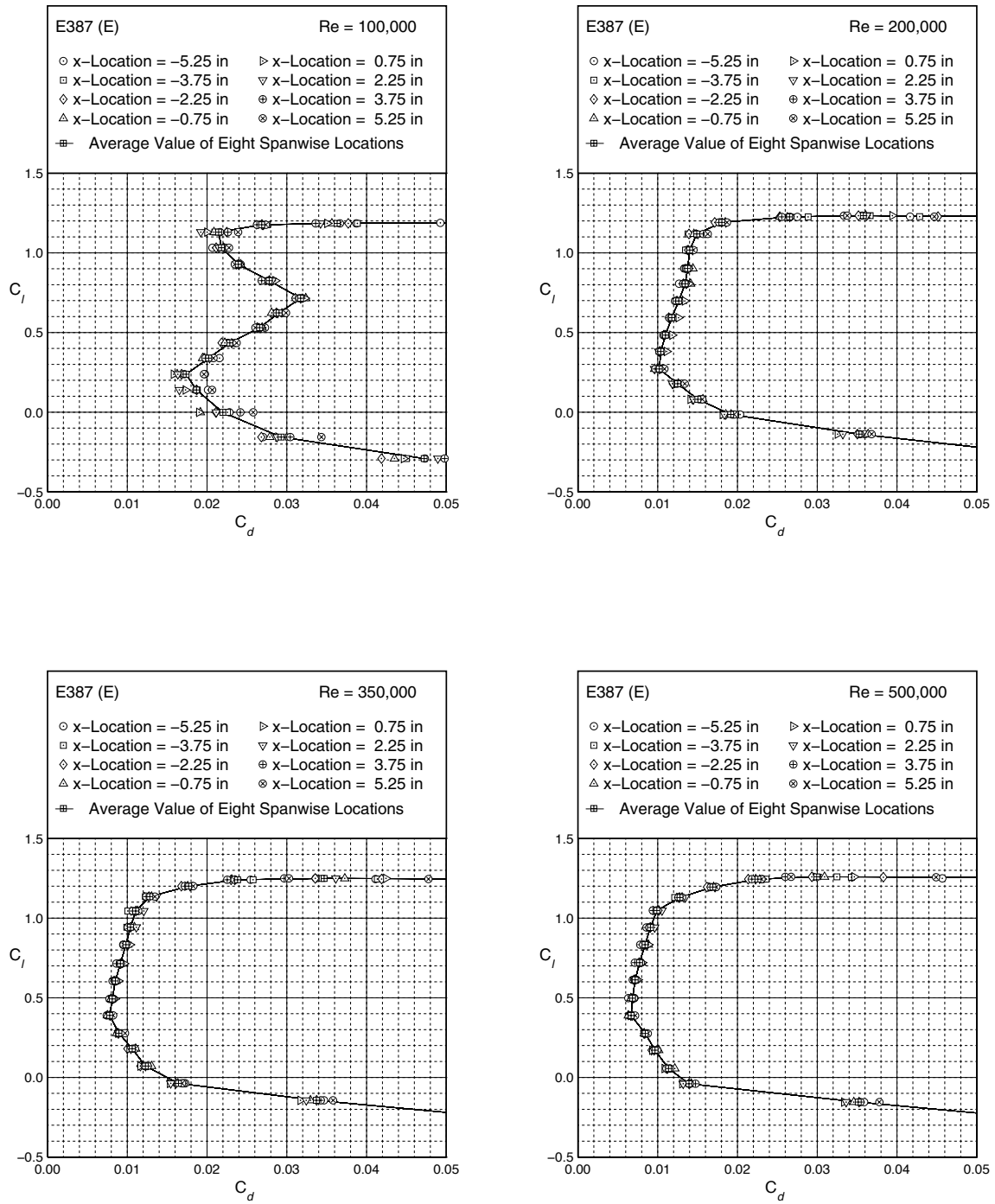


**Fig. 2.15** Drag results for the E387 (E) airfoil depicting typical spanwise drag variations for the eight spanwise stations for  $Re = 100,000, 200,000, 350,000,$  and  $500,000$ .

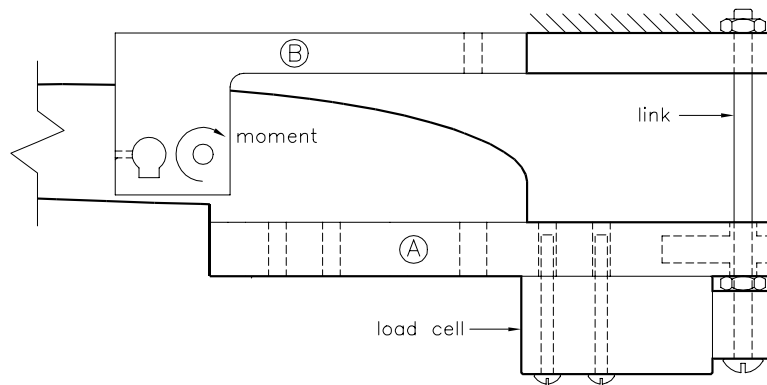


**Fig. 2.16** Moment measurement apparatus.

occurred for the E387, S822, S834, and SD2030 airfoils, but not for the FX 63-137 and SH3055 airfoils. For the former group, the angle of attack range for moment data was reduced to avoid flutter at the higher Reynolds numbers tested ( $Re = 350,000$  and  $500,000$ ). For this group of airfoils, a special lift-only carriage was designed in an attempt to acquire more stall data (absent the moment data), and to some extent this was achieved. However, despite the robust design of the new carriage, in some cases the runs could not be extended to the desired 20 deg condition because of the aero-structural stall-induced unsteadiness.

## 2.4 Data Acquisition and Reduction

All analog data were recorded on a Dell 1.4-GHz Precision-330 computer workstation. The data were digitized using a National Instruments NI PCI-6031E 16-bit analog-to-digital data acquisition board. The NI PCI-6031E has a resolution of 0.0015% of full-scale reading, 32 differential input channels, and two 16-bit digital-to-analog output channels. The 16-bit resolution of the board provided an accuracy of  $\pm 0.305$  mV when set for a full-scale range of  $\pm 10$  V.

At the low speeds required for low Reynolds number tests, small time-dependent fluctuations in tunnel speed were caused by inertia of both the fan drive system and the air. Thus, all quantities (dynamic pressure, total pressure, lift, angle of attack, probe  $x$ - $y$  position, and temperature) were measured simultaneously. Once a run started, the entire data acquisition process was completely automated as previously described. This automation included setting and maintaining a constant Reynolds number within the test section, acquiring data, and plotting raw data graphically to the computer screen and numerically to a printer. All raw data were also saved to a separate output file for later in-depth data reduction.

Since the wind-tunnel model was mounted between splitter plates, the amount of flow (or spillage) between the splitter plates and the sidewalls of the test section

could not be easily determined. Consequently, measurement of the freestream flow speed ahead of the splitter plates could not be used to determine the true freestream experienced by the model. Rather, the upstream dynamic pressure was measured between the two splitter plates 15.9 in. ahead of the quarter-chord point of the airfoil models and 5.2 in. above the test section floor. Since the upstream pitot-static probe was close to the leading edge of the airfoil, the measured velocity was corrected for circulation effects, as discussed in Section 2.4.2.

In order to convert the upstream dynamic pressure into velocity, the air density was calculated from the ideal gas law

$$\rho = \frac{P_{atm}}{RT} \quad (2.9)$$

with ambient temperature obtained from an Omega Model CJ thermocouple (accurate to within 1 deg Rankine) located next to the wind tunnel. The velocity was then calculated from

$$V_{\infty} = \sqrt{\frac{2q_{\infty}}{\rho}} \quad (2.10)$$

The Reynolds number based on the airfoil chord is given by

$$Re = \frac{\rho V_{\infty} c}{\mu} \quad (2.11)$$

where  $\mu$  for air was calculated using the Sutherland viscosity law<sup>14</sup> expressed as

$$\frac{\mu}{\mu_0} = \left(\frac{T}{T_0}\right)^{3/2} \left(\frac{T_0 + S}{T + S}\right) \quad (2.12)$$

The physical boundaries of a closed test section restrict the flow and, as a result, produce extraneous forces on the model that must be subtracted out. These extraneous aerodynamic forces occur mainly because the velocity of the air increases as it flows over the model owing to the restraining effect of the wind-tunnel boundaries combined with the physical presence of the model and its wake. This effect is minimized when the model is small in relation to the size of the test section. Unfortunately, smaller models are more difficult to build accurately. Hence, 12-in. chord airfoil models were selected as a compromise, even though this required measuring smaller forces and a more complicated data reduction process.

In the following three sections, only an overview of the two-dimensional wind-tunnel corrections and their causes is presented.

### 2.4.1 Wind-Tunnel Boundary Corrections

The presence of the wind-tunnel walls increases the measured lift, drag, and pitching moment because of the increase in velocity at the model. More specifically, the lateral boundaries in a two-dimensional testing context cause four phenomena to occur<sup>8</sup>: buoyancy, solid blockage, wake blockage, and streamline curvature.

**Buoyancy:** Buoyancy is an additional drag force that results from a decrease in static pressure along the test section due to the growth of the boundary layer at the walls. Although buoyancy effects are usually insignificant even for airfoils tested within test having a constant area, the main effect of buoyancy was taken into account directly in corrections of the freestream velocity.

**Solid Blockage:** The physical presence of a model within a test section is known as solid blockage, which produces a decrease in the effective area. From the continuity and Bernoulli's equation, the velocity of the air must increase as it flows over the model, increasing all aerodynamic forces and moments at a given angle of attack. Solid blockage is a function of the model size and test section dimensions.

$$\varepsilon_{sb} = \frac{K_1 M_v}{A_{ts}^{3/2}} \quad (2.13)$$

**Wake Blockage:** The second type of blockage is known as wake blockage, which results from a velocity within the airfoil wake that is lower than the freestream velocity. For closed test sections, in order to satisfy the continuity equation the velocity at the model (outside of the wake) must increase. The effect of wake blockage is proportional to the wake size and thus to the measured drag force on the model.

$$\varepsilon_{wb} = \left( \frac{c}{2h_{ts}} \right) C_{du} \quad (2.14)$$

**Streamline Curvature:** Because of the physical constraints of the tunnel boundaries, the normal curvature of the free air as it passes over a lifting body (such as an airfoil) is altered, increasing the airfoil effective camber as the streamlines are "squeezed" together. For closed wind-tunnel sections, the increase in camber results in an increase in lift, pitching moment about the quarter-chord point, and angle of attack; the drag is unaffected.

$$\Delta C_{l_{sc}} = \sigma C_l \quad (2.15)$$

$$\Delta \alpha_{sc} = \frac{57.3 \sigma}{2\pi} (C_l + 4 C_{m,c/4}) \quad (2.16)$$

where

$$\sigma = \frac{\pi^2}{48} \left( \frac{c}{h_{ts}} \right)^2 \quad (2.17)$$

### 2.4.2 Additional Velocity Corrections

When splitter plates are used, an additional velocity correction is required to correct for the so-called circulation effect.<sup>15</sup> As discussed previously, the freestream velocity must be measured between the splitter plates, and as a result the pitot-static tube used to measure dynamic pressure is influenced by the circulation on the airfoil model. Consequently, at the pitot-static tube, there is an induced velocity that depends on the amount of lift generated by the airfoil model—the greater the lift on the model (and thus the greater the circulation), the greater the induced velocity at the pitot-static tube. This circulation effect is, of course, also a function of the distance between the airfoil and the pitot-static tube. In most practical situations, however, the length of the splitter plates in front of the airfoil is usually small, since one of the main advantages of using splitter plates is to minimize the wall boundary-layer thickness at the model/wall juncture.

A detailed development of this correction procedure can be found in Ref. 15. To some degree, the effects of this correction can be gleaned from the results shown in Fig. 2.17 (taken from Ref. 5). Included in the figure are the reduced data for a prior version of the E387 airfoil, in particular model C, both with and without the circulation correction included. As clearly seen, this correction increases as the circulation increases, as one would expect, and overall the correction is substantial and should be included.

Finally, the velocity was also corrected to account for the boundary-layer growth along the tunnel walls, which resulted in a slightly higher than freestream velocity at the model. By using a second velocity measuring probe at the model quarter-chord point with the model removed and then measuring the upstream and downstream velocities simultaneously over a wide range in the Reynolds number, a calibration curve was obtained. Thus, for a measured upstream velocity, the actual velocity at the model could be calculated. The resulting velocity correction curve used to account for boundary-layer growth is shown in Fig. 2.18 and given by the equation

$$K_{vel} = 1.015755 - 0.0002391 V_u + 0.00001712 \sqrt{V_u} + \frac{0.1296}{\sqrt{V_u}} \quad (2.18)$$

### 2.4.3 Corrections to Measured Quantities

The measured quantities that must be corrected can be subdivided into two categories:

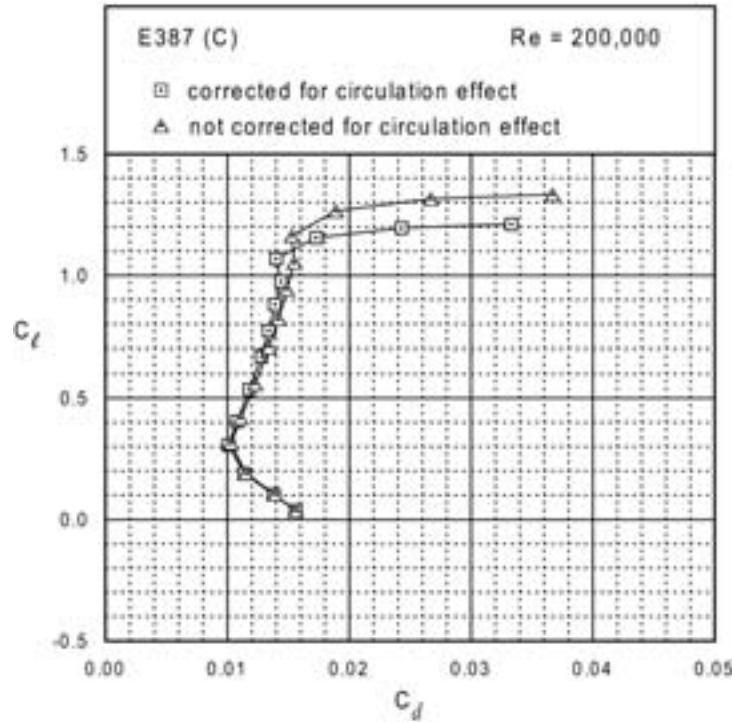


**Fig. 2.17** Drag polars for the E387 (C) with and without the necessary circulation correction (taken from Ref. 5).

stream and model quantities. The most important stream quantity is the velocity at the model. This velocity was obtained from the freestream velocity measurements and by applying the proper corrections to account for solid and wake blockage as well as boundary-layer growth. Combining the velocity corrections in a single expression gives

$$V_c = V_u K_{vel} (1 + \varepsilon_{sb} + \varepsilon_{wb}) \quad (2.19)$$

Other freestream quantities, such as the Reynolds number and dynamic pressure, were then obtained directly from the corrected value of the velocity.

The model quantities of interest are the lift, drag, moment, and angle of attack, which were corrected in their nondimensional form to account for solid and wake blockage as well as streamline curvature. These correction equations for lift, drag, moment, and angle of attack are expressed as

$$C_l = C_{lu} \frac{1 - \sigma}{(1 + \varepsilon_b)^2} \quad (2.20)$$

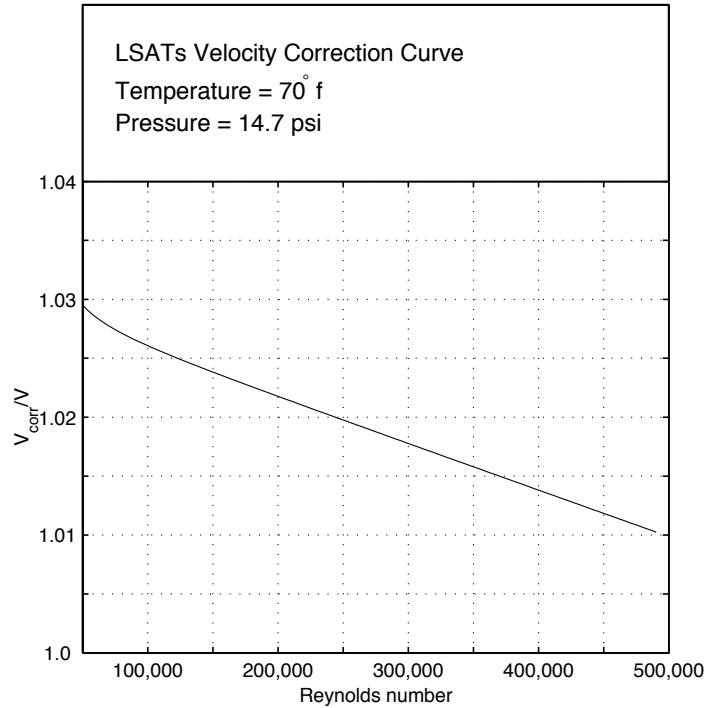


**Fig. 2.18** Velocity correction curve to account for boundary-layer growth between the splitter plates.

$$C_d = C_{du} \frac{1 - \varepsilon_{sb}}{(1 + \varepsilon_b)^2} \quad (2.21)$$

$$C_m = \frac{C_{m_u} + C_l \sigma (1 - \sigma) / 4}{(1 + \varepsilon_b)^2} \quad (2.22)$$

$$\alpha = \alpha_u + \frac{57.3 \sigma}{2\pi} (C_{l_u} + 4 C_{m,c/4_u}) \quad (2.23)$$

It is important to note that the use of drag coefficient data is required to correct the model quantities since wake blockage is proportional to the measured drag coefficient. For the lift runs, however, drag was not measured, which has an effect on the lift data reduction. For the lift curves, the wake blockage correction was computed using a constant value for the drag coefficient of 0.04, which was representative for conditions close to maximum lift. This method ensured more accurate values for the maximum lift coefficients even though it overcorrected lift coefficient values in the normal low-drag operating range of the airfoil. This “overcorrection” was not significant, as can be seen by comparing lift data taken from a lift run with that from a drag run.

## 2.5 Calibrations and Uncertainty Analysis

By applying the general uncertainty analysis presented in Coleman & Steele,<sup>16</sup> the uncertainties in the velocity, lift coefficient, and drag coefficient were found in a relatively straightforward manner. Further details describing the uncertainty analysis are presented in Ref. 12.

First, consider the case of measuring the upstream velocity, which is used to normalize the lift and drag forces. The highest uncertainty in the pressure readings due to fluctuations in flow angle is 1%, resulting in a freestream velocity uncertainty within 0.5%. If no errors related to the probes are included, the uncertainty in pressure readings and the velocity measurements reduce to less than approximately 0.5% and 0.3%, respectively.

The lift balance was calibrated over a range that depended on the loads expected for a given run—the higher the Reynolds number, the larger the range. Overall uncertainty in the lift coefficient is estimated to be 1.5%. The accuracy of the lift calibrations was the main contribution to this small error.

The drag measurement error comes from three sources: accuracy of the data acquisition instruments, the repeatability of the measurements, and spanwise variation in the downstream momentum deficit. Based partly on the error analysis method presented in McGhee<sup>17</sup> and Coleman & Steele,<sup>16</sup> the uncertainties caused by the instruments and measurement repeatability are less than 1% and 1.5%, respectively. Based on a statistical analysis of a representative low Reynolds number airfoil,<sup>5</sup> the uncertainties caused by the spanwise variations are estimated at 3% for  $Re = 100,000$  and reduce to approximately 1.5% at and above  $Re = 200,000$ .

For the angle of attack sensor, calibration measurements were taken at six different angles of attack incremented from 0 to 25 deg in 5-deg steps. Overall uncertainty in the angle of attack is estimated at 0.08 deg, based on the calibration results.





---

## Chapter 3

# Data Validation

---

In this chapter, data taken on the E387 are compared with results from NASA Langley in the Low-Turbulence Pressure Tunnel (NASA LTPT).<sup>17,18</sup> Four types of data are compared: surface oil flow visualization, lift data, moment data, and drag polars. In this order, these data are presented and discussed below.

### 3.1 Surface Oil Flow Measurements

Low Reynolds number airfoil flows are distinguished principally by the associated flow phenomenon termed a laminar separation bubble, which is the leading culprit in the degradation of low Reynolds number airfoil performance relative to the performance of airfoils at higher Reynolds numbers. When laminar separation bubbles do appear, they are caused by the inability of the flow to make a transition to turbulent flow in the attached boundary layer on the surface of the airfoil. Instead, the laminar flow separates before transition. When this happens, transition occurs in the free shear layer, and the so-called laminar separation bubble is formed when the turbulent flow reattaches to the airfoil surface downstream of the transition. For the most part, the resulting pressure drag over the region of the laminar separation bubble is responsible for the relatively high drag that can sometimes accompany airfoils at low Reynolds numbers. The existence of a laminar separation bubble and its extent can be deduced by examining surface oil flow visualization, as was done in the study.

The surface oil flow visualization technique made use of a fluorescent pigment (Kent-Moore 28431-1) suspended in a light, household-grade mineral oil that was sprayed onto the surface of the model using a Paasche Model VL airbrush. The model was then subjected to 20–45 min of continuous wind-tunnel run time at a fixed speed and angle of attack. During this period, the oil moved in the direction of the local flow velocity at a rate dependent on the balance of forces dictated by the boundary-layer skin friction  $C_f$  and surface tension of the oil. As a result, discernible regions of the flow could be identified for comparison with the NASA LTPT data.<sup>17,18</sup>

Figure 3.1 is a photograph of the surface oil flow pattern made visible under fluorescent light. Figure 3.2 conceptually illustrates the connection between the salient surface oil flow features and the skin friction distribution. Note that the skin friction distribution, though conceptual, is consistent with the results of many computational studies.<sup>19–24</sup> The authors believe that the unique shape of the  $C_f$  distribution, in particular the strong negative  $C_f$  spike, has yet to be experimentally

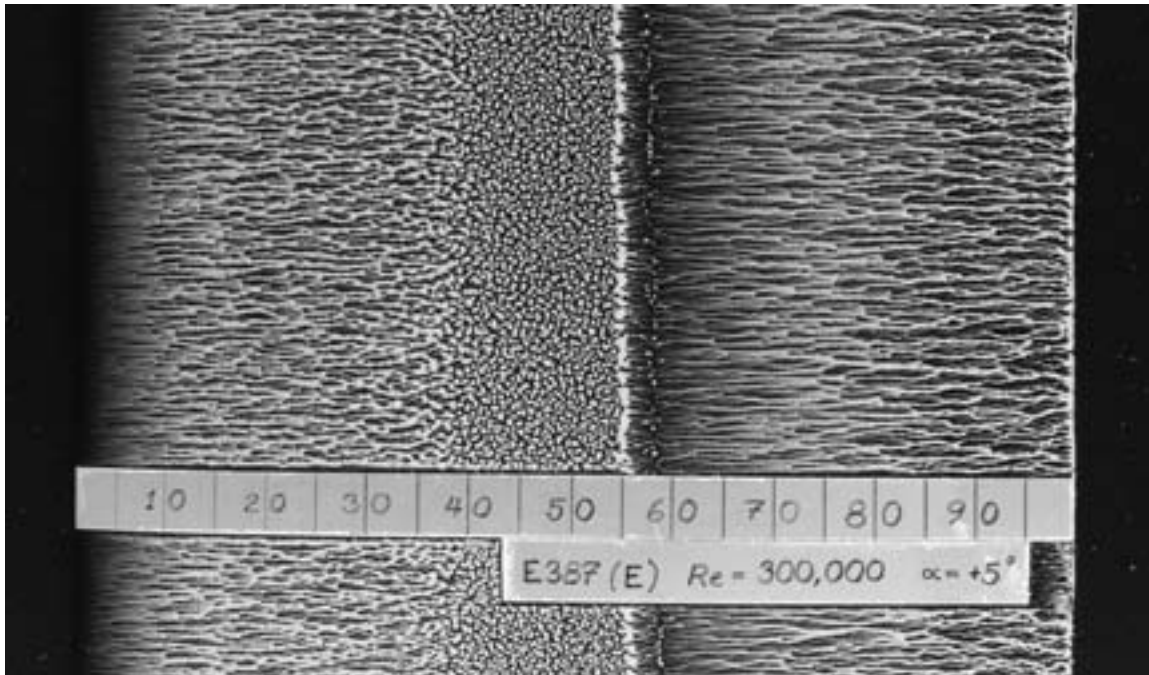


**Fig. 3.1** Representative upper-surface oil flow visualization on the E387 (E) airfoil.

verified (as no data could be found); however, the oil flow patterns observed are in general consistent with the predictions.

Several important flow features can be identified and related to the underlying skin friction and surface tension forces. In Fig. 3.1, laminar flow is seen to exist from the leading edge to approximately  $x/c = 40\%$ . The oil streaks are characteristically smooth in this region until laminar separation, which has been identified in Fig. 3.2 as the point where  $C_f = 0$ . (Note again that the flow shown in Fig. 3.2 is conceptual, and it is not intended to match Fig. 3.1 in detail.) Downstream of the point of laminar separation, the original airbrushed “orange-peel” texture that existed before running the tunnel test still exists, indicating that the flow is stagnant in this region. This stagnant flow is consistent with the known behavior of the interior leading-edge region of a laminar separation bubble. As sketched, the magnitude of the  $C_f$  in this region is quite small because of the low flow speed and negative in sign because of reverse flow at the surface.

In the presence of a laminar separation bubble, transition takes place in the free shear layer above the airfoil surface. Downstream of this point, reattachment occurs in a process that is known to be unsteady as vortices are periodically generated and impinge on the airfoil surface.<sup>24,25</sup> These unsteady vortices colliding with the surface lead to a relatively high shear stress that tends to scour away the oil at the mean reattachment point, pushing the oil upstream or downstream in a random walk of sorts. As seen in Fig. 3.2, the reattachment line is less distinct because the bulk of the

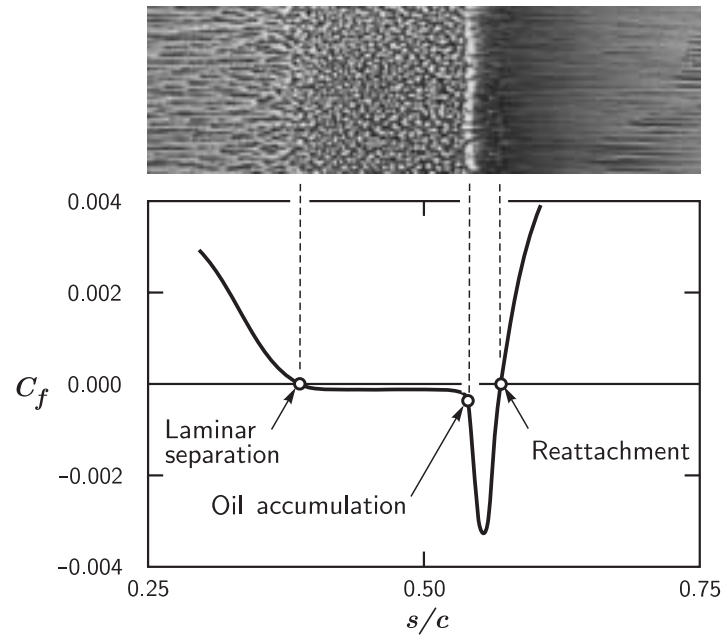


**Fig. 3.2** Conceptual illustration of the relationship between the surface oil flow features and skin friction distribution in the region of a laminar separation bubble.

oil has been pushed away, revealing the underlying black airfoil surface. In Fig. 3.1, the tunnel run time was long enough that the reattachment line at  $x/c = 58\%$  is even harder to see. In the original high-resolution color photographs that were archived, this feature is clear and easily quantifiable.

Downstream of reattachment, the boundary layer is, of course, turbulent. The high skin friction in this area relative to the laminar boundary layer tends to clear away more oil, again making the black surface downstream more visible than it was upstream, where it was laminar.

The remaining feature of the flow is a line where the oil tends to pool, termed here the “oil accumulation line.” This intrinsic feature of the oil flow has no direct connection to laminar flow, reverse flow in the bubble, or the ensuing turbulent flow downstream. However, it does indicate a relatively important feature of the flow, if the myriad predictions are to be believed, in the vicinity of reattachment. The negative  $C_f$  spike shown in predictions and sketched conceptually in Fig. 3.2 is most likely responsible for generating the oil accumulation line. Assuming that this is the case, the fluctuating high skin friction that is generated over the unsteady reattachment zone will tend to push the oil upstream ahead of the mean reattachment point. At some location on the airfoil, however, the oil moving upstream will experience a balance of forces between the rapidly weakening skin friction force (at the edge of the negative  $C_f$  spike) and the surface tension or oil adhesion that is retarding its motion. Where these two forces balance, the oil accumulates into a line that becomes

the single most visible feature of the oil flow. Moreover, there is speculation that this flow feature is further distinguished by sometimes being mislabeled as “reattachment” as will be discussed below.

The upper-surface oil flow features, as just described, were obtained over a range of angles of attack for Reynolds numbers of 200,000 and 300,000. These results are shown in Fig. 3.3 and compared with the NASA Langley LTPT data. Over the low drag range from  $-2$  deg to  $7$  deg, the agreement in the laminar separation line between the data sets is mostly within 1–2% of  $x/c$ , which is very near the uncertainty of the method. As previously discussed, the next feature to appear is the oil accumulation line. The UIUC oil accumulation line agrees fairly well with the “reattachment” line identified in the NASA experiment. It is believed, however, on the basis of the previous reasoning, that this label in the original reference<sup>17</sup> is a misnomer. Had the UIUC tests been performed for a longer time, the reattachment zone would be scoured clean with no distinguishing feature, leaving only the oil accumulation line to be labeled as the “reattachment line,” since one must exist. Hence, here and in prior UIUC work<sup>5</sup> there is speculation that such a scenario took place in the NASA study, i.e., the oil-accumulation line was misinterpreted as the reattachment line.

Given this working assumption, the two results again are in good agreement. It must be stated, however, that the oil accumulation line might change slightly from one facility to the next, because again it is dictated by a force balance that depends on the skin friction forces of the boundary layer relative to the adhesion forces of the particular oil used. The predictions, however, show that the  $C_f$  “well” has a sharp upstream edge, and that is most likely where the oil accumulates regardless of the surface tension characteristics. Thus differences in the oil accumulation line owing to differences in the oil are believed to be small. The good comparisons between UIUC and Langley tend to support this assumption.

Moving further downstream, the UIUC reattachment data are plotted, but unfortunately no direct comparison can be made because reattachment proper was not reported in the NASA study. However, close inspection of the data suggests that at a Reynolds of 300,000 and between  $5$  deg and  $7$  deg, the LTPT line merges with the UIUC reattachment line. Perhaps in this case, the measurements at Langley were indeed the reattachment points.

It is worth mentioning that surface oil flow data were not taken at a Reynolds number of 100,000 during these tests because the run times would be in excess of 2 hrs per data point. Over this period of time, the droplets of oil spray that initially give rise to the “orange peel” texture tend to smooth out. This reduces the contrast between the different regions of the flow, thereby making it difficult to ascertain the distinguishing features of the flow.

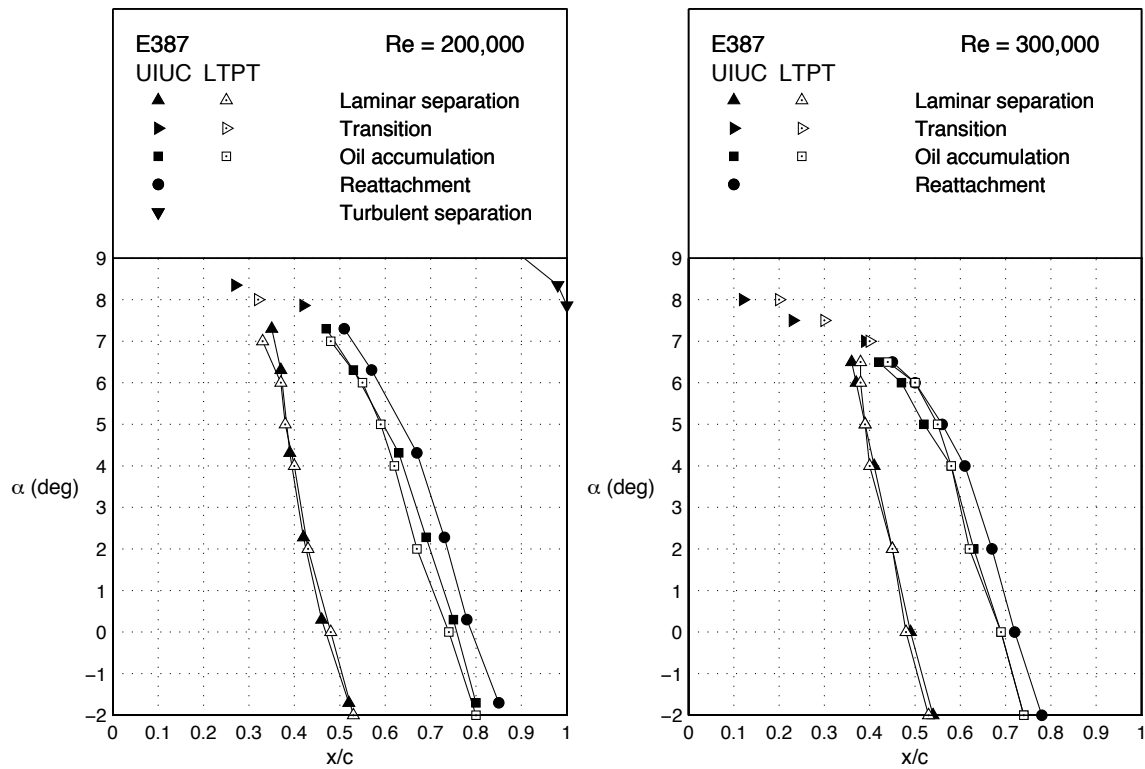


**Fig. 3.3** Comparison of major E387 (E) upper-surface flow features between UIUC and LTPT for  $Re = 200,000$  and  $300,000$ .

The conclusion to be drawn from this comparison of the oil flow visualization results is that the two facilities produce airfoil flows that are in close agreement. Moreover, assuming that the arguments regarding the oil accumulation line are correct, then the agreement is excellent and within the uncertainty of the measurements.

## 3.2 Lift and Moment Data

Lift and moment data comparisons between the UIUC and LTPT data are shown in Fig. 3.4. Discrepancies can be seen for a Reynolds number of  $100,000$  as well as in the stalled regime. For  $Re = 100,000$ , differences are most likely attributable to measurement accuracy. In stall for  $\alpha > 12$  deg, taking the Langley data as the benchmark, the UIUC data differ most likely as result of three-dimensional end effects. Nevertheless, the results show good agreement over the unstalled range, and this agreement improves with higher Reynolds number.

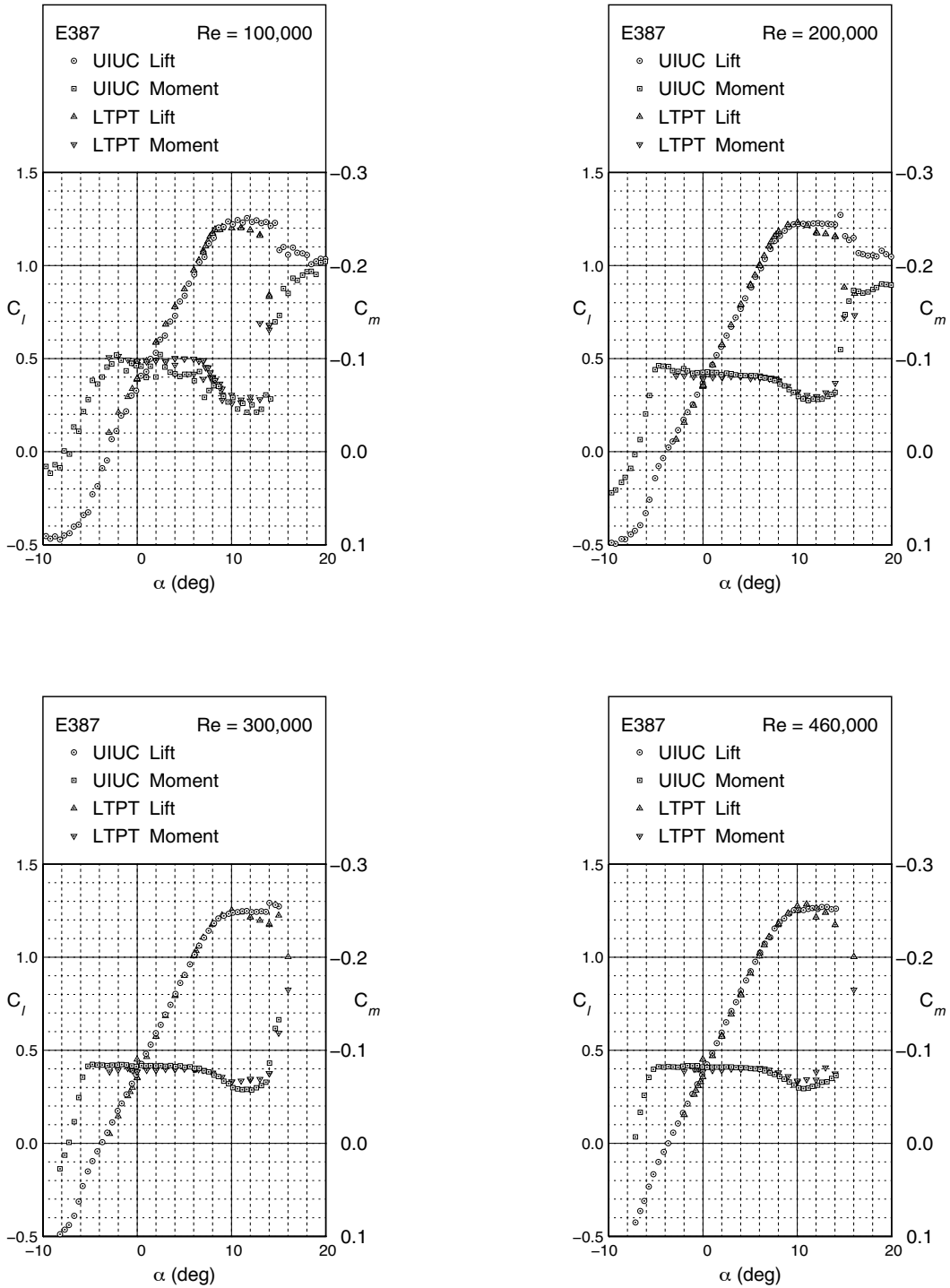


**Fig. 3.4** Comparison between UIUC and LTPT E387 lift and moment coefficient data for  $Re = 100,000, 200,000, 300,000,$  and  $460,000$ .

### 3.3 Drag Polars

Figure 3.5 shows a comparison between UIUC and NASA LTPT drag data for the Reynolds numbers of 100,000, 200,000, 300,000, and 460,000. To begin this discussion, data at a Reynolds number of 200,000 and 300,000 are considered. For these cases, the oil flow results were in close agreement as well as the lift data, which, taken together, suggest that the drag data should likewise be in good agreement. Indeed, for  $Re = 200,000$ , there is close agreement. However, for  $Re = 300,000$ , the agreement is not as good. As for the other cases, for a  $Re = 460,000$ , the agreement improves, while for  $Re = 100,000$ , there is less agreement. When these cases are studied in more detail, it is seen that the edges of the drag polar are in quite close agreement for each case, with the  $Re = 100,000$  perhaps being the exception.

There can be many reasons for the observed discrepancies, not the least of which is the fact that at low Reynolds numbers the drag data, when determined from downstream wake measurements, vary along the span—the further downstream, the more variation. The current measurements were taken 1.25 chord lengths downstream of the trailing edge, while those in the NASA study were taken 1.5 chord lengths downstream. Because of this variation in spanwise drag, ideally many wake profile measurements should be taken along the span and the resulting drag coefficients summed and averaged. This approach of performing multiple wake surveys was taken in the current study (as mentioned previously, eight wake surveys were taken), but in the NASA study, wake rake data were taken at only one station for the purpose of acquiring the full polar data reported. However, in the NASA study, some limited spanwise data were taken at angles of attack of 0 and 5 deg. For these cases, the degree of spanwise variation observed is quite similar to the current data shown in Fig. 2.15. Consequently, the discrepancies in part must be related to the variation in drag along the span. In the NASA study, had data been taken at many stations for all conditions, it is likely that better agreement would be observed.

For the Reynolds number of 100,000, which was not critical to the current investigation, the discrepancies are larger. This result cannot be attributed solely to spanwise drag variation. Figure 2.15 shows that at a  $C_l = 0.7$  and  $Re = 100,000$ , the eight  $C_d$  data points obtained from the eight wake measurements fall nearly one on top of the other. Therefore, the spanwise variation in drag is small on a percentage basis, and a similar variation in  $C_d$  was seen in the NASA data. Consequently, for  $Re = 100,000$ , the cause for the bulk of the difference in the drag measurements must be something other than spanwise drag variation.

When sources of error were being considered to explain the discrepancies, several factors were ruled out in light of the excellent agreement in surface oil flow visualization as well as lift and moment data. Of those that remained, no sources of uncertainty in the current data lingered after investigation. Thus, the state of the agreement for the Reynolds number of 100,000 remains unexplained. It is recognized that the source of this discrepancy might relate to some of the discrepancies for the



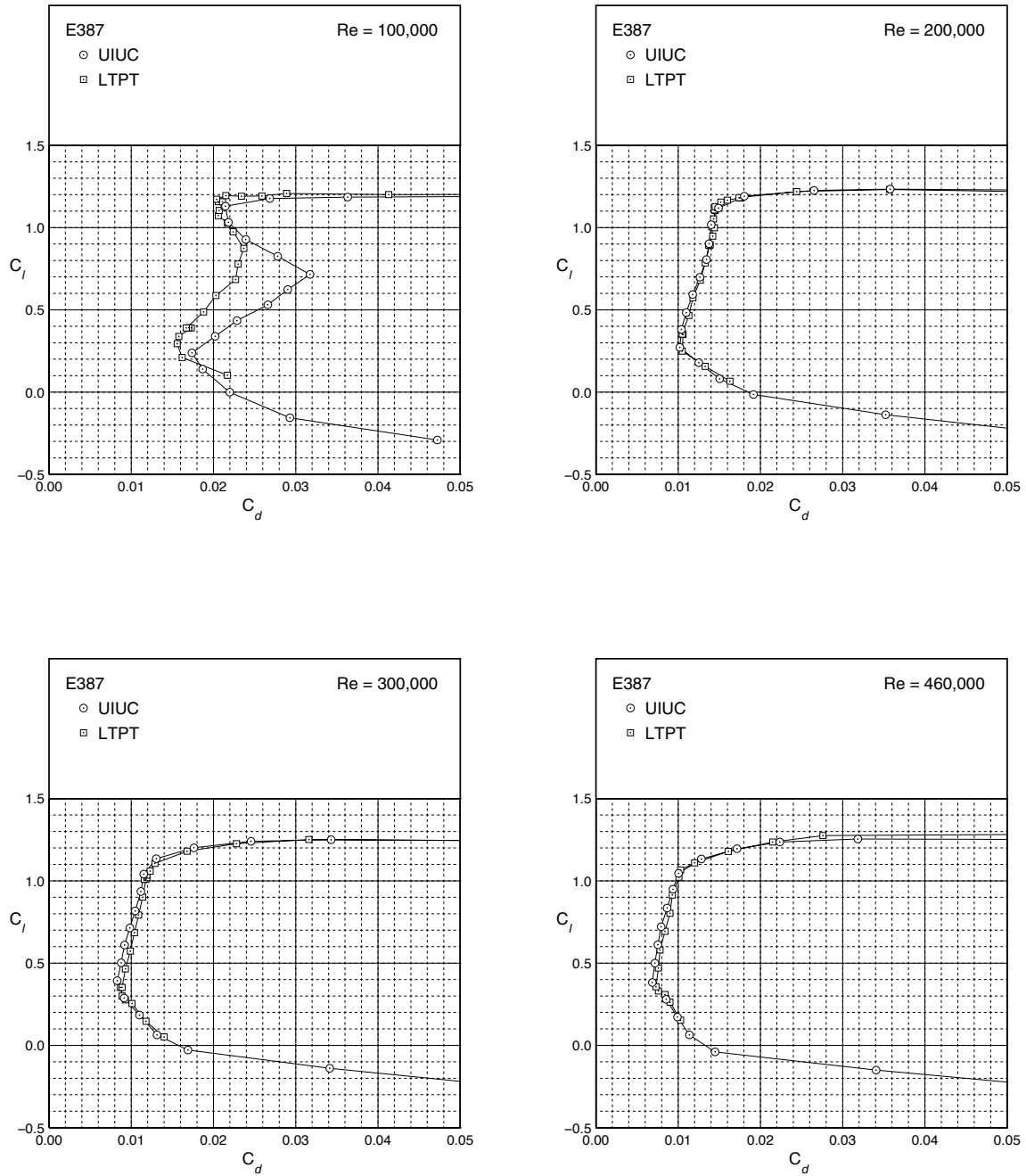


**Fig. 3.5** Comparison between UIUC and LTPT E387 drag coefficient data for  $Re = 100,000, 200,000, 300,000,$  and  $460,000$ .

higher Reynolds number cases, as well. Nevertheless, the agreement overall is good, especially in light of past historical comparisons of low Reynolds number airfoil data, which vary widely.<sup>2,3</sup>

### 3.4 Summary

Regarding the accuracy of the current data overall, this chapter has made several important points that should instill confidence in the data presented in the following chapters. First, it was shown that surface oil flow data obtained on the E387 airfoil exhibited excellent agreement with NASA LTPT data for  $Re = 200,000$  and  $300,000$ . Second, current lift data were shown to have good agreement with LTPT data for all Reynolds numbers up to stall, after which three-dimensional end effects and unsteady aerodynamics produced slight discrepancies. Third, the pitching moment data were shown to agree well with LTPT data over a broad range of angles of attack. Lastly, in support of the three previous conclusions, the drag data showed good agreement, with some discrepancies yet to be fully explained.



---

## Chapter 4

# Summary of Airfoil Data

---

In this chapter the airfoils are discussed, and the corresponding performance data are given in Chapter 5, which follows. Table 4.1 lists each airfoil along with its thickness, camber, and representative quarter chord pitching moment ( $C_{m,c/4}$ ). The  $C_{m,c/4}$  values correspond to the current measurements for the clean airfoils at a Reynolds number of 350,000 and angle of attack near zero. Table 4.2 lists the model construction method (surface finish), model accuracy, and model builder. As an aid to the reader, the following comments apply:

- The suffixes ‘(B)’, ‘(C)’, and ‘(E)’ refer to multiple versions of those particular airfoils. For instance, the E387 (E) model is the 5th model in the UIUC collection.
- When characterizing surface finish qualities in Table 4.2, the term “smooth” refers to a fiberglass surface applied via the vacuum bag method.
- The inviscid velocity distributions shown for the true airfoils in Chapter 5 were determined using the Eppler code.<sup>26,27</sup> With experience, these velocity distributions, when viewed in light of the experimental results, can be used to obtain additional insight into the airfoil performance characteristics.
- The figures in Chapter 5 list the nominal Reynolds numbers. Actual Reynolds numbers are listed in Appendix B.
- As previously stated, all drag coefficients were obtained by averaging spanwise drag coefficients from eight wake surveys spaced 1.5 in. (3.81 cm) apart approximately 1.25 chord lengths downstream of the model trailing edge. Although these spanwise coefficients are not documented in this volume, they are available upon request.

**Table 4.1: Characteristics of the Airfoils Tested for Wind Turbines**

| Airfoils for:       | Airfoil       | Thickness (%) | Camber (%) | $C_{m,c/4}$ |
|---------------------|---------------|---------------|------------|-------------|
| Small Wind Turbines | E387 (E)      | 9.07          | 3.78       | -0.083      |
|                     | FX 63-137 (C) | 13.66         | 5.79       | -0.202      |
|                     | S822 (B)      | 16.00         | 1.89       | -0.068      |
|                     | S834          | 15.00         | 1.63       | -0.075      |
|                     | SD2030 (B)    | 8.56          | 2.23       | -0.075      |
|                     | SH3055        | 16.50         | 6.42       | -0.246      |

**Table 4.2: Wind Tunnel Model Characteristics**

| Airfoil       | Surface Finish | Avg. Diff.            | Builder  |
|---------------|----------------|-----------------------|----------|
| E387 (E)      | smooth         | 0.0091 in. (0.231 mm) | Y. Tinel |
| FX 63-137 (C) | smooth         | 0.0031 in. (0.079 mm) | Y. Tinel |
| S822 (B)      | smooth         | 0.0074 in. (0.188 mm) | Y. Tinel |
| S834          | smooth         | 0.0056 in. (0.142 mm) | Y. Tinel |
| SD2030 (B)    | smooth         | 0.0060 in. (0.152 mm) | Y. Tinel |
| SH3055        | smooth         | 0.0037 in. (0.094 mm) | Y. Tinel |

- For the lift curves, increasing and decreasing angles of attack are denoted by solid triangles and open circles, respectively.
- For the moment curves, increasing and decreasing angles of attack are denoted by inverted solid triangles and open rectangles, respectively. As has become convention when plotting airfoil pitching-moment data, positive values of  $C_{m,c/4}$  are at the bottom of the plot (i.e., the  $C_{m,c/4}$  axis is inverted).
- For some of the data, the lift curves cover a wider angle of attack range than the moment curves. In such cases, the data are a composite of two separate runs. First, lift and moment data were taken up to a point where stall flutter was about to occur. Beyond this point, a more-rigid lift carriage without moment measuring capability was used to obtain lift data into the unsteady stalled region. In contrast, when the lift and moment data cover the same range, it is an indication that the stall was a relatively steady process. (Note that in the tabulated data in Appendix B, data taken with the new lift carriage list “N/A” for the moment.)
- The moment data presented in Table 4.1 are representative values for the typical operating point of the airfoil. As observed in the experimental data, many airfoils exhibit significant changes in  $C_{m,c/4}$  as both angle of attack and Reynolds number change. Because of these changes, the values listed in Table 4.1 should be used only for comparative purposes.
- For ease of comparison, the symbols used for the various Reynolds numbers in the drag polars are consistent with those used in past volumes.<sup>2-5</sup>
- Finally, Table 4.3 includes a drawing of the boundary-layer trip used in this study. It is denoted as “zigzag trip type F” because it is the 6th different zigzag trip geometry tested at UIUC. The locations of the trip along the airfoil chord are drawn together with the airfoil geometries in Chapter 5.

In the remainder of this chapter, the performance characteristics of each of the airfoils are discussed in detail. Rather than organizing this discussion by commenting on broad categories of various effects, which would lead to much jumping around in viewing the related figures, the airfoils are discussed in the order of their appearance in Chapter 5. In so doing, a repertoire of performance characteristics will be introduced

**Table 4.3: Three-Dimensional Zigzag Trip Geometry**

| Trip Name             | Airfoils  | Trip Geometry | Trip Height                      |
|-----------------------|---|---------------|----------------------------------|
| zigzag trip<br>type F | E387 (E)<br>FX 63-137 (C)<br>S822 (B)<br>S834<br>SD2030 (B)<br>SH3055 |               | 0.013 in. (0.33 mm)<br>0.11% $c$ |

Trip geometry dimensions in inches.

and discussed in turn, along with references to past observations.

It should also be stated from the outset that each airfoil was designed with unique constraints and desired performance characteristics in mind. Consequently, the airfoils collectively represent a broad range of performance characteristics and geometric properties. Hence, to compare directly the performance of one airfoil to the next and declare one airfoil better than another would be misleading. Therefore, the focus will be on highlighting interesting and important performance characteristics while leaving design decisions and the establishment of various figures of merit to the wind turbine blade designer, whose task goes beyond the scope of topics discussed in this report.

**E387.** The E387 airfoil was originally designed in the early 1960s by Richard Eppler for model sailplanes; it was quickly successful and is still used. Beyond this, it has taken on the additional role of becoming a benchmark section used to compare low-Reynolds-number airfoil measurements from one wind tunnel facility with those of another. In fact, the E387 airfoil is likely the most widely tested low-Reynolds-number section, having been tested at Delft in the Netherlands, Stuttgart, Princeton, NASA Langley and UIUC both before and during the current tests. Because the comparison between the UIUC data and that of NASA Langley has been discussed already, the focus in this chapter is on elucidating the low Reynolds number performance characteristics.

Figures 5.3–5.6 show the drag polars and the lift and drag characteristics at Reynolds numbers of 100,000, 150,000, 200,000, 300,000, 460,000, and 500,000. [The  $Re = 460,000$  case was added for comparison with Langley (see Chapter 3).] For the lowest Reynolds number of 100,000, the most prominent manifestation of a laminar separation bubble is observed in the drag polar. Between the limits of the low drag range, there is an increase in drag associated principally with a laminar separation bubble. In the vicinity of corners of the low drag range, the laminar separation bubble is short or nonexistent, in which case the drag is not as high. However, as the angle of attack is increased from the lower corner, the adverse pressure gradient on the upper surface becomes stronger; as a result, the bubble drag grows until the drag is a maximum near a lift coefficient of 0.7 ( $\alpha \approx 3$  deg). Beyond this point, the size of the bubble begins to decrease (see Fig. 21 of Ref. 17), which results in lower drag until the

upper corner of the polar is reached. There, a transition takes place on the surface without a drag-producing bubble being present. As the Reynolds number increases, the advantages of higher Reynolds number as well as a reduction in the length of the bubble (due to an earlier transition, see Fig. 3.3) leads to correspondingly lower drag.

Other things to note for the untripped airfoil include the following. In the moment data for  $Re = 100,000$ , there is some scatter. This is an artifact resulting from stiction in the moment measurement apparatus, not some intrinsic unsteady flow effects. However, it should be mentioned that at an angle of attack of 14 deg, this airfoil exhibited considerable fluctuations in the lift force measurement due to unsteady stalled flow. Corresponding to this condition for this airfoil, there occur unusual peaks in the lift curves for  $Re = 200,000$  and above at  $\alpha \approx 14$  deg, as seen in the plots. This type of unsteadiness has been previously observed and discussed in Ref. 28. In essence, the unsteady fluctuations result from a change in the upper surface (suction side) flow state from a short leading edge bubble to a longer bubble, back to a short bubble and so on. It is this destructive unsteadiness that was referred to in Chapter 2, and it has in some cases limited the angle of attack range of the lift runs (e.g., see data for  $Re = 460,000$  and  $500,000$ ).

For this airfoil and all of the others, a zigzag boundary layer trip was added on the top and bottom surfaces near the leading edge to simulate the effects of roughness caused by debris and erosion that occurs on wind turbine blades over time. In general, the main effect of the trip is to promote transition shortly downstream of the trip. If a bubble is present in the “clean” case (i.e., the case without a boundary layer trip), the trip has the effect of shortening the laminar separation bubble should it be present. When there is no bubble, transition is forced to occur sooner than it otherwise would.

In terms of performance, the beneficial effect of shortening the bubble and hence lowering the drag is to some degree offset by the increased length of turbulent flow. The net effect can be either beneficial when the bubble is otherwise large or a hindrance when the bubble is small or not present at all. As a result, the performance with boundary layer trips used at low Reynolds numbers is often complex.

For the E387, the effects of the trip are clearly seen in the drag polar shown in Fig. 5.5. For  $Re = 100,000$ , the drag is reduced overall as a result of the shortened laminar separation bubble. In the middle of the polar, the kink where the drag begins to reduce with increasing angle of attack occurs at a lower lift coefficient ( $C_l \approx 0.55$ ) because of the transition promoted by the boundary layer trip and because of the pressure gradient effect, which is beneficial in both the clean and tripped cases.

The effects of the trip are also apparent in the lift curves that are shown with the polars (see Figs. 5.3 and 5.5). For the clean case at  $Re = 100,000$ , the lift curve is offset slightly below the curves for the higher Reynolds numbers. This offset is caused by a decambering effect that results from the added displacement thickness produced by the large bubble. When the bubble is reduced in size by using a trip,

this displacement thickness effect is smaller, and the lift curve at  $Re = 100,000$  nearly coincides with the higher Reynolds number cases that have smaller bubbles.

For  $Re = 200,000$  with the boundary layer trip, only at a lift coefficient of  $\approx 0.47$  is the drag lower than the clean case. Thus, for this condition, the trade-off between having lower bubble drag and higher turbulent skin friction drag leads to lower net drag, while for all other points the added turbulent skin friction drag outweighs the reduction in the bubble drag, resulting in higher drag with the trip. This trade-off leading to higher drag is particularly true for the high-Reynolds-number cases (see Fig. 5.5).

Finally, it is interesting to note that there is a negligible drop in the maximum lift coefficient due to roughness effects for this case. This results from transition occurring very near the leading edge before reaching the airfoil maximum lift coefficient. Thus, at maximum lift, the flow on the upper surface behaves the same for the most part, whether or not there is a trip; hence, the stall performance has little dependence on the presence of the trip. This general understanding, which is further discussed in Ref. 29, can be amplified if at stall there exists a leading edge separation bubble. In such a case, the boundary layer trip can be completely or partially immersed in the recirculating zone of the bubble. When this occurs, the airfoil stall can be quite insensitive to a discrete roughness element such as the type tested in this study.

**FX 63-137.** This airfoil was designed by F.X. Wortmann for the Liver Puffin human-powered aircraft. It has since been used for many low-Reynolds-number applications because of its high-lift, soft-stall characteristics in addition to its overall good performance. In particular, in the small wind turbine arena, it has been used by Aeromag (Lakota wind turbine) and Worldpower Technologies/Southwest Windpower (H-40 and H-80 wind turbines).

The original coordinates for this section as well as several other early Wortmann sections<sup>30</sup> are not analytically smooth, presumably because of a small numerical error in the design method. As described in Ref. 31, the original coordinates were smoothed for use in computations, and those coordinates have been used in this study and are tabulated in Appendix A.

As seen in the inviscid velocity distributions (Fig. 5.8) and deduced from the high camber, this airfoil should be expected to produce considerably more lift than the E387. Indeed, as shown in Fig. 5.9, the FX 63-137 produces a  $C_{l,max}$  of approximately 1.7. However, for  $Re = 100,000$ , the airfoil suffers the consequences of a large laminar separation bubble. In fact, at the lower angles of attack, it is likely that the bubble does not close on the airfoil, but instead extends into the wake. Two observations support this assumption. First, the lift curve at  $Re = 100,000$  for low angles of attack falls considerably below the curves for higher Reynolds numbers. Second, for the same low-Reynolds-number condition, the drag is quite high. At an angle of attack of approximately 4 deg, the situation improves as the bubble begins to attach to the airfoil. The lift increases and the drag is correspondingly reduced.



This airfoil, along with the S822 and S834 airfoils, was tested at an intermediate Reynolds number of 150,000 to obtain more resolution in the low Reynolds number range, where the drag changes dramatically. As seen in Fig. 5.9, a large drag reduction is observed for the  $Re = 150,000$  case. Concurrent with this, the large offset in the lift curve is absent. Both of these observations indicate a reduction in the size of the laminar separation bubble vs. the  $Re = 100,000$  case. As would be expected, performance continues to improve at higher Reynolds numbers.

When boundary layer trips are applied, the performance follows trends similar to those described for the E387. First, for  $Re = 100,000$ , the effects of the bubble are mitigated as seen by the slight rise in the lift curve and by the reduction in drag. For the higher Reynolds numbers, the polars tend to collapse onto an envelope, which indicates that the flow on the upper surface is similar indicating early transition and the absence of a laminar separation bubble. For points that fall on either side of this envelope, a bubble still exists.

In the polars, there is an interesting trend reversal where the drag first decreases and then increases as the Reynolds number is increased for a fixed angle of attack. One instance of this is seen for an angle of attack of 4 deg, which corresponds to a lift coefficient of approximately 0.7. This same type of behavior was seen for the E387 at an angle of attack of 1 deg ( $C_l \approx 0.47$ ). As previously described, there is first a reduction in drag due to a shortening of the bubble and then a rise in drag due to the added turbulent flow as the Reynolds number is increased. This same behavior can be identified in the performance of all of the tripped airfoil polars.

Other items to note include the following. Unlike the E387 airfoil, the maximum lift performance of the FX 63-137 suffers from the addition of simulated roughness. Overall, the drop in  $C_{l,max}$  is 0.2. Another difference is that, while the E387 had a highly unsteady stall leading to a sharp break, the FX 63-137 exhibited a soft stall with little unsteadiness. Finally, the pitching moment curves, unlike those of the E387, do not show nearly constant  $C_{m,c/4}$  over the low drag range. Instead, the nose-down moment is gradually reduced with increasing angle of attack. This behavior is largely produced by a decambering effect resulting from a rapid growth in the displacement thickness at the trailing edge with increasing angle of attack.

**S822 and S834.** As described in Ref. 31, the S822 and S834 were both designed for small wind turbines and are proprietary to NREL.<sup>32–35</sup> The S822 airfoil has been used on the AOC/Windlite small wind turbine. Briefly, the S822 and S834 were designed for the outer blade span of rotors having diameters in the 3–10 meter and 1–3 meter range, respectively. As reported elsewhere,<sup>35</sup> the newer S834 was designed for low noise, which was not a consideration in the design of the S822 section.

The performance of these airfoils is shown in Figs. 5.15–5.24. Many of the general characteristics previously described are exhibited by these two airfoils. Differences in the details are of course dictated by the associated design goals, which collectively lead to the performance discussed below.

For both airfoils, an often characteristic high-drag knee in the drag polar due to the presence of a laminar separation at the lower Reynolds numbers is observed. The associated nonlinearities (offsets) in the lift curves are also seen, except for these airfoils, as compared with the Wortmann section, the offsets occur for  $Re = 100,000$  and  $150,000$  as well as  $200,000$  to a slight extent. This behavior is also reflected in the drag polars where the high-drag knee is more exaggerated than that for the FX 63-137.

Overlaying the S822 and FX 63-137 polars shows that the S822 achieves its highest lift-to-drag ratio at the upper corner where it nearly coincides with the lower corner of the FX 63-137 for  $Re = 500,000$ . Note the different scales in the  $C_l$  axis. This is one illustration of the considerable differences between these airfoils and the Wortmann section.

Adding the zigzag boundary layer trips to both airfoils yields lower drag at the lower Reynolds numbers, as would be expected from the past cases examined. Also, as would be expected, the nonlinearities seen in the lift curves are mitigated somewhat by the boundary layer trips. However, the boundary layer trip on the upper surface is not large enough to completely eliminate the bubble for  $Re = 100,000$ , where, over a 2-deg range in the middle of the polar, the lift increases nonlinearly ( $\Delta C_l \approx 0.5$ ) for both airfoils. As seen in Figs. 5.18 and 5.24, some peculiar remnant of this exists for  $Re = 150,000$  at  $\alpha \approx 5$  deg.

The S834, being designed for smaller rotors, was designed for lower Reynolds numbers. This trend is apparent in the drag polars, where the S834 is observed to have better performance than the S822 at low Reynolds numbers. The differences are mostly slight, as one might expect from the similarities in the geometries and pressure distributions.

For both airfoils, unsteadiness at stall prevented taking high-angle-of-attack data for  $Re = 500,000$ . The degree of the unsteadiness during the tests was observed to be somewhat less than that for the E387.

**SD2030.** This Selig/Donovan airfoil, presented in Ref. 2, was originally designed for model sailplanes. It has since been used on the Southwest Windpower Air 403 and Air X small wind turbines. Figures 5.27–5.30 show its performance characteristics.

As compared with the other airfoils discussed, this airfoil has quite low drag at the expense of a narrower drag polar. A high-drag knee is present for  $Re = 100,000$ ; however, the peak drag at the kink is much lower than that seen for the other airfoils tested. This low drag is achieved by having a long transition ramp, or “bubble ramp,”<sup>2</sup> that leads to a thin laminar separation bubble. The causes for other general effects seen in the figures have been previously explained.

Of the six airfoils tested, this airfoil displayed the most unsteadiness in stall, and this limited the angle-of-attack range for the  $Re = 500,000$  case.

**SH3055.** The Selig/Hanley airfoil, derived from prior SH/Bergey designs, is intended for a 7-meter diameter variable-speed wind turbine to be manufactured by Bergey Windpower, Co. For the lowest Reynolds number case ( $Re = 100,000$ ), there is a considerable drop in lift, in contrast to the higher Reynolds number cases. This drop and associated high drag is likely caused by a laminar separation bubble that does not reattach to the airfoil over the majority of the lift range. Moreover, at the lowest angles of attack tested, the lower surface of the airfoil appears to be stalled as well, which further decambers the section. For the higher Reynolds numbers, the performance improves, as seen in past examples. Boundary layer trips applied to the airfoil lead to improved performance for  $Re = 100,000$ , but at higher Reynolds numbers the performance is mostly handicapped, as observed in the other sections. Finally, for this airfoil, the stall behavior was quite gentle.

---

## Chapter 5

# Airfoil Profiles and Performance Plots

---

Chapter 5 presents the airfoil profiles and performance plots that were previously discussed in Chapter 4. For quick reference, the airfoil names are listed in the margins. As a matter of record, a table listing all the data sets, associated figures, figure page numbers, and run numbers is included on the following page.

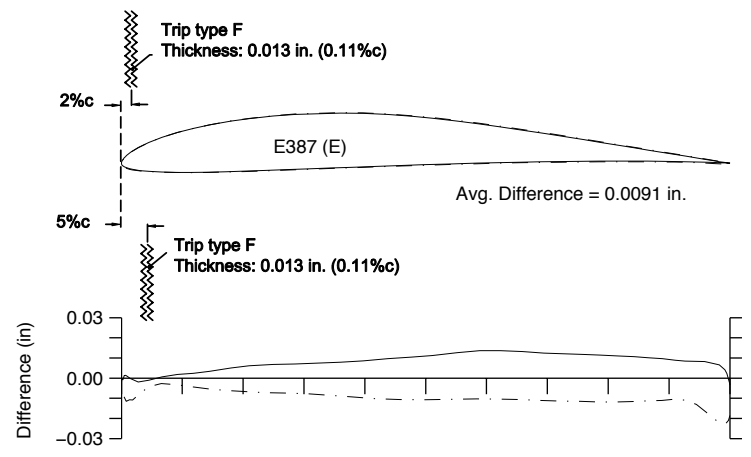
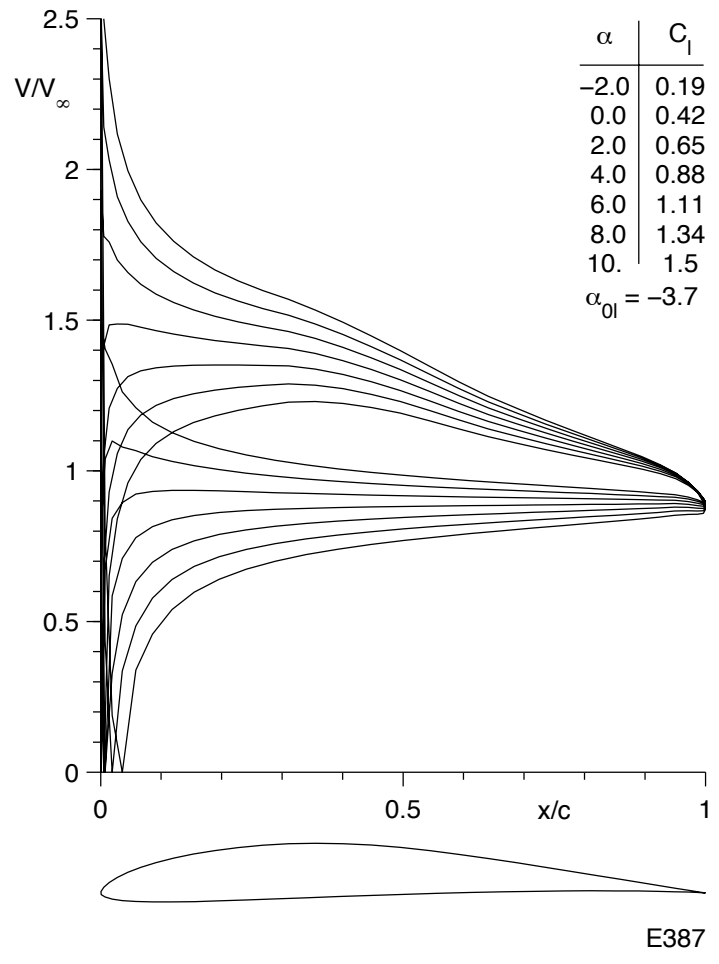
In several cases, two runs are listed for a given airfoil/Reynolds number combination. There can be two reasons for this. First, as previously mentioned, some airfoils exhibited significant unsteadiness in stall, and two different runs were required to cover a full angle-of-attack range. Second, for some drag runs, supplemental runs had to be performed to complete the drag polar.

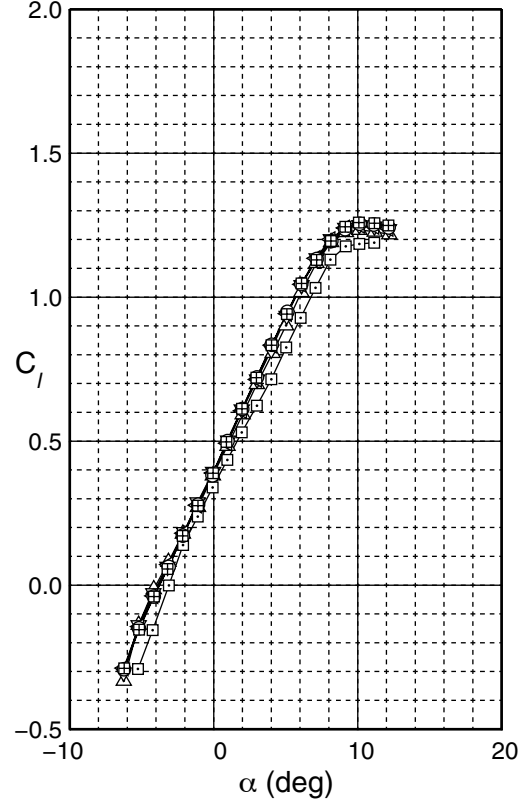
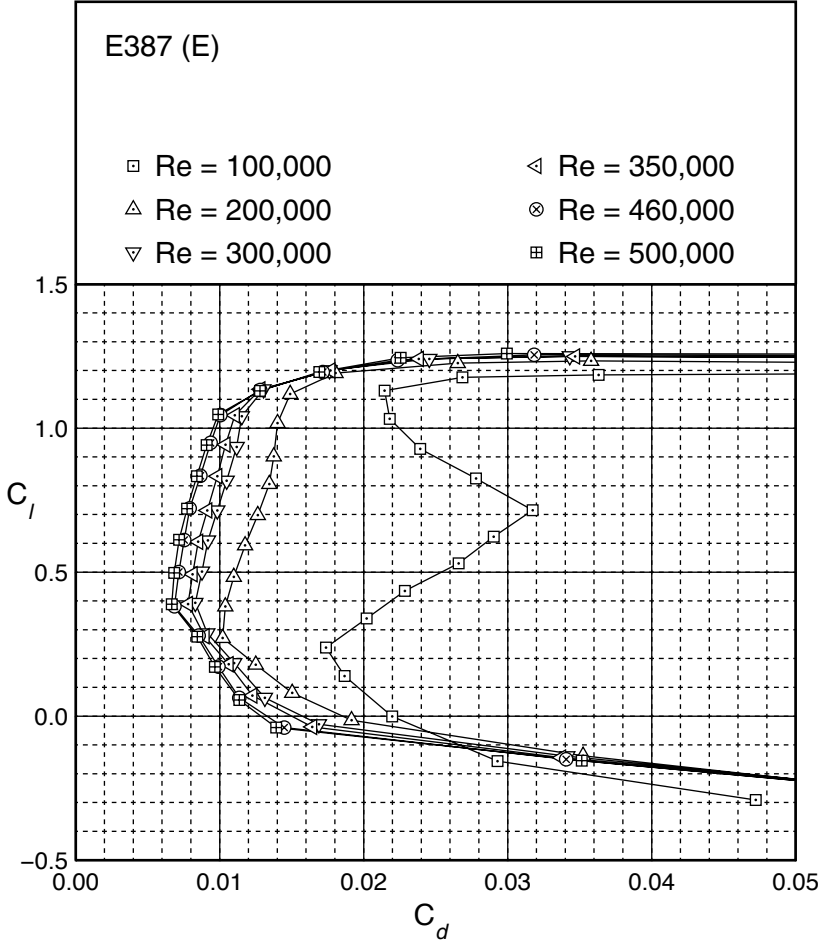
Table 5.1: Test Matrix and Run Number Index

| Model<br>(Builder)<br>Designer          | Configuration         | V-dist &<br>Profile |    | Drag Data |     |         |         | Lift & Moment Data |     |         |                 |         |
|---|-----------------------|---------------------|----|-----------|-----|---------|---------|--------------------|-----|---------|-----------------|---------|
|   |                       | Fig.                | p. | Fig.      | p.  | Re      | Run #   | Fig.               | p.  | Re      | Run #           |         |
| E387 (E)<br>(Y. Tinel)<br>Eppler        | clean                 | 5.1                 | 46 | 5.3       | 47  | 100,000 | BM05141 | 5.4                | 48  | 100,000 | BM05140         |         |
|   |                       | 5.2                 |    |           |     | 200,000 | BM04979 |                    |     | 200,000 | BM04978         |         |
|   | Zigzag trip<br>type F |                     |    |           | 5.5 | 51      | 100,000 | BM04989            | 5.6 | 52      | 100,000         | BM04988 |
|   |                       |                     |    |           |     |         | 200,000 | BM04991            |     |         | 200,000         | BM04990 |
| FX 63-137 (C)<br>(Y. Tinel)<br>Wortmann | clean                 | 5.7                 | 54 | 5.9       | 55  | 100,000 | BM04997 | 5.10               | 56  | 100,000 | BM04996         |         |
|   |                       | 5.8                 |    |           |     | 150,000 | BM04999 |                    |     | 150,000 | BM04998         |         |
| Zigzag trip<br>type F                   |                       |                     |    | 5.11      | 59  | 100,000 | BM05001 | 5.12               | 57  | 200,000 | BM05000         |         |
|   |                       |                     |    |           |     | 200,000 | BM05003 |                    |     | 200,000 | BM05002         |         |
| S822 (B)<br>(Y. Tinel)<br>Somers        | clean                 | 5.13                | 64 | 5.15      | 65  | 100,000 | BM05005 | 5.16               | 58  | 500,000 | BM05004         |         |
|   |                       | 5.14                |    |           |     | 100,000 | BM05007 |                    |     | 100,000 | BM05006         |         |
| Zigzag trip<br>type F                   |                       |                     |    | 5.11      | 59  | 150,000 | BM05009 | 5.12               | 60  | 150,000 | BM05008         |         |
|   |                       |                     |    |           |     | 200,000 | BM05011 |                    |     | 200,000 | BM05010         |         |
| S822 (B)<br>(Y. Tinel)<br>Somers        | clean                 | 5.13                | 64 | 5.15      | 65  | 200,000 | BM05013 | 5.16               | 61  | 200,000 | BM05010         |         |
|   |                       | 5.14                |    |           |     | 350,000 | BM05015 |                    |     | 350,000 | BM05012         |         |
| Zigzag trip<br>type F                   |                       |                     |    | 5.11      | 59  | 350,000 | BM05017 | 5.12               | 62  | 350,000 | BM05012         |         |
|   |                       |                     |    |           |     | 500,000 | BM05015 |                    |     | 500,000 | BM05014         |         |
| S822 (B)<br>(Y. Tinel)<br>Somers        | clean                 | 5.13                | 64 | 5.15      | 65  | 100,000 | BM05017 | 5.16               | 66  | 100,000 | BM05016         |         |
|   |                       | 5.14                |    |           |     | 150,000 | BM05019 |                    |     | 150,000 | BM05018         |         |
| Zigzag trip<br>type F                   |                       |                     |    | 5.17      | 69  | 100,000 | BM05021 | 5.18               | 67  | 200,000 | BM05020         |         |
|   |                       |                     |    |           |     | 200,000 | BM05023 |                    |     | 200,000 | BM05020         |         |
| S822 (B)<br>(Y. Tinel)<br>Somers        | clean                 | 5.13                | 64 | 5.15      | 65  | 350,000 | BM05025 | 5.16               | 68  | 350,000 | BM05022/BM05125 |         |
|   |                       | 5.14                |    |           |     | 500,000 | BM05025 |                    |     | 500,000 | BM05024         |         |
| Zigzag trip<br>type F                   |                       |                     |    | 5.17      | 69  | 100,000 | BM05027 | 5.18               | 70  | 100,000 | BM05026         |         |
|   |                       |                     |    |           |     | 150,000 | BM05029 |                    |     | 150,000 | BM05028         |         |
| S822 (B)<br>(Y. Tinel)<br>Somers        | clean                 | 5.13                | 64 | 5.15      | 65  | 200,000 | BM05031 | 5.18               | 71  | 200,000 | BM05030         |         |
|   |                       | 5.14                |    |           |     | 350,000 | BM05033 |                    |     | 350,000 | BM05032/BM05124 |         |
| Zigzag trip<br>type F                   |                       |                     |    | 5.17      | 69  | 350,000 | BM05033 | 5.18               | 72  | 350,000 | BM05032/BM05124 |         |
|   |                       |                     |    |           |     | 500,000 | BM05035 |                    |     | 500,000 | BM05034         |         |

|   |                       |              |    |      |     |   |  |      |                        |   |   |
|---|-----------------------|--------------|----|------|-----|---|--|------|------------------------|---|---|
| S834<br>(Y. Tinel)<br>Somers              | clean                 | 5.19<br>5.20 | 78 | 5.21 | 79  | 100,000<br>150,000<br>200,000<br>350,000<br>500,000 | BM05037<br>BM05039<br>BM05041<br>BM05043<br>BM05045              | 5.22 | 80<br><br>81<br><br>82 | 100,000<br>150,000<br>200,000<br>350,000<br>500,000 | BM05036<br>BM05038<br>BM05040<br>BM05042/BM05129<br>BM05044/BM05130 |
|   | Zigzag trip<br>type F |              |    | 5.23 | 83  | 100,000<br>150,000<br>200,000<br>350,000<br>500,000 | BM05047<br>BM05049<br>BM05051<br>BM05053<br>BM05055              | 5.24 | 84<br><br>85<br><br>86 | 100,000<br>150,000<br>200,000<br>350,000<br>500,000 | BM05046<br>BM05048<br>BM05050<br>BM05052/BM05128<br>BM05054/BM05127 |
| SD2030 (B)<br>(Y. Tinel)<br>Selig/Donovan | clean                 | 5.25<br>5.26 | 88 | 5.27 | 89  | 100,000<br>200,000<br>350,000<br>500,000            | BM05077<br>BM05079/BM05133<br>BM05081/BM05134<br>BM05083/BM05135 | 5.28 | 90<br><br>91           | 100,000<br>200,000<br>350,000<br>500,000            | BM05094<br>BM05078<br>BM05080/BM05132<br>BM05082                    |
|   | Zigzag trip<br>type F |              |    | 5.29 | 92  | 100,000<br>200,000<br>350,000<br>500,000            | BM05085<br>BM05087<br>BM05089<br>BM05091                         | 5.30 | 93<br><br>94           | 100,000<br>200,000<br>350,000<br>500,000            | BM05095<br>BM05086<br>BM05088/BM05131<br>BM05090                    |
| SH3055<br>(Y. Tinel)<br>Selig/Hanley      | clean                 | 5.31<br>5.32 | 96 | 5.33 | 97  | 100,000<br>200,000<br>350,000<br>500,000            | BM05057<br>BM05059<br>BM05061<br>BM05063                         | 5.34 | 98<br><br>99           | 100,000<br>200,000<br>350,000<br>500,000            | BM05056<br>BM05058<br>BM05060<br>BM05062                            |
|   | Zigzag trip<br>type F |              |    | 5.35 | 100 | 100,000<br>200,000<br>350,000<br>500,000            | BM05065<br>BM05067<br>BM05069<br>BM05071                         | 5.36 | 101<br><br>102         | 100,000<br>200,000<br>350,000<br>500,000            | BM05117<br>BM05066<br>BM05068<br>BM05070                            |

E387 (E)





E387 (E)



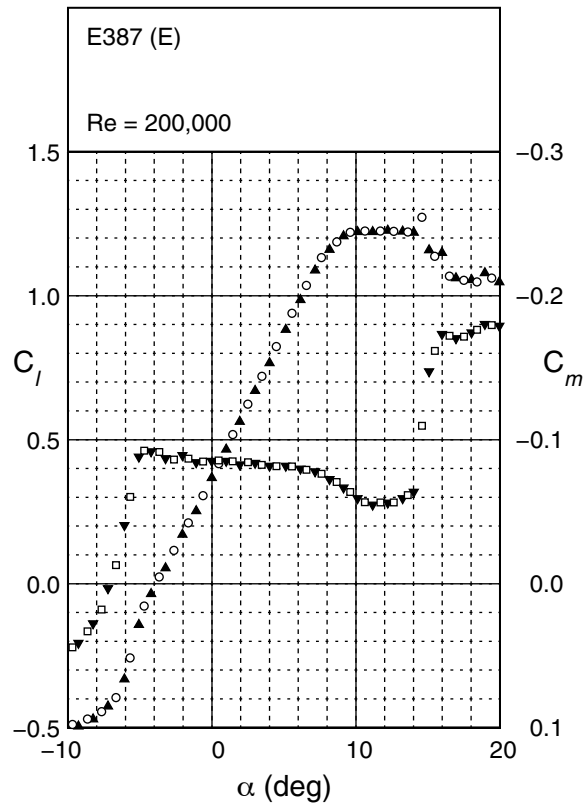
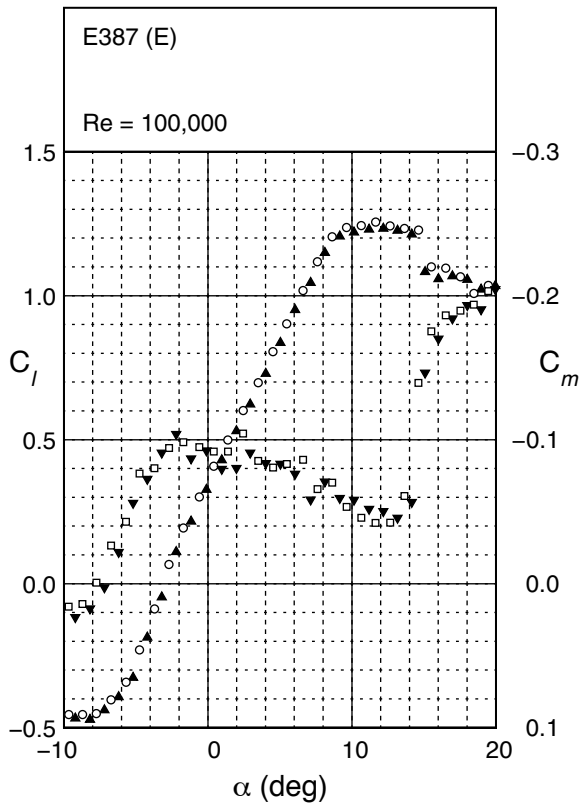
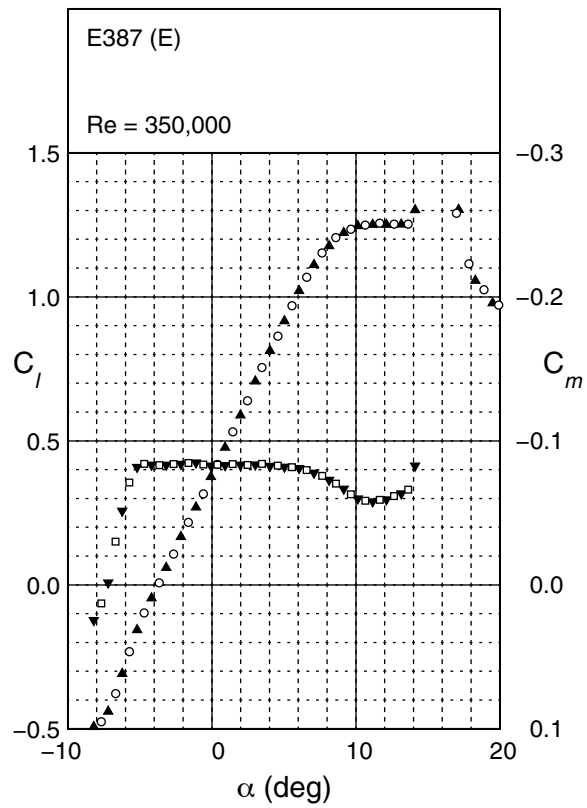
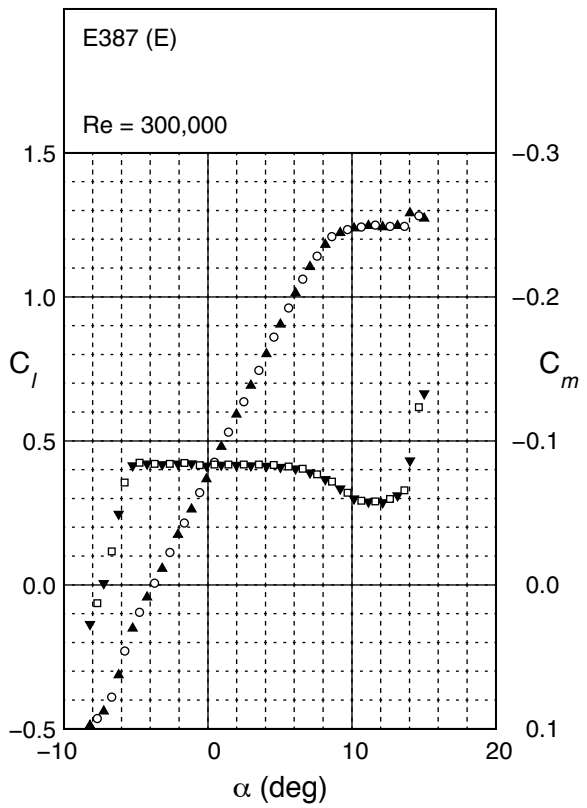


Fig. 5.4



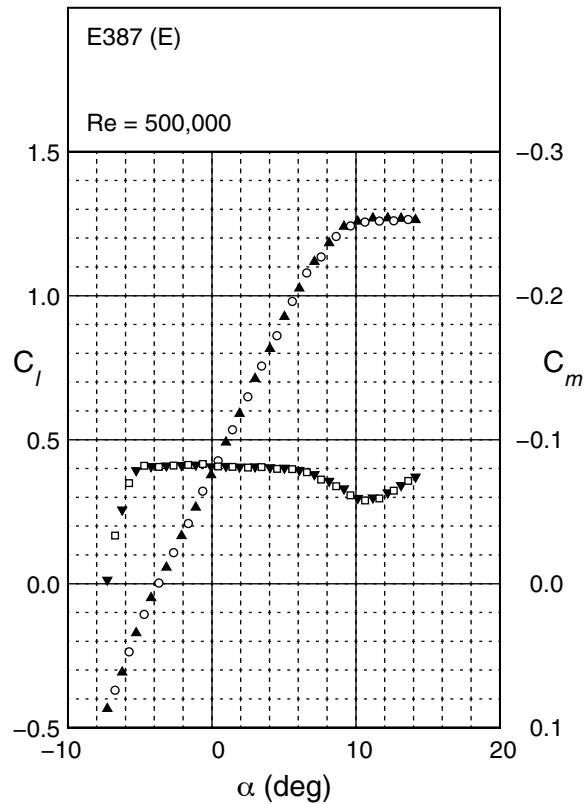
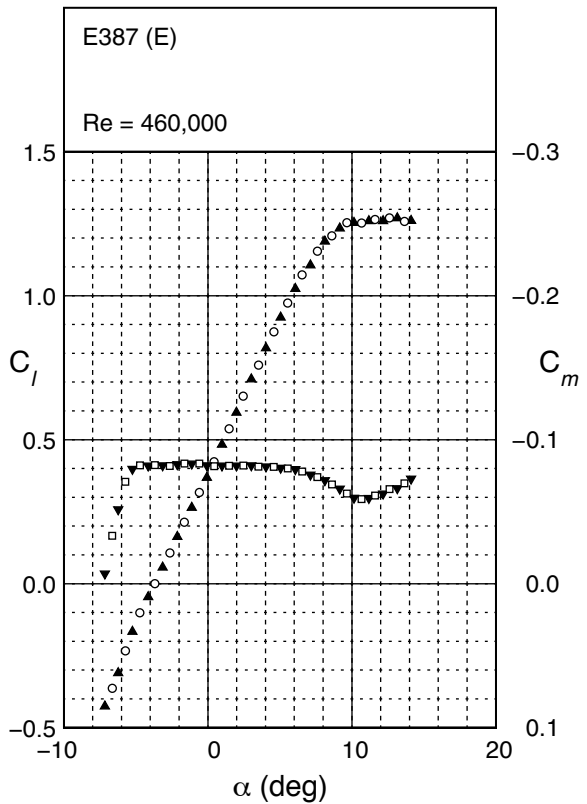
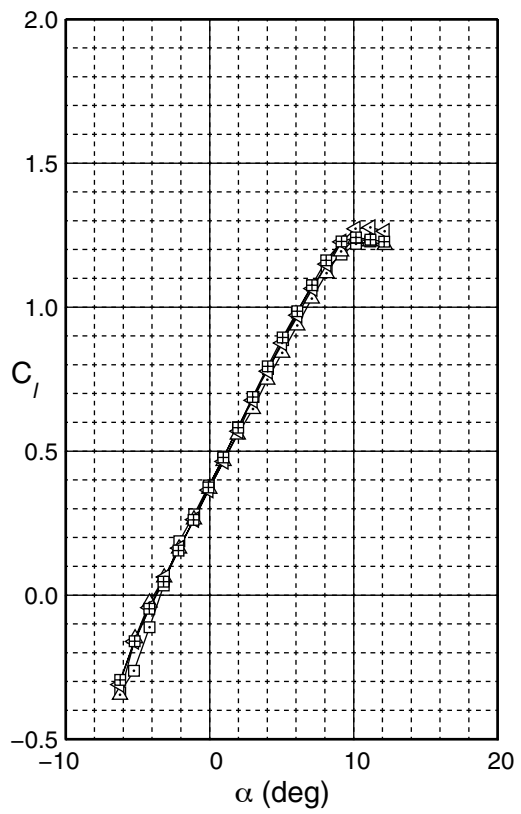
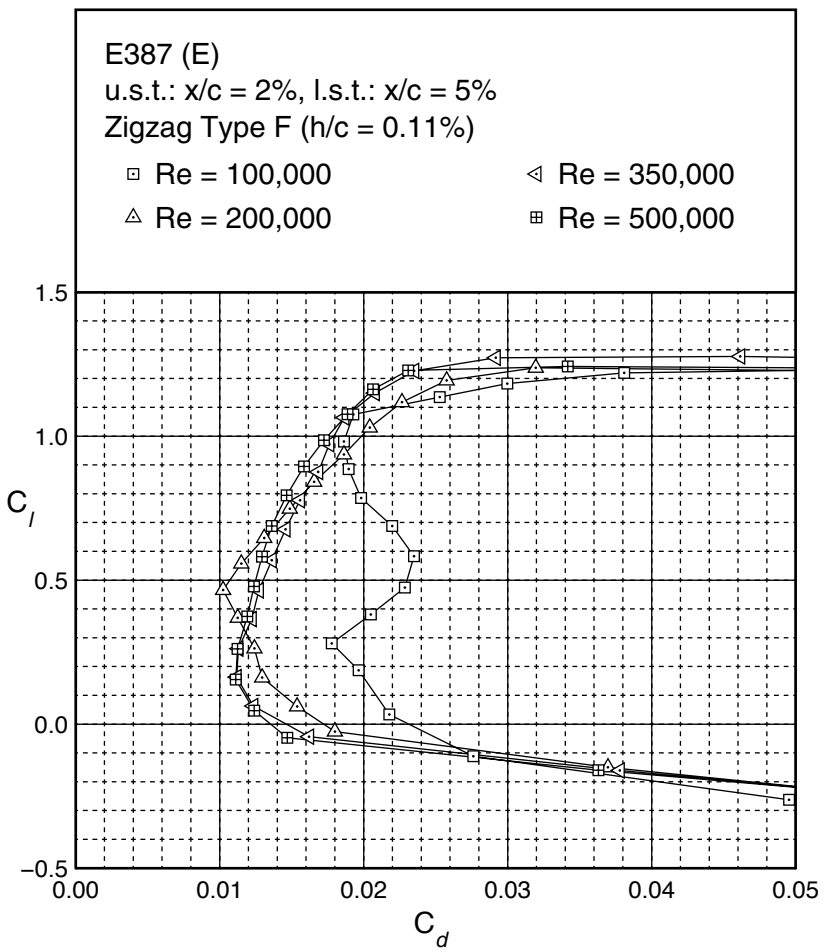
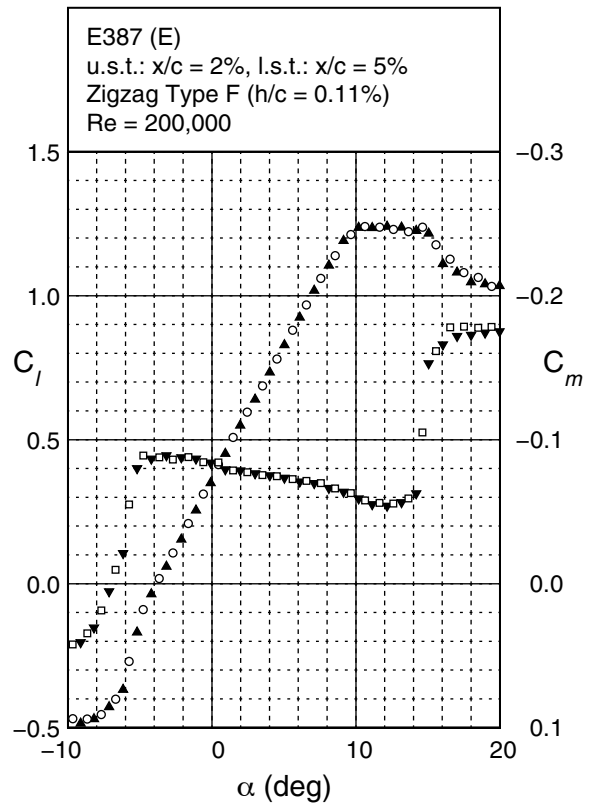
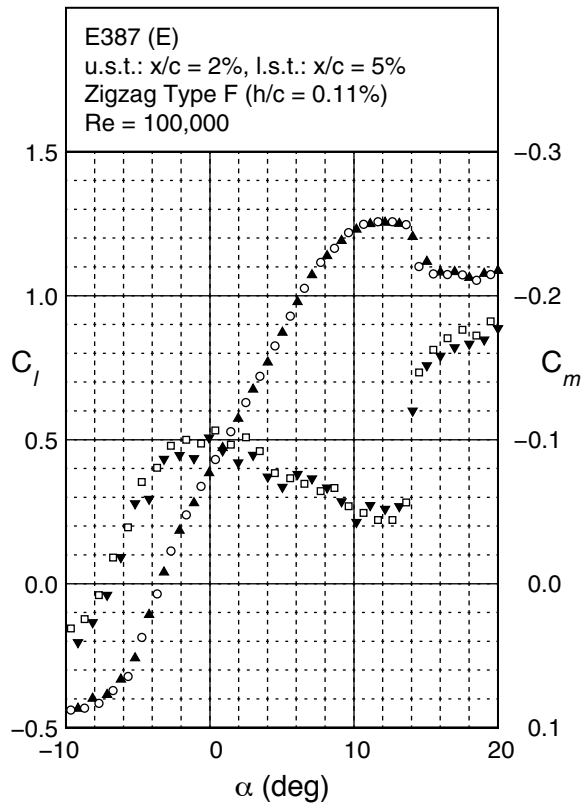
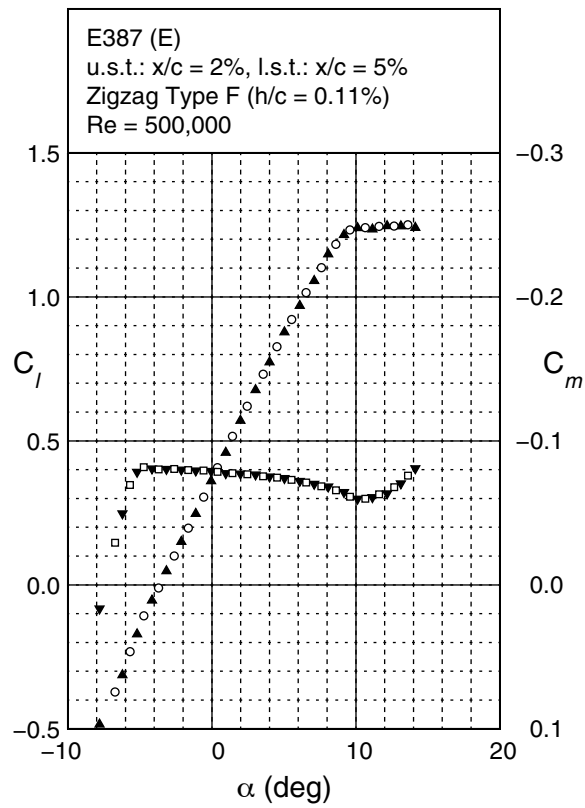
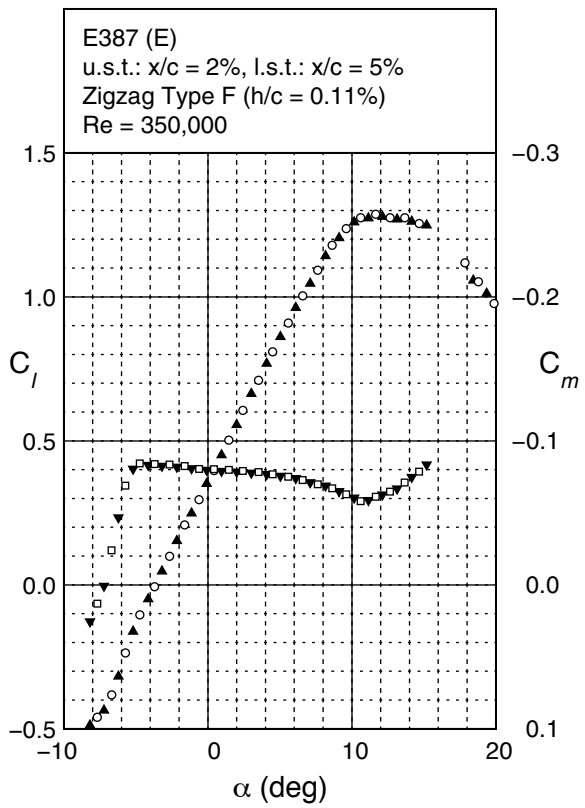


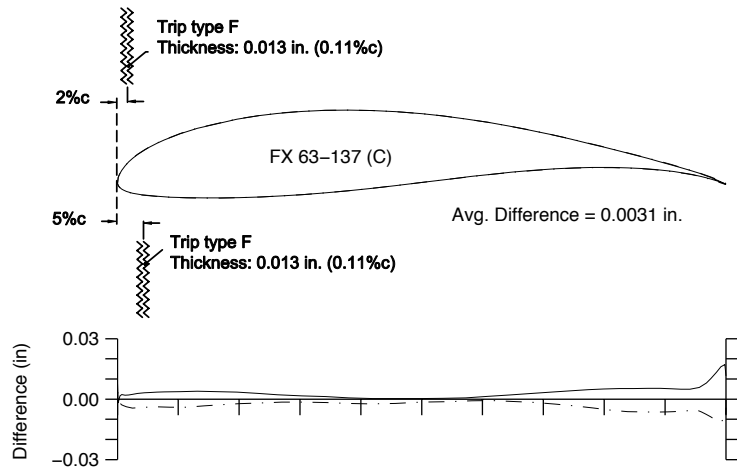
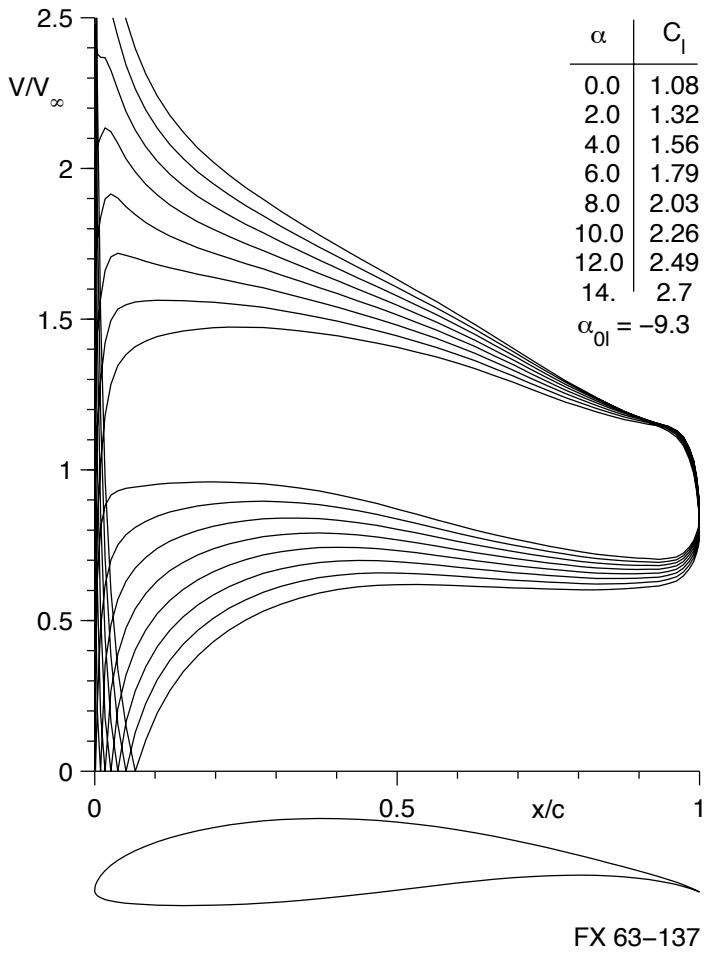
Fig. 5.4 (continued)

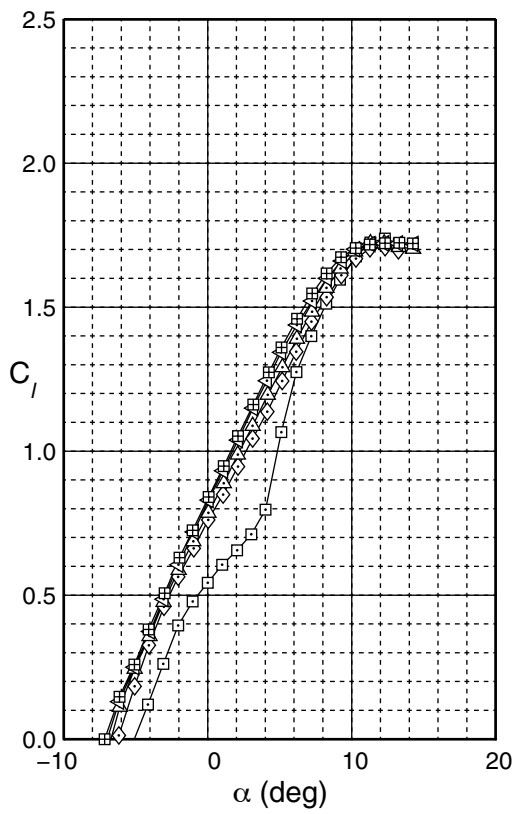
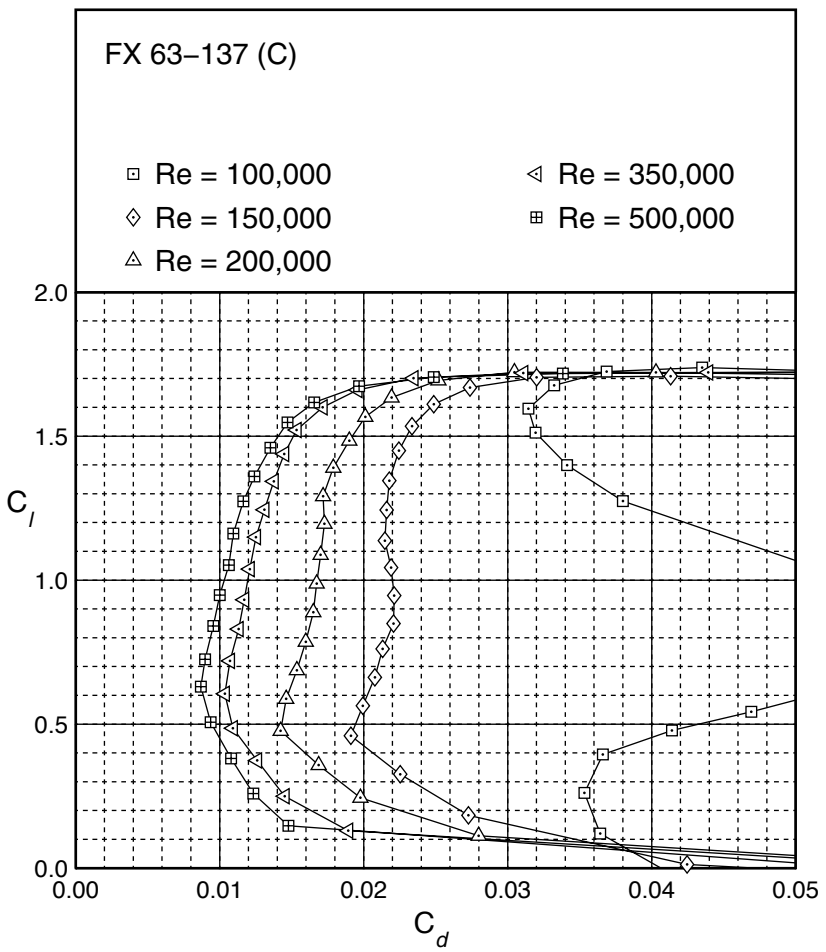


E387 (E)









FX 63-137 (C)



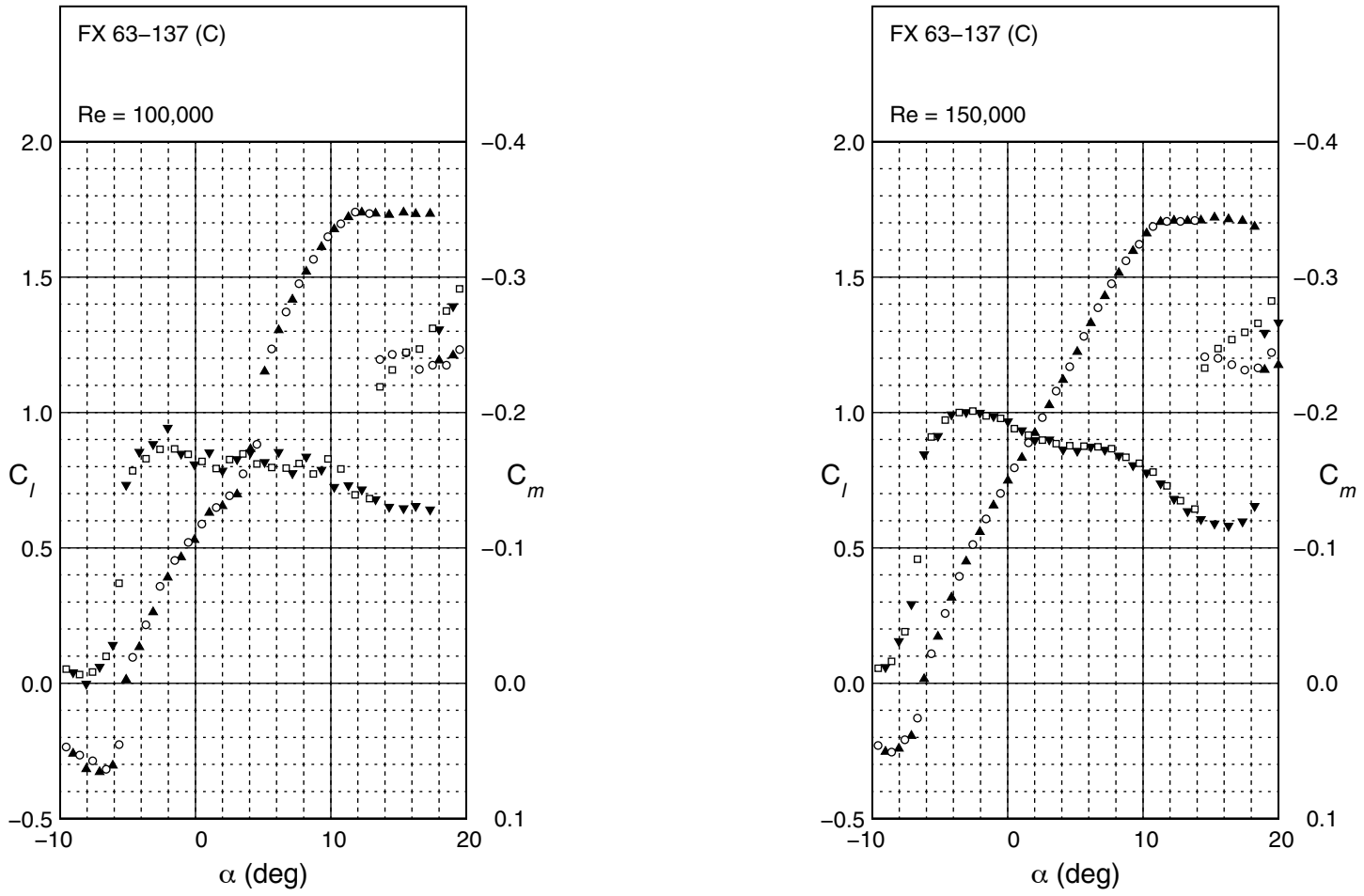
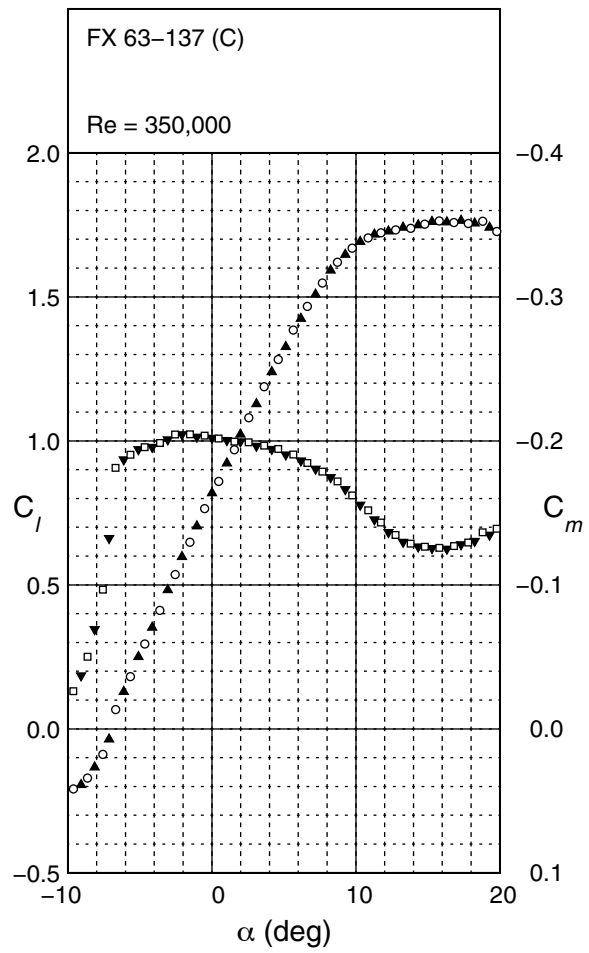
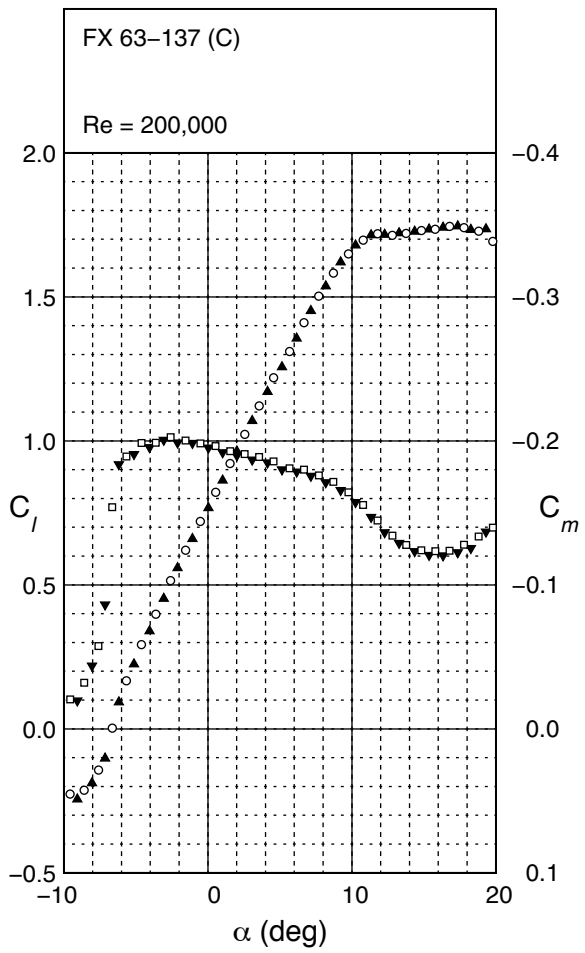
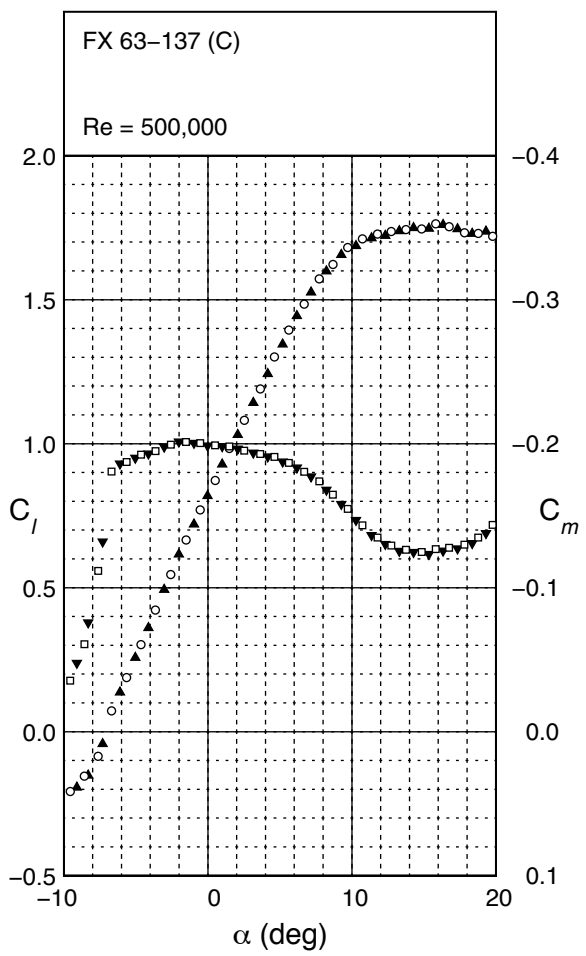


Fig. 5.10



FX 63-137 (C)



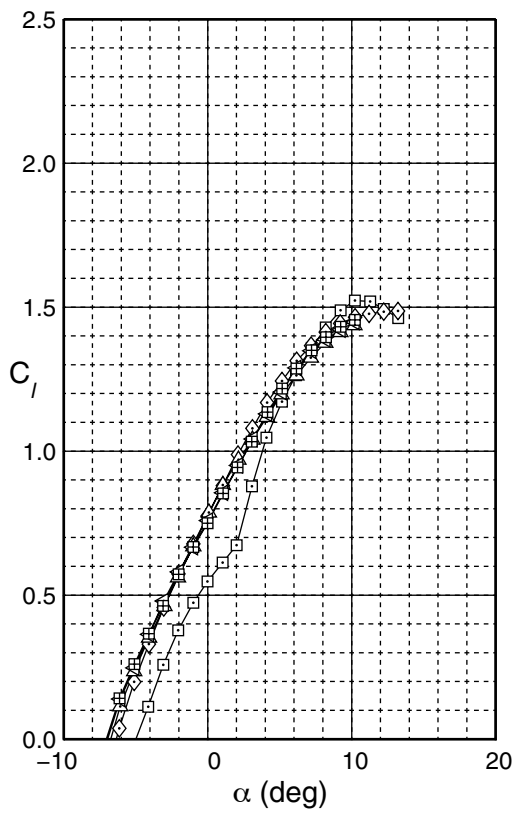
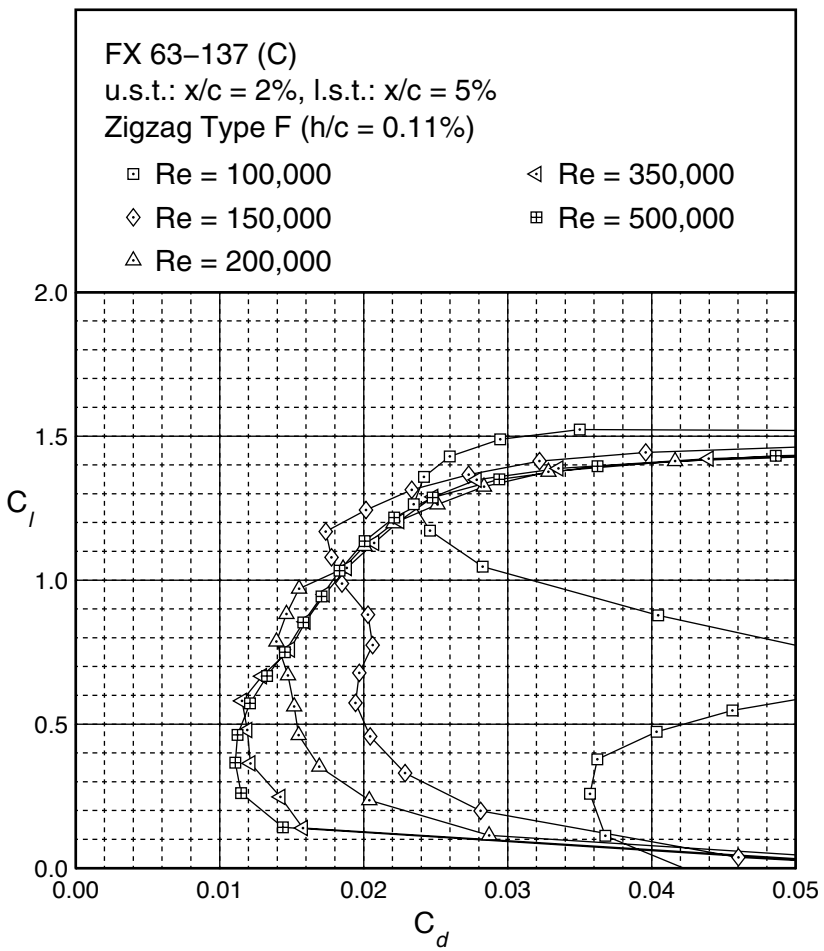


Fig. 5.11

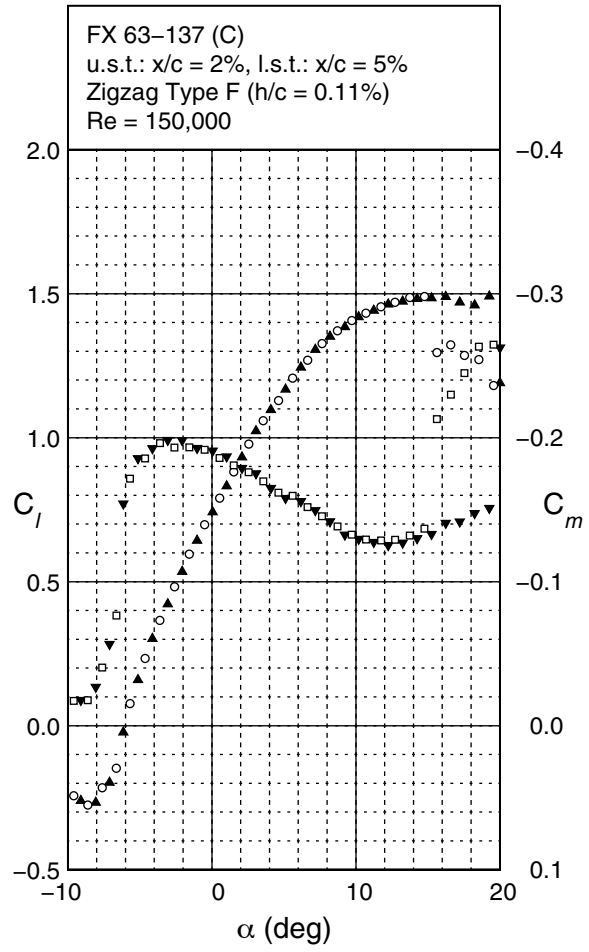
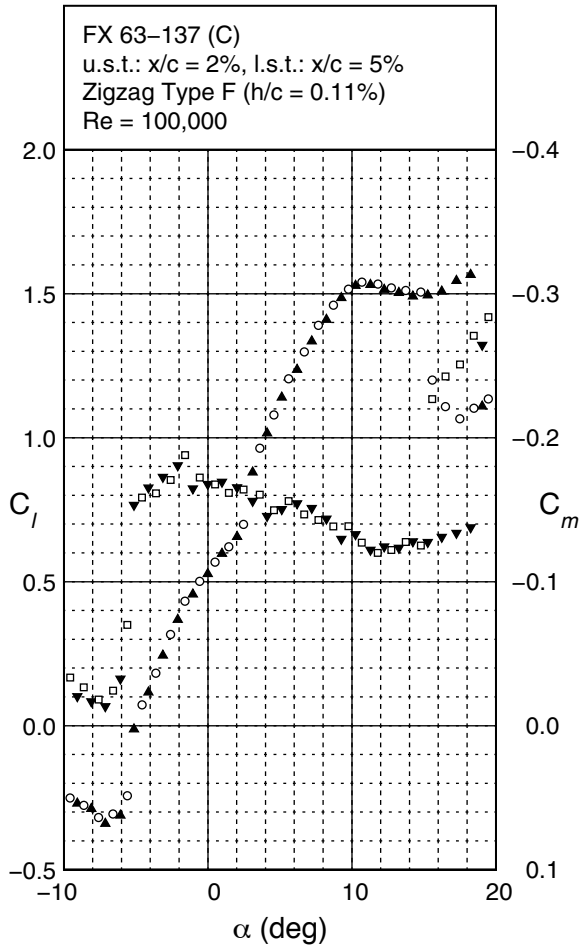
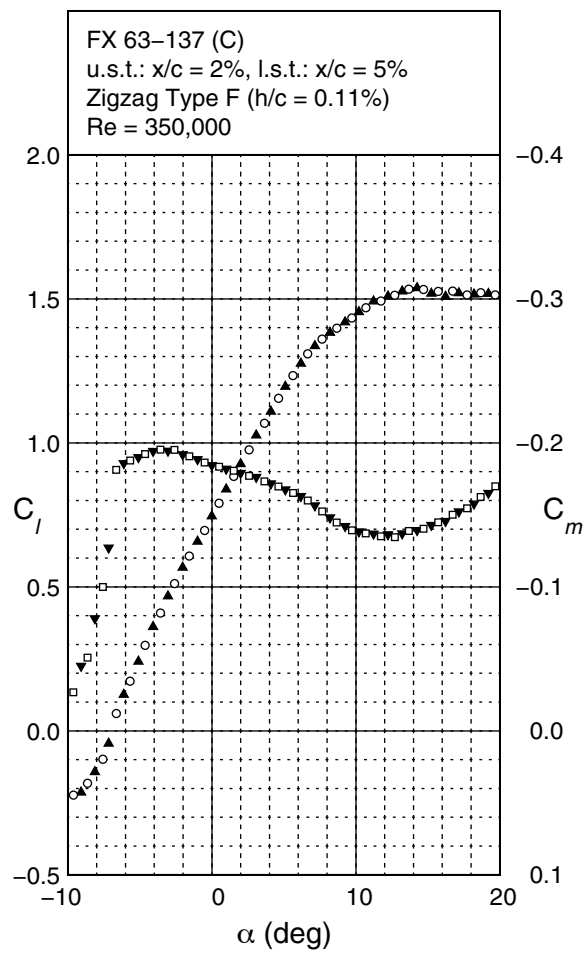
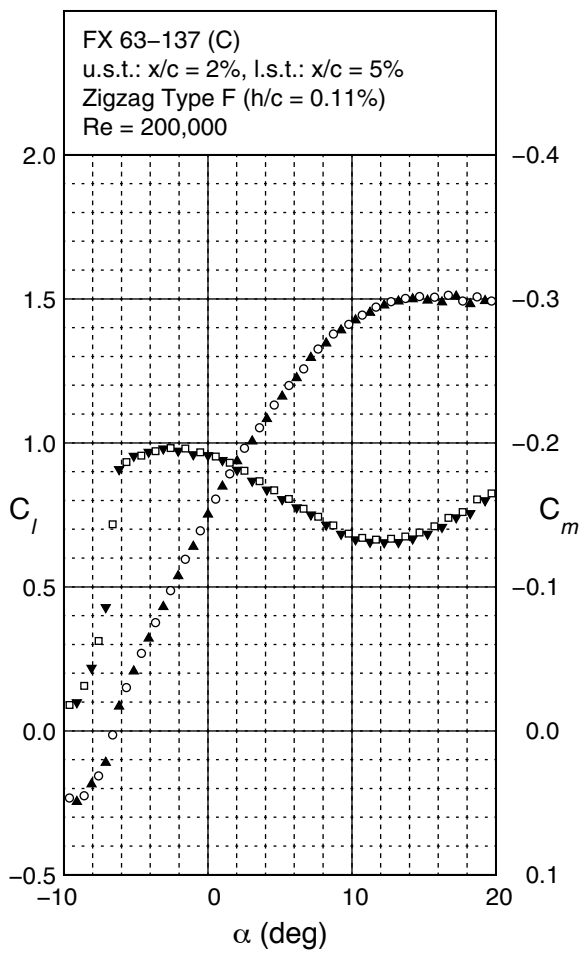
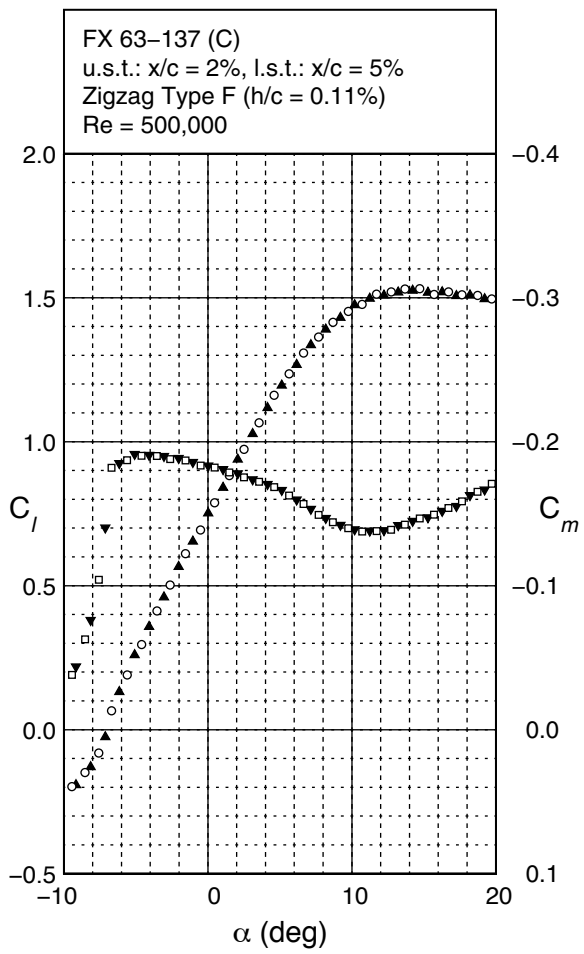


Fig. 5.12



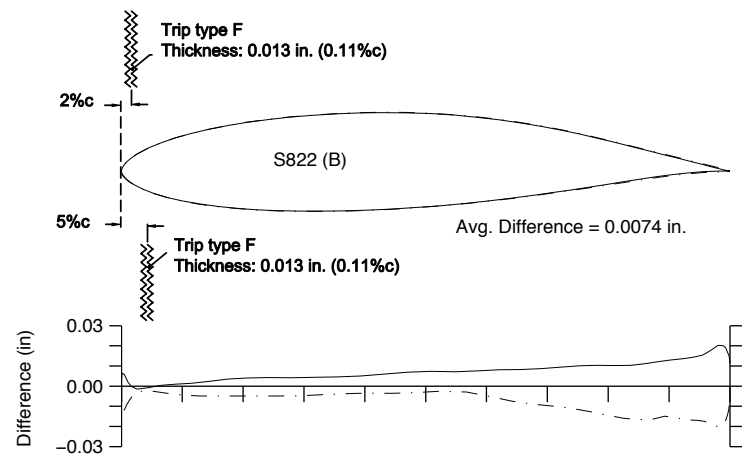
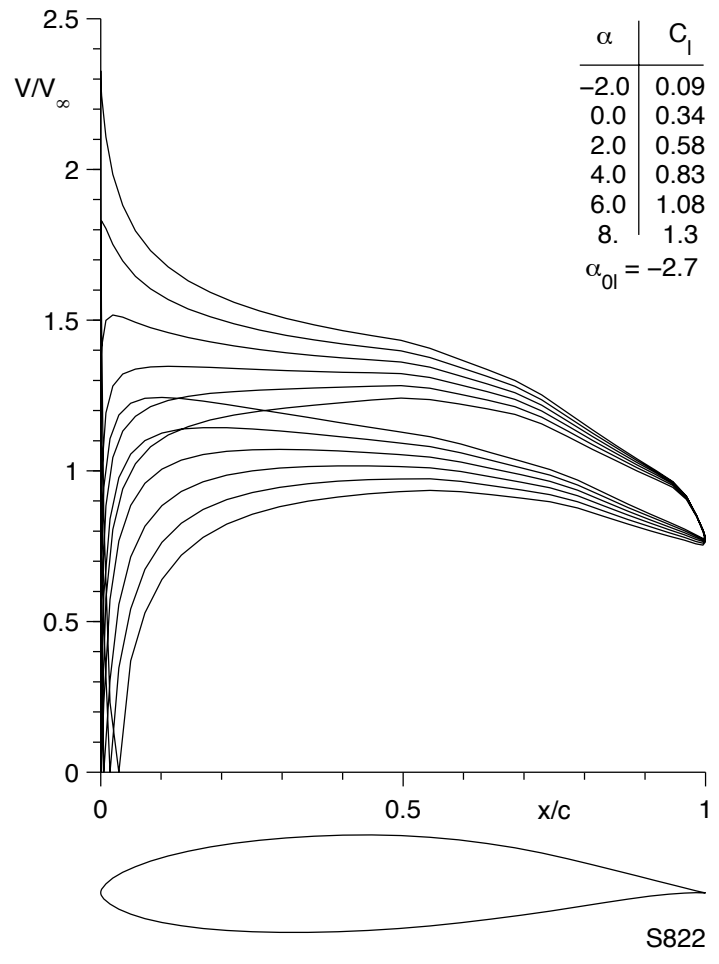
FX 63-137 (C)

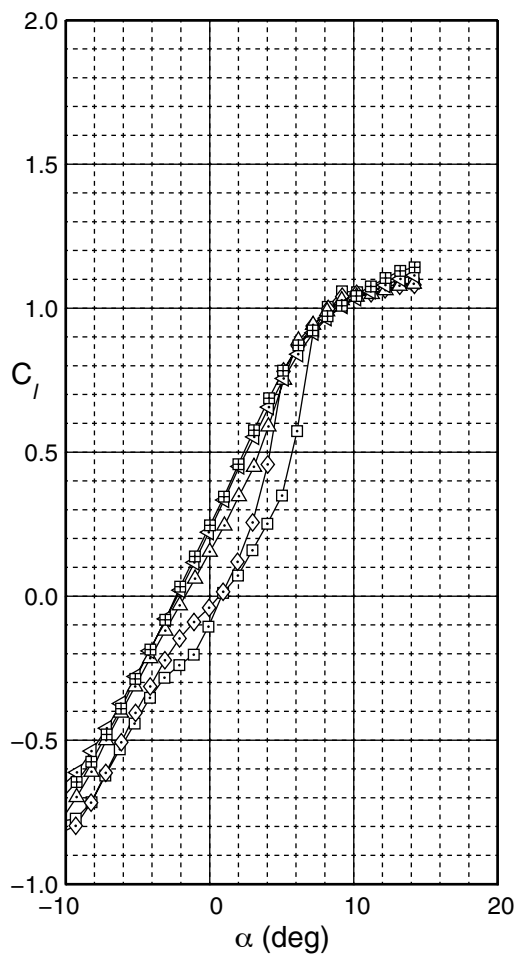
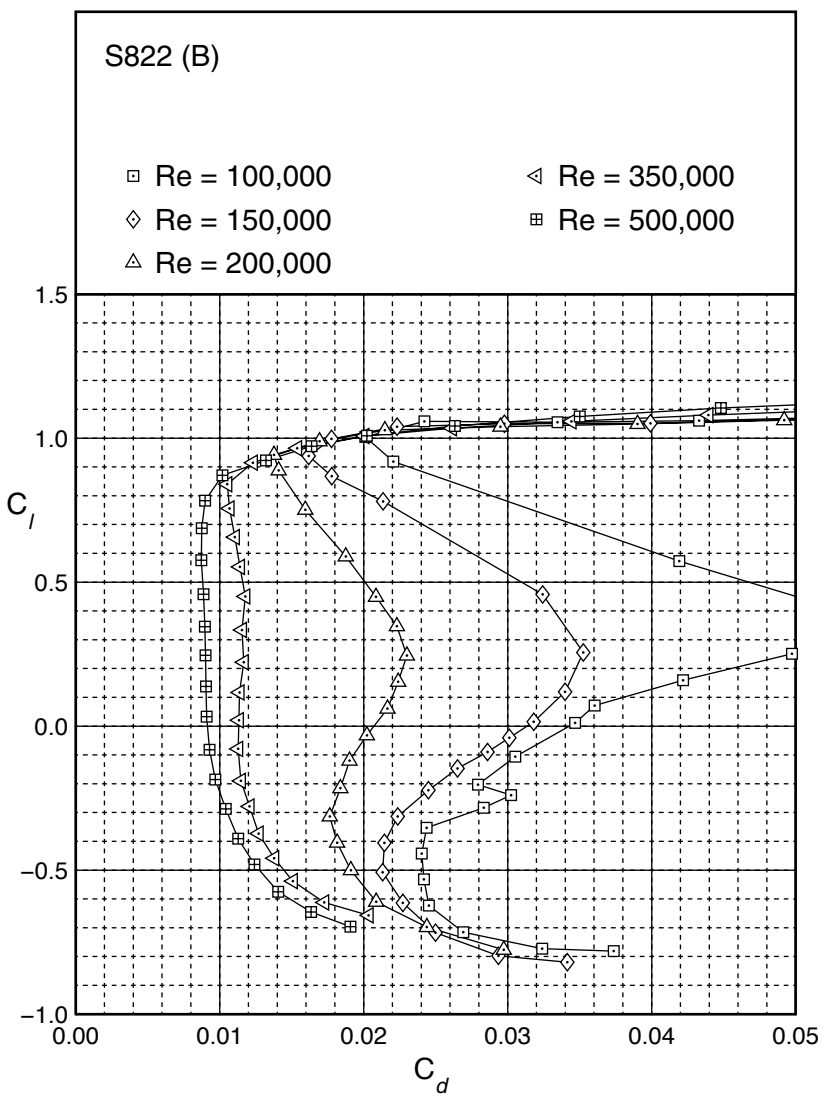






S822 (B)





S822 (B)

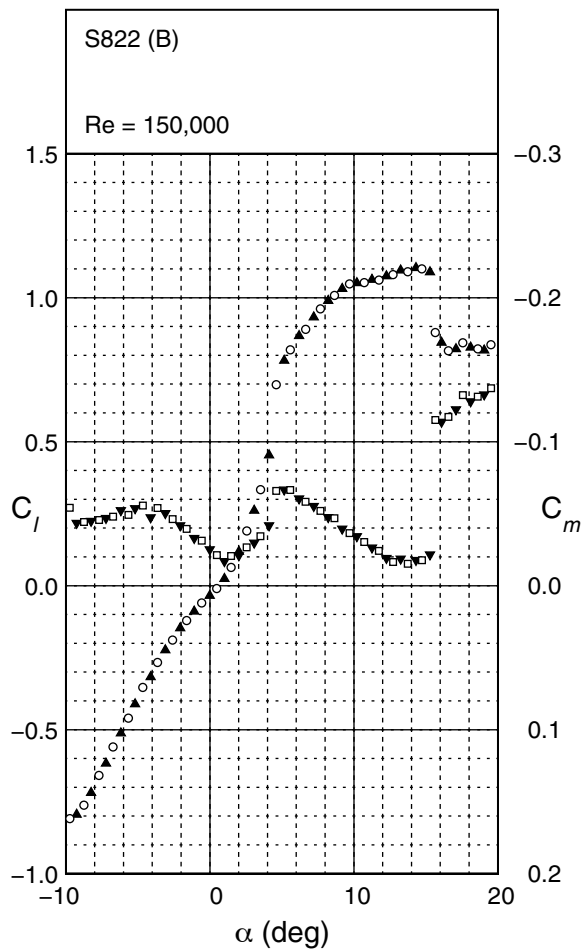
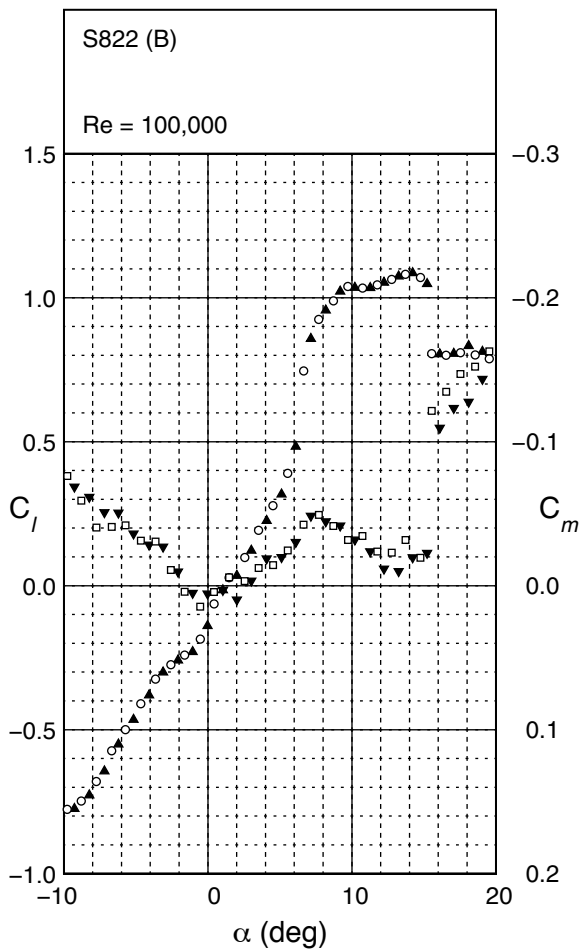
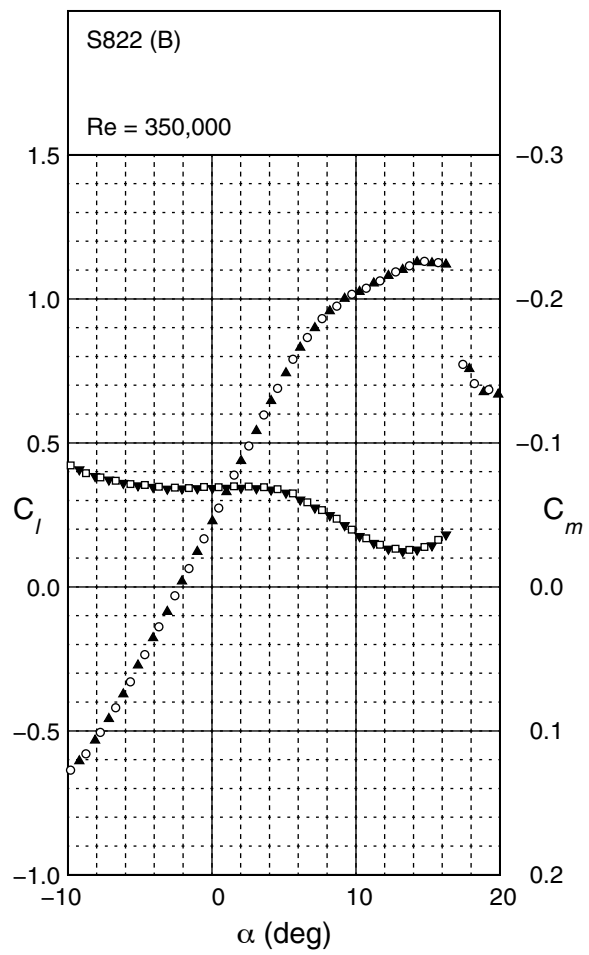
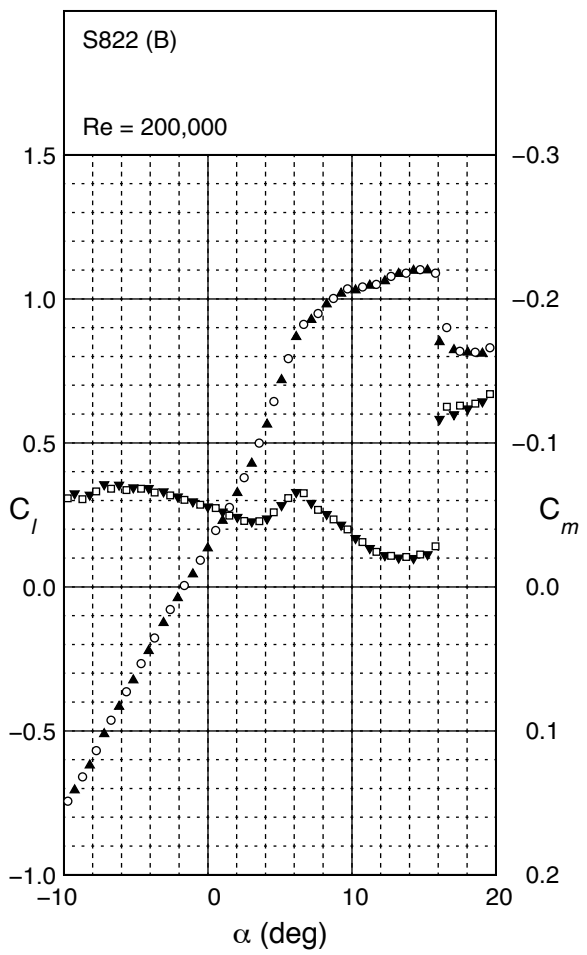
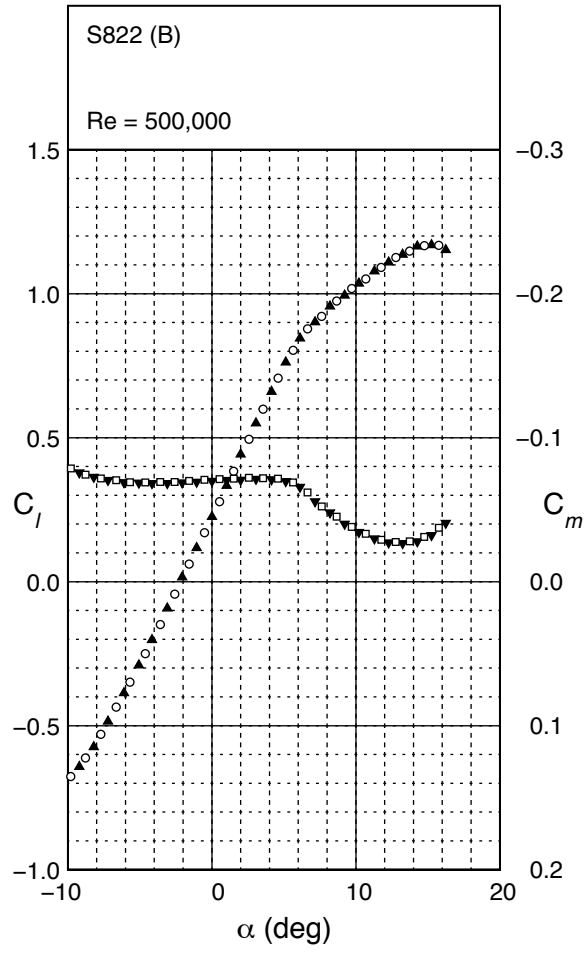
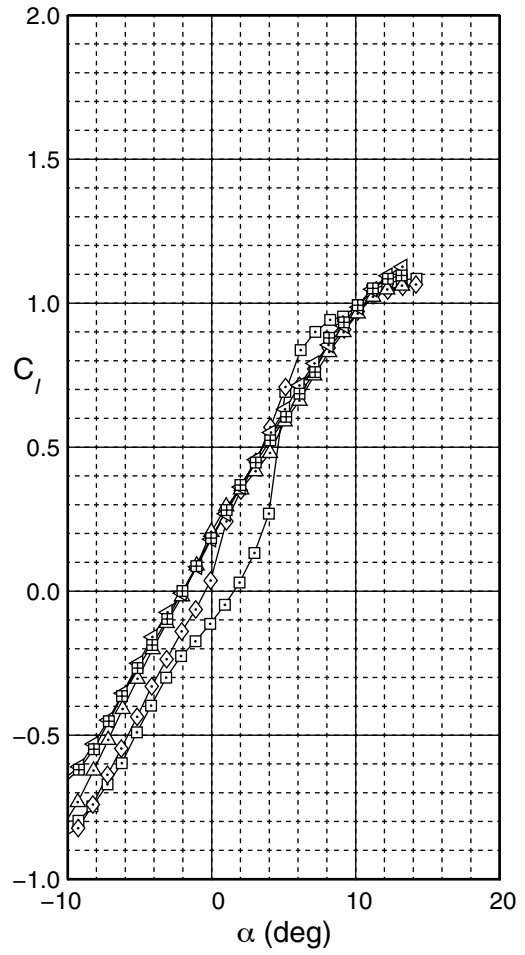
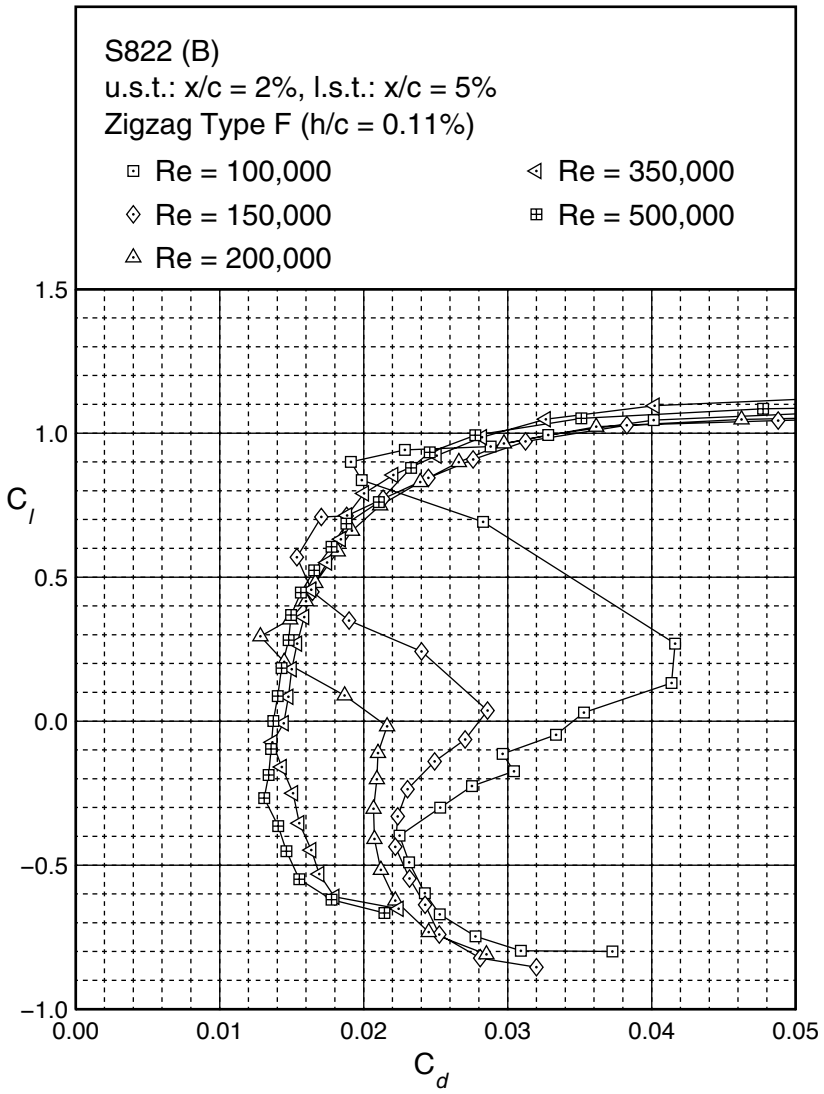


Fig. 5.16



S822 (B)





S822 (B)

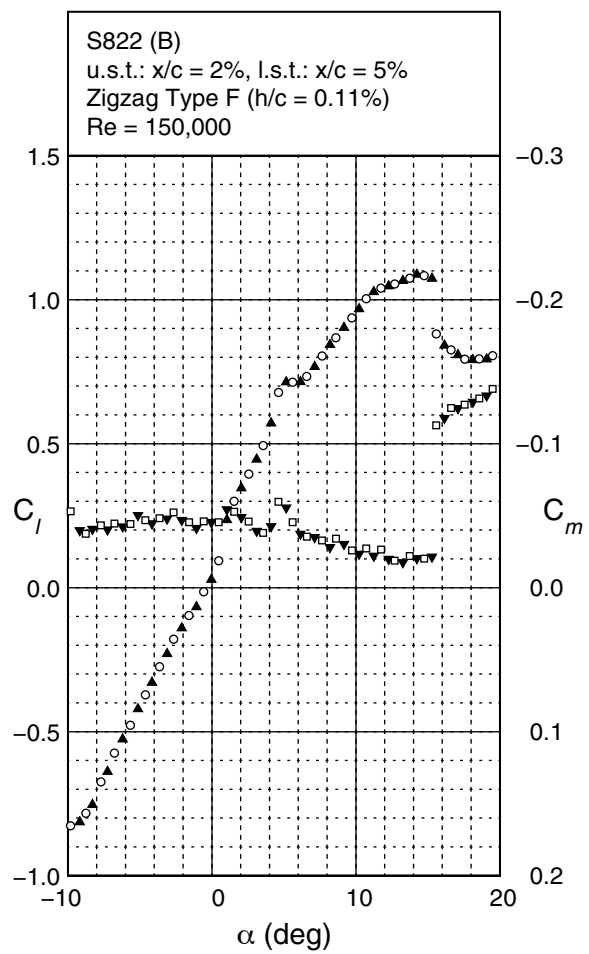
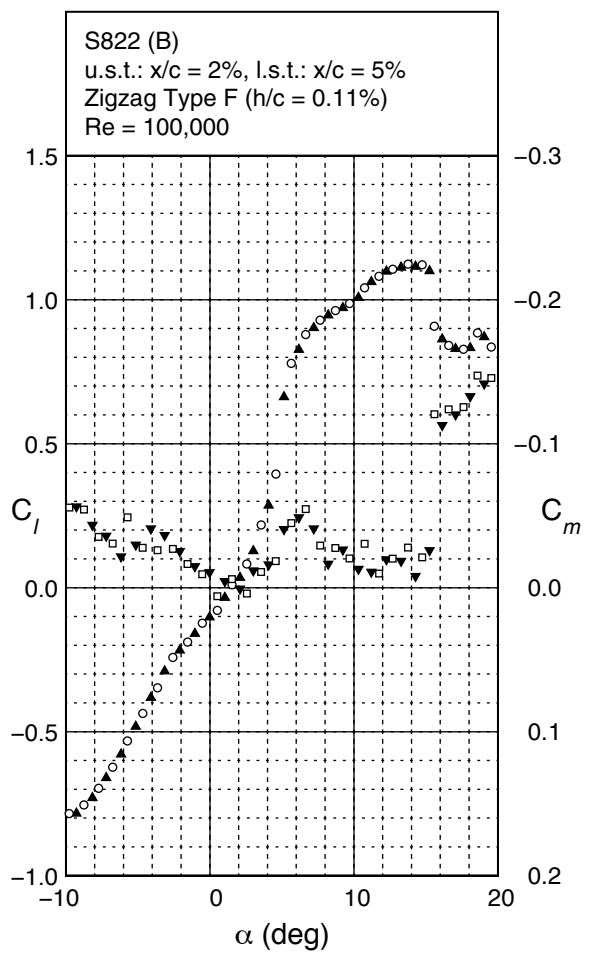
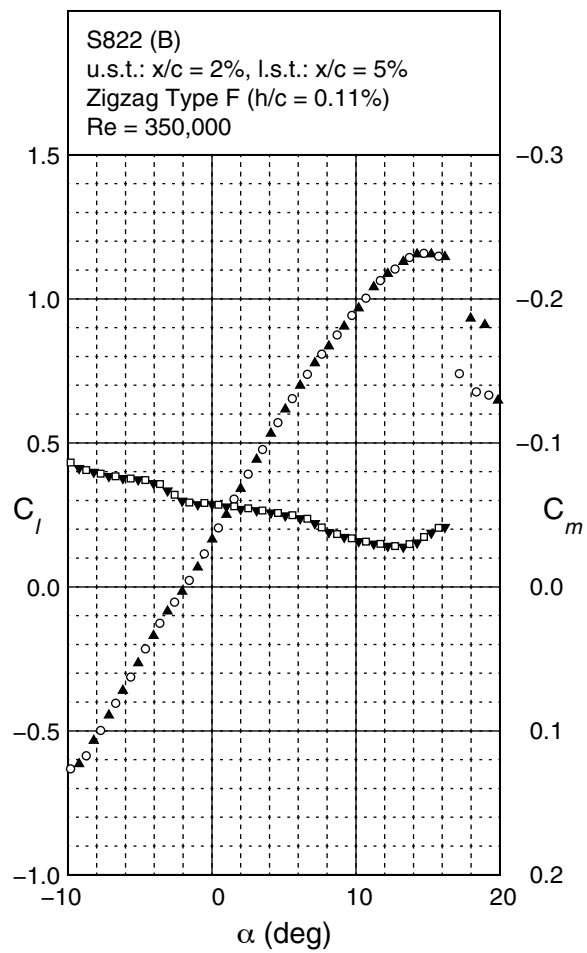
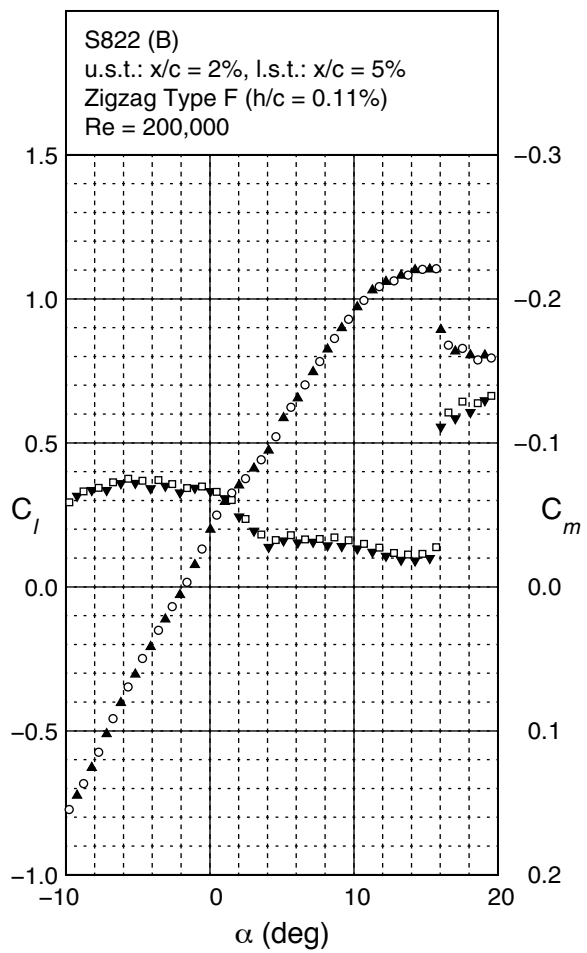
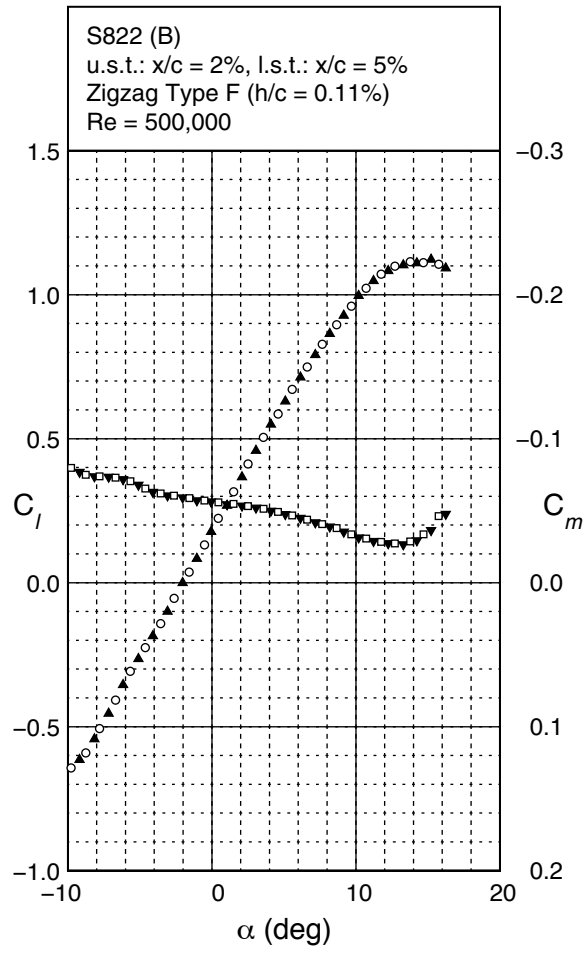


Fig. 5.18

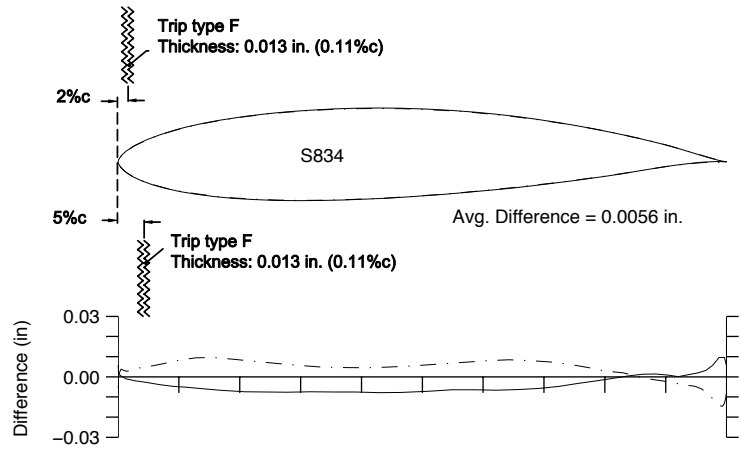
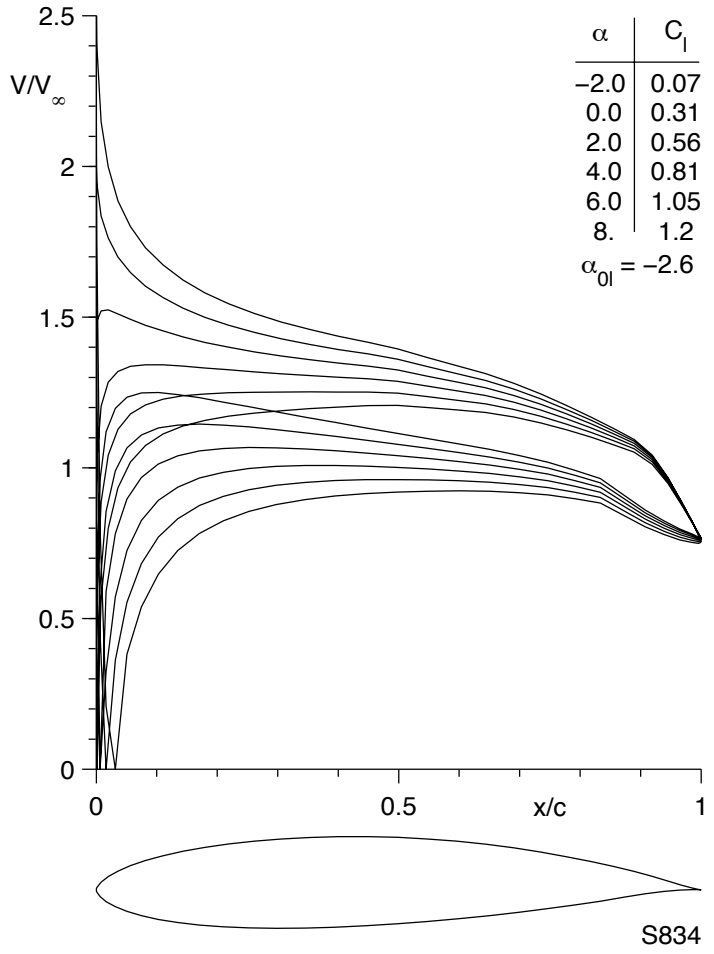




S822 (B)

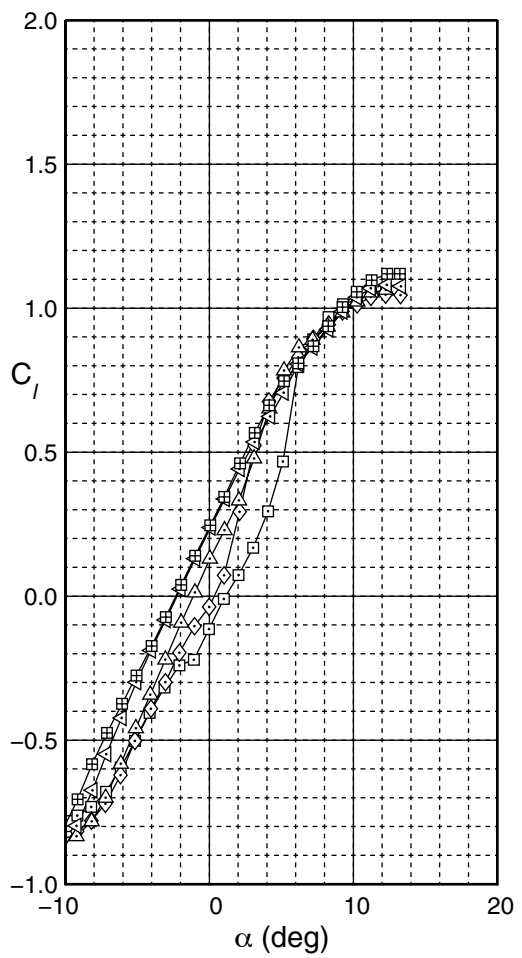
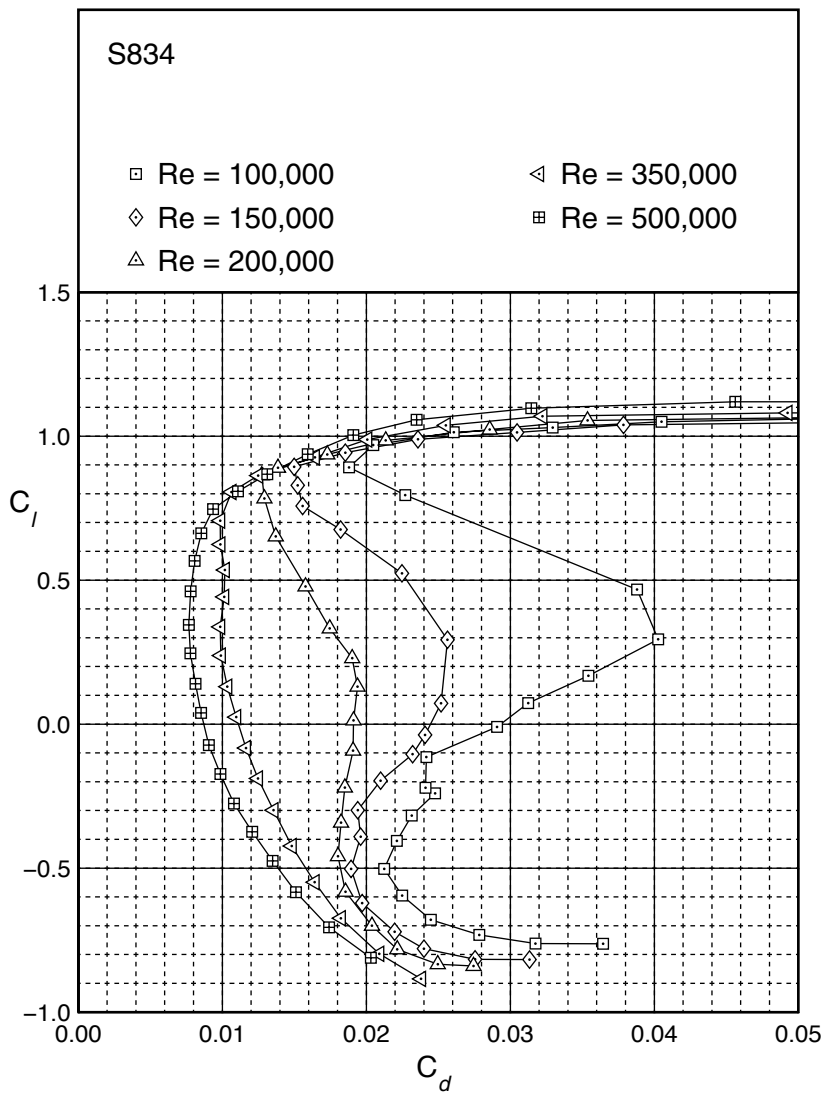




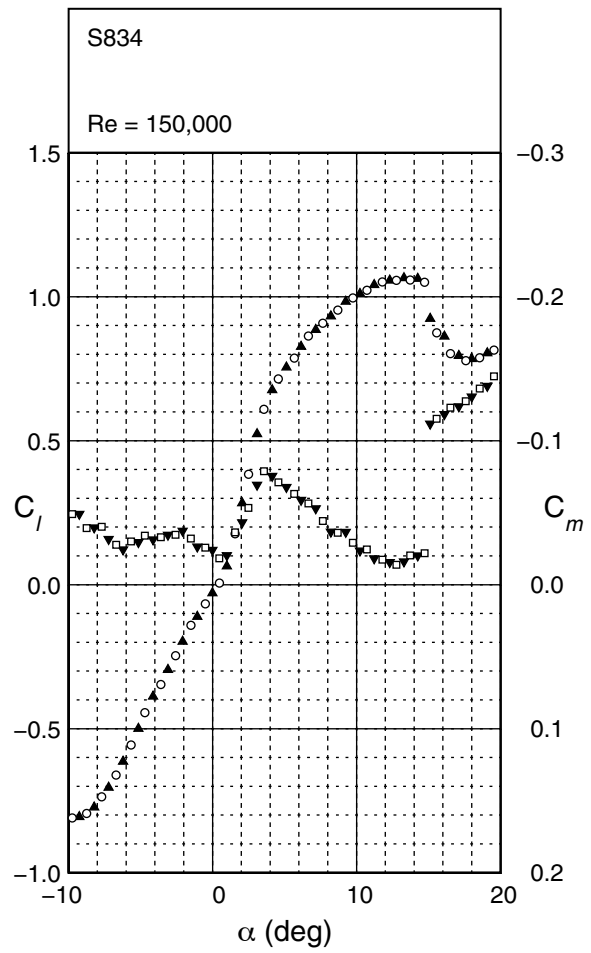
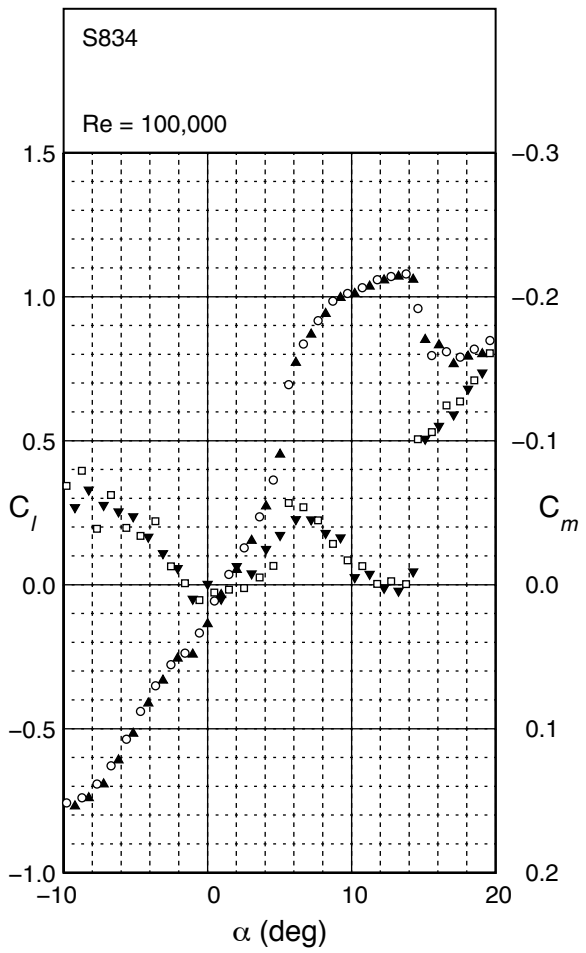


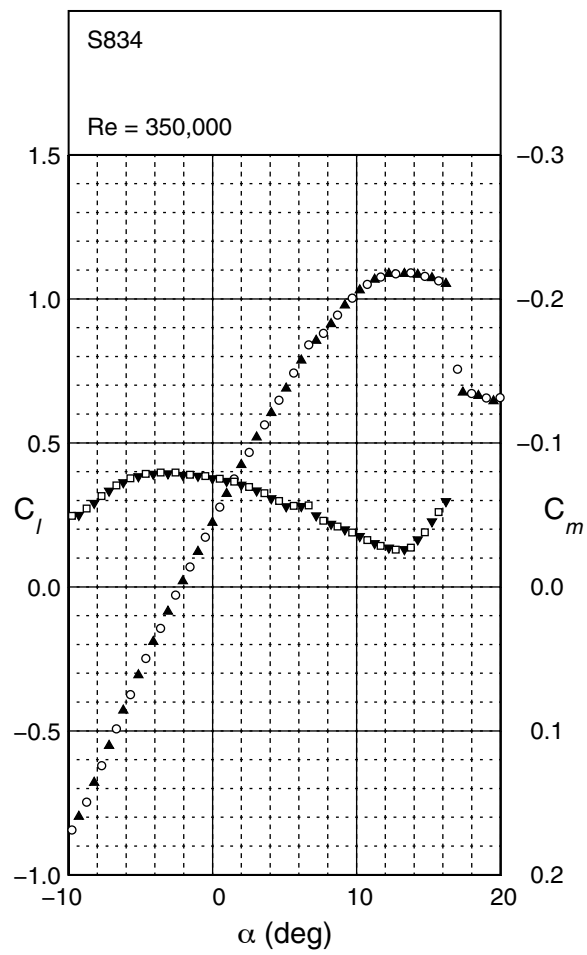
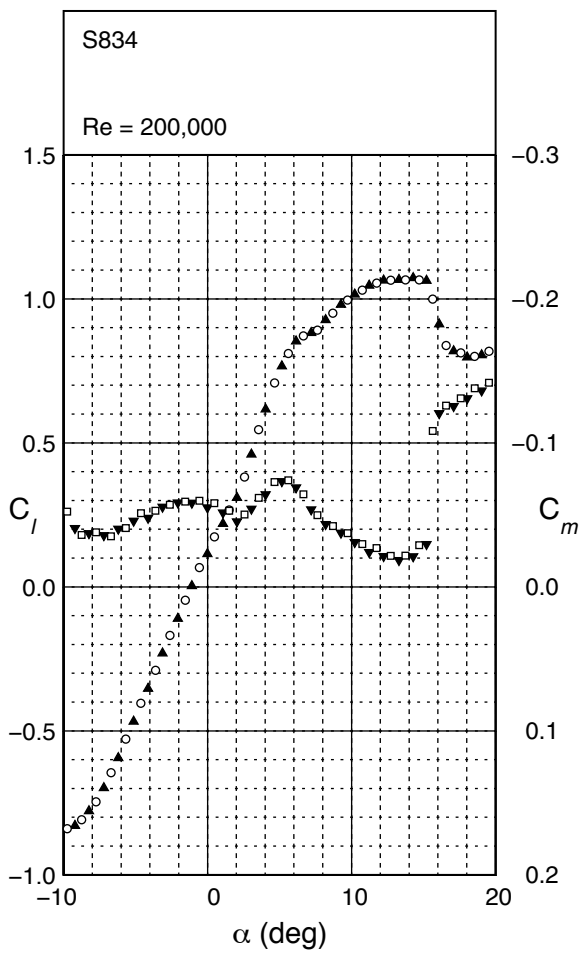
Figs. 5.19 & 5.20

Fig. 5.21

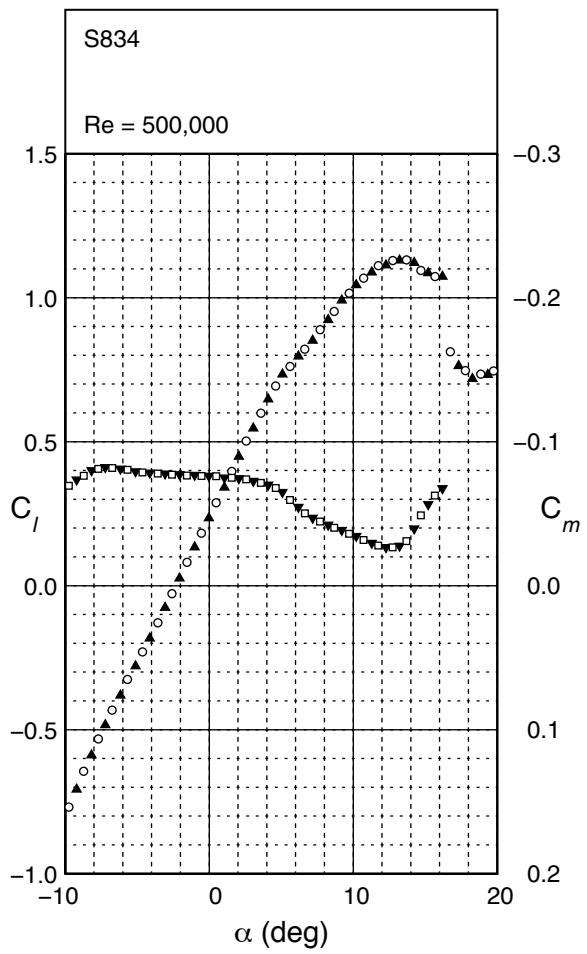


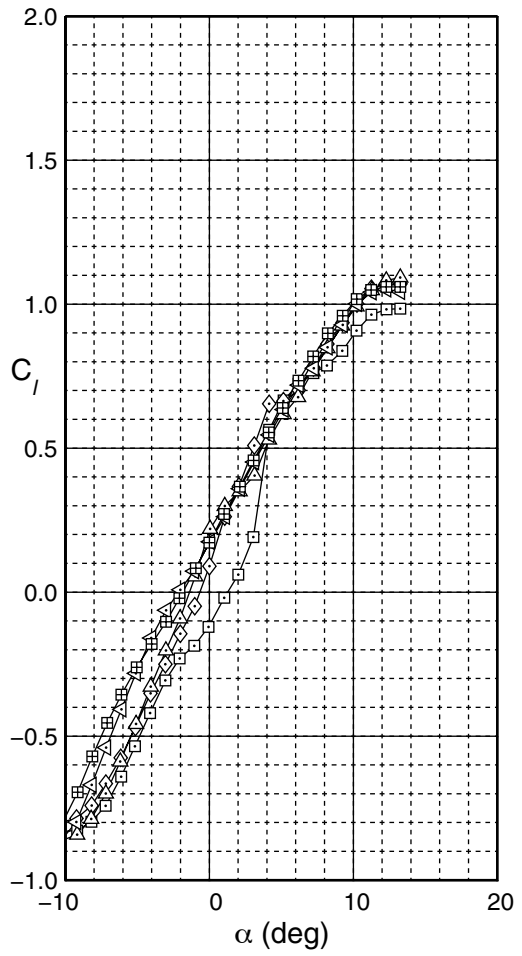
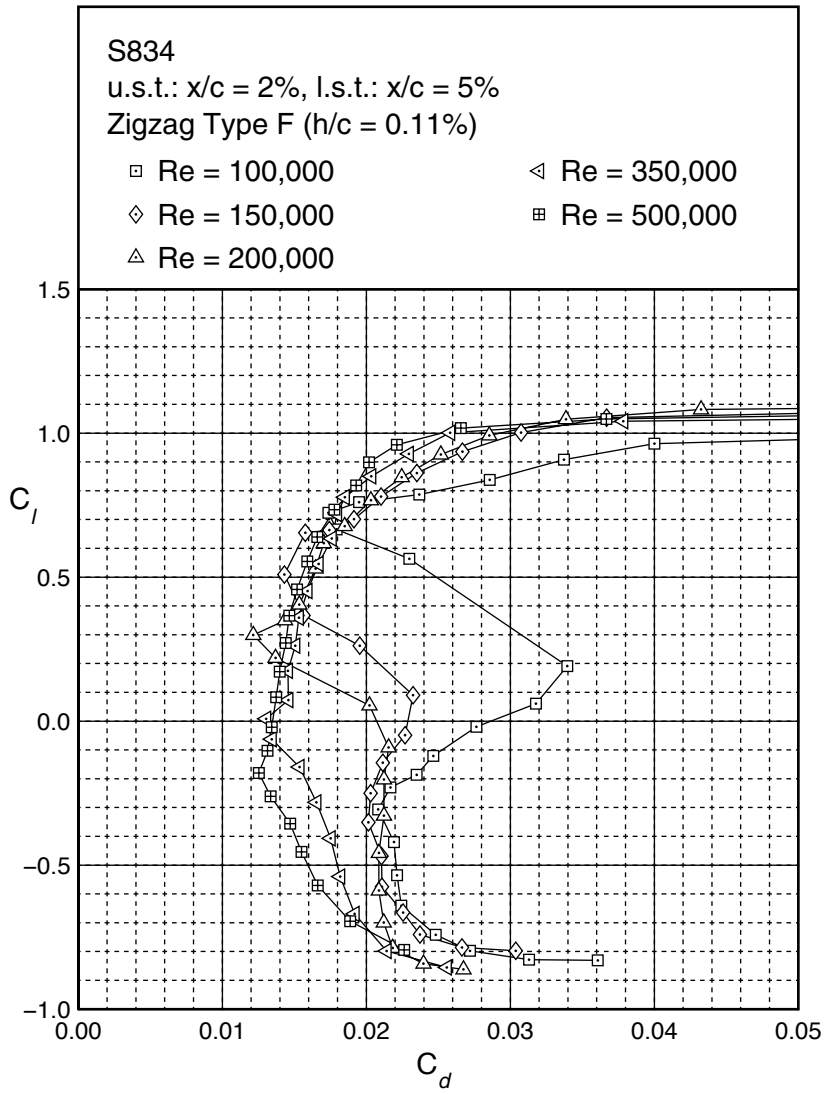
S834





S834





S834



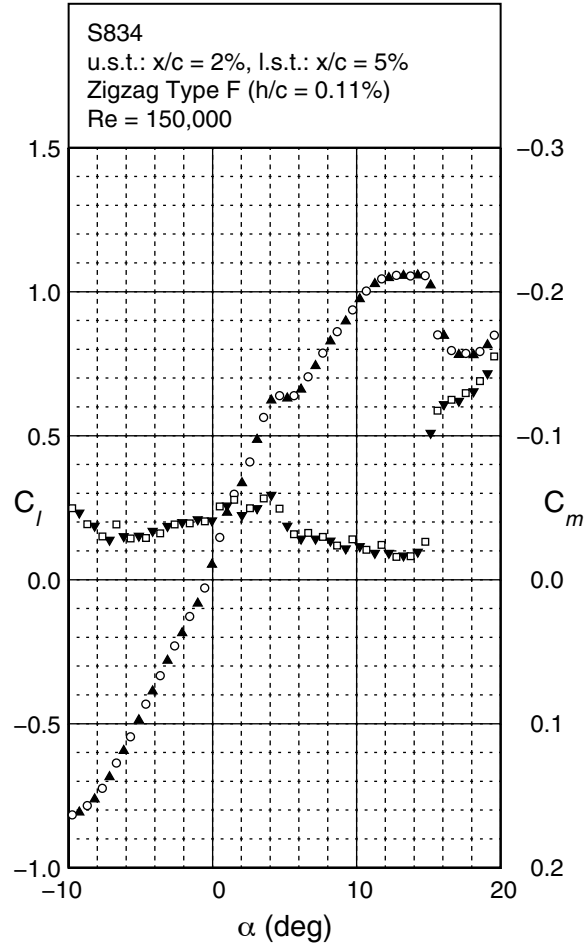
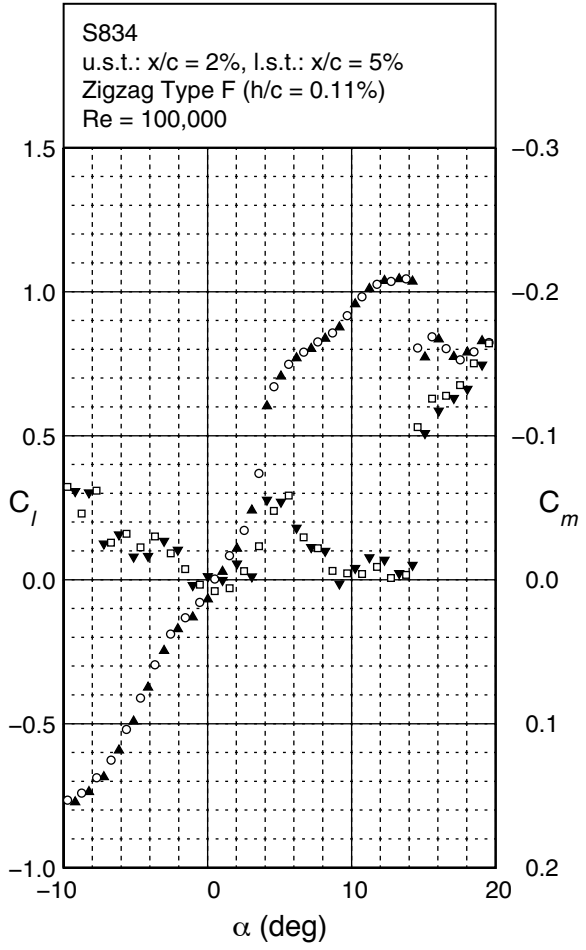
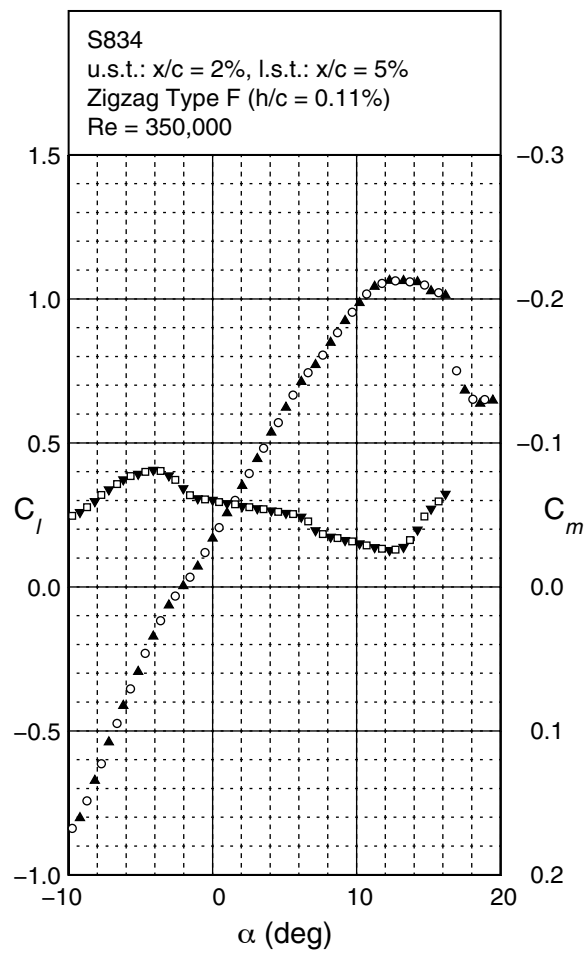
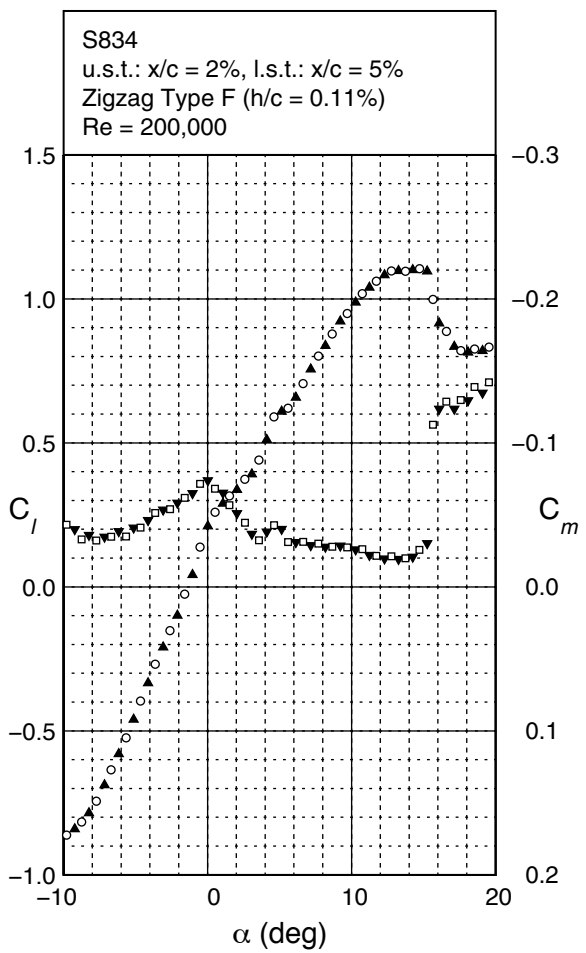
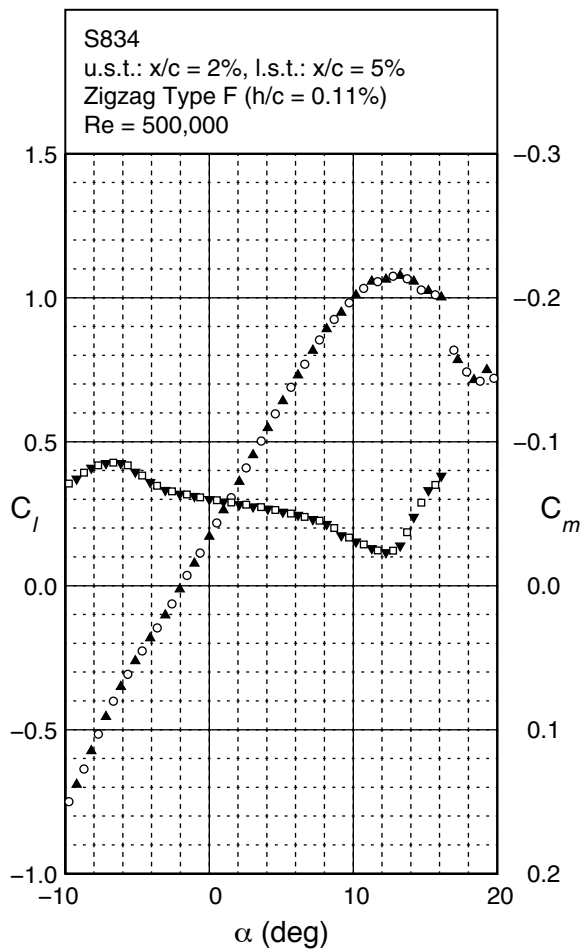


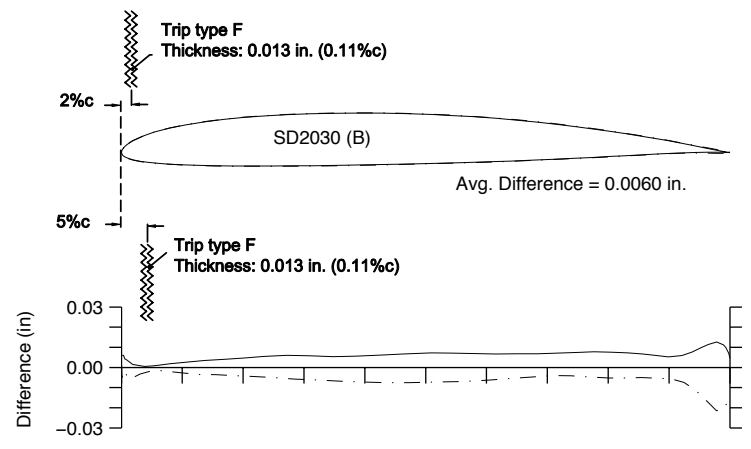
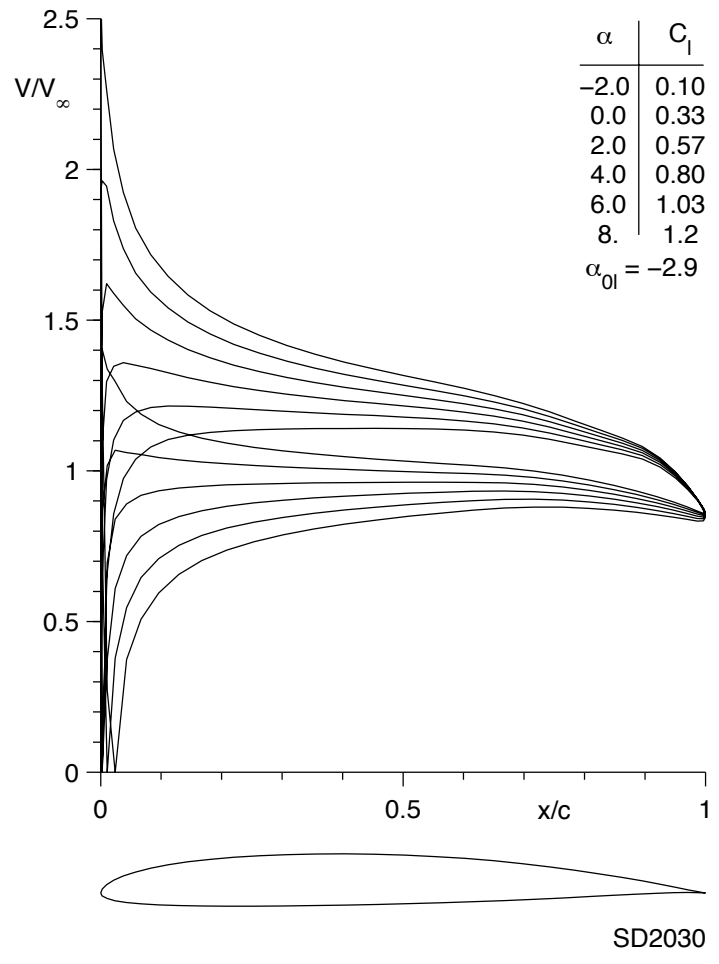
Fig. 5.24



S834







Figs. 5.25 & 5.26

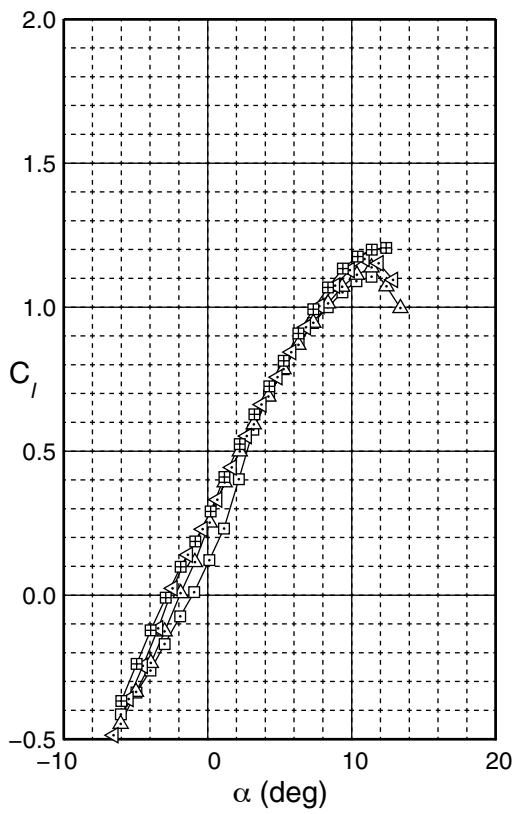
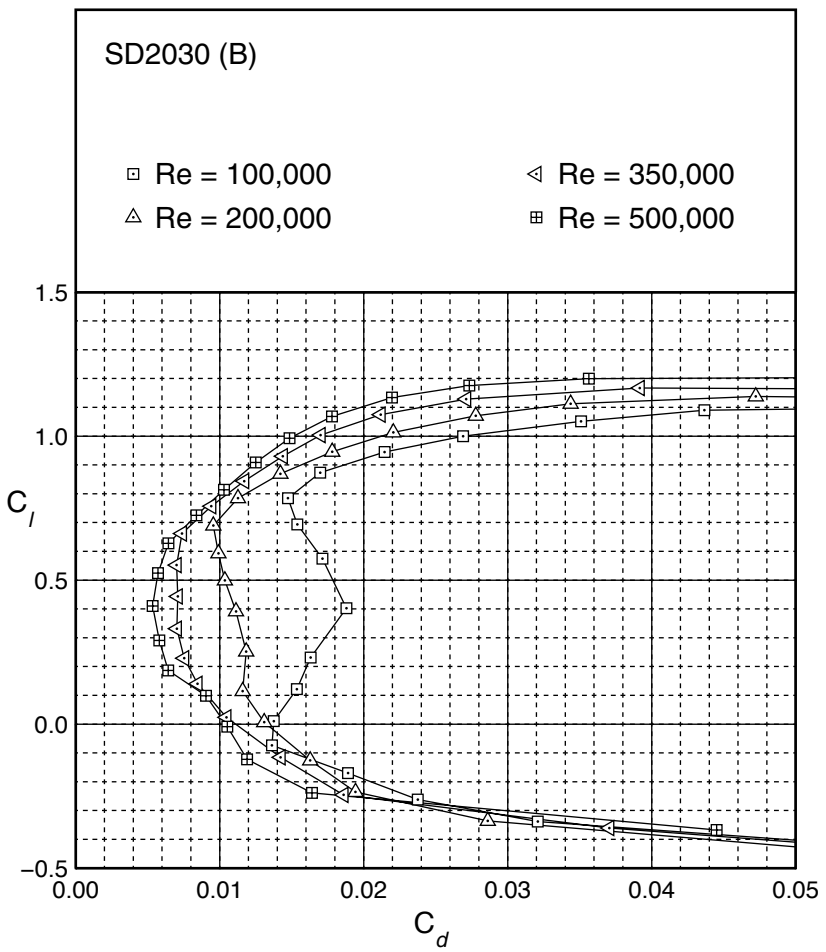


Fig. 5.27

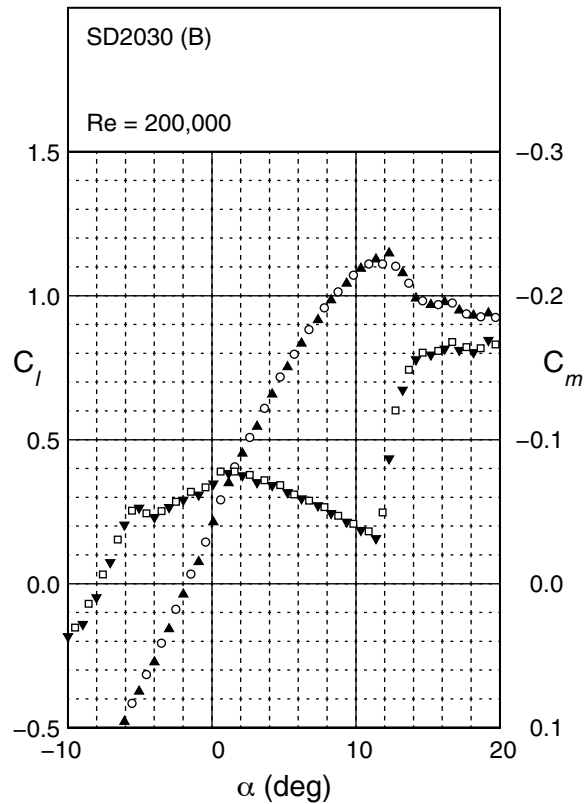
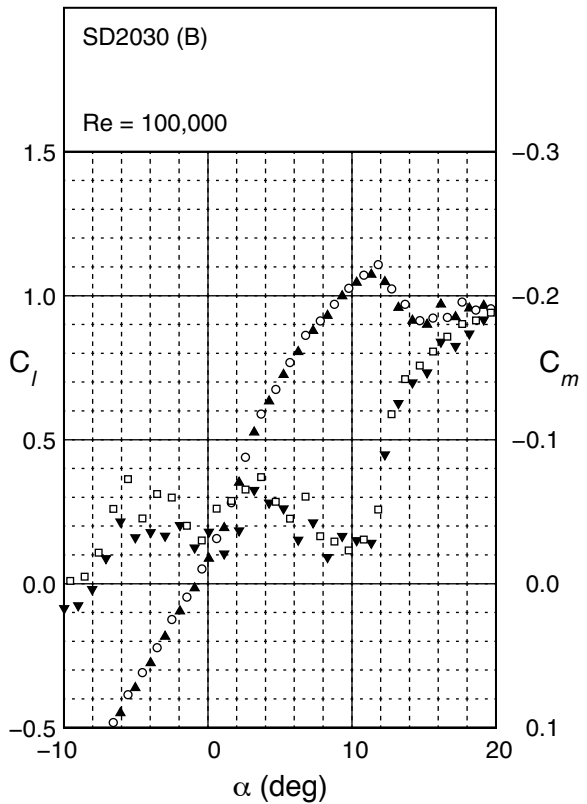
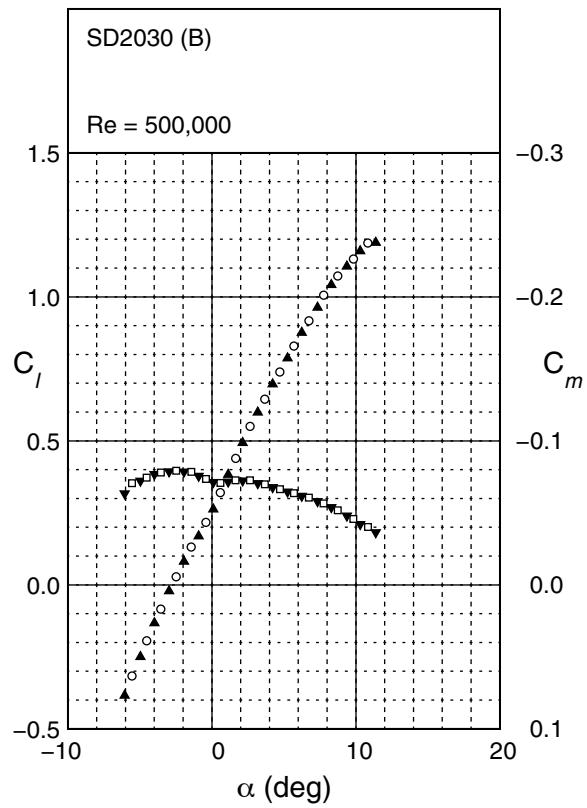
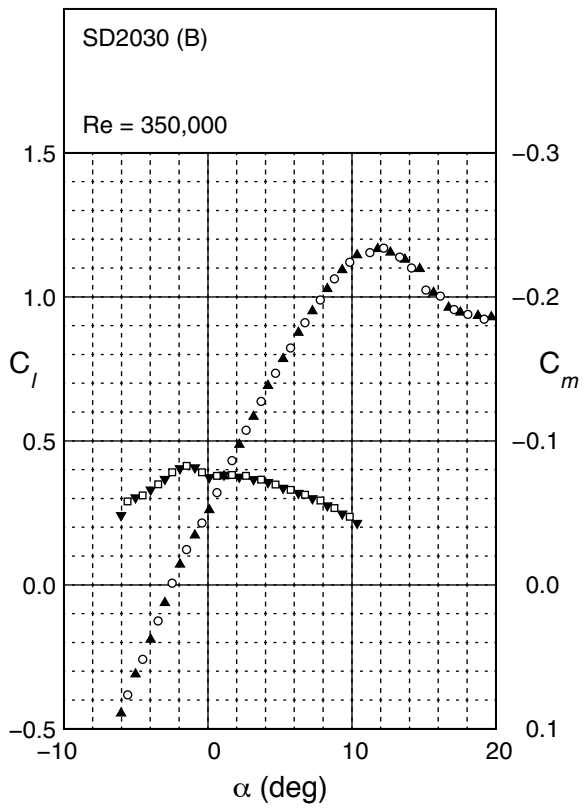


Fig. 5.28





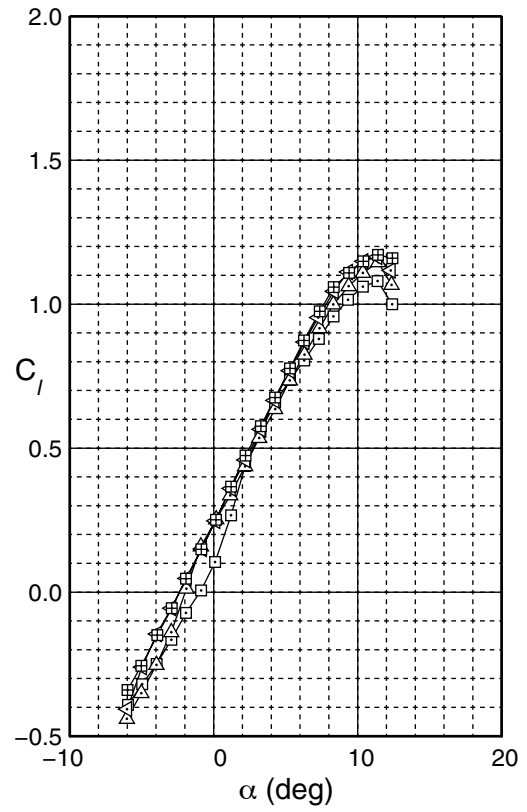
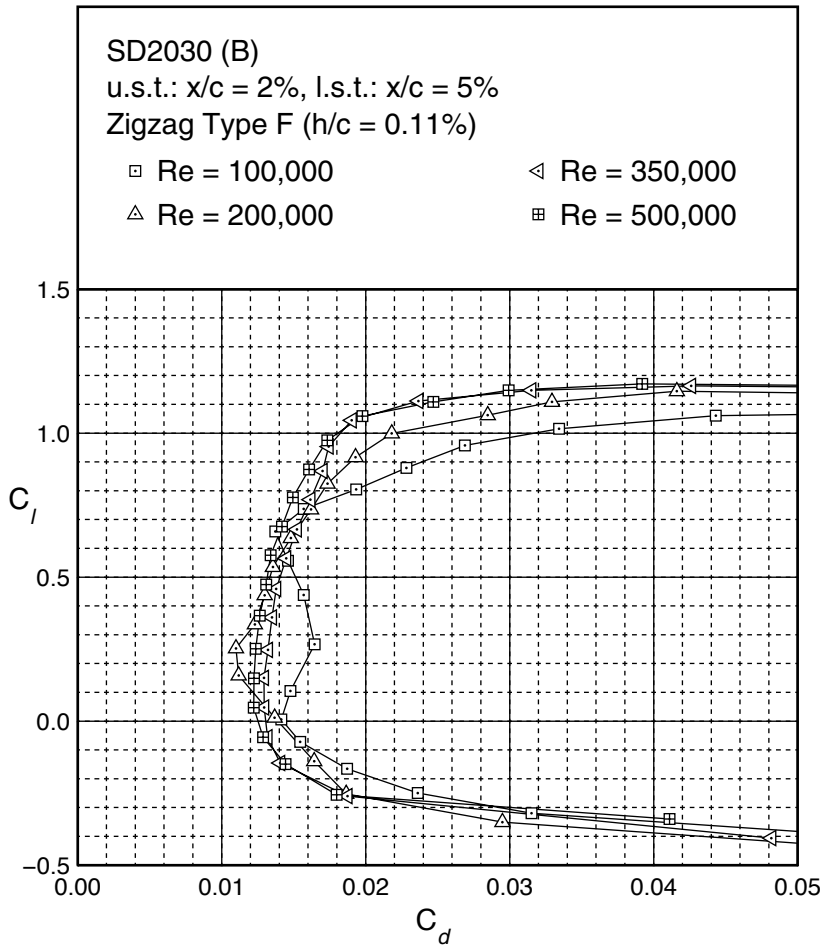
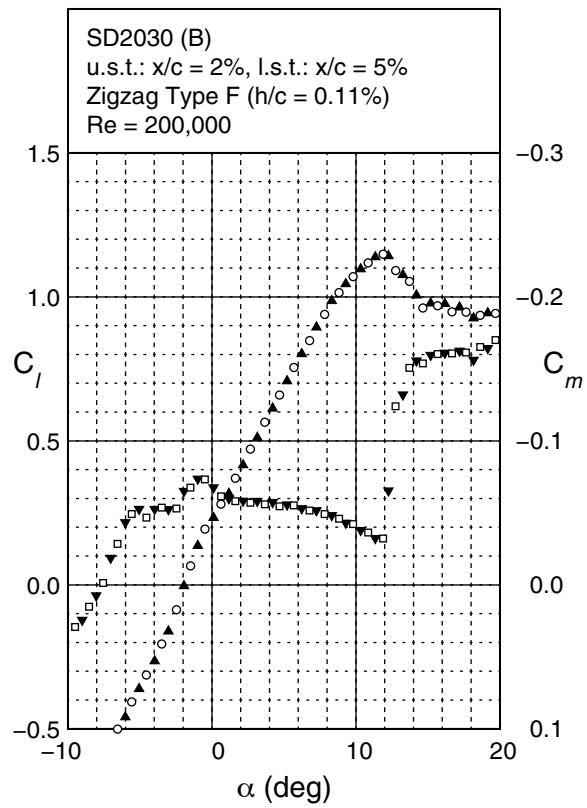
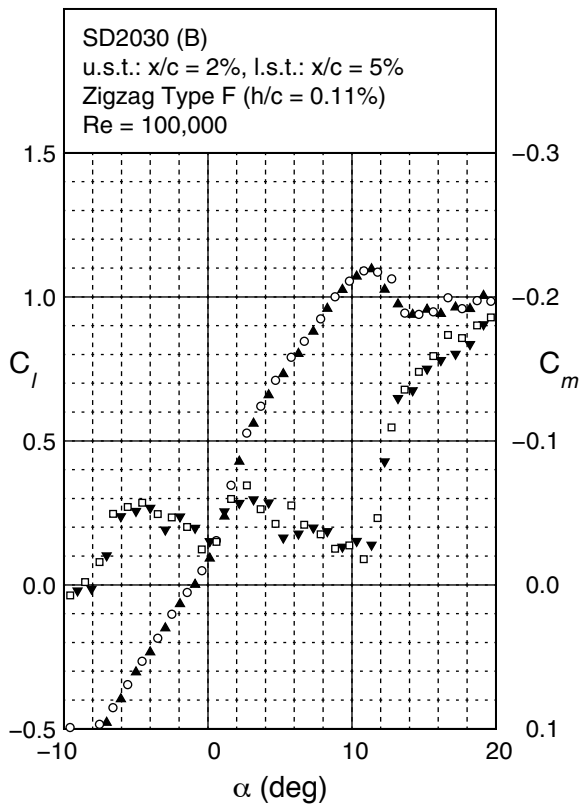


Fig. 5.29



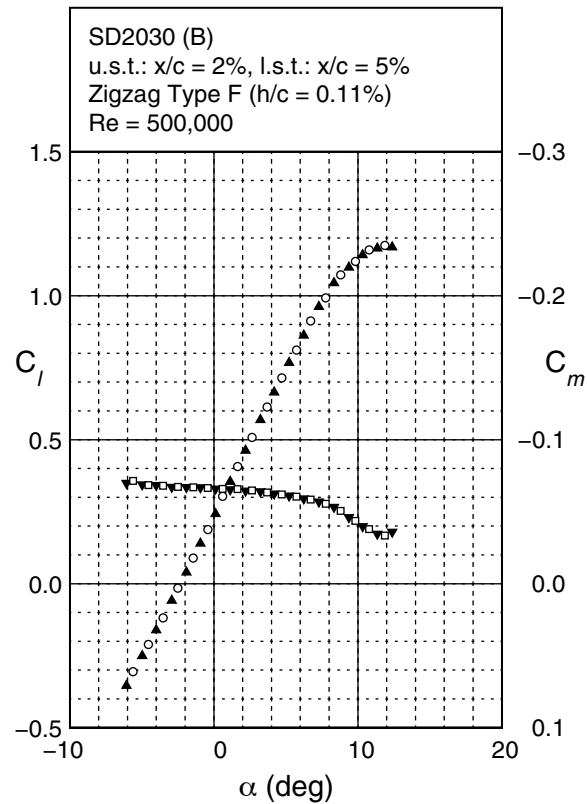
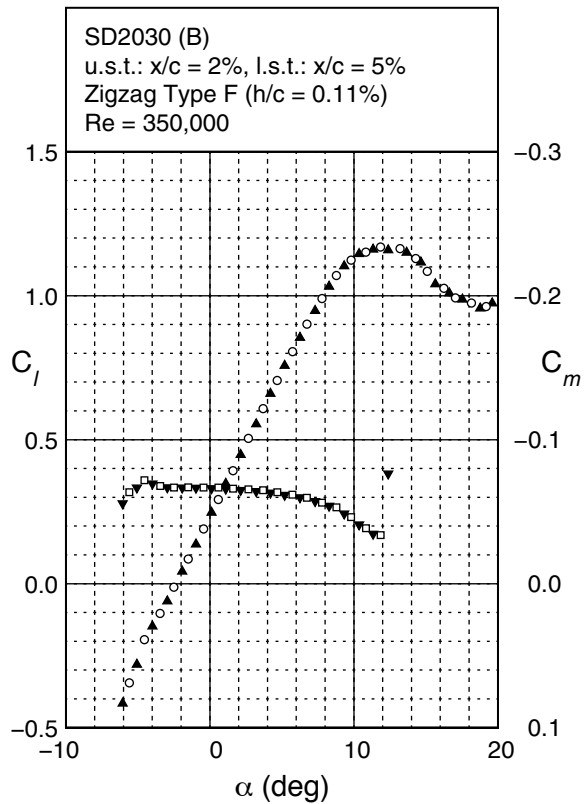
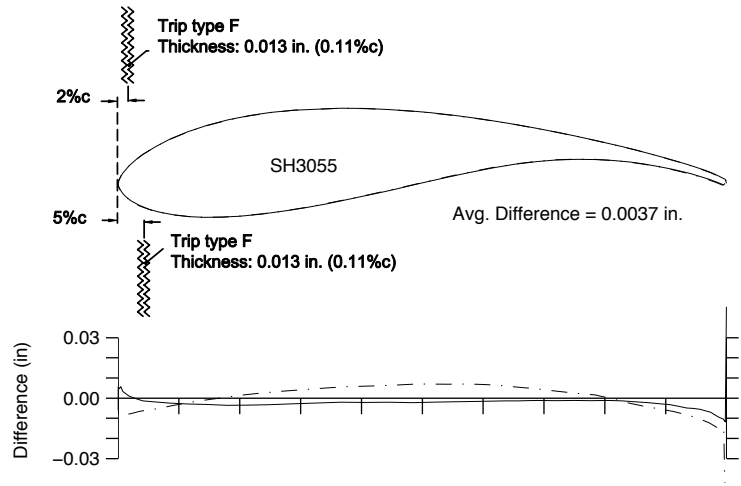
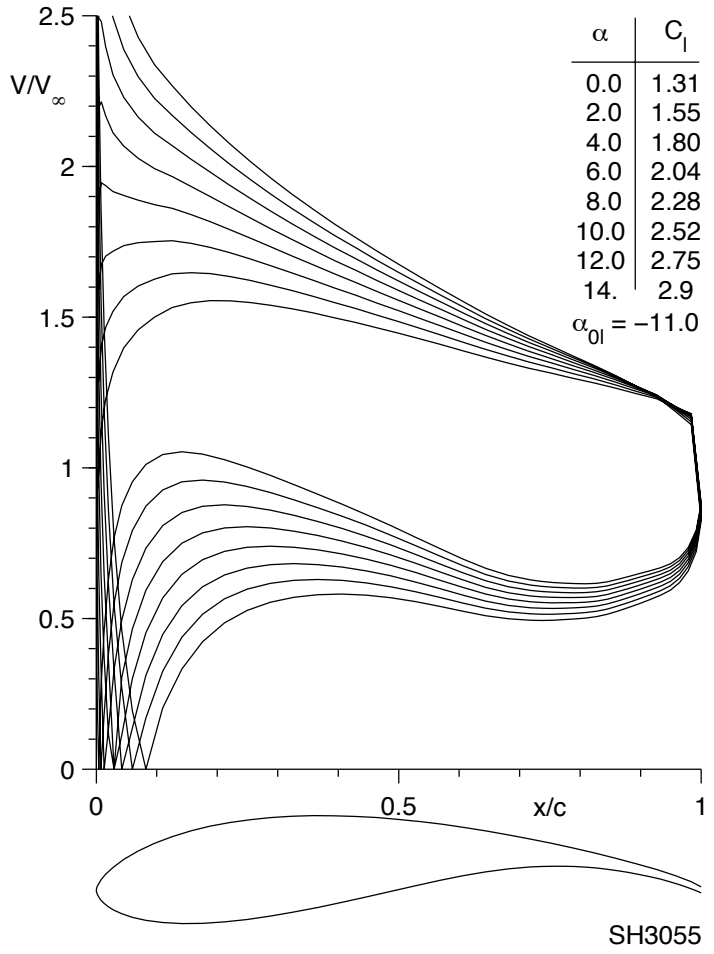


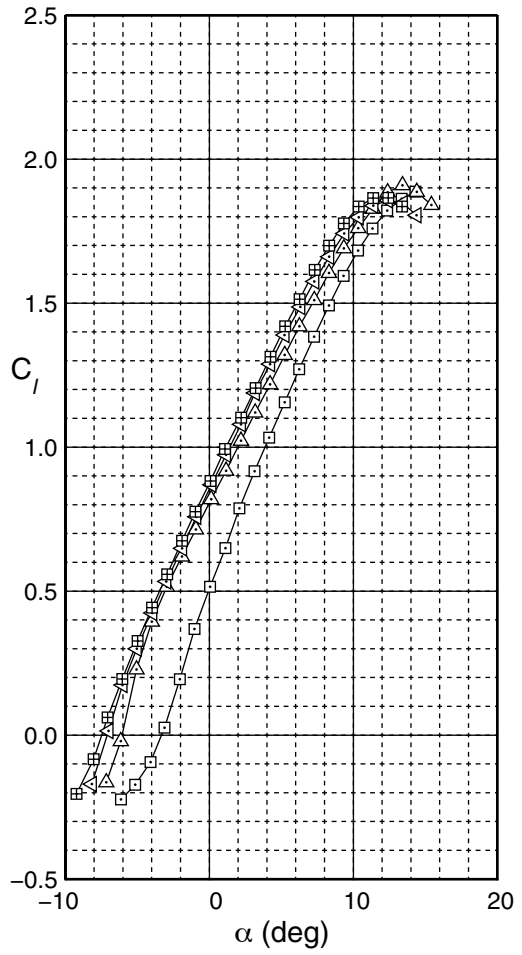
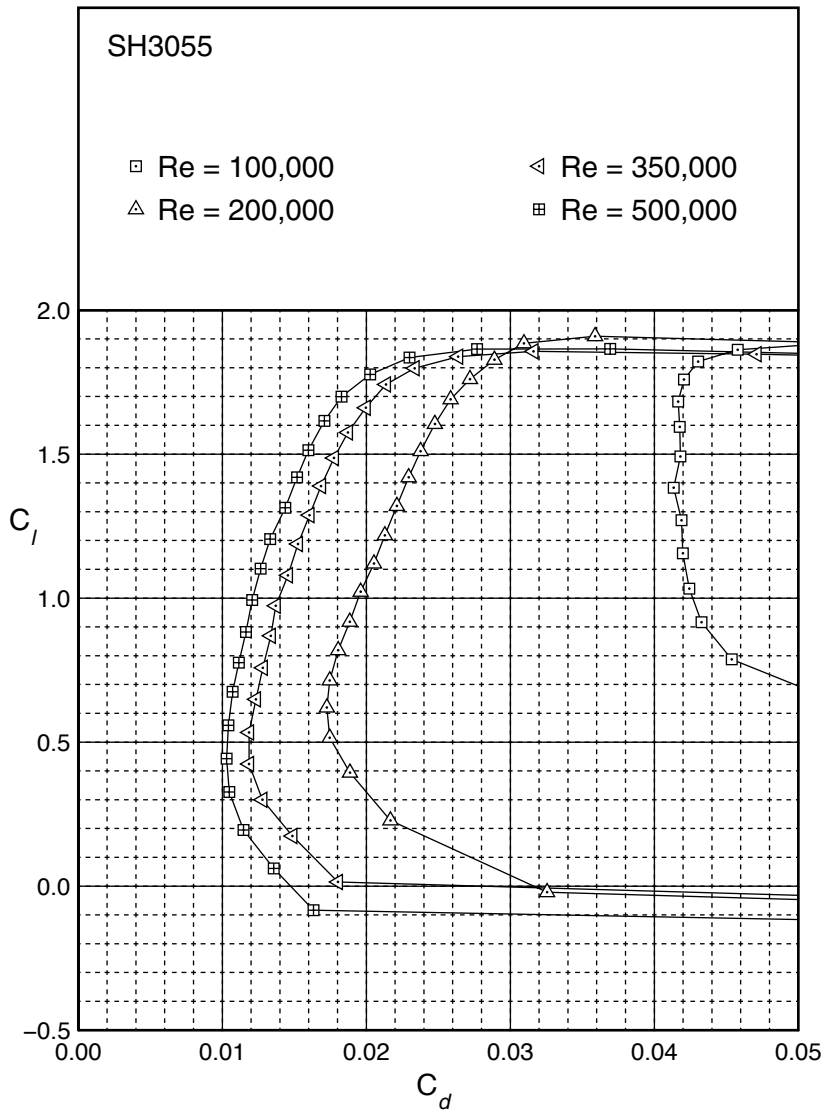
Fig. 5.30 (continued)





Figs. 5.31 & 5.32

Fig. 5.33



SH3055

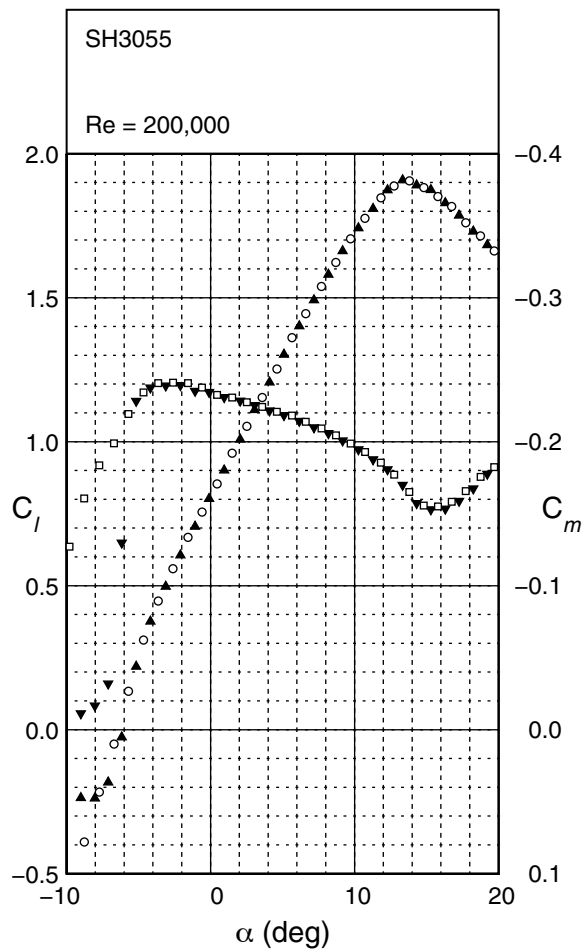
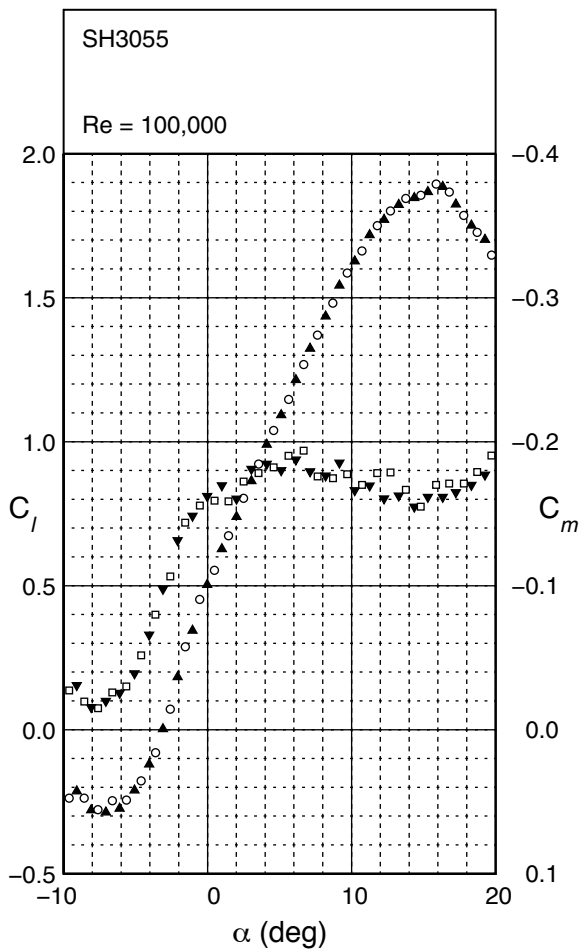


Fig. 5.34

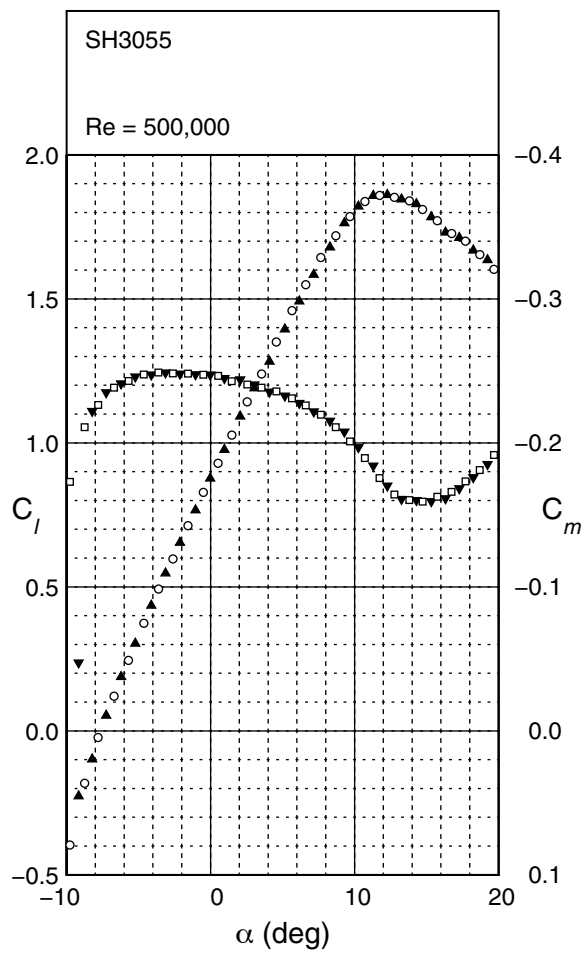
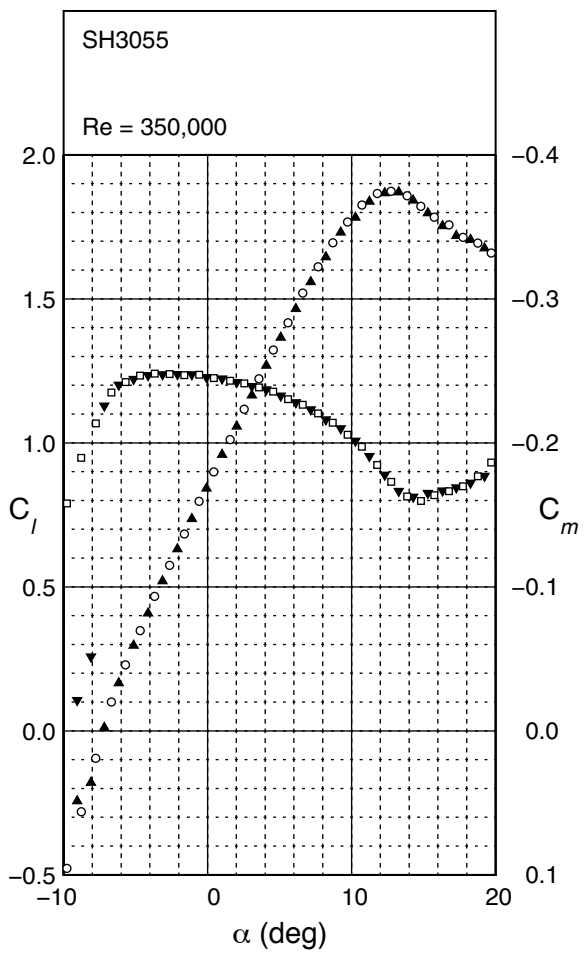




Fig. 5.35

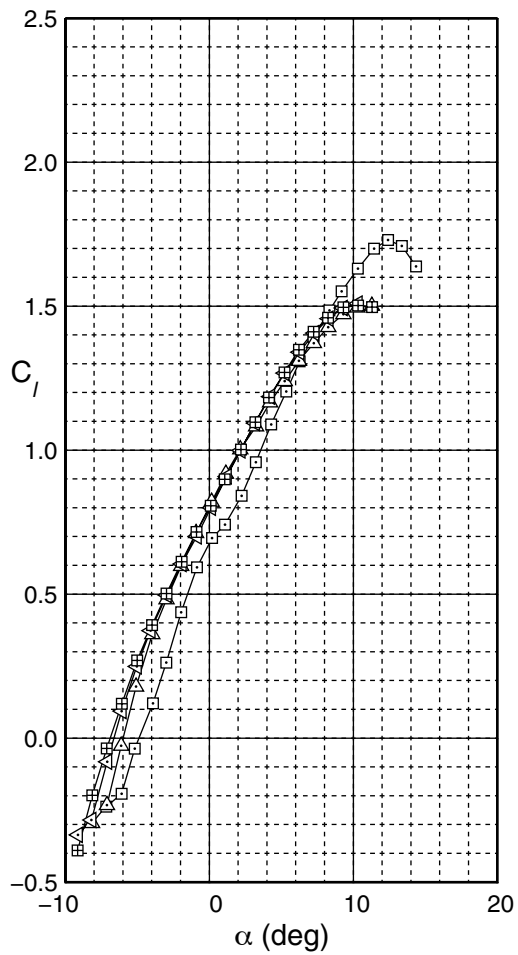
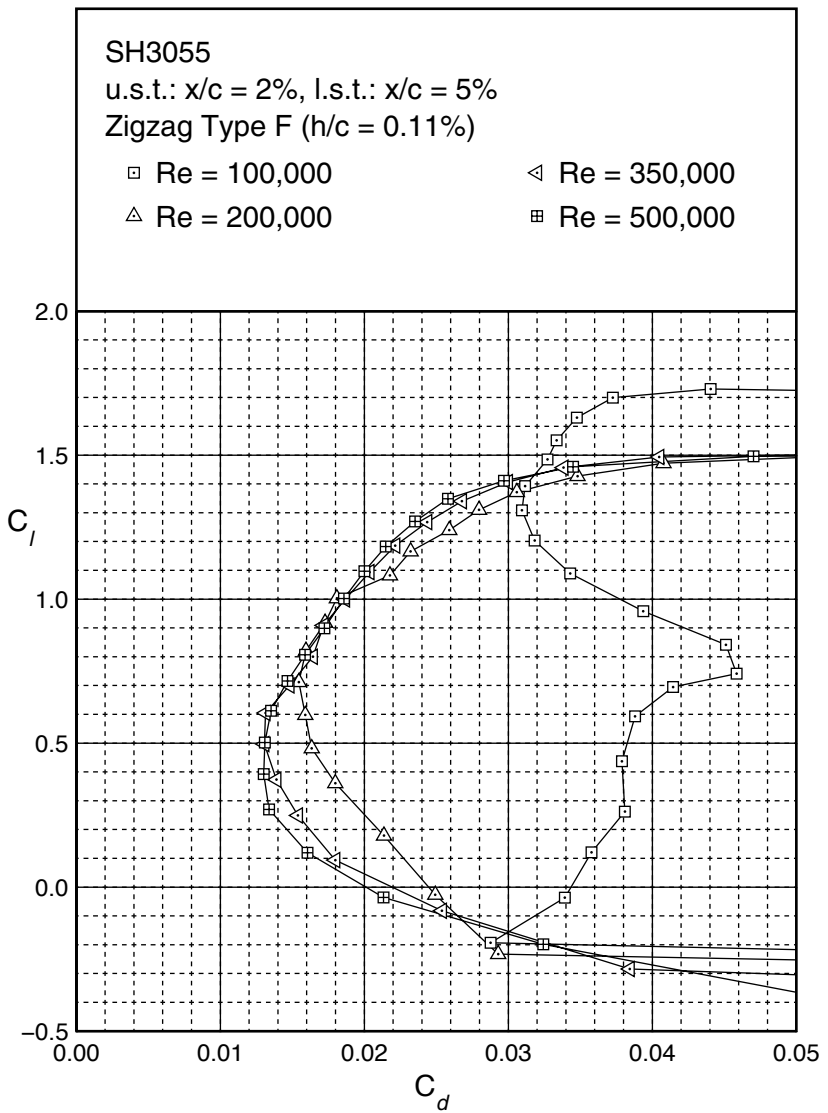
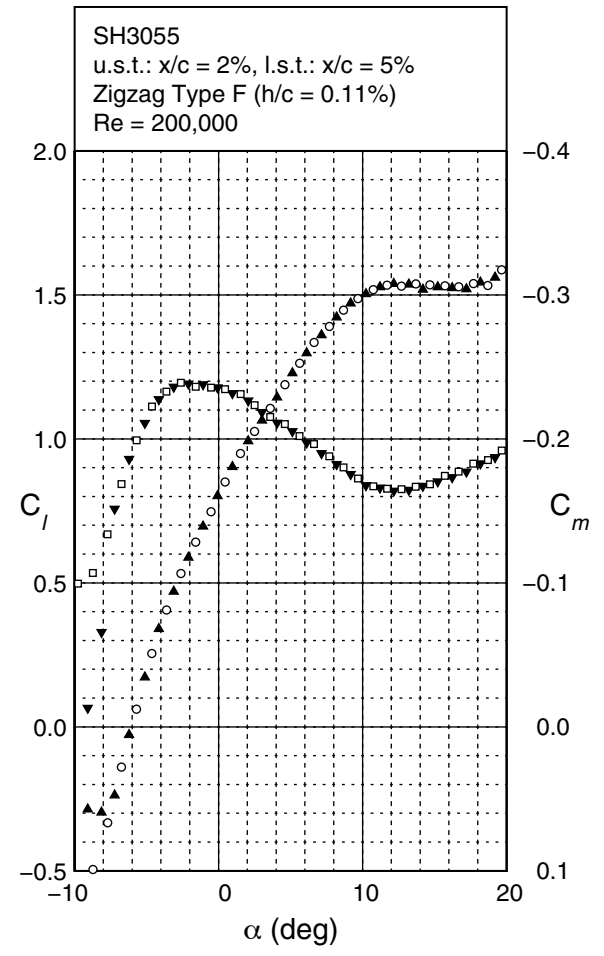
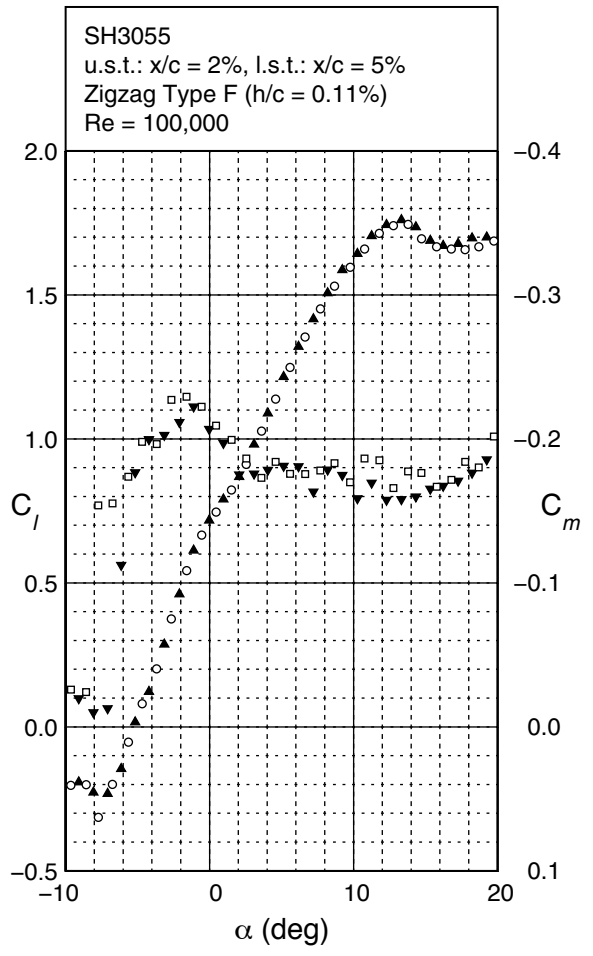


Fig. 5.36



SH3055

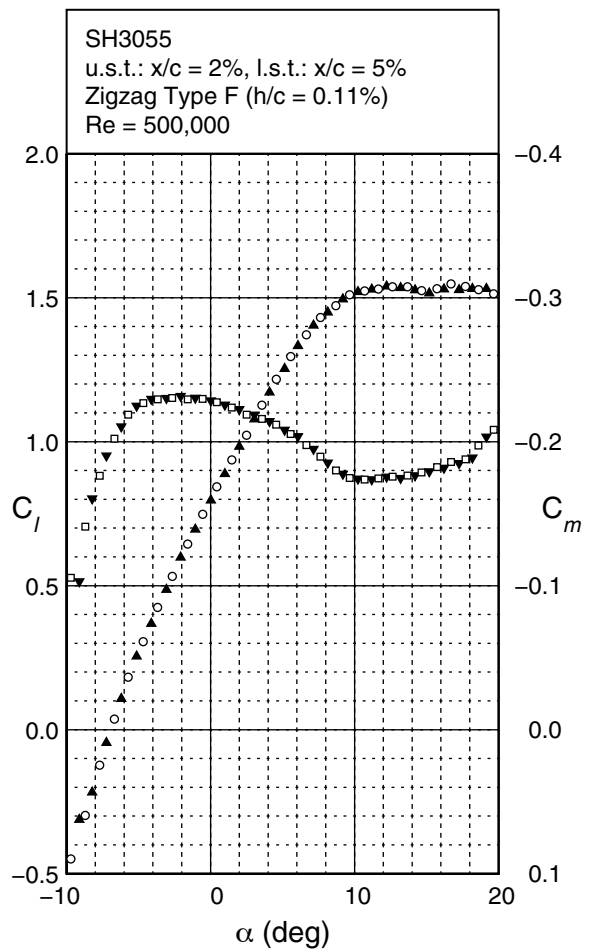
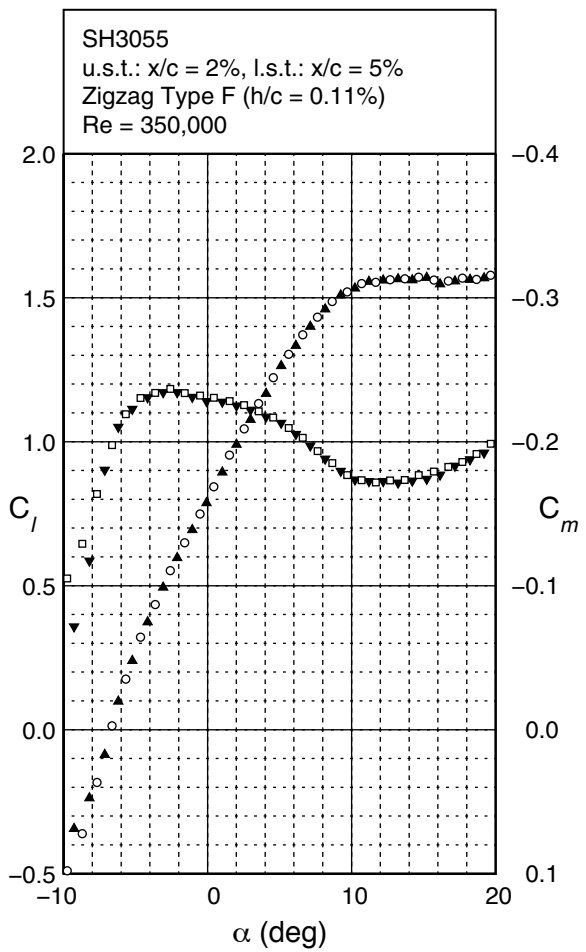


Fig. 5.36 (continued)





---

## References

---

- [1] Oerlemans, S., and Migliore, P., “Wind Tunnel Aeroacoustic Tests of Six Airfoils for Use on Small Wind Turbines,” in preparation, National Renewable Energy Laboratory, Golden, CO, 2003.
- [2] Selig, M.S., Donovan, J.F., and Fraser, D.B., *Airfoils at Low Speeds*, Soartech 8, SoarTech Publications, Virginia Beach, VA, 1989.
- [3] Selig, M.S., Guglielmo, J.J., Broeren, A.P., and Giguère, P., *Summary of Low-Speed Airfoil Data – Vol. 1*, SoarTech Publications, Virginia Beach, VA, 1995.
- [4] Selig, M.S., Lyon, C.A., Giguère, P., Ninham, C.P., and Guglielmo, J.J., *Summary of Low-Speed Airfoil Data – Vol. 2*, SoarTech Publications, Virginia Beach, VA, 1996.
- [5] Lyon, C.A., Broeren, A.P., Giguère, P., Gopalarathnam, A., and Selig, M.S., *Summary of Low-Speed Airfoil Data – Vol. 3*, SoarTech Publications, Virginia Beach, VA, 1997.
- [6] Khodadoust, A., “An Experimental Study of the Flowfield on a Semispan Rectangular Wing with a Simulated Glaze Ice Accretion,” Ph.D. Thesis, University of Illinois at Urbana-Champaign, Dept. of Aeronautical and Astronautical Engineering, 1993.
- [7] Henze, C.M., and Bragg, M.B., “Turbulence Intensity Measurements Technique for Use in Icing Wind Tunnels,” *Journal of Aircraft*, Vol. 36, No. 3, May–June 1999, pp. 577–583.
- [8] Rae, W.H., Jr., and Pope, A., *Low-speed Wind Tunnel Testing*, John Wiley and Sons, New York, 1984.
- [9] Bragg, M.B., and Lu, B., “Experimental Investigation of Airfoil Drag Measurement with Simulated Leading-Edge Ice Using the Wake Survey Method,” AIAA 2000-3919, August 2000.
- [10] Jones, B.M., “The Measurement of Profile Drag by the Pitot Traverse Method,” Aeronautical Research Council, R&M 1688, 1936.
- [11] Schlichting, H., *Boundary Layer Theory*, McGraw-Hill Book Company, New York, 1979.
- [12] Guglielmo, J.J., “Spanwise Variations in Profile Drag for Airfoils at Low Reynolds Numbers,” Master’s Thesis, University of Illinois at Urbana-Champaign, Dept. of Aeronautical and Astronautical Engineering, 1995.
- [13] Guglielmo, J.J., and Selig, M.S., “Spanwise Variations in Profile Drag for Airfoils

- at Low Reynolds Numbers,” *Journal of Aircraft*, Vol. 33, No. 4, July–August 1996, pp. 699–707.
- [14] White, F.M., *Viscous Fluid Flow*, McGraw-Hill, Inc., New York, 1991.
- [15] Giguère, P., and Selig, M.S., “Freestream Velocity Corrections for Two-Dimensional Testing with Splitter Plates,” *AIAA Journal*, Vol. 35, No. 7, July 1997, pp. 1195–1200.
- [16] Coleman, H.W., and Steele, W.G., Jr., *Experimentation and Uncertainty Analysis For Engineers*, John Wiley and Sons, New York, 1989.
- [17] McGhee, R.J., Walker, B.S., and Millard, B.F., “Experimental Results for the Eppler 387 Airfoil at Low Reynolds Numbers in the Langley Low-Turbulence Pressure Tunnel,” NASA TM 4062, October 1988.
- [18] Evangelista, R., McGhee, R.J., and Walker, B.S., “Correlation of Theory to Wind-Tunnel Data at Reynolds Numbers below 500,000,” *Lecture Notes in Engineering: Low Reynolds Number Aerodynamics*, T.J. Mueller (ed.), Vol. 54, Springer-Verlag, New York, June 1989, pp. 131–145.
- [19] Briley, R.W., and McDonald, H., “Numerical Prediction of Incompressible Separation Bubbles,” *Journal of Fluid Mechanics*, Vol. 69, Part 4, 1975, pp. 631–656.
- [20] Kwon, O.K., and Pletcher, R.H., “Prediction of Incompressible Separated Boundary Layers Including Viscous-Inviscid Interaction,” *Transactions of the ASME*, Vol. 101, December 1979, pp. 466–472.
- [21] Davis, R.L., and Carter, J.E., “Analysis of Airfoil Transitional Separation Bubbles,” NASA CR-3791, July 1984.
- [22] Walker, G.J., Subroto, P.H., and Platzler, M.F., “Transition Modeling Effects on Viscous/Inviscid Interaction Analysis of Low Reynolds Number Airfoil Flows Involving Laminar Separation Bubbles,” ASME Paper 88-GT-32, 1988.
- [23] Huebsch, W.W., and Rothmayer, A.P., “The Effects of Small-Scale Surface Roughness on Laminar Airfoil-Scale Trailing Edge Separation Bubbles,” AIAA Paper 98-0103, January 1998.
- [24] Alam, M., and Sandham, N.D., “Direct Numerical Simulation of ‘Short’ Laminar Separation Bubbles with Turbulent Reattachment,” *Journal of Fluid Mechanics*, Vol. 403, 2000, pp. 223–250.
- [25] Lin, J.C.M., and Pauley, L.L., “Low-Reynolds-Number Separation on an Airfoil,” *AIAA Journal*, Vol. 34, No. 8, 1996, pp. 1570–1577.
- [26] Eppler, R. and Somers, D.M., “A Computer Program for the Design and Analysis of Low-Speed Airfoils,” NASA TM 80210, August 1980.
- [27] Eppler, R., *Airfoil Design and Data*, Springer-Verlag, New York, 1990.

- [28] Broeren, A.P., and Bragg, M.B., “Unsteady Stalling Characteristics of Thin Airfoils at Low-Reynolds Numbers,” *Fixed and Flapping Wing Aerodynamics for Micro Air Vehicle Applications*, T.J. Mueller (ed.), *AIAA Progress in Astronautics and Aeronautics*, Vol. 195, AIAA, 2001.
- [29] Somers, D.M., “Subsonic Natural-Laminar-Flow Airfoils,” in *Natural Laminar Flow and Laminar Flow Control*, R.W. Barnwell and M.Y. Hussaini (eds.), Springer-Verlag, New York, 1992, pp. 143–176.
- [30] Althaus, D. and Wortmann, F.X., “Stuttgarter Profilkatalog I,” Friedr. Vieweg & Sohn, Braunschweig/Wiesbaden, 1981. ISBN 3-528-08464-2
- [31] Somers, D.M., and Maughmer, M.D., “Theoretical Aerodynamic Analyses of Six Airfoils for Use on Small Wind Turbines,” National Renewable Energy Laboratory, NREL/SR-500-33295, Golden, CO, April 2003.
- [32] Somers, D.M., “The S822 and S823 Airfoils,” Airfoils, Inc., 1993. [Proprietary to the National Renewable Energy Laboratory]
- [33] Tangler, J.L., and Somers, D.M., “NREL Airfoil Families for HAWTs,” National Renewable Energy Laboratory, TP-442-7109, Golden, CO, Jan 1995.
- [34] Tangler, J.L., and Somers, D.M., “Airfoils for Wind Turbine,” U.S. Patent Number 5562420, October 8, 1996.
- [35] Somers, D.M., “The S833, S834, and S835 Airfoils,” Airfoils, Inc., 2002. [Proprietary to the National Renewable Energy Laboratory]





---

## Appendix A

# Tabulated Airfoil Coordinates

---

This appendix lists both the true (as designed) and actual (as built) airfoil coordinates. For any given airfoil, the true airfoil coordinates are listed first. The S822, S834 and SH3055 coordinates are not listed because they are proprietary.

| <b>E387</b> |          | 1.00000         | 0.00000   | 0.089604          | -0.014936 | 0.597679 | 0.103443  |
|-------------|----------|-----------------|-----------|-------------------|-----------|----------|-----------|
| true        |          |                 |           | 0.114136          | -0.015007 | 0.565416 | 0.108227  |
| $x/c$       | $y/c$    |                 |           | 0.143028          | -0.014687 | 0.532860 | 0.112363  |
| 1.00000     | 0.00000  | <b>E387 (E)</b> |           | 0.171384          | -0.014074 | 0.500172 | 0.115800  |
| 0.99677     | 0.00043  | actual          |           | 0.202734          | -0.013178 | 0.467482 | 0.118486  |
| 0.98729     | 0.00180  | $x/c$           | $y/c$     | 0.235535          | -0.012082 | 0.434928 | 0.120402  |
| 0.97198     | 0.00423  | 1.000000        | 0.000706  | 0.273934          | -0.010661 | 0.402662 | 0.121516  |
| 0.95128     | 0.00763  | 0.999678        | 0.000791  | 0.306347          | -0.009442 | 0.370803 | 0.121810  |
| 0.92554     | 0.01184  | 0.995017        | 0.001842  | 0.342832          | -0.008082 | 0.339511 | 0.121281  |
| 0.89510     | 0.01679  | 0.991921        | 0.002437  | 0.378570          | -0.006776 | 0.308896 | 0.119930  |
| 0.86035     | 0.02242  | 0.982490        | 0.004061  | 0.416413          | -0.005431 | 0.279098 | 0.117766  |
| 0.82183     | 0.02866  | 0.973277        | 0.005591  | 0.457857          | -0.003984 | 0.250257 | 0.114799  |
| 0.78007     | 0.03540  | 0.958633        | 0.008062  | 0.496093          | -0.002702 | 0.222474 | 0.111077  |
| 0.73567     | 0.04249  | 0.926344        | 0.013343  | 0.539972          | -0.001324 | 0.195888 | 0.106652  |
| 0.68922     | 0.04975  | 0.909852        | 0.016057  | 0.583917          | -0.000082 | 0.170610 | 0.101562  |
| 0.64136     | 0.05696  | 0.889160        | 0.019465  | 0.620305          | 0.000811  | 0.146729 | 0.095877  |
| 0.59272     | 0.06390  | 0.866125        | 0.023222  | 0.656351          | 0.001577  | 0.124377 | 0.089656  |
| 0.54394     | 0.07020  | 0.842670        | 0.027047  | 0.688568          | 0.002129  | 0.103623 | 0.082960  |
| 0.49549     | 0.07546  | 0.817387        | 0.031154  | 0.723435          | 0.002627  | 0.084568 | 0.075838  |
| 0.44767     | 0.07936  | 0.787247        | 0.036040  | 0.754643          | 0.002982  | 0.067301 | 0.068359  |
| 0.40077     | 0.08173  | 0.759532        | 0.040496  | 0.785321          | 0.003185  | 0.051883 | 0.060564  |
| 0.35505     | 0.08247  | 0.726804        | 0.045702  | 0.811327          | 0.003292  | 0.038374 | 0.052482  |
| 0.31078     | 0.08156  | 0.694176        | 0.050803  | 0.839117          | 0.003322  | 0.026854 | 0.044103  |
| 0.26813     | 0.07908  | 0.659004        | 0.056198  | 0.864230          | 0.003255  | 0.017353 | 0.035426  |
| 0.22742     | 0.07529  | 0.622656        | 0.061560  | 0.888306          | 0.003076  | 0.009932 | 0.026653  |
| 0.18906     | 0.07037  | 0.589064        | 0.066242  | 0.910334          | 0.002841  | 0.004602 | 0.018262  |
| 0.15345     | 0.06448  | 0.551907        | 0.070969  | 0.926935          | 0.002510  | 0.001396 | 0.010983  |
| 0.12094     | 0.05775  | 0.510670        | 0.075532  | 0.944962          | 0.001938  | 0.000000 | 0.003558  |
| 0.09185     | 0.05033  | 0.476873        | 0.078647  | 0.961010          | 0.001195  | 0.000329 | 0.000467  |
| 0.06643     | 0.04238  | 0.437853        | 0.081396  | 0.973032          | 0.000543  | 0.001389 | -0.002407 |
| 0.04493     | 0.03408  | 0.397082        | 0.083151  | 0.988335          | -0.000256 | 0.004595 | -0.006298 |
| 0.02748     | 0.02562  | 0.359760        | 0.083690  | 0.993532          | -0.000492 | 0.009923 | -0.009727 |
| 0.01423     | 0.01726  | 0.284936        | 0.081342  | 0.997747          | -0.000619 | 0.017353 | -0.012634 |
| 0.00519     | 0.00931  | 0.249194        | 0.078551  | 0.999577          | -0.000588 | 0.026844 | -0.015058 |
| 0.00044     | 0.00234  | 0.209825        | 0.074182  | 0.999959          | -0.000562 | 0.038367 | -0.017059 |
| 0.00091     | -0.00286 | 0.179829        | 0.069843  |                   |           | 0.051871 | -0.018697 |
| 0.00717     | -0.00682 | 0.144677        | 0.063511  | <b>FX 63-137</b>  |           | 0.067287 | -0.020021 |
| 0.01890     | -0.01017 | 0.118041        | 0.057682  | smoothed, Ref. 31 |           | 0.084563 | -0.021073 |
| 0.03596     | -0.01265 | 0.092257        | 0.050985  | true              |           | 0.103610 | -0.021871 |
| 0.05827     | -0.01425 | 0.066657        | 0.042878  | $x/c$             | $y/c$     | 0.124359 | -0.022385 |
| 0.08569     | -0.01500 | 0.045215        | 0.034472  | 1.000000          | 0.000001  | 0.146718 | -0.022604 |
| 0.11800     | -0.01502 | 0.027607        | 0.025873  | 0.998926          | 0.000545  | 0.170588 | -0.022519 |
| 0.15490     | -0.01441 | 0.015156        | 0.018258  | 0.995721          | 0.002116  | 0.195880 | -0.022099 |
| 0.19599     | -0.01329 | 0.008243        | 0.012848  | 0.990390          | 0.004625  | 0.222463 | -0.021323 |
| 0.24083     | -0.01177 | 0.006684        | 0.011366  | 0.982962          | 0.007902  | 0.250237 | -0.020162 |
| 0.28892     | -0.00998 | 0.004741        | 0.009284  | 0.973465          | 0.011745  | 0.279083 | -0.018615 |
| 0.33968     | -0.00804 | 0.003353        | 0.007609  | 0.961950          | 0.015966  | 0.308880 | -0.016641 |
| 0.39252     | -0.00605 | 0.002206        | 0.006012  | 0.948446          | 0.020465  | 0.339489 | -0.014250 |
| 0.44679     | -0.00410 | 0.001354        | 0.004632  | 0.933033          | 0.025219  | 0.370789 | -0.011461 |
| 0.50182     | -0.00228 | 0.000639        | 0.003148  | 0.915761          | 0.030251  | 0.402640 | -0.008274 |
| 0.55694     | -0.00065 | 0.000136        | 0.001489  | 0.896710          | 0.035579  | 0.434913 | -0.004759 |
| 0.61147     | 0.00074  | 0.000002        | 0.000164  | 0.875959          | 0.041202  | 0.500161 | 0.002959  |
| 0.66472     | 0.00186  | 0.000017        | -0.000523 | 0.853600          | 0.047122  | 0.532845 | 0.006943  |
| 0.71602     | 0.00268  | 0.000245        | -0.001706 | 0.829732          | 0.053297  | 0.565400 | 0.010847  |
| 0.76475     | 0.00320  | 0.000972        | -0.003167 | 0.804445          | 0.059687  | 0.597673 | 0.014552  |
| 0.81027     | 0.00342  | 0.001656        | -0.004032 | 0.777858          | 0.066232  | 0.629525 | 0.017929  |
| 0.85202     | 0.00337  | 0.004841        | -0.006361 | 0.750081          | 0.072870  | 0.660826 | 0.020888  |
| 0.88944     | 0.00307  | 0.007808        | -0.007724 | 0.721245          | 0.079493  | 0.691435 | 0.023369  |
| 0.92205     | 0.00258  | 0.013461        | -0.009542 | 0.691448          | 0.085989  | 0.721232 | 0.025313  |
| 0.94942     | 0.00196  | 0.018565        | -0.010677 | 0.660840          | 0.092218  | 0.750077 | 0.026690  |
| 0.97118     | 0.00132  | 0.030536        | -0.012338 | 0.629540          | 0.098079  | 0.777860 | 0.027481  |
| 0.98705     | 0.00071  | 0.045514        | -0.013506 |                   |           | 0.804441 | 0.027687  |
| 0.99674     | 0.00021  | 0.065671        | -0.014411 |                   |           | 0.829730 | 0.027297  |
|             |          |                 |           |                   |           | 0.853596 | 0.026332  |

|          |          |          |           |         |          |          |           |
|----------|----------|----------|-----------|---------|----------|----------|-----------|
| 0.875961 | 0.024852 | 0.000239 | -0.002725 | 0.86252 | 0.02564  | 0.978111 | 0.005632  |
| 0.896705 | 0.022919 | 0.000554 | -0.004175 | 0.82542 | 0.03150  | 0.964628 | 0.008198  |
| 0.915756 | 0.020611 | 0.001879 | -0.007373 | 0.78512 | 0.03742  | 0.952429 | 0.010534  |
| 0.933027 | 0.017999 | 0.003306 | -0.009321 | 0.74219 | 0.04320  | 0.937969 | 0.013285  |
| 0.948447 | 0.015124 | 0.006598 | -0.012181 | 0.69709 | 0.04856  | 0.921246 | 0.016435  |
| 0.961946 | 0.012096 | 0.010118 | -0.014205 | 0.65019 | 0.05328  | 0.898887 | 0.020559  |
| 0.973466 | 0.009025 | 0.014800 | -0.016199 | 0.60189 | 0.05724  | 0.876788 | 0.024469  |
| 0.982965 | 0.006112 | 0.024765 | -0.019038 | 0.55259 | 0.06038  | 0.856660 | 0.027843  |
| 0.990386 | 0.003585 | 0.039500 | -0.021554 | 0.50273 | 0.06268  | 0.832654 | 0.031657  |
| 0.995719 | 0.001636 | 0.062720 | -0.023874 | 0.45282 | 0.06415  | 0.805844 | 0.035693  |
| 0.998925 | 0.000415 | 0.086431 | -0.025281 | 0.40336 | 0.06478  | 0.776443 | 0.039874  |
| 1.000000 | 0.000001 | 0.113905 | -0.026153 | 0.35488 | 0.06460  | 0.749193 | 0.043482  |
|          |          | 0.141969 | -0.026389 | 0.30788 | 0.06360  | 0.716934 | 0.047411  |
|          |          | 0.169331 | -0.026170 | 0.26288 | 0.06179  | 0.684588 | 0.050959  |
|          |          | 0.199932 | -0.025452 | 0.22034 | 0.05917  | 0.650257 | 0.054286  |
|          |          | 0.234658 | -0.024121 | 0.18069 | 0.05576  | 0.614913 | 0.057225  |
|          |          | 0.270149 | -0.022201 | 0.14432 | 0.05157  | 0.578935 | 0.059754  |
|          |          | 0.306575 | -0.019712 | 0.11158 | 0.04664  | 0.541977 | 0.061855  |
|          |          | 0.343245 | -0.016692 | 0.08273 | 0.04100  | 0.509502 | 0.063300  |
|          |          | 0.379412 | -0.013261 | 0.05798 | 0.03475  | 0.462396 | 0.064715  |
|          |          | 0.415039 | -0.009441 | 0.03752 | 0.02803  | 0.425852 | 0.065293  |
|          |          | 0.456772 | -0.004530 | 0.02150 | 0.02096  | 0.382439 | 0.065404  |
|          |          | 0.498683 | 0.000739  | 0.00995 | 0.01371  | 0.347597 | 0.065041  |
|          |          | 0.544736 | 0.006575  | 0.00281 | 0.00657  | 0.309062 | 0.064166  |
|          |          | 0.582318 | 0.011214  | 0.00000 | 0.00017  | 0.271723 | 0.062729  |
|          |          | 0.614845 | 0.014968  | 0.00249 | -0.00501 | 0.233653 | 0.060516  |
|          |          | 0.648353 | 0.018421  | 0.01071 | -0.00935 | 0.202194 | 0.058060  |
|          |          | 0.683009 | 0.021515  | 0.02419 | -0.01306 | 0.169023 | 0.054766  |
|          |          | 0.719669 | 0.024104  | 0.04296 | -0.01601 | 0.137449 | 0.050782  |
|          |          | 0.751225 | 0.025679  | 0.06693 | -0.01829 | 0.105676 | 0.045635  |
|          |          | 0.780586 | 0.026524  | 0.09584 | -0.01997 | 0.079389 | 0.040180  |
|          |          | 0.813195 | 0.026666  | 0.12941 | -0.02113 | 0.054264 | 0.033490  |
|          |          | 0.838777 | 0.026107  | 0.16727 | -0.02183 | 0.037618 | 0.027841  |
|          |          | 0.862827 | 0.024999  | 0.20896 | -0.02213 | 0.018425 | 0.019152  |
|          |          | 0.882701 | 0.023575  | 0.25401 | -0.02207 | 0.009028 | 0.013011  |
|          |          | 0.903888 | 0.021510  | 0.30191 | -0.02170 | 0.005563 | 0.009948  |
|          |          | 0.913534 | 0.020353  | 0.35208 | -0.02106 | 0.003232 | 0.007386  |
|          |          | 0.927285 | 0.018453  | 0.40396 | -0.02018 | 0.003452 | 0.007653  |
|          |          | 0.934256 | 0.017361  | 0.45693 | -0.01908 | 0.001999 | 0.005682  |
|          |          | 0.944892 | 0.015498  | 0.51038 | -0.01780 | 0.001216 | 0.004364  |
|          |          | 0.951641 | 0.014145  | 0.56368 | -0.01634 | 0.001083 | 0.004099  |
|          |          | 0.959647 | 0.012300  | 0.61621 | -0.01471 | 0.000700 | 0.003220  |
|          |          | 0.967000 | 0.010398  | 0.66738 | -0.01286 | 0.000365 | 0.002331  |
|          |          | 0.974946 | 0.008106  | 0.71670 | -0.01076 | 0.000291 | 0.002044  |
|          |          | 0.981085 | 0.006159  | 0.76373 | -0.00848 | 0.000084 | 0.001117  |
|          |          | 0.985996 | 0.004491  | 0.80802 | -0.00616 | 0.000055 | 0.000849  |
|          |          | 0.991222 | 0.002657  | 0.84906 | -0.00398 | 0.000002 | -0.000169 |
|          |          | 0.995348 | 0.001256  | 0.88632 | -0.00210 | 0.000367 | -0.002179 |
|          |          | 0.997500 | 0.000367  | 0.91925 | -0.00066 | 0.001105 | -0.003732 |
|          |          | 0.999500 | -0.000200 | 0.94728 | 0.00024  | 0.002386 | -0.005317 |
|          |          | 1.000000 | 0.000000  | 0.96985 | 0.00059  | 0.004827 | -0.007260 |
|          |          |          |           | 0.98643 | 0.00049  | 0.008782 | -0.009345 |
|          |          |          |           | 0.99659 | 0.00017  | 0.012457 | -0.010770 |
|          |          |          |           | 1.00000 | 0.00000  | 0.020021 | -0.012860 |
|          |          |          |           |         |          | 0.030924 | -0.014875 |
|          |          |          |           |         |          | 0.045480 | -0.016743 |
|          |          |          |           |         |          | 0.060281 | -0.018141 |
|          |          |          |           |         |          | 0.078760 | -0.019477 |
|          |          |          |           |         |          | 0.103394 | -0.020723 |
|          |          |          |           |         |          | 0.127385 | -0.021533 |
|          |          |          |           |         |          | 0.155387 | -0.022099 |
|          |          |          |           |         |          | 0.182581 | -0.022426 |
|          |          |          |           |         |          | 0.215392 | -0.022576 |
|          |          |          |           |         |          | 0.250143 | -0.022531 |
|          |          |          |           |         |          | 0.284425 | -0.022325 |

|                      |          |  |  |  |  |  |  |
|----------------------|----------|--|--|--|--|--|--|
| <b>FX 63-137 (C)</b> |          |  |  |  |  |  |  |
| actual               |          |  |  |  |  |  |  |
| $x/c$                | $y/c$    |  |  |  |  |  |  |
| 1.000000             | 0.001313 |  |  |  |  |  |  |
| 0.998244             | 0.002655 |  |  |  |  |  |  |
| 0.991870             | 0.005587 |  |  |  |  |  |  |
| 0.984488             | 0.008637 |  |  |  |  |  |  |
| 0.975411             | 0.012071 |  |  |  |  |  |  |
| 0.967994             | 0.014670 |  |  |  |  |  |  |
| 0.956278             | 0.018539 |  |  |  |  |  |  |
| 0.940983             | 0.023300 |  |  |  |  |  |  |
| 0.925965             | 0.027731 |  |  |  |  |  |  |
| 0.910530             | 0.032107 |  |  |  |  |  |  |
| 0.892025             | 0.037167 |  |  |  |  |  |  |
| 0.871596             | 0.042586 |  |  |  |  |  |  |
| 0.849029             | 0.048423 |  |  |  |  |  |  |
| 0.824949             | 0.054516 |  |  |  |  |  |  |
| 0.799019             | 0.060894 |  |  |  |  |  |  |
| 0.774258             | 0.066824 |  |  |  |  |  |  |
| 0.745917             | 0.073388 |  |  |  |  |  |  |
| 0.712650             | 0.080748 |  |  |  |  |  |  |
| 0.675421             | 0.088419 |  |  |  |  |  |  |
| 0.644195             | 0.094320 |  |  |  |  |  |  |
| 0.609250             | 0.100263 |  |  |  |  |  |  |
| 0.572616             | 0.105691 |  |  |  |  |  |  |
| 0.534589             | 0.110443 |  |  |  |  |  |  |
| 0.500139             | 0.113917 |  |  |  |  |  |  |
| 0.457814             | 0.117057 |  |  |  |  |  |  |
| 0.419094             | 0.118802 |  |  |  |  |  |  |
| 0.380510             | 0.119413 |  |  |  |  |  |  |
| 0.341855             | 0.118831 |  |  |  |  |  |  |
| 0.303394             | 0.116934 |  |  |  |  |  |  |
| 0.263286             | 0.113454 |  |  |  |  |  |  |
| 0.232180             | 0.109598 |  |  |  |  |  |  |
| 0.196149             | 0.103709 |  |  |  |  |  |  |
| 0.131179             | 0.088412 |  |  |  |  |  |  |
| 0.103669             | 0.079594 |  |  |  |  |  |  |
| 0.077368             | 0.069346 |  |  |  |  |  |  |
| 0.065275             | 0.063834 |  |  |  |  |  |  |
| 0.052393             | 0.057195 |  |  |  |  |  |  |
| 0.044238             | 0.052481 |  |  |  |  |  |  |
| 0.032913             | 0.044958 |  |  |  |  |  |  |
| 0.025099             | 0.038803 |  |  |  |  |  |  |
| 0.018504             | 0.032701 |  |  |  |  |  |  |
| 0.012711             | 0.026302 |  |  |  |  |  |  |
| 0.007208             | 0.018783 |  |  |  |  |  |  |
| 0.004261             | 0.013634 |  |  |  |  |  |  |
| 0.002778             | 0.010443 |  |  |  |  |  |  |
| 0.001421             | 0.006806 |  |  |  |  |  |  |

|  |  |               |         |  |  |  |  |
|--|--|---------------|---------|--|--|--|--|
|  |  | <b>SD2030</b> |         |  |  |  |  |
|  |  | true          |         |  |  |  |  |
|  |  | $x/c$         | $y/c$   |  |  |  |  |
|  |  | 1.00000       | 0.00000 |  |  |  |  |
|  |  | 0.99665       | 0.00049 |  |  |  |  |
|  |  | 0.98686       | 0.00212 |  |  |  |  |
|  |  | 0.97128       | 0.00510 |  |  |  |  |
|  |  | 0.95059       | 0.00930 |  |  |  |  |
|  |  | 0.92535       | 0.01438 |  |  |  |  |
|  |  | 0.89593       | 0.01992 |  |  |  |  |

|  |  |  |  |                   |          |  |  |
|--|--|--|--|-------------------|----------|--|--|
|  |  |  |  | <b>SD2030 (B)</b> |          |  |  |
|  |  |  |  | actual            |          |  |  |
|  |  |  |  | $x/c$             | $y/c$    |  |  |
|  |  |  |  | 1.000000          | 0.001244 |  |  |
|  |  |  |  | 0.997810          | 0.001763 |  |  |
|  |  |  |  | 0.993566          | 0.002637 |  |  |
|  |  |  |  | 0.989659          | 0.003401 |  |  |

|          |           |
|----------|-----------|
| 0.315982 | -0.021997 |
| 0.356811 | -0.021449 |
| 0.394872 | -0.020804 |
| 0.434925 | -0.019996 |
| 0.473638 | -0.019089 |
| 0.517944 | -0.017910 |
| 0.559838 | -0.016689 |
| 0.601458 | -0.015331 |
| 0.640293 | -0.013892 |
| 0.672580 | -0.012581 |
| 0.708510 | -0.010954 |
| 0.738725 | -0.009514 |
| 0.772357 | -0.007844 |
| 0.801698 | -0.006311 |
| 0.827471 | -0.004908 |
| 0.854750 | -0.003410 |
| 0.880418 | -0.002111 |
| 0.903866 | -0.001022 |
| 0.924746 | -0.000303 |
| 0.943464 | -0.000008 |
| 0.962993 | -0.000062 |
| 0.977885 | -0.000365 |
| 0.987624 | -0.000465 |
| 0.995730 | -0.000397 |
| 0.997387 | -0.000385 |
| 0.998748 | -0.000325 |
| 1.000000 | -0.000243 |

---

## Appendix B

# Tabulated Polar Data

---

All of the polar data shown in Chapter 5 are listed in this appendix and identified by airfoil name, figure number, and run number. Also included here is the lift and moment data presented in the  $C_l$ - $\alpha$  and  $C_m$ - $\alpha$  curves of Chapter 5. Note that runs using the more-rigid lift carriage (mentioned in Chapter 4) do not include moment data, and thus the moment column shows “N/A” where the moment data would otherwise be.

|                            |        |        |                |        |        |                            |        |        |                            |        |        |
|----------------------------|--------|--------|----------------|--------|--------|----------------------------|--------|--------|----------------------------|--------|--------|
| <hr/>                      |        |        | 8.14           | 1.201  | 0.0176 | 5.08                       | 0.941  | 0.0091 | -2.13                      | 0.163  | 0.0112 |
| <b>E387 (E)</b>            |        |        | 9.15           | 1.241  | 0.0246 | 6.11                       | 1.047  | 0.0099 | -1.09                      | 0.262  | 0.0113 |
| Fig. 5.3 ( $C_l$ & $C_d$ ) |        |        | 10.12          | 1.250  | 0.0343 | 7.15                       | 1.129  | 0.0128 | -0.09                      | 0.364  | 0.0122 |
| Run: BM05141               |        |        | 11.16          | 1.245  | 0.0537 | 8.14                       | 1.195  | 0.0169 | 0.97                       | 0.464  | 0.0127 |
| $Re = 100,029$             |        |        | 12.17          | 1.236  | 0.0774 | 9.14                       | 1.244  | 0.0226 | 2.00                       | 0.569  | 0.0136 |
| $\alpha$                   | $C_l$  | $C_d$  | Run: BM04983   |        |        | 10.09                      | 1.259  | 0.0300 | 2.98                       | 0.677  | 0.0146 |
| -5.25                      | -0.292 | 0.0472 | $Re = 349,865$ |        |        | 11.17                      | 1.257  | 0.0548 | 4.04                       | 0.777  | 0.0156 |
| -4.24                      | -0.156 | 0.0293 | $\alpha$       | $C_l$  | $C_d$  | 12.13                      | 1.248  | 0.0804 | 5.02                       | 0.876  | 0.0168 |
| -3.12                      | -0.001 | 0.0220 | -6.25          | -0.288 | 0.0647 | <hr/>                      |        |        | 6.09                       | 0.972  | 0.0176 |
| -2.13                      | 0.139  | 0.0187 | -5.18          | -0.144 | 0.0337 | <b>E387 (E)</b>            |        |        | 7.14                       | 1.065  | 0.0187 |
| -1.11                      | 0.238  | 0.0174 | -4.19          | -0.038 | 0.0164 | Fig. 5.5 ( $C_l$ & $C_d$ ) |        |        | 8.11                       | 1.150  | 0.0208 |
| -0.08                      | 0.339  | 0.0202 | -3.15          | 0.071  | 0.0123 | Run: BM04989               |        |        | 9.14                       | 1.227  | 0.0235 |
| 0.95                       | 0.435  | 0.0229 | -2.11          | 0.180  | 0.0106 | $Re = 100,062$             |        |        | 10.13                      | 1.272  | 0.0292 |
| 1.96                       | 0.530  | 0.0266 | -1.16          | 0.277  | 0.0090 | $\alpha$                   | $C_l$  | $C_d$  | 11.17                      | 1.277  | 0.0462 |
| 3.00                       | 0.623  | 0.0290 | -0.05          | 0.389  | 0.0078 | -6.21                      | -0.338 | 0.0754 | 12.15                      | 1.264  | 0.0643 |
| 4.00                       | 0.715  | 0.0317 | 0.94           | 0.493  | 0.0081 | -5.25                      | -0.262 | 0.0495 | Run: BM04995               |        |        |
| 5.04                       | 0.825  | 0.0278 | 1.97           | 0.605  | 0.0085 | -4.17                      | -0.111 | 0.0276 | $Re = 500,060$             |        |        |
| 6.04                       | 0.928  | 0.0239 | 3.00           | 0.714  | 0.0091 | -3.18                      | 0.034  | 0.0218 | $\alpha$                   | $C_l$  | $C_d$  |
| 7.07                       | 1.032  | 0.0218 | 4.03           | 0.833  | 0.0098 | -2.10                      | 0.187  | 0.0197 | -6.22                      | -0.295 | 0.0674 |
| 8.11                       | 1.130  | 0.0215 | 5.08           | 0.942  | 0.0104 | -1.07                      | 0.280  | 0.0178 | -5.20                      | -0.160 | 0.0363 |
| 9.17                       | 1.176  | 0.0269 | 6.08           | 1.045  | 0.0111 | -0.05                      | 0.381  | 0.0205 | -4.19                      | -0.047 | 0.0147 |
| 10.11                      | 1.185  | 0.0363 | 7.08           | 1.134  | 0.0128 | 0.93                       | 0.474  | 0.0229 | -3.20                      | 0.047  | 0.0124 |
| 11.14                      | 1.188  | 0.0526 | 8.11           | 1.200  | 0.0177 | 1.97                       | 0.583  | 0.0235 | -2.16                      | 0.155  | 0.0111 |
| Run: BM04979               |        |        | 9.11           | 1.240  | 0.0238 | 3.05                       | 0.688  | 0.0220 | -1.12                      | 0.261  | 0.0112 |
| $Re = 199,879$             |        |        | 10.14          | 1.249  | 0.0347 | 4.05                       | 0.785  | 0.0198 | -0.08                      | 0.374  | 0.0119 |
| $\alpha$                   | $C_l$  | $C_d$  | 11.15          | 1.245  | 0.0564 | 5.10                       | 0.885  | 0.0190 | 0.95                       | 0.478  | 0.0124 |
| -6.24                      | -0.332 | 0.0705 | 12.14          | 1.238  | 0.0781 | 6.06                       | 0.981  | 0.0186 | 1.98                       | 0.582  | 0.0129 |
| -5.20                      | -0.138 | 0.0352 | Run: BM04985   |        |        | 7.14                       | 1.075  | 0.0193 | 2.99                       | 0.688  | 0.0136 |
| -4.17                      | -0.015 | 0.0192 | $Re = 459,961$ |        |        | 8.13                       | 1.136  | 0.0253 | 4.04                       | 0.794  | 0.0147 |
| -3.14                      | 0.081  | 0.0150 | $\alpha$       | $C_l$  | $C_d$  | 9.15                       | 1.183  | 0.0300 | 5.06                       | 0.894  | 0.0159 |
| -2.14                      | 0.178  | 0.0125 | -6.23          | -0.292 | 0.0651 | 10.16                      | 1.220  | 0.0381 | 6.08                       | 0.986  | 0.0172 |
| -1.09                      | 0.271  | 0.0102 | -5.20          | -0.150 | 0.0341 | 11.14                      | 1.228  | 0.0510 | 7.11                       | 1.076  | 0.0189 |
| -0.05                      | 0.381  | 0.0104 | -4.16          | -0.040 | 0.0145 | Run: BM04991               |        |        | 8.09                       | 1.162  | 0.0207 |
| 0.97                       | 0.483  | 0.0110 | -3.13          | 0.064  | 0.0114 | $Re = 199,800$             |        |        | 9.16                       | 1.228  | 0.0231 |
| 2.01                       | 0.593  | 0.0118 | -2.13          | 0.172  | 0.0099 | $\alpha$                   | $C_l$  | $C_d$  | 10.16                      | 1.242  | 0.0342 |
| 3.00                       | 0.698  | 0.0126 | -1.08          | 0.280  | 0.0085 | -6.22                      | -0.346 | 0.0754 | 11.16                      | 1.234  | 0.0585 |
| 4.09                       | 0.806  | 0.0134 | -0.09          | 0.382  | 0.0069 | -5.18                      | -0.150 | 0.0370 | 12.12                      | 1.227  | 0.0809 |
| 5.02                       | 0.902  | 0.0138 | 0.96           | 0.500  | 0.0072 | -4.17                      | -0.026 | 0.0180 | <hr/>                      |        |        |
| 6.09                       | 1.017  | 0.0140 | 1.98           | 0.611  | 0.0075 | -3.15                      | 0.062  | 0.0154 | <b>FX 63-137 (C)</b>       |        |        |
| 7.14                       | 1.119  | 0.0149 | 3.00           | 0.721  | 0.0079 | -2.12                      | 0.162  | 0.0130 | Fig. 5.9 ( $C_l$ & $C_d$ ) |        |        |
| 8.15                       | 1.191  | 0.0181 | 4.03           | 0.835  | 0.0087 | -1.09                      | 0.263  | 0.0124 | Run: BM04997               |        |        |
| 9.18                       | 1.226  | 0.0265 | 5.12           | 0.948  | 0.0094 | -0.02                      | 0.369  | 0.0113 | $Re = 100,019$             |        |        |
| 10.12                      | 1.234  | 0.0358 | 6.09           | 1.045  | 0.0101 | 0.96                       | 0.465  | 0.0102 | $\alpha$                   | $C_l$  | $C_d$  |
| 11.18                      | 1.227  | 0.0550 | 7.15           | 1.132  | 0.0128 | 1.96                       | 0.558  | 0.0115 | -7.24                      | -0.320 | 0.1437 |
| 12.20                      | 1.218  | 0.0774 | 8.18           | 1.195  | 0.0172 | 3.00                       | 0.646  | 0.0131 | -6.23                      | -0.296 | 0.1195 |
| Run: BM04981               |        |        | 9.12           | 1.236  | 0.0224 | 4.00                       | 0.748  | 0.0149 | -5.19                      | -0.012 | 0.0411 |
| $Re = 300,289$             |        |        | 10.14          | 1.255  | 0.0318 | 5.03                       | 0.842  | 0.0166 | -4.14                      | 0.120  | 0.0364 |
| $\alpha$                   | $C_l$  | $C_d$  | 11.12          | 1.252  | 0.0543 | 6.09                       | 0.937  | 0.0186 | -3.09                      | 0.261  | 0.0353 |
| -6.25                      | -0.304 | 0.0669 | 12.16          | 1.242  | 0.0790 | 7.10                       | 1.030  | 0.0204 | -2.05                      | 0.394  | 0.0366 |
| -5.21                      | -0.139 | 0.0341 | Run: BM04987   |        |        | 8.12                       | 1.117  | 0.0227 | -1.05                      | 0.478  | 0.0414 |
| -4.18                      | -0.028 | 0.0169 | $Re = 500,094$ |        |        | 9.12                       | 1.194  | 0.0258 | 0.00                       | 0.543  | 0.0469 |
| -3.20                      | 0.064  | 0.0131 | $\alpha$       | $C_l$  | $C_d$  | 10.13                      | 1.237  | 0.0320 | 1.02                       | 0.605  | 0.0517 |
| -2.07                      | 0.184  | 0.0110 | -6.20          | -0.289 | 0.0643 | 11.13                      | 1.228  | 0.0503 | 2.05                       | 0.655  | 0.0587 |
| -1.11                      | 0.288  | 0.0092 | -5.18          | -0.155 | 0.0352 | 12.17                      | 1.215  | 0.0733 | 3.04                       | 0.711  | 0.0655 |
| -0.04                      | 0.393  | 0.0083 | -4.15          | -0.040 | 0.0139 | Run: BM04993               |        |        | 4.01                       | 0.797  | 0.0760 |
| 1.02                       | 0.502  | 0.0088 | -3.20          | 0.056  | 0.0114 | $Re = 349,749$             |        |        | 5.12                       | 1.066  | 0.0501 |
| 1.96                       | 0.610  | 0.0092 | -2.16          | 0.171  | 0.0097 | $\alpha$                   | $C_l$  | $C_d$  | 6.17                       | 1.274  | 0.0380 |
| 3.02                       | 0.714  | 0.0098 | -1.09          | 0.276  | 0.0085 | -6.28                      | -0.311 | 0.0700 | 7.20                       | 1.399  | 0.0341 |
| 4.00                       | 0.817  | 0.0105 | -0.04          | 0.388  | 0.0067 | -5.26                      | -0.161 | 0.0378 | 8.23                       | 1.512  | 0.0319 |
| 5.06                       | 0.935  | 0.0112 | 0.88           | 0.497  | 0.0068 | -4.19                      | -0.044 | 0.0162 | 9.19                       | 1.595  | 0.0314 |
| 6.11                       | 1.041  | 0.0115 | 1.97           | 0.613  | 0.0072 | -3.12                      | 0.063  | 0.0123 | 10.30                      | 1.676  | 0.0332 |
| 7.15                       | 1.135  | 0.0131 | 2.98           | 0.720  | 0.0077 |                            |        |        | 11.31                      | 1.724  | 0.0369 |
|                            |        |        | 4.02           | 0.833  | 0.0084 |                            |        |        |                            |        |        |







|                             |        |        |                |        |        |                             |        |        |                |        |        |
|-----------------------------|--------|--------|----------------|--------|--------|-----------------------------|--------|--------|----------------|--------|--------|
| <b>S834</b>                 |        |        | -7.20          | -0.700 | 0.0204 | 3.15                        | 0.566  | 0.0081 | 8.20           | 0.862  | 0.0235 |
| Fig. 5.21 ( $C_l$ & $C_d$ ) |        |        | -6.15          | -0.582 | 0.0186 | 4.17                        | 0.662  | 0.0085 | 9.25           | 0.936  | 0.0267 |
| Run: BM05037                |        |        | -5.10          | -0.458 | 0.0180 | 5.20                        | 0.747  | 0.0094 | 10.25          | 1.002  | 0.0307 |
| $Re = 99,982$               |        |        | -4.10          | -0.342 | 0.0183 | 6.19                        | 0.808  | 0.0111 | 11.25          | 1.054  | 0.0367 |
| $\alpha$                    | $C_l$  | $C_d$  | -3.04          | -0.221 | 0.0185 | 7.24                        | 0.868  | 0.0131 | 12.24          | 1.069  | 0.0507 |
| -10.13                      | -0.763 | 0.0364 | -1.95          | -0.092 | 0.0191 | 8.26                        | 0.937  | 0.0159 | 13.28          | 1.071  | 0.0676 |
| -9.15                       | -0.762 | 0.0317 | -1.00          | 0.012  | 0.0191 | 9.25                        | 1.003  | 0.0191 | Run: BM05051   |        |        |
| -8.21                       | -0.732 | 0.0278 | 0.03           | 0.130  | 0.0194 | 10.24                       | 1.056  | 0.0235 | $Re = 199,613$ |        |        |
| -7.16                       | -0.680 | 0.0245 | 1.05           | 0.229  | 0.0190 | 11.27                       | 1.097  | 0.0315 | $\alpha$       | $C_l$  | $C_d$  |
| -6.14                       | -0.595 | 0.0225 | 2.06           | 0.332  | 0.0175 | 12.36                       | 1.119  | 0.0456 | -10.21         | -0.862 | 0.0268 |
| -5.16                       | -0.503 | 0.0212 | 3.12           | 0.478  | 0.0158 | 13.24                       | 1.119  | 0.0682 | -9.17          | -0.843 | 0.0240 |
| -4.14                       | -0.406 | 0.0221 | 4.18           | 0.651  | 0.0137 | <b>S834</b>                 |        |        | -8.21          | -0.787 | 0.0218 |
| -3.10                       | -0.317 | 0.0232 | 5.19           | 0.784  | 0.0129 | Fig. 5.23 ( $C_l$ & $C_d$ ) |        |        | -7.18          | -0.700 | 0.0212 |
| -2.07                       | -0.241 | 0.0248 | 6.23           | 0.864  | 0.0127 | Run: BM05047                |        |        | -6.18          | -0.589 | 0.0209 |
| -1.07                       | -0.221 | 0.0241 | 7.17           | 0.890  | 0.0139 | $Re = 100,159$              |        |        | -5.09          | -0.458 | 0.0209 |
| -0.02                       | -0.115 | 0.0242 | 8.22           | 0.936  | 0.0173 | $\alpha$                    | $C_l$  | $C_d$  | -4.06          | -0.329 | 0.0212 |
| 1.01                        | -0.009 | 0.0291 | 9.23           | 0.985  | 0.0213 | -10.18                      | -0.830 | 0.0361 | -3.01          | -0.202 | 0.0212 |
| 2.02                        | 0.073  | 0.0312 | 10.27          | 1.023  | 0.0286 | -9.17                       | -0.828 | 0.0313 | -2.03          | -0.091 | 0.0216 |
| 3.04                        | 0.168  | 0.0354 | 11.26          | 1.055  | 0.0354 | -8.19                       | -0.798 | 0.0272 | -0.97          | 0.054  | 0.0202 |
| 4.09                        | 0.295  | 0.0403 | 12.27          | 1.064  | 0.0505 | -7.20                       | -0.742 | 0.0248 | 0.06           | 0.219  | 0.0137 |
| 5.12                        | 0.467  | 0.0388 | Run: BM05043   |        |        | -6.11                       | -0.641 | 0.0224 | 1.07           | 0.299  | 0.0122 |
| 6.17                        | 0.795  | 0.0227 | $Re = 349,949$ |        |        | -5.16                       | -0.535 | 0.0221 | 2.10           | 0.350  | 0.0144 |
| 7.21                        | 0.891  | 0.0188 | $\alpha$       | $C_l$  | $C_d$  | -4.11                       | -0.420 | 0.0219 | 3.14           | 0.405  | 0.0154 |
| 8.28                        | 0.969  | 0.0205 | -10.21         | -0.885 | 0.0238 | -3.04                       | -0.307 | 0.0208 | 4.14           | 0.530  | 0.0165 |
| 9.28                        | 1.013  | 0.0261 | -9.22          | -0.797 | 0.0209 | -2.06                       | -0.231 | 0.0217 | 5.16           | 0.618  | 0.0170 |
| 10.26                       | 1.030  | 0.0329 | -8.12          | -0.674 | 0.0182 | -1.04                       | -0.186 | 0.0235 | 6.17           | 0.677  | 0.0185 |
| 11.22                       | 1.049  | 0.0405 | -7.15          | -0.549 | 0.0164 | -0.05                       | -0.121 | 0.0247 | 7.17           | 0.767  | 0.0203 |
| 12.27                       | 1.063  | 0.0534 | -6.08          | -0.423 | 0.0148 | 1.05                        | -0.020 | 0.0276 | 8.20           | 0.847  | 0.0225 |
| Run: BM05039                |        |        | -5.08          | -0.299 | 0.0136 | 2.02                        | 0.061  | 0.0318 | 9.22           | 0.926  | 0.0252 |
| $Re = 149,734$              |        |        | -4.04          | -0.189 | 0.0125 | 3.06                        | 0.191  | 0.0340 | 10.22          | 0.992  | 0.0285 |
| $\alpha$                    | $C_l$  | $C_d$  | -3.03          | -0.083 | 0.0116 | 4.16                        | 0.564  | 0.0230 | 11.28          | 1.048  | 0.0339 |
| -10.21                      | -0.818 | 0.0313 | -2.00          | 0.024  | 0.0110 | 5.17                        | 0.665  | 0.0179 | 12.30          | 1.082  | 0.0432 |
| -9.17                       | -0.817 | 0.0276 | -0.98          | 0.130  | 0.0104 | 6.20                        | 0.723  | 0.0174 | 13.27          | 1.092  | 0.0622 |
| -8.18                       | -0.780 | 0.0240 | 0.08           | 0.238  | 0.0099 | 7.22                        | 0.760  | 0.0195 | Run: BM05053   |        |        |
| -7.21                       | -0.721 | 0.0220 | 1.07           | 0.337  | 0.0099 | 8.17                        | 0.786  | 0.0237 | $Re = 350,082$ |        |        |
| -6.17                       | -0.622 | 0.0197 | 2.11           | 0.441  | 0.0101 | 9.23                        | 0.838  | 0.0286 | $\alpha$       | $C_l$  | $C_d$  |
| -5.16                       | -0.503 | 0.0189 | 3.14           | 0.535  | 0.0102 | 10.23                       | 0.908  | 0.0337 | -10.20         | -0.855 | 0.0256 |
| -4.06                       | -0.391 | 0.0196 | 4.22           | 0.624  | 0.0099 | 11.26                       | 0.963  | 0.0400 | -9.24          | -0.798 | 0.0214 |
| -3.05                       | -0.299 | 0.0194 | 5.16           | 0.707  | 0.0099 | 12.31                       | 0.982  | 0.0537 | -8.18          | -0.670 | 0.0192 |
| -2.08                       | -0.196 | 0.0210 | 6.18           | 0.806  | 0.0106 | 13.26                       | 0.984  | 0.0701 | -7.16          | -0.540 | 0.0182 |
| -1.02                       | -0.104 | 0.0232 | 7.17           | 0.863  | 0.0125 | Run: BM05049                |        |        | -6.11          | -0.407 | 0.0175 |
| -0.01                       | -0.038 | 0.0241 | 8.27           | 0.926  | 0.0164 | $Re = 150,195$              |        |        | -5.10          | -0.282 | 0.0165 |
| 1.03                        | 0.072  | 0.0252 | 9.25           | 0.988  | 0.0201 | $\alpha$                    | $C_l$  | $C_d$  | -4.04          | -0.159 | 0.0154 |
| 2.10                        | 0.293  | 0.0256 | 10.25          | 1.037  | 0.0255 | -10.19                      | -0.798 | 0.0304 | -3.00          | -0.063 | 0.0134 |
| 3.15                        | 0.524  | 0.0225 | 11.22          | 1.069  | 0.0322 | -9.22                       | -0.786 | 0.0266 | -2.02          | 0.008  | 0.0131 |
| 4.14                        | 0.676  | 0.0182 | 12.32          | 1.081  | 0.0492 | -8.18                       | -0.741 | 0.0237 | -1.06          | 0.073  | 0.0146 |
| 5.17                        | 0.757  | 0.0156 | 13.31          | 1.076  | 0.0722 | -7.18                       | -0.665 | 0.0226 | 0.03           | 0.175  | 0.0146 |
| 6.18                        | 0.829  | 0.0152 | Run: BM05045   |        |        | -6.15                       | -0.575 | 0.0211 | 1.08           | 0.262  | 0.0151 |
| 7.24                        | 0.893  | 0.0150 | $Re = 499,497$ |        |        | -5.13                       | -0.469 | 0.0211 | 2.12           | 0.359  | 0.0153 |
| 8.30                        | 0.943  | 0.0185 | $\alpha$       | $C_l$  | $C_d$  | -4.08                       | -0.352 | 0.0201 | 3.11           | 0.452  | 0.0159 |
| 9.26                        | 0.989  | 0.0236 | -10.17         | -0.811 | 0.0203 | -3.05                       | -0.250 | 0.0203 | 4.17           | 0.546  | 0.0167 |
| 10.27                       | 1.013  | 0.0305 | -9.14          | -0.706 | 0.0174 | -2.02                       | -0.144 | 0.0211 | 5.17           | 0.634  | 0.0176 |
| 11.23                       | 1.039  | 0.0379 | -8.14          | -0.584 | 0.0151 | -1.01                       | -0.049 | 0.0227 | 6.20           | 0.718  | 0.0180 |
| 12.25                       | 1.047  | 0.0514 | -7.11          | -0.475 | 0.0135 | 0.01                        | 0.090  | 0.0232 | 7.26           | 0.777  | 0.0185 |
| 13.28                       | 1.045  | 0.0692 | -6.06          | -0.374 | 0.0121 | 1.08                        | 0.262  | 0.0195 | 8.22           | 0.850  | 0.0204 |
| Run: BM05041                |        |        | -5.06          | -0.276 | 0.0108 | 2.07                        | 0.367  | 0.0156 | 9.26           | 0.928  | 0.0230 |
| $Re = 199,914$              |        |        | -4.00          | -0.173 | 0.0099 | 3.13                        | 0.509  | 0.0143 | 10.26          | 1.001  | 0.0258 |
| $\alpha$                    | $C_l$  | $C_d$  | -3.01          | -0.073 | 0.0091 | 4.16                        | 0.654  | 0.0158 | 11.28          | 1.041  | 0.0379 |
| -10.20                      | -0.840 | 0.0274 | -1.96          | 0.039  | 0.0085 | 5.15                        | 0.663  | 0.0174 | 12.30          | 1.051  | 0.0573 |
| -9.22                       | -0.834 | 0.0250 | -0.98          | 0.140  | 0.0081 | 6.21                        | 0.701  | 0.0191 | 13.25          | 1.043  | 0.0845 |
| -8.17                       | -0.782 | 0.0221 | 0.07           | 0.246  | 0.0078 | 7.23                        | 0.780  | 0.0210 | Run: BM05055   |        |        |
|                             |        |        | 1.04           | 0.345  | 0.0077 |                             |        |        | $Re = 499,211$ |        |        |
|                             |        |        | 2.14           | 0.461  | 0.0078 |                             |        |        | $\alpha$       | $C_l$  | $C_d$  |



|                |        |        |                             |        |        |                            |        |        |              |        |        |
|----------------|--------|--------|-----------------------------|--------|--------|----------------------------|--------|--------|--------------|--------|--------|
| $\alpha$       | $C_l$  | $C_d$  | 1.09                        | 0.994  | 0.0121 | 10.28                      | 1.495  | 0.0516 | -6.19        | -0.393 | -0.022 |
| -7.15          | -0.164 | 0.1329 | 2.21                        | 1.102  | 0.0127 | 11.28                      | 1.501  | 0.0767 | -5.20        | -0.326 | -0.056 |
| -6.14          | -0.021 | 0.0326 | 3.22                        | 1.205  | 0.0133 | 13.37                      | 1.709  | 0.0695 | -4.20        | -0.186 | -0.073 |
| -5.05          | 0.228  | 0.0217 | 4.25                        | 1.313  | 0.0144 | 14.36                      | 1.638  | 0.1178 | -3.20        | -0.047 | -0.091 |
| -3.99          | 0.394  | 0.0189 | 5.27                        | 1.419  | 0.0152 |                            |        |        | -2.20        | 0.110  | -0.104 |
| -2.95          | 0.515  | 0.0175 | 6.27                        | 1.513  | 0.0160 | Run: BM05069               |        |        | -1.16        | 0.216  | -0.087 |
| -1.90          | 0.620  | 0.0173 | 7.32                        | 1.616  | 0.0171 | $Re = 350,134$             |        |        | -0.11        | 0.327  | -0.092 |
| -0.93          | 0.714  | 0.0175 | 8.33                        | 1.700  | 0.0183 | $\alpha$                   | $C_l$  | $C_d$  | 0.96         | 0.429  | -0.080 |
| 0.13           | 0.819  | 0.0180 | 9.35                        | 1.777  | 0.0203 | -9.12                      | -0.336 | 0.0687 | 1.98         | 0.530  | -0.080 |
| 1.16           | 0.918  | 0.0188 | 10.38                       | 1.836  | 0.0230 | -8.19                      | -0.285 | 0.0384 | 2.94         | 0.623  | -0.091 |
| 2.21           | 1.022  | 0.0196 | 11.39                       | 1.864  | 0.0277 | -7.09                      | -0.082 | 0.0254 | 4.02         | 0.730  | -0.084 |
| 3.19           | 1.120  | 0.0205 | 12.43                       | 1.865  | 0.0369 | -6.09                      | 0.094  | 0.0180 | 5.03         | 0.836  | -0.083 |
| 4.22           | 1.218  | 0.0213 | 13.39                       | 1.835  | 0.0625 | -5.03                      | 0.249  | 0.0154 | 6.05         | 0.951  | -0.076 |
| 5.24           | 1.320  | 0.0221 |                             |        |        | -4.08                      | 0.373  | 0.0139 | 7.14         | 1.045  | -0.058 |
| 6.26           | 1.419  | 0.0229 |                             |        |        | -2.95                      | 0.496  | 0.0131 | 8.13         | 1.149  | -0.071 |
| 7.29           | 1.510  | 0.0238 |                             |        |        | -1.93                      | 0.605  | 0.0131 | 9.16         | 1.207  | -0.059 |
| 8.32           | 1.604  | 0.0248 | <b>SH3055</b>               |        |        | -0.88                      | 0.701  | 0.0148 | 10.15        | 1.221  | -0.058 |
| 9.34           | 1.690  | 0.0259 | Fig. 5.35 ( $C_l$ & $C_d$ ) |        |        | 0.12                       | 0.799  | 0.0164 | 11.19        | 1.230  | -0.052 |
| 10.35          | 1.760  | 0.0272 | Run: BM05118                |        |        | 1.22                       | 0.908  | 0.0172 | 12.19        | 1.234  | -0.050 |
| 11.37          | 1.828  | 0.0289 | $Re = 100,002$              |        |        | 2.17                       | 0.999  | 0.0187 | 13.17        | 1.226  | -0.046 |
| 12.38          | 1.885  | 0.0309 | $\alpha$                    | $C_l$  | $C_d$  | 3.18                       | 1.094  | 0.0204 | 14.16        | 1.214  | -0.057 |
| 13.41          | 1.909  | 0.0359 | -7.16                       | -0.238 | 0.0684 | 4.22                       | 1.186  | 0.0221 | 15.08        | 1.083  | -0.146 |
| 14.41          | 1.886  | 0.0528 | -6.09                       | -0.193 | 0.0288 | 5.22                       | 1.267  | 0.0244 | 16.01        | 1.058  | -0.170 |
| 15.42          | 1.841  | 0.0861 | -5.18                       | -0.036 | 0.0339 | 6.25                       | 1.340  | 0.0268 | 16.99        | 1.068  | -0.184 |
|                |        |        | -3.91                       | 0.121  | 0.0358 | 7.30                       | 1.406  | 0.0300 | 18.02        | 1.056  | -0.193 |
| Run: BM05061   |        |        | -2.98                       | 0.262  | 0.0381 | 8.28                       | 1.456  | 0.0338 | 18.97        | 1.022  | -0.190 |
| $Re = 349,811$ |        |        | -1.95                       | 0.437  | 0.0379 | 9.26                       | 1.494  | 0.0405 | 19.96        | 1.034  | -0.204 |
| $\alpha$       | $C_l$  | $C_d$  | -0.86                       | 0.593  | 0.0388 | 10.30                      | 1.509  | 0.0607 | 19.46        | 1.036  | -0.203 |
| -8.16          | -0.170 | 0.1455 | 0.19                        | 0.695  | 0.0414 |                            |        |        | 18.46        | 1.008  | -0.194 |
| -7.00          | 0.015  | 0.0180 | 1.10                        | 0.741  | 0.0458 | Run: BM05071               |        |        | 17.53        | 1.065  | -0.190 |
| -6.02          | 0.174  | 0.0149 | 2.25                        | 0.842  | 0.0451 | $Re = 499,693$             |        |        | 16.52        | 1.096  | -0.186 |
| -5.05          | 0.300  | 0.0128 | 3.24                        | 0.958  | 0.0394 | $\alpha$                   | $C_l$  | $C_d$  | 15.51        | 1.100  | -0.175 |
| -3.96          | 0.424  | 0.0119 | 4.30                        | 1.089  | 0.0343 | -9.15                      | -0.390 | 0.0526 | 14.63        | 1.228  | -0.140 |
| -2.98          | 0.534  | 0.0119 | 5.35                        | 1.203  | 0.0318 | -8.13                      | -0.198 | 0.0324 | 13.65        | 1.234  | -0.061 |
| -1.90          | 0.648  | 0.0123 | 6.28                        | 1.308  | 0.0309 | -7.12                      | -0.036 | 0.0213 | 12.66        | 1.242  | -0.042 |
| -0.90          | 0.758  | 0.0128 | 7.23                        | 1.393  | 0.0312 | -6.07                      | 0.119  | 0.0161 | 11.65        | 1.255  | -0.042 |
| 0.14           | 0.869  | 0.0134 | 8.34                        | 1.485  | 0.0327 | -5.01                      | 0.270  | 0.0134 | 10.65        | 1.244  | -0.046 |
| 1.16           | 0.973  | 0.0137 | 9.19                        | 1.551  | 0.0334 | -3.97                      | 0.392  | 0.0130 | 9.63         | 1.236  | -0.053 |
| 2.20           | 1.079  | 0.0146 | 10.32                       | 1.630  | 0.0348 | -2.98                      | 0.502  | 0.0131 | 8.63         | 1.204  | -0.070 |
| 3.17           | 1.188  | 0.0153 | 11.45                       | 1.700  | 0.0373 | -1.92                      | 0.612  | 0.0135 | 7.62         | 1.118  | -0.066 |
| 4.21           | 1.288  | 0.0161 | 12.41                       | 1.729  | 0.0440 | -0.89                      | 0.715  | 0.0147 | 6.61         | 1.018  | -0.086 |
| 5.23           | 1.389  | 0.0169 | 13.37                       | 1.709  | 0.0695 | 0.10                       | 0.807  | 0.0159 | 5.49         | 0.902  | -0.083 |
| 6.32           | 1.486  | 0.0178 | 14.36                       | 1.638  | 0.1178 | 1.08                       | 0.898  | 0.0172 | 4.53         | 0.806  | -0.081 |
| 7.29           | 1.575  | 0.0187 |                             |        |        | 2.19                       | 1.002  | 0.0186 | 3.50         | 0.698  | -0.085 |
| 8.33           | 1.661  | 0.0200 | Run: BM05067                |        |        | 3.20                       | 1.097  | 0.0200 | 2.44         | 0.601  | -0.104 |
| 9.37           | 1.742  | 0.0214 | $Re = 181,773$              |        |        | 4.15                       | 1.183  | 0.0215 | 1.40         | 0.499  | -0.092 |
| 10.38          | 1.798  | 0.0234 | $\alpha$                    | $C_l$  | $C_d$  | 5.22                       | 1.270  | 0.0235 | 0.41         | 0.408  | -0.092 |
| 11.39          | 1.838  | 0.0264 | -8.14                       | -0.295 | 0.0931 | 6.22                       | 1.348  | 0.0258 | -0.60        | 0.301  | -0.095 |
| 12.39          | 1.857  | 0.0316 | -7.11                       | -0.233 | 0.0293 | 7.24                       | 1.411  | 0.0297 | -1.70        | 0.193  | -0.098 |
| 13.43          | 1.847  | 0.0471 | -6.12                       | -0.027 | 0.0249 | 8.24                       | 1.460  | 0.0345 | -2.69        | 0.067  | -0.094 |
| 14.38          | 1.805  | 0.0858 | -5.09                       | 0.178  | 0.0214 | 9.31                       | 1.496  | 0.0470 | -3.72        | -0.088 | -0.080 |
|                |        |        | -3.96                       | 0.361  | 0.0180 | 10.33                      | 1.502  | 0.0737 | -4.75        | -0.230 | -0.076 |
| Run: BM05063   |        |        | -2.98                       | 0.482  | 0.0163 | 11.30                      | 1.497  | 0.1020 | -5.68        | -0.342 | -0.043 |
| $Re = 499,564$ |        |        | -1.95                       | 0.598  | 0.0159 |                            |        |        | -6.73        | -0.403 | -0.026 |
| $\alpha$       | $C_l$  | $C_d$  | -0.92                       | 0.712  | 0.0155 |                            |        |        | -7.74        | -0.451 | -0.001 |
| -9.22          | -0.204 | 0.1408 | 0.17                        | 0.821  | 0.0159 | <b>E387 (E)</b>            |        |        | -8.71        | -0.455 | 0.014  |
| -8.04          | -0.084 | 0.0163 | 1.15                        | 0.918  | 0.0173 | Fig. 5.4 ( $C_l$ & $C_m$ ) |        |        | -9.67        | -0.454 | 0.016  |
| -7.06          | 0.062  | 0.0136 | 2.16                        | 1.003  | 0.0181 | Run: BM05140               |        |        |              |        |        |
| -6.04          | 0.195  | 0.0115 | 3.24                        | 1.082  | 0.0218 | $Re = 100,064$             |        |        | Run: BM04978 |        |        |
| -4.97          | 0.327  | 0.0105 | 4.23                        | 1.165  | 0.0232 | $\alpha$                   | $C_l$  | $C_m$  | $\alpha$     | $C_l$  | $C_m$  |
| -3.97          | 0.443  | 0.0103 | 5.24                        | 1.240  | 0.0259 | -10.21                     | -0.454 | 0.027  | -10.14       | -0.495 | 0.049  |
| -2.92          | 0.558  | 0.0104 | 6.23                        | 1.309  | 0.0280 | -9.21                      | -0.467 | 0.023  | -9.26        | -0.495 | 0.041  |
| -1.89          | 0.675  | 0.0107 | 7.25                        | 1.372  | 0.0306 | -8.19                      | -0.472 | 0.017  | -8.25        | -0.470 | 0.028  |
| -0.96          | 0.776  | 0.0112 | 8.26                        | 1.427  | 0.0348 | -7.19                      | -0.439 | 0.003  | -7.21        | -0.425 | 0.003  |
| 0.09           | 0.882  | 0.0116 | 9.31                        | 1.472  | 0.0408 |                            |        |        |              |        |        |

|       |        |        |              |        |        |              |        |        |              |        |        |
|-------|--------|--------|--------------|--------|--------|--------------|--------|--------|--------------|--------|--------|
| -6.08 | -0.331 | -0.041 | -4.22        | -0.043 | -0.084 | 10.14        | 1.246  | -0.060 | -2.12        | 0.163  | -0.083 |
| -5.08 | -0.142 | -0.088 | -3.18        | 0.057  | -0.084 | 11.17        | 1.251  | -0.058 | -1.11        | 0.264  | -0.083 |
| -4.22 | -0.035 | -0.092 | -2.07        | 0.174  | -0.084 | 12.12        | 1.251  | -0.059 | -0.07        | 0.369  | -0.082 |
| -3.22 | 0.055  | -0.087 | -1.14        | 0.263  | -0.084 | 13.16        | 1.252  | -0.063 | 0.98         | 0.484  | -0.082 |
| -2.04 | 0.171  | -0.089 | -0.10        | 0.368  | -0.083 | 14.11        | 1.302  | -0.083 | 1.98         | 0.594  | -0.082 |
| -1.09 | 0.253  | -0.084 | 0.94         | 0.480  | -0.083 | 14.78        | 1.303  | -0.125 | 3.02         | 0.710  | -0.082 |
| 0.00  | 0.367  | -0.085 | 1.98         | 0.592  | -0.083 | 14.64        | 1.290  | -0.115 | 4.03         | 0.819  | -0.081 |
| 0.99  | 0.467  | -0.085 | 2.99         | 0.692  | -0.083 | 13.64        | 1.252  | -0.066 | 5.06         | 0.925  | -0.080 |
| 1.93  | 0.563  | -0.083 | 4.06         | 0.802  | -0.083 | 12.64        | 1.253  | -0.062 | 6.07         | 1.025  | -0.079 |
| 3.01  | 0.670  | -0.084 | 5.03         | 0.905  | -0.082 | 11.66        | 1.256  | -0.059 | 7.12         | 1.106  | -0.076 |
| 4.00  | 0.766  | -0.082 | 6.08         | 1.013  | -0.081 | 10.66        | 1.249  | -0.058 | 8.13         | 1.189  | -0.072 |
| 5.12  | 0.882  | -0.082 | 7.08         | 1.104  | -0.078 | 9.65         | 1.235  | -0.063 | 9.16         | 1.234  | -0.066 |
| 6.15  | 0.986  | -0.080 | 8.16         | 1.182  | -0.073 | 8.62         | 1.206  | -0.070 | 10.14        | 1.253  | -0.060 |
| 7.17  | 1.088  | -0.078 | 9.19         | 1.223  | -0.067 | 7.66         | 1.152  | -0.076 | 11.19        | 1.260  | -0.059 |
| 8.18  | 1.160  | -0.072 | 10.15        | 1.239  | -0.060 | 6.59         | 1.067  | -0.080 | 12.17        | 1.260  | -0.063 |
| 9.15  | 1.207  | -0.067 | 11.15        | 1.247  | -0.058 | 5.57         | 0.968  | -0.082 | 13.15        | 1.269  | -0.066 |
| 10.11 | 1.222  | -0.059 | 12.13        | 1.243  | -0.057 | 4.58         | 0.863  | -0.083 | 14.12        | 1.261  | -0.073 |
| 11.17 | 1.222  | -0.055 | 13.17        | 1.247  | -0.062 | 3.49         | 0.754  | -0.084 | 13.65        | 1.258  | -0.070 |
| 12.22 | 1.227  | -0.056 | 14.04        | 1.291  | -0.086 | 2.47         | 0.639  | -0.083 | 12.62        | 1.270  | -0.066 |
| 13.24 | 1.224  | -0.059 | 15.02        | 1.273  | -0.133 | 1.44         | 0.532  | -0.084 | 11.61        | 1.264  | -0.061 |
| 14.03 | 1.219  | -0.064 | 14.65        | 1.281  | -0.123 | 0.38         | 0.418  | -0.084 | 10.68        | 1.252  | -0.059 |
| 15.08 | 1.158  | -0.147 | 13.65        | 1.245  | -0.066 | -0.59        | 0.316  | -0.084 | 9.66         | 1.253  | -0.063 |
| 15.98 | 1.149  | -0.173 | 12.64        | 1.244  | -0.060 | -1.63        | 0.217  | -0.085 | 8.63         | 1.208  | -0.069 |
| 16.95 | 1.061  | -0.170 | 11.62        | 1.249  | -0.058 | -2.66        | 0.107  | -0.084 | 7.60         | 1.154  | -0.074 |
| 18.03 | 1.055  | -0.174 | 10.65        | 1.242  | -0.058 | -3.65        | 0.007  | -0.083 | 6.54         | 1.072  | -0.078 |
| 18.95 | 1.079  | -0.180 | 9.69         | 1.233  | -0.064 | -4.70        | -0.097 | -0.084 | 5.54         | 0.975  | -0.080 |
| 19.96 | 1.048  | -0.179 | 8.62         | 1.209  | -0.072 | -5.73        | -0.232 | -0.071 | 4.57         | 0.874  | -0.081 |
| 19.44 | 1.061  | -0.179 | 7.59         | 1.142  | -0.077 | -6.69        | -0.377 | -0.030 | 3.52         | 0.759  | -0.081 |
| 18.41 | 1.049  | -0.176 | 6.58         | 1.061  | -0.081 | -7.68        | -0.475 | 0.013  | 2.46         | 0.650  | -0.082 |
| 17.52 | 1.054  | -0.172 | 5.61         | 0.962  | -0.082 |              |        |        | 1.48         | 0.538  | -0.082 |
| 16.50 | 1.068  | -0.172 | 4.58         | 0.861  | -0.083 | Run: BM05121 |        |        | 0.44         | 0.423  | -0.082 |
| 15.49 | 1.137  | -0.162 | 3.55         | 0.745  | -0.084 | Re = 349,714 |        |        | -0.60        | 0.317  | -0.083 |
| 14.59 | 1.272  | -0.110 | 2.50         | 0.636  | -0.084 | $\alpha$     | $C_l$  | $C_m$  | -1.62        | 0.213  | -0.083 |
| 13.61 | 1.221  | -0.061 | 1.43         | 0.530  | -0.084 | 10.21        | 1.248  | N/A    | -2.65        | 0.106  | -0.082 |
| 12.63 | 1.224  | -0.056 | 0.45         | 0.427  | -0.084 | 11.19        | 1.255  | N/A    | -3.68        | 0.000  | -0.082 |
| 11.70 | 1.225  | -0.056 | -0.56        | 0.320  | -0.083 | 12.23        | 1.260  | N/A    | -4.71        | -0.101 | -0.082 |
| 10.62 | 1.224  | -0.057 | -1.62        | 0.214  | -0.085 | 13.14        | 1.258  | N/A    | -5.73        | -0.233 | -0.071 |
| 9.61  | 1.220  | -0.064 | -2.64        | 0.112  | -0.084 | 14.19        | 1.308  | N/A    | -6.65        | -0.363 | -0.033 |
| 8.66  | 1.186  | -0.071 | -3.70        | 0.006  | -0.084 | 15.06        | 1.272  | N/A    |              |        |        |
| 7.61  | 1.132  | -0.076 | -4.74        | -0.095 | -0.085 | 16.05        | 1.201  | N/A    | Run: BM04986 |        |        |
| 6.57  | 1.035  | -0.079 | -5.78        | -0.230 | -0.071 | 17.28        | 1.122  | N/A    | Re = 499,909 |        |        |
| 5.56  | 0.939  | -0.081 | -6.67        | -0.390 | -0.023 | 18.18        | 1.072  | N/A    | $\alpha$     | $C_l$  | $C_m$  |
| 4.49  | 0.823  | -0.082 | -7.68        | -0.464 | 0.013  | 19.19        | 1.059  | N/A    | -7.26        | -0.434 | -0.003 |
| 3.46  | 0.720  | -0.082 |              |        |        | 20.12        | 1.063  | N/A    | -6.23        | -0.307 | -0.051 |
| 2.51  | 0.623  | -0.084 | Run: BM04982 |        |        | 19.63        | 1.055  | N/A    | -5.25        | -0.171 | -0.079 |
| 1.44  | 0.518  | -0.085 | Re = 350,282 |        |        | 18.65        | 1.053  | N/A    | -4.22        | -0.049 | -0.082 |
| 0.47  | 0.416  | -0.086 | $\alpha$     | $C_l$  | $C_m$  | 17.69        | 1.115  | N/A    | -3.15        | 0.057  | -0.082 |
| -0.62 | 0.305  | -0.085 | -8.20        | -0.492 | 0.025  | 16.67        | 1.168  | N/A    | -2.10        | 0.166  | -0.082 |
| -1.62 | 0.211  | -0.087 | -7.20        | -0.439 | -0.002 | 15.64        | 1.257  | N/A    | -1.12        | 0.265  | -0.083 |
| -2.63 | 0.115  | -0.086 | -6.23        | -0.308 | -0.051 | 14.69        | 1.326  | N/A    | -0.06        | 0.377  | -0.081 |
| -3.65 | 0.023  | -0.091 | -5.19        | -0.156 | -0.082 | 13.63        | 1.253  | N/A    | 0.99         | 0.491  | -0.082 |
| -4.70 | -0.077 | -0.092 | -4.19        | -0.046 | -0.083 | 12.66        | 1.255  | N/A    | 1.92         | 0.590  | -0.081 |
| -5.67 | -0.258 | -0.060 | -3.16        | 0.060  | -0.083 | 11.75        | 1.261  | N/A    | 3.00         | 0.712  | -0.081 |
| -6.65 | -0.396 | -0.013 | -2.15        | 0.167  | -0.084 | 10.68        | 1.252  | N/A    | 4.04         | 0.816  | -0.081 |
| -7.66 | -0.444 | 0.018  | -1.10        | 0.270  | -0.085 |              |        |        | 5.04         | 0.927  | -0.080 |
| -8.63 | -0.470 | 0.033  | -0.07        | 0.375  | -0.083 |              |        |        | 6.08         | 1.026  | -0.079 |
| -9.69 | -0.489 | 0.044  | 0.92         | 0.477  | -0.083 |              |        |        | 7.12         | 1.118  | -0.076 |
|       |        |        | 1.99         | 0.589  | -0.083 | Run: BM04984 |        |        | 8.14         | 1.183  | -0.071 |
|       |        |        | 3.02         | 0.707  | -0.083 | Re = 460,154 |        |        | 9.17         | 1.240  | -0.066 |
|       |        |        | 4.03         | 0.813  | -0.082 | $\alpha$     | $C_l$  | $C_m$  | 10.14        | 1.258  | -0.059 |
|       |        |        | 5.04         | 0.916  | -0.082 | -7.16        | -0.425 | -0.007 | 11.19        | 1.269  | -0.060 |
|       |        |        | 6.05         | 1.021  | -0.081 | -6.22        | -0.310 | -0.051 | 12.21        | 1.269  | -0.063 |
|       |        |        | 7.09         | 1.112  | -0.078 | -5.23        | -0.166 | -0.080 | 13.14        | 1.268  | -0.068 |
|       |        |        | 8.15         | 1.177  | -0.073 | -4.15        | -0.046 | -0.082 | 14.15        | 1.264  | -0.074 |
|       |        |        | 9.15         | 1.223  | -0.067 | -3.14        | 0.057  | -0.082 | 13.63        | 1.264  | -0.071 |

|       |        |        |       |        |        |       |        |        |       |        |        |
|-------|--------|--------|-------|--------|--------|-------|--------|--------|-------|--------|--------|
| 12.63 | 1.261  | -0.065 | 13.64 | 1.246  | -0.057 | 13.65 | 1.223  | -0.059 | 1.46  | 0.502  | -0.080 |
| 11.63 | 1.259  | -0.059 | 12.67 | 1.257  | -0.044 | 12.60 | 1.230  | -0.056 | 0.42  | 0.397  | -0.080 |
| 10.63 | 1.256  | -0.058 | 11.67 | 1.256  | -0.044 | 11.64 | 1.237  | -0.056 | -0.61 | 0.296  | -0.081 |
| 9.63  | 1.243  | -0.061 | 10.67 | 1.247  | -0.049 | 10.63 | 1.240  | -0.058 | -1.61 | 0.208  | -0.083 |
| 8.63  | 1.205  | -0.068 | 9.64  | 1.219  | -0.054 | 9.66  | 1.213  | -0.063 | -2.66 | 0.099  | -0.084 |
| 7.59  | 1.134  | -0.072 | 8.65  | 1.165  | -0.066 | 8.56  | 1.138  | -0.066 | -3.70 | -0.007 | -0.084 |
| 6.60  | 1.078  | -0.077 | 7.69  | 1.115  | -0.064 | 7.57  | 1.060  | -0.070 | -4.73 | -0.104 | -0.084 |
| 5.58  | 0.979  | -0.080 | 6.56  | 1.026  | -0.069 | 6.57  | 0.968  | -0.071 | -5.73 | -0.236 | -0.069 |
| 4.52  | 0.861  | -0.080 | 5.59  | 0.928  | -0.073 | 5.62  | 0.880  | -0.073 | -6.69 | -0.382 | -0.024 |
| 3.44  | 0.755  | -0.081 | 4.51  | 0.825  | -0.077 | 4.52  | 0.780  | -0.075 | -7.68 | -0.460 | 0.013  |
| 2.51  | 0.649  | -0.081 | 3.46  | 0.719  | -0.092 | 3.50  | 0.687  | -0.075 |       |        |        |
| 1.42  | 0.535  | -0.081 | 2.50  | 0.629  | -0.102 | 2.46  | 0.596  | -0.077 |       |        |        |
| 0.43  | 0.426  | -0.081 | 1.45  | 0.528  | -0.097 | 1.47  | 0.507  | -0.079 |       |        |        |
| -0.62 | 0.320  | -0.083 | 0.38  | 0.431  | -0.106 | 0.46  | 0.413  | -0.084 |       |        |        |
| -1.65 | 0.209  | -0.083 | -0.60 | 0.338  | -0.097 | -0.59 | 0.311  | -0.084 |       |        |        |
| -2.67 | 0.108  | -0.082 | -1.65 | 0.239  | -0.100 | -1.63 | 0.208  | -0.088 |       |        |        |
| -3.68 | 0.002  | -0.081 | -2.71 | 0.114  | -0.096 | -2.71 | 0.107  | -0.086 |       |        |        |
| -4.71 | -0.107 | -0.082 | -3.67 | -0.036 | -0.080 | -3.65 | 0.018  | -0.088 |       |        |        |
| -5.75 | -0.236 | -0.070 | -4.73 | -0.187 | -0.071 | -4.76 | -0.090 | -0.089 |       |        |        |
| -6.73 | -0.370 | -0.033 | -5.69 | -0.322 | -0.039 | -5.75 | -0.270 | -0.055 |       |        |        |
|       |        |        | -6.72 | -0.372 | -0.018 | -6.69 | -0.401 | -0.010 |       |        |        |
|       |        |        | -7.71 | -0.415 | 0.008  | -7.68 | -0.454 | 0.019  |       |        |        |
|       |        |        | -8.69 | -0.433 | 0.025  | -8.65 | -0.470 | 0.034  |       |        |        |
|       |        |        | -9.65 | -0.440 | 0.031  | -9.66 | -0.469 | 0.042  |       |        |        |

**E387 (E)**

Fig. 5.6 ( $C_l$  &  $C_m$ )

Run: BM04988  
 $Re = 99,963$

| $\alpha$ | $C_l$  | $C_m$  |
|----------|--------|--------|
| -10.17   | -0.471 | 0.053  |
| -9.16    | -0.434 | 0.041  |
| -8.15    | -0.398 | 0.027  |
| -7.14    | -0.386 | 0.008  |
| -6.18    | -0.332 | -0.018 |
| -5.19    | -0.258 | -0.056 |
| -4.21    | -0.108 | -0.059 |
| -3.18    | 0.039  | -0.086 |
| -2.11    | 0.185  | -0.089 |
| -1.11    | 0.280  | -0.087 |
| -0.06    | 0.385  | -0.101 |
| 0.89     | 0.472  | -0.092 |
| 1.96     | 0.573  | -0.084 |
| 3.00     | 0.675  | -0.089 |
| 4.02     | 0.769  | -0.074 |
| 5.04     | 0.872  | -0.067 |
| 6.08     | 0.979  | -0.076 |
| 7.09     | 1.072  | -0.073 |
| 8.14     | 1.138  | -0.067 |
| 9.15     | 1.191  | -0.057 |
| 10.17    | 1.230  | -0.043 |
| 11.13    | 1.250  | -0.054 |
| 12.16    | 1.254  | -0.052 |
| 13.16    | 1.251  | -0.054 |
| 14.08    | 1.205  | -0.120 |
| 15.08    | 1.119  | -0.152 |
| 16.01    | 1.082  | -0.158 |
| 17.00    | 1.083  | -0.164 |
| 18.02    | 1.063  | -0.167 |
| 19.05    | 1.077  | -0.169 |
| 20.01    | 1.087  | -0.177 |
| 19.50    | 1.074  | -0.182 |
| 18.52    | 1.054  | -0.172 |
| 17.54    | 1.073  | -0.176 |
| 16.50    | 1.074  | -0.170 |
| 15.51    | 1.076  | -0.163 |
| 14.53    | 1.100  | -0.147 |

Run: BM04990  
 $Re = 200,028$

| $\alpha$ | $C_l$  | $C_m$  |
|----------|--------|--------|
| -10.17   | -0.477 | 0.047  |
| -9.12    | -0.485 | 0.041  |
| -8.19    | -0.469 | 0.031  |
| -7.14    | -0.428 | 0.005  |
| -6.17    | -0.368 | -0.021 |
| -5.19    | -0.169 | -0.080 |
| -4.21    | -0.036 | -0.087 |
| -3.16    | 0.059  | -0.089 |
| -2.13    | 0.154  | -0.087 |
| -1.11    | 0.255  | -0.087 |
| -0.08    | 0.350  | -0.084 |
| 0.94     | 0.452  | -0.079 |
| 1.97     | 0.550  | -0.078 |
| 3.00     | 0.640  | -0.076 |
| 4.02     | 0.734  | -0.075 |
| 5.04     | 0.829  | -0.073 |
| 6.10     | 0.925  | -0.071 |
| 7.10     | 1.018  | -0.070 |
| 8.13     | 1.105  | -0.066 |
| 9.15     | 1.191  | -0.064 |
| 10.19    | 1.237  | -0.059 |
| 11.14    | 1.236  | -0.055 |
| 12.17    | 1.240  | -0.054 |
| 13.17    | 1.237  | -0.056 |
| 14.19    | 1.225  | -0.063 |
| 15.05    | 1.216  | -0.153 |
| 16.04    | 1.110  | -0.166 |
| 17.03    | 1.081  | -0.172 |
| 18.00    | 1.047  | -0.173 |
| 18.97    | 1.040  | -0.174 |
| 19.98    | 1.035  | -0.175 |
| 19.42    | 1.032  | -0.178 |
| 18.49    | 1.063  | -0.178 |
| 17.51    | 1.080  | -0.178 |
| 16.55    | 1.127  | -0.178 |
| 15.57    | 1.177  | -0.161 |
| 14.63    | 1.238  | -0.105 |

Run: BM04992  
 $Re = 350,084$

| $\alpha$ | $C_l$  | $C_m$  |
|----------|--------|--------|
| -8.18    | -0.487 | 0.026  |
| -7.22    | -0.435 | 0.001  |
| -6.21    | -0.317 | -0.047 |
| -5.19    | -0.161 | -0.081 |
| -4.14    | -0.049 | -0.083 |
| -3.19    | 0.048  | -0.083 |
| -2.15    | 0.153  | -0.082 |
| -1.14    | 0.249  | -0.081 |
| -0.08    | 0.351  | -0.080 |
| 0.94     | 0.451  | -0.079 |
| 1.99     | 0.556  | -0.079 |
| 3.02     | 0.664  | -0.078 |
| 4.08     | 0.769  | -0.077 |
| 5.04     | 0.862  | -0.075 |
| 6.10     | 0.963  | -0.074 |
| 7.10     | 1.047  | -0.071 |
| 8.18     | 1.142  | -0.069 |
| 9.11     | 1.205  | -0.065 |
| 10.16    | 1.260  | -0.060 |
| 11.15    | 1.274  | -0.059 |
| 12.13    | 1.279  | -0.063 |
| 13.15    | 1.269  | -0.067 |
| 14.15    | 1.262  | -0.075 |
| 15.19    | 1.249  | -0.083 |
| 14.66    | 1.254  | -0.079 |
| 13.66    | 1.275  | -0.071 |
| 12.64    | 1.275  | -0.065 |
| 11.66    | 1.287  | -0.061 |
| 10.61    | 1.275  | -0.058 |
| 9.61     | 1.236  | -0.063 |
| 8.63     | 1.179  | -0.067 |
| 7.63     | 1.092  | -0.070 |
| 6.58     | 1.003  | -0.073 |
| 5.57     | 0.909  | -0.075 |
| 4.50     | 0.809  | -0.077 |
| 3.52     | 0.710  | -0.078 |
| 2.44     | 0.605  | -0.079 |

Run: BM05120  
 $Re = 349,956$

| $\alpha$ | $C_l$ | $C_m$ |
|----------|-------|-------|
| 10.25    | 1.270 | N/A   |
| 11.27    | 1.285 | N/A   |
| 12.29    | 1.281 | N/A   |
| 13.22    | 1.280 | N/A   |
| 14.18    | 1.278 | N/A   |
| 15.23    | 1.259 | N/A   |
| 16.22    | 1.197 | N/A   |
| 17.17    | 1.151 | N/A   |
| 18.21    | 1.061 | N/A   |
| 19.18    | 1.049 | N/A   |
| 20.13    | 1.054 | N/A   |
| 19.66    | 1.056 | N/A   |
| 18.66    | 1.058 | N/A   |
| 17.63    | 1.120 | N/A   |
| 16.57    | 1.192 | N/A   |
| 15.62    | 1.258 | N/A   |
| 14.60    | 1.270 | N/A   |
| 13.81    | 1.280 | N/A   |
| 12.81    | 1.281 | N/A   |
| 11.74    | 1.278 | N/A   |
| 10.70    | 1.281 | N/A   |

Run: BM04994  
 $Re = 499,933$

| $\alpha$ | $C_l$  | $C_m$  |
|----------|--------|--------|
| -7.81    | -0.484 | 0.017  |
| -6.21    | -0.313 | -0.050 |
| -5.19    | -0.171 | -0.078 |
| -4.16    | -0.054 | -0.081 |
| -3.16    | 0.048  | -0.080 |
| -2.13    | 0.150  | -0.080 |
| -1.12    | 0.247  | -0.079 |
| -0.06    | 0.360  | -0.079 |
| 0.97     | 0.459  | -0.077 |
| 1.98     | 0.570  | -0.077 |
| 3.03     | 0.677  | -0.076 |
| 4.00     | 0.774  | -0.075 |
| 5.04     | 0.877  | -0.074 |
| 6.10     | 0.970  | -0.072 |
| 7.11     | 1.056  | -0.070 |
| 8.07     | 1.149  | -0.068 |
| 9.18     | 1.216  | -0.064 |
| 10.12    | 1.239  | -0.060 |
| 11.15    | 1.235  | -0.061 |
| 12.17    | 1.247  | -0.063 |
| 13.13    | 1.246  | -0.070 |
| 14.12    | 1.240  | -0.081 |
| 13.62    | 1.251  | -0.076 |
| 12.66    | 1.246  | -0.068 |

|       |        |        |       |        |        |       |        |        |       |        |        |
|-------|--------|--------|-------|--------|--------|-------|--------|--------|-------|--------|--------|
| 11.61 | 1.245  | -0.063 | 12.86 | 1.734  | -0.136 | 12.76 | 1.706  | -0.135 | 12.81 | 1.713  | -0.134 |
| 10.65 | 1.240  | -0.060 | 11.80 | 1.740  | -0.139 | 11.76 | 1.706  | -0.146 | 11.78 | 1.719  | -0.145 |
| 9.60  | 1.233  | -0.061 | 10.74 | 1.698  | -0.158 | 10.75 | 1.686  | -0.156 | 10.78 | 1.697  | -0.155 |
| 8.62  | 1.183  | -0.066 | 9.79  | 1.649  | -0.166 | 9.73  | 1.621  | -0.162 | 9.76  | 1.650  | -0.164 |
| 7.60  | 1.102  | -0.068 | 8.72  | 1.565  | -0.155 | 8.74  | 1.560  | -0.167 | 8.71  | 1.582  | -0.172 |
| 6.56  | 1.014  | -0.071 | 7.66  | 1.476  | -0.162 | 7.68  | 1.476  | -0.173 | 7.71  | 1.503  | -0.176 |
| 5.53  | 0.922  | -0.073 | 6.70  | 1.371  | -0.159 | 6.67  | 1.387  | -0.175 | 6.68  | 1.410  | -0.180 |
| 4.53  | 0.827  | -0.074 | 5.65  | 1.235  | -0.159 | 5.64  | 1.281  | -0.175 | 5.67  | 1.310  | -0.181 |
| 3.55  | 0.732  | -0.075 | 4.54  | 0.883  | -0.162 | 4.59  | 1.169  | -0.175 | 4.56  | 1.219  | -0.186 |
| 2.47  | 0.620  | -0.077 | 3.51  | 0.773  | -0.169 | 3.58  | 1.079  | -0.177 | 3.55  | 1.122  | -0.189 |
| 1.43  | 0.516  | -0.077 | 2.52  | 0.692  | -0.165 | 2.57  | 0.981  | -0.180 | 2.56  | 1.023  | -0.191 |
| 0.39  | 0.407  | -0.079 | 1.53  | 0.649  | -0.159 | 1.54  | 0.888  | -0.183 | 1.55  | 0.921  | -0.193 |
| -0.58 | 0.305  | -0.079 | 0.48  | 0.587  | -0.164 | 0.49  | 0.795  | -0.188 | 0.54  | 0.822  | -0.196 |
| -1.64 | 0.196  | -0.080 | -0.53 | 0.520  | -0.169 | -0.52 | 0.701  | -0.196 | -0.52 | 0.721  | -0.198 |
| -2.62 | 0.101  | -0.081 | -1.54 | 0.453  | -0.173 | -1.57 | 0.607  | -0.198 | -1.55 | 0.620  | -0.200 |
| -3.70 | -0.010 | -0.080 | -2.61 | 0.358  | -0.173 | -2.57 | 0.512  | -0.201 | -2.59 | 0.514  | -0.203 |
| -4.73 | -0.107 | -0.082 | -3.65 | 0.216  | -0.166 | -3.57 | 0.395  | -0.200 | -3.61 | 0.397  | -0.199 |
| -5.69 | -0.232 | -0.069 | -4.64 | 0.096  | -0.157 | -4.61 | 0.258  | -0.194 | -4.61 | 0.292  | -0.199 |
| -6.72 | -0.372 | -0.029 | -5.64 | -0.227 | -0.074 | -5.64 | 0.109  | -0.182 | -5.65 | 0.167  | -0.189 |
|       |        |        | -6.60 | -0.318 | -0.020 | -6.66 | -0.129 | -0.092 | -6.65 | 0.002  | -0.154 |
|       |        |        | -7.61 | -0.287 | -0.008 | -7.59 | -0.209 | -0.038 | -7.60 | -0.143 | -0.058 |
|       |        |        | -8.56 | -0.266 | -0.006 | -8.58 | -0.254 | -0.016 | -8.58 | -0.213 | -0.032 |
|       |        |        | -9.55 | -0.236 | -0.010 | -9.56 | -0.230 | -0.011 | -9.55 | -0.226 | -0.021 |

**FX 63-137 (C)**Fig. 5.10 ( $C_l$  &  $C_m$ )Run: BM04996  
 $Re = 100,019$ 

| $\alpha$ | $C_l$  | $C_m$  |
|----------|--------|--------|
| -10.08   | -0.223 | -0.021 |
| -9.04    | -0.260 | -0.008 |
| -8.07    | -0.317 | 0.001  |
| -7.08    | -0.328 | -0.012 |
| -6.10    | -0.304 | -0.028 |
| -5.11    | 0.013  | -0.146 |
| -4.14    | 0.134  | -0.171 |
| -3.12    | 0.263  | -0.176 |
| -2.04    | 0.391  | -0.189 |
| -1.05    | 0.466  | -0.169 |
| -0.07    | 0.530  | -0.162 |
| 1.02     | 0.630  | -0.170 |
| 2.00     | 0.655  | -0.157 |
| 3.08     | 0.698  | -0.165 |
| 4.06     | 0.864  | -0.170 |
| 5.11     | 1.152  | -0.163 |
| 6.16     | 1.304  | -0.171 |
| 7.16     | 1.417  | -0.155 |
| 8.18     | 1.520  | -0.167 |
| 9.31     | 1.611  | -0.157 |
| 10.26    | 1.677  | -0.145 |
| 11.31    | 1.722  | -0.146 |
| 12.29    | 1.739  | -0.143 |
| 13.30    | 1.735  | -0.136 |
| 14.31    | 1.731  | -0.130 |
| 15.37    | 1.739  | -0.129 |
| 16.28    | 1.733  | -0.131 |
| 17.33    | 1.734  | -0.128 |
| 17.99    | 1.193  | -0.261 |
| 19.03    | 1.211  | -0.278 |
| 20.03    | 1.244  | -0.284 |
| 19.51    | 1.232  | -0.291 |
| 18.54    | 1.175  | -0.275 |
| 17.52    | 1.174  | -0.262 |
| 16.56    | 1.159  | -0.247 |
| 15.56    | 1.219  | -0.244 |
| 14.54    | 1.214  | -0.231 |
| 13.63    | 1.196  | -0.219 |

Run: BM04998  
 $Re = 150,054$ 

| $\alpha$ | $C_l$  | $C_m$  |
|----------|--------|--------|
| -10.02   | -0.224 | -0.015 |
| -9.02    | -0.253 | -0.012 |
| -8.04    | -0.241 | -0.031 |
| -7.11    | -0.194 | -0.058 |
| -6.16    | 0.016  | -0.169 |
| -5.15    | 0.172  | -0.183 |
| -4.14    | 0.316  | -0.198 |
| -3.06    | 0.451  | -0.200 |
| -2.05    | 0.559  | -0.200 |
| -1.04    | 0.657  | -0.197 |
| 0.02     | 0.749  | -0.193 |
| 1.06     | 0.833  | -0.187 |
| 2.02     | 0.925  | -0.179 |
| 3.09     | 1.028  | -0.180 |
| 4.10     | 1.121  | -0.172 |
| 5.14     | 1.224  | -0.172 |
| 6.15     | 1.331  | -0.175 |
| 7.18     | 1.430  | -0.172 |
| 8.21     | 1.516  | -0.168 |
| 9.27     | 1.597  | -0.161 |
| 10.26    | 1.662  | -0.156 |
| 11.31    | 1.704  | -0.147 |
| 12.30    | 1.708  | -0.136 |
| 13.30    | 1.708  | -0.127 |
| 14.28    | 1.709  | -0.121 |
| 15.28    | 1.720  | -0.118 |
| 16.33    | 1.714  | -0.116 |
| 17.35    | 1.708  | -0.119 |
| 18.25    | 1.686  | -0.131 |
| 18.98    | 1.158  | -0.259 |
| 20.01    | 1.176  | -0.266 |
| 19.49    | 1.221  | -0.282 |
| 18.50    | 1.165  | -0.266 |
| 17.52    | 1.156  | -0.259 |
| 16.56    | 1.177  | -0.254 |
| 15.54    | 1.201  | -0.247 |
| 14.56    | 1.206  | -0.233 |
| 13.83    | 1.709  | -0.129 |

Run: BM05000  
 $Re = 199,952$ 

| $\alpha$ | $C_l$  | $C_m$  |
|----------|--------|--------|
| -10.07   | -0.227 | -0.011 |
| -9.06    | -0.244 | -0.020 |
| -8.05    | -0.188 | -0.044 |
| -7.14    | -0.102 | -0.086 |
| -6.18    | 0.093  | -0.184 |
| -5.13    | 0.225  | -0.191 |
| -4.06    | 0.340  | -0.196 |
| -3.07    | 0.452  | -0.201 |
| -2.10    | 0.559  | -0.199 |
| -1.08    | 0.660  | -0.198 |
| 0.04     | 0.767  | -0.195 |
| 1.03     | 0.863  | -0.192 |
| 2.01     | 0.964  | -0.190 |
| 3.08     | 1.070  | -0.187 |
| 4.14     | 1.171  | -0.185 |
| 5.15     | 1.257  | -0.180 |
| 6.17     | 1.356  | -0.178 |
| 7.16     | 1.452  | -0.176 |
| 8.19     | 1.538  | -0.171 |
| 9.23     | 1.621  | -0.166 |
| 10.25    | 1.679  | -0.157 |
| 11.34    | 1.715  | -0.147 |
| 12.28    | 1.717  | -0.136 |
| 13.28    | 1.722  | -0.129 |
| 14.35    | 1.727  | -0.123 |
| 15.36    | 1.735  | -0.121 |
| 16.34    | 1.741  | -0.120 |
| 17.35    | 1.746  | -0.123 |
| 18.27    | 1.734  | -0.125 |
| 19.31    | 1.736  | -0.137 |
| 20.27    | 1.685  | -0.143 |
| 19.79    | 1.692  | -0.140 |
| 18.81    | 1.728  | -0.134 |
| 17.79    | 1.741  | -0.128 |
| 16.78    | 1.745  | -0.124 |
| 15.80    | 1.735  | -0.124 |
| 14.83    | 1.731  | -0.124 |
| 13.77    | 1.720  | -0.128 |

Run: BM05002  
 $Re = 349,860$ 

| $\alpha$ | $C_l$  | $C_m$  |
|----------|--------|--------|
| -10.05   | -0.215 | -0.020 |
| -9.08    | -0.194 | -0.037 |
| -8.15    | -0.133 | -0.069 |
| -7.14    | -0.036 | -0.132 |
| -6.12    | 0.129  | -0.187 |
| -5.09    | 0.251  | -0.194 |
| -4.15    | 0.352  | -0.196 |
| -3.07    | 0.483  | -0.201 |
| -2.08    | 0.598  | -0.204 |
| -1.05    | 0.704  | -0.203 |
| 0.01     | 0.819  | -0.202 |
| 1.04     | 0.922  | -0.200 |
| 1.99     | 1.023  | -0.200 |
| 3.09     | 1.129  | -0.196 |
| 4.15     | 1.240  | -0.194 |
| 5.13     | 1.327  | -0.190 |
| 6.18     | 1.425  | -0.186 |
| 7.19     | 1.509  | -0.180 |
| 8.24     | 1.593  | -0.175 |
| 9.26     | 1.647  | -0.166 |
| 10.31    | 1.692  | -0.155 |
| 11.28    | 1.717  | -0.145 |
| 12.27    | 1.728  | -0.137 |
| 13.28    | 1.741  | -0.130 |
| 14.33    | 1.749  | -0.126 |
| 15.29    | 1.762  | -0.125 |
| 16.32    | 1.759  | -0.125 |
| 17.30    | 1.765  | -0.128 |
| 18.25    | 1.756  | -0.130 |
| 19.28    | 1.741  | -0.135 |
| 20.30    | 1.724  | -0.141 |
| 19.77    | 1.726  | -0.139 |
| 18.80    | 1.763  | -0.137 |
| 17.80    | 1.754  | -0.129 |
| 16.81    | 1.758  | -0.127 |
| 15.80    | 1.763  | -0.126 |
| 14.80    | 1.753  | -0.127 |
| 13.81    | 1.738  | -0.129 |

|       |        |        |       |        |        |       |        |        |       |        |        |
|-------|--------|--------|-------|--------|--------|-------|--------|--------|-------|--------|--------|
| 12.76 | 1.733  | -0.135 | 12.74 | 1.736  | -0.129 | 16.50 | 1.107  | -0.242 | 16.60 | 1.322  | -0.230 |
| 11.74 | 1.723  | -0.143 | 11.79 | 1.727  | -0.135 | 15.57 | 1.199  | -0.227 | 15.62 | 1.296  | -0.213 |
| 10.85 | 1.705  | -0.152 | 10.74 | 1.711  | -0.143 | 14.80 | 1.506  | -0.125 | 14.76 | 1.489  | -0.137 |
| 9.74  | 1.669  | -0.162 | 9.71  | 1.681  | -0.155 | 13.74 | 1.511  | -0.128 | 13.74 | 1.486  | -0.132 |
| 8.72  | 1.621  | -0.172 | 8.68  | 1.622  | -0.165 | 12.74 | 1.520  | -0.122 | 12.72 | 1.470  | -0.129 |
| 7.68  | 1.547  | -0.179 | 7.74  | 1.572  | -0.174 | 11.80 | 1.534  | -0.120 | 11.75 | 1.454  | -0.129 |
| 6.62  | 1.467  | -0.185 | 6.68  | 1.485  | -0.180 | 10.69 | 1.540  | -0.127 | 10.71 | 1.432  | -0.129 |
| 5.65  | 1.385  | -0.191 | 5.62  | 1.395  | -0.187 | 9.76  | 1.515  | -0.139 | 9.72  | 1.407  | -0.133 |
| 4.61  | 1.283  | -0.194 | 4.62  | 1.300  | -0.191 | 8.71  | 1.461  | -0.138 | 8.73  | 1.372  | -0.138 |
| 3.63  | 1.188  | -0.197 | 3.63  | 1.189  | -0.193 | 7.68  | 1.390  | -0.143 | 7.65  | 1.327  | -0.145 |
| 2.55  | 1.080  | -0.199 | 2.52  | 1.081  | -0.195 | 6.68  | 1.299  | -0.147 | 6.64  | 1.269  | -0.152 |
| 1.57  | 0.969  | -0.200 | 1.49  | 0.984  | -0.198 | 5.61  | 1.205  | -0.156 | 5.61  | 1.207  | -0.160 |
| 0.46  | 0.859  | -0.202 | 0.50  | 0.873  | -0.199 | 4.59  | 1.079  | -0.150 | 4.62  | 1.129  | -0.162 |
| -0.49 | 0.764  | -0.204 | -0.54 | 0.770  | -0.201 | 3.60  | 0.963  | -0.160 | 3.57  | 1.059  | -0.170 |
| -1.53 | 0.648  | -0.204 | -1.52 | 0.666  | -0.201 | 2.48  | 0.699  | -0.164 | 2.56  | 0.977  | -0.176 |
| -2.56 | 0.536  | -0.204 | -2.57 | 0.546  | -0.199 | 1.45  | 0.620  | -0.162 | 1.52  | 0.881  | -0.181 |
| -3.61 | 0.411  | -0.199 | -3.63 | 0.422  | -0.195 | 0.50  | 0.568  | -0.168 | 0.54  | 0.790  | -0.186 |
| -4.67 | 0.295  | -0.196 | -4.64 | 0.302  | -0.192 | -0.56 | 0.501  | -0.172 | -0.51 | 0.698  | -0.192 |
| -5.65 | 0.181  | -0.190 | -5.64 | 0.188  | -0.187 | -1.59 | 0.432  | -0.188 | -1.57 | 0.595  | -0.193 |
| -6.69 | 0.067  | -0.181 | -6.69 | 0.072  | -0.181 | -2.59 | 0.316  | -0.171 | -2.61 | 0.483  | -0.193 |
| -7.57 | -0.089 | -0.097 | -7.62 | -0.085 | -0.112 | -3.60 | 0.181  | -0.161 | -3.60 | 0.365  | -0.196 |
| -8.63 | -0.171 | -0.050 | -8.57 | -0.155 | -0.061 | -4.57 | 0.073  | -0.159 | -4.64 | 0.233  | -0.186 |
| -9.62 | -0.209 | -0.026 | -9.55 | -0.208 | -0.035 | -5.60 | -0.244 | -0.070 | -5.68 | 0.077  | -0.172 |
|       |        |        |       |        |        | -6.59 | -0.307 | -0.024 | -6.63 | -0.147 | -0.076 |
|       |        |        |       |        |        | -7.59 | -0.319 | -0.018 | -7.61 | -0.216 | -0.040 |
|       |        |        |       |        |        | -8.62 | -0.277 | -0.027 | -8.62 | -0.275 | -0.018 |
|       |        |        |       |        |        | -9.56 | -0.251 | -0.034 | -9.58 | -0.244 | -0.017 |

Run: BM05004  
 $Re = 499,848$

| $\alpha$ | $C_l$  | $C_m$  |
|----------|--------|--------|
| -10.20   | -0.235 | -0.025 |
| -9.10    | -0.193 | -0.048 |
| -8.32    | -0.152 | -0.076 |
| -7.31    | -0.042 | -0.132 |
| -6.11    | 0.137  | -0.186 |
| -5.04    | 0.257  | -0.190 |
| -4.13    | 0.361  | -0.193 |
| -3.04    | 0.493  | -0.198 |
| -2.02    | 0.616  | -0.201 |
| -0.97    | 0.720  | -0.200 |
| -0.02    | 0.819  | -0.199 |
| 1.00     | 0.928  | -0.198 |
| 2.08     | 1.031  | -0.196 |
| 3.15     | 1.143  | -0.194 |
| 4.17     | 1.243  | -0.191 |
| 5.19     | 1.345  | -0.187 |
| 6.17     | 1.444  | -0.183 |
| 7.17     | 1.525  | -0.177 |
| 8.23     | 1.599  | -0.168 |
| 9.27     | 1.656  | -0.158 |
| 10.28    | 1.687  | -0.147 |
| 11.37    | 1.714  | -0.136 |
| 12.32    | 1.723  | -0.130 |
| 13.30    | 1.739  | -0.125 |
| 14.28    | 1.749  | -0.125 |
| 15.35    | 1.747  | -0.123 |
| 16.34    | 1.760  | -0.126 |
| 17.34    | 1.746  | -0.127 |
| 18.35    | 1.729  | -0.131 |
| 19.31    | 1.737  | -0.138 |
| 20.29    | 1.715  | -0.145 |
| 19.77    | 1.720  | -0.144 |
| 18.77    | 1.730  | -0.135 |
| 17.82    | 1.732  | -0.130 |
| 16.74    | 1.753  | -0.128 |
| 15.82    | 1.763  | -0.127 |
| 14.86    | 1.745  | -0.125 |
| 13.75    | 1.744  | -0.126 |

**FX 63-137 (C)**  
 Fig. 5.12 ( $C_l$  &  $C_m$ )

Run: BM05006  
 $Re = 99,985$

| $\alpha$ | $C_l$  | $C_m$  |
|----------|--------|--------|
| -10.08   | -0.218 | -0.034 |
| -9.07    | -0.270 | -0.020 |
| -8.09    | -0.288 | -0.017 |
| -7.12    | -0.340 | -0.013 |
| -6.08    | -0.312 | -0.033 |
| -5.13    | -0.012 | -0.153 |
| -4.14    | 0.116  | -0.165 |
| -3.12    | 0.244  | -0.173 |
| -2.09    | 0.368  | -0.181 |
| -1.05    | 0.456  | -0.165 |
| -0.01    | 0.527  | -0.168 |
| 0.98     | 0.598  | -0.169 |
| 2.03     | 0.656  | -0.165 |
| 3.11     | 0.880  | -0.156 |
| 4.11     | 1.016  | -0.145 |
| 5.13     | 1.140  | -0.150 |
| 6.19     | 1.237  | -0.154 |
| 7.21     | 1.336  | -0.151 |
| 8.23     | 1.410  | -0.144 |
| 9.26     | 1.485  | -0.130 |
| 10.26    | 1.528  | -0.133 |
| 11.29    | 1.532  | -0.122 |
| 12.24    | 1.514  | -0.124 |
| 13.27    | 1.503  | -0.123 |
| 14.24    | 1.491  | -0.128 |
| 15.27    | 1.495  | -0.127 |
| 16.24    | 1.508  | -0.131 |
| 17.26    | 1.545  | -0.134 |
| 18.26    | 1.566  | -0.138 |
| 19.05    | 1.109  | -0.264 |
| 20.03    | 1.191  | -0.286 |
| 19.48    | 1.134  | -0.284 |
| 18.47    | 1.102  | -0.271 |
| 17.50    | 1.066  | -0.251 |

Run: BM05008  
 $Re = 149,980$

| $\alpha$ | $C_l$  | $C_m$  |
|----------|--------|--------|
| -10.13   | -0.239 | -0.014 |
| -9.09    | -0.261 | -0.018 |
| -8.07    | -0.267 | -0.027 |
| -7.11    | -0.197 | -0.057 |
| -6.16    | -0.023 | -0.154 |
| -5.14    | 0.159  | -0.186 |
| -4.12    | 0.302  | -0.193 |
| -3.06    | 0.422  | -0.198 |
| -2.06    | 0.535  | -0.198 |
| -1.03    | 0.643  | -0.193 |
| 0.05     | 0.742  | -0.191 |
| 1.03     | 0.832  | -0.187 |
| 2.09     | 0.933  | -0.179 |
| 3.07     | 1.024  | -0.175 |
| 4.10     | 1.097  | -0.165 |
| 5.12     | 1.168  | -0.158 |
| 6.18     | 1.244  | -0.156 |
| 7.18     | 1.306  | -0.149 |
| 8.21     | 1.352  | -0.142 |
| 9.23     | 1.384  | -0.132 |
| 10.19    | 1.420  | -0.130 |
| 11.25    | 1.442  | -0.127 |
| 12.24    | 1.463  | -0.125 |
| 13.25    | 1.474  | -0.127 |
| 14.24    | 1.483  | -0.130 |
| 15.26    | 1.485  | -0.133 |
| 16.24    | 1.489  | -0.141 |
| 17.21    | 1.470  | -0.142 |
| 18.24    | 1.460  | -0.147 |
| 19.26    | 1.491  | -0.151 |
| 20.00    | 1.190  | -0.262 |
| 19.56    | 1.181  | -0.265 |
| 18.54    | 1.271  | -0.263 |
| 17.54    | 1.285  | -0.245 |

Run: BM05010  
 $Re = 200,005$

| $\alpha$ | $C_l$  | $C_m$  |
|----------|--------|--------|
| -10.11   | -0.212 | -0.016 |
| -9.09    | -0.246 | -0.020 |
| -8.08    | -0.185 | -0.044 |
| -7.09    | -0.110 | -0.086 |
| -6.17    | 0.085  | -0.181 |
| -5.15    | 0.207  | -0.191 |
| -4.11    | 0.321  | -0.194 |
| -3.10    | 0.431  | -0.196 |
| -2.07    | 0.538  | -0.194 |
| -1.01    | 0.640  | -0.192 |
| 0.01     | 0.752  | -0.191 |
| 1.01     | 0.849  | -0.188 |
| 2.03     | 0.937  | -0.181 |
| 3.07     | 1.006  | -0.173 |
| 4.09     | 1.084  | -0.167 |
| 5.17     | 1.162  | -0.161 |
| 6.16     | 1.225  | -0.155 |
| 7.15     | 1.296  | -0.150 |
| 8.22     | 1.346  | -0.143 |
| 9.25     | 1.392  | -0.137 |
| 10.26    | 1.426  | -0.133 |
| 11.27    | 1.453  | -0.131 |
| 12.25    | 1.478  | -0.131 |
| 13.23    | 1.492  | -0.131 |
| 14.22    | 1.500  | -0.133 |
| 15.26    | 1.495  | -0.137 |
| 16.25    | 1.489  | -0.141 |
| 17.24    | 1.509  | -0.148 |
| 18.21    | 1.482  | -0.151 |
| 19.25    | 1.494  | -0.160 |
| 20.17    | 1.496  | -0.163 |
| 19.70    | 1.493  | -0.165 |
| 18.70    | 1.506  | -0.161 |
| 17.70    | 1.492  | -0.152 |



|       |        |        |       |        |        |       |        |        |       |        |        |
|-------|--------|--------|-------|--------|--------|-------|--------|--------|-------|--------|--------|
| 16.71 | 1.512  | -0.148 | 16.72 | 1.527  | -0.150 | 16.71 | 1.520  | -0.154 | 20.07 | 0.825  | -0.152 |
| 15.73 | 1.506  | -0.142 | 15.72 | 1.526  | -0.145 | 15.71 | 1.511  | -0.149 | 19.54 | 0.788  | -0.163 |
| 14.71 | 1.508  | -0.138 | 14.70 | 1.532  | -0.140 | 14.72 | 1.531  | -0.147 | 18.56 | 0.800  | -0.152 |
| 13.71 | 1.501  | -0.135 | 13.68 | 1.534  | -0.139 | 13.67 | 1.530  | -0.142 | 17.54 | 0.809  | -0.147 |
| 12.72 | 1.491  | -0.133 | 12.71 | 1.512  | -0.134 | 12.72 | 1.520  | -0.139 | 16.55 | 0.799  | -0.135 |
| 11.67 | 1.471  | -0.133 | 11.74 | 1.492  | -0.135 | 11.72 | 1.512  | -0.138 | 15.55 | 0.806  | -0.121 |
| 10.72 | 1.444  | -0.134 | 10.69 | 1.469  | -0.137 | 10.72 | 1.476  | -0.138 | 14.77 | 1.070  | -0.019 |
| 9.77  | 1.411  | -0.137 | 9.73  | 1.433  | -0.139 | 9.75  | 1.452  | -0.140 | 13.73 | 1.081  | -0.032 |
| 8.71  | 1.379  | -0.143 | 8.67  | 1.398  | -0.145 | 8.67  | 1.414  | -0.144 | 12.77 | 1.064  | -0.023 |
| 7.67  | 1.326  | -0.149 | 7.66  | 1.361  | -0.152 | 7.69  | 1.364  | -0.149 | 11.76 | 1.044  | -0.024 |
| 6.64  | 1.257  | -0.154 | 6.65  | 1.309  | -0.160 | 6.64  | 1.308  | -0.157 | 10.73 | 1.033  | -0.034 |
| 5.62  | 1.199  | -0.161 | 5.64  | 1.233  | -0.165 | 5.64  | 1.236  | -0.163 | 9.74  | 1.039  | -0.032 |
| 4.60  | 1.131  | -0.167 | 4.61  | 1.155  | -0.170 | 4.60  | 1.161  | -0.168 | 8.71  | 0.989  | -0.042 |
| 3.59  | 1.052  | -0.173 | 3.64  | 1.068  | -0.173 | 3.56  | 1.065  | -0.172 | 7.70  | 0.925  | -0.049 |
| 2.54  | 0.981  | -0.181 | 2.59  | 0.976  | -0.177 | 2.50  | 0.973  | -0.175 | 6.65  | 0.745  | -0.042 |
| 1.51  | 0.892  | -0.186 | 1.52  | 0.884  | -0.181 | 1.49  | 0.883  | -0.179 | 5.55  | 0.390  | -0.025 |
| 0.55  | 0.805  | -0.191 | 0.49  | 0.790  | -0.183 | 0.47  | 0.787  | -0.182 | 4.52  | 0.278  | -0.014 |
| -0.53 | 0.695  | -0.193 | -0.50 | 0.696  | -0.186 | -0.51 | 0.693  | -0.183 | 3.52  | 0.192  | -0.012 |
| -1.56 | 0.595  | -0.196 | -1.57 | 0.607  | -0.191 | -1.54 | 0.611  | -0.187 | 2.55  | 0.098  | -0.003 |
| -2.59 | 0.487  | -0.197 | -2.60 | 0.511  | -0.195 | -2.61 | 0.503  | -0.188 | 1.47  | 0.028  | -0.006 |
| -3.64 | 0.377  | -0.194 | -3.58 | 0.409  | -0.195 | -3.54 | 0.412  | -0.190 | 0.42  | -0.063 | 0.004  |
| -4.62 | 0.269  | -0.191 | -4.63 | 0.297  | -0.192 | -4.61 | 0.296  | -0.190 | -0.53 | -0.186 | 0.015  |
| -5.66 | 0.150  | -0.187 | -5.67 | 0.172  | -0.188 | -5.60 | 0.190  | -0.187 | -1.61 | -0.241 | 0.004  |
| -6.61 | -0.014 | -0.143 | -6.64 | 0.060  | -0.181 | -6.69 | 0.066  | -0.182 | -2.56 | -0.274 | -0.011 |
| -7.59 | -0.156 | -0.063 | -7.56 | -0.099 | -0.100 | -7.57 | -0.081 | -0.104 | -3.63 | -0.325 | -0.031 |
| -8.59 | -0.225 | -0.031 | -8.63 | -0.181 | -0.051 | -8.53 | -0.150 | -0.063 | -4.65 | -0.410 | -0.031 |
| -9.61 | -0.233 | -0.018 | -9.62 | -0.223 | -0.027 | -9.43 | -0.198 | -0.038 | -5.72 | -0.499 | -0.042 |
|       |        |        |       |        |        |       |        |        | -6.67 | -0.574 | -0.041 |
|       |        |        |       |        |        |       |        |        | -7.74 | -0.680 | -0.040 |
|       |        |        |       |        |        |       |        |        | -8.79 | -0.748 | -0.059 |
|       |        |        |       |        |        |       |        |        | -9.77 | -0.777 | -0.076 |

Run: BM05012  
Re = 349,891

| $\alpha$ | $C_l$  | $C_m$  |
|----------|--------|--------|
| -10.15   | -0.252 | -0.030 |
| -9.08    | -0.213 | -0.045 |
| -8.12    | -0.143 | -0.078 |
| -7.17    | -0.044 | -0.127 |
| -6.13    | 0.126  | -0.186 |
| -5.09    | 0.241  | -0.190 |
| -4.08    | 0.362  | -0.194 |
| -3.05    | 0.468  | -0.194 |
| -2.02    | 0.568  | -0.192 |
| -1.00    | 0.658  | -0.189 |
| -0.01    | 0.746  | -0.184 |
| 1.00     | 0.839  | -0.182 |
| 2.01     | 0.927  | -0.179 |
| 3.08     | 1.027  | -0.176 |
| 4.10     | 1.109  | -0.172 |
| 5.10     | 1.195  | -0.168 |
| 6.19     | 1.276  | -0.163 |
| 7.15     | 1.337  | -0.156 |
| 8.20     | 1.383  | -0.148 |
| 9.25     | 1.419  | -0.142 |
| 10.21    | 1.455  | -0.138 |
| 11.23    | 1.492  | -0.137 |
| 12.23    | 1.509  | -0.136 |
| 13.21    | 1.527  | -0.137 |
| 14.25    | 1.538  | -0.139 |
| 15.24    | 1.519  | -0.143 |
| 16.22    | 1.508  | -0.146 |
| 17.16    | 1.521  | -0.152 |
| 18.20    | 1.516  | -0.158 |
| 19.20    | 1.518  | -0.165 |
| 20.19    | 1.500  | -0.171 |
| 19.69    | 1.514  | -0.170 |
| 18.67    | 1.521  | -0.162 |
| 17.72    | 1.513  | -0.155 |

Run: BM05014  
Re = 499,970

| $\alpha$ | $C_l$  | $C_m$  |
|----------|--------|--------|
| -10.10   | -0.218 | -0.023 |
| -9.16    | -0.191 | -0.044 |
| -8.14    | -0.129 | -0.076 |
| -7.12    | -0.025 | -0.140 |
| -6.16    | 0.132  | -0.185 |
| -5.08    | 0.259  | -0.191 |
| -4.08    | 0.358  | -0.191 |
| -3.05    | 0.460  | -0.190 |
| -2.03    | 0.566  | -0.189 |
| -1.04    | 0.654  | -0.186 |
| 0.02     | 0.752  | -0.183 |
| 1.06     | 0.841  | -0.181 |
| 2.08     | 0.939  | -0.178 |
| 3.10     | 1.028  | -0.174 |
| 4.15     | 1.118  | -0.171 |
| 5.13     | 1.195  | -0.166 |
| 6.17     | 1.267  | -0.160 |
| 7.15     | 1.336  | -0.153 |
| 8.18     | 1.390  | -0.147 |
| 9.20     | 1.431  | -0.142 |
| 10.19    | 1.475  | -0.139 |
| 11.24    | 1.497  | -0.138 |
| 12.24    | 1.508  | -0.138 |
| 13.22    | 1.519  | -0.142 |
| 14.22    | 1.525  | -0.145 |
| 15.28    | 1.519  | -0.147 |
| 16.28    | 1.519  | -0.152 |
| 17.26    | 1.506  | -0.155 |
| 18.20    | 1.509  | -0.163 |
| 19.22    | 1.496  | -0.167 |
| 20.20    | 1.516  | -0.177 |
| 19.71    | 1.495  | -0.171 |
| 18.73    | 1.507  | -0.165 |
| 17.65    | 1.511  | -0.159 |

**S822 (B)**

Fig. 5.16 ( $C_l$  &  $C_m$ )

Run: BM05016  
Re = 100,027

| $\alpha$ | $C_l$  | $C_m$  |
|----------|--------|--------|
| -10.26   | -0.782 | -0.067 |
| -9.26    | -0.775 | -0.069 |
| -8.23    | -0.727 | -0.061 |
| -7.19    | -0.644 | -0.051 |
| -6.21    | -0.550 | -0.051 |
| -5.16    | -0.465 | -0.036 |
| -4.09    | -0.380 | -0.028 |
| -3.10    | -0.301 | -0.027 |
| -2.07    | -0.259 | -0.010 |
| -1.06    | -0.230 | 0.005  |
| -0.03    | -0.140 | 0.006  |
| 1.05     | -0.015 | 0.003  |
| 2.01     | 0.035  | 0.010  |
| 3.01     | 0.122  | -0.003 |
| 4.08     | 0.226  | -0.019 |
| 5.11     | 0.318  | -0.020 |
| 6.10     | 0.483  | -0.030 |
| 7.16     | 0.858  | -0.048 |
| 8.18     | 0.957  | -0.044 |
| 9.19     | 1.022  | -0.042 |
| 10.21    | 1.035  | -0.032 |
| 11.27    | 1.034  | -0.024 |
| 12.24    | 1.053  | -0.012 |
| 13.25    | 1.074  | -0.010 |
| 14.23    | 1.086  | -0.020 |
| 15.23    | 1.048  | -0.023 |
| 16.10    | 0.804  | -0.110 |
| 17.07    | 0.806  | -0.123 |
| 18.10    | 0.833  | -0.128 |
| 19.07    | 0.813  | -0.143 |

Run: BM05018  
Re = 149,914

| $\alpha$ | $C_l$  | $C_m$  |
|----------|--------|--------|
| -10.24   | -0.814 | -0.053 |
| -9.26    | -0.794 | -0.043 |
| -8.24    | -0.719 | -0.045 |
| -7.21    | -0.617 | -0.047 |
| -6.18    | -0.512 | -0.052 |
| -5.19    | -0.411 | -0.054 |
| -4.11    | -0.316 | -0.047 |
| -3.09    | -0.224 | -0.050 |
| -2.06    | -0.147 | -0.042 |
| -1.09    | -0.089 | -0.033 |
| -0.01    | -0.035 | -0.025 |
| 1.01     | 0.025  | -0.017 |
| 2.01     | 0.118  | -0.021 |
| 3.08     | 0.261  | -0.030 |
| 4.11     | 0.453  | -0.042 |
| 5.17     | 0.782  | -0.067 |
| 6.20     | 0.868  | -0.060 |
| 7.21     | 0.932  | -0.055 |
| 8.21     | 0.990  | -0.048 |
| 9.19     | 1.031  | -0.039 |
| 10.20    | 1.052  | -0.034 |
| 11.25    | 1.063  | -0.026 |
| 12.27    | 1.075  | -0.019 |
| 13.25    | 1.095  | -0.018 |
| 14.31    | 1.104  | -0.018 |
| 15.29    | 1.089  | -0.021 |
| 16.08    | 0.844  | -0.114 |
| 17.09    | 0.822  | -0.122 |
| 18.11    | 0.828  | -0.128 |
| 19.05    | 0.818  | -0.133 |

|              |        |        |              |        |        |              |        |        |        |        |        |
|--------------|--------|--------|--------------|--------|--------|--------------|--------|--------|--------|--------|--------|
| 20.06        | 0.808  | -0.138 | 20.07        | 0.857  | -0.143 | 12.76        | 1.094  | -0.026 | 1.03   | 0.333  | -0.070 |
| 19.53        | 0.837  | -0.137 | 19.60        | 0.830  | -0.134 | 11.68        | 1.063  | -0.029 | 2.00   | 0.442  | -0.071 |
| 18.60        | 0.822  | -0.131 | 18.57        | 0.815  | -0.127 | 10.72        | 1.037  | -0.034 | 3.06   | 0.550  | -0.071 |
| 17.57        | 0.844  | -0.132 | 17.51        | 0.818  | -0.126 | 9.71         | 1.016  | -0.040 | 4.14   | 0.660  | -0.071 |
| 16.57        | 0.816  | -0.117 | 16.60        | 0.900  | -0.125 | 8.67         | 0.975  | -0.047 | 5.12   | 0.762  | -0.070 |
| 15.66        | 0.879  | -0.115 | 15.81        | 1.089  | -0.028 | 7.65         | 0.931  | -0.053 | 6.13   | 0.846  | -0.066 |
| 14.73        | 1.100  | -0.018 | 14.74        | 1.101  | -0.022 | 6.62         | 0.865  | -0.059 | 7.17   | 0.902  | -0.056 |
| 13.74        | 1.090  | -0.015 | 13.78        | 1.089  | -0.021 | 5.62         | 0.790  | -0.065 | 8.20   | 0.957  | -0.048 |
| 12.73        | 1.080  | -0.016 | 12.72        | 1.078  | -0.022 | 4.56         | 0.689  | -0.068 | 9.21   | 0.994  | -0.040 |
| 11.74        | 1.062  | -0.024 | 11.71        | 1.051  | -0.024 | 3.61         | 0.597  | -0.069 | 10.21  | 1.036  | -0.034 |
| 10.72        | 1.052  | -0.030 | 10.74        | 1.042  | -0.031 | 2.55         | 0.490  | -0.070 | 11.28  | 1.079  | -0.030 |
| 9.70         | 1.048  | -0.036 | 9.70         | 1.034  | -0.040 | 1.53         | 0.388  | -0.070 | 12.28  | 1.109  | -0.027 |
| 8.65         | 1.008  | -0.047 | 8.73         | 1.001  | -0.047 | 0.47         | 0.273  | -0.069 | 13.25  | 1.136  | -0.027 |
| 7.67         | 0.961  | -0.052 | 7.64         | 0.949  | -0.053 | -0.56        | 0.167  | -0.069 | 14.26  | 1.165  | -0.028 |
| 6.65         | 0.890  | -0.058 | 6.66         | 0.911  | -0.065 | -1.60        | 0.063  | -0.069 | 15.25  | 1.169  | -0.032 |
| 5.58         | 0.819  | -0.067 | 5.57         | 0.793  | -0.062 | -2.57        | -0.031 | -0.069 | 16.25  | 1.152  | -0.041 |
| 4.60         | 0.698  | -0.066 | 4.57         | 0.644  | -0.052 | -3.68        | -0.139 | -0.070 | 15.76  | 1.168  | -0.037 |
| 3.51         | 0.333  | -0.034 | 3.58         | 0.499  | -0.045 | -4.65        | -0.236 | -0.071 | 14.75  | 1.166  | -0.031 |
| 2.55         | 0.190  | -0.027 | 2.52         | 0.379  | -0.046 | -5.66        | -0.330 | -0.071 | 13.73  | 1.147  | -0.028 |
| 1.47         | 0.063  | -0.021 | 1.49         | 0.276  | -0.049 | -6.67        | -0.420 | -0.074 | 12.76  | 1.126  | -0.028 |
| 0.49         | -0.010 | -0.021 | 0.54         | 0.196  | -0.055 | -7.73        | -0.505 | -0.076 | 11.77  | 1.090  | -0.029 |
| -0.56        | -0.060 | -0.031 | -0.53        | 0.093  | -0.057 | -8.75        | -0.580 | -0.079 | 10.68  | 1.051  | -0.033 |
| -1.62        | -0.121 | -0.040 | -1.63        | 0.004  | -0.060 | -9.80        | -0.637 | -0.084 | 9.71   | 1.018  | -0.038 |
| -2.59        | -0.189 | -0.046 | -2.61        | -0.078 | -0.064 |              |        |        | 8.66   | 0.975  | -0.045 |
| -3.63        | -0.267 | -0.054 | -3.70        | -0.178 | -0.066 | Run: BM05125 |        |        | 7.64   | 0.921  | -0.052 |
| -4.66        | -0.354 | -0.056 | -4.64        | -0.267 | -0.068 | Re = 349,855 |        |        | 6.64   | 0.878  | -0.062 |
| -5.66        | -0.460 | -0.049 | -5.66        | -0.364 | -0.067 | $\alpha$     | $C_l$  | $C_m$  | 5.63   | 0.803  | -0.069 |
| -6.71        | -0.560 | -0.048 | -6.72        | -0.464 | -0.068 | 10.33        | 1.036  | N/A    | 4.59   | 0.707  | -0.072 |
| -7.69        | -0.659 | -0.045 | -7.75        | -0.568 | -0.066 | 11.20        | 1.064  | N/A    | 3.56   | 0.599  | -0.072 |
| -8.74        | -0.762 | -0.044 | -8.71        | -0.660 | -0.061 | 12.25        | 1.090  | N/A    | 2.56   | 0.494  | -0.072 |
| -9.73        | -0.809 | -0.054 | -9.73        | -0.744 | -0.062 | 13.27        | 1.122  | N/A    | 1.51   | 0.383  | -0.071 |
|              |        |        |              |        |        | 14.35        | 1.134  | N/A    | 0.53   | 0.278  | -0.071 |
| Run: BM05020 |        |        | Run: BM05022 |        |        | 15.15        | 1.157  | N/A    | -0.52  | 0.170  | -0.071 |
| Re = 199,832 |        |        | Re = 349,869 |        |        | 16.19        | 1.136  | N/A    | -1.59  | 0.061  | -0.070 |
| $\alpha$     | $C_l$  | $C_m$  | $\alpha$     | $C_l$  | $C_m$  | 17.24        | 0.910  | N/A    | -2.58  | -0.043 | -0.069 |
| -10.30       | -0.787 | -0.059 | -10.30       | -0.660 | -0.086 | 18.24        | 0.829  | N/A    | -3.59  | -0.148 | -0.069 |
| -9.24        | -0.705 | -0.065 | -9.21        | -0.604 | -0.081 | 19.24        | 0.822  | N/A    | -4.63  | -0.250 | -0.069 |
| -8.21        | -0.619 | -0.064 | -8.11        | -0.532 | -0.077 | 20.24        | 0.839  | N/A    | -5.69  | -0.348 | -0.069 |
| -7.19        | -0.511 | -0.071 | -7.15        | -0.458 | -0.074 | 19.73        | 0.832  | N/A    | -6.64  | -0.435 | -0.070 |
| -6.16        | -0.416 | -0.071 | -6.15        | -0.372 | -0.072 | 18.60        | 0.838  | N/A    | -7.70  | -0.529 | -0.072 |
| -5.18        | -0.324 | -0.069 | -5.13        | -0.272 | -0.070 | 17.60        | 0.857  | N/A    | -8.77  | -0.612 | -0.074 |
| -4.11        | -0.222 | -0.069 | -4.07        | -0.177 | -0.069 | 16.80        | 0.922  | N/A    | -9.80  | -0.677 | -0.079 |
| -3.08        | -0.125 | -0.066 | -3.09        | -0.086 | -0.068 | 15.69        | 1.141  | N/A    |        |        |        |
| -2.09        | -0.039 | -0.063 | -2.08        | 0.020  | -0.068 | 14.85        | 1.147  | N/A    |        |        |        |
| -1.03        | 0.044  | -0.059 | -1.01        | 0.123  | -0.068 | 13.78        | 1.129  | N/A    |        |        |        |
| -0.02        | 0.135  | -0.056 | 0.03         | 0.229  | -0.068 | 12.76        | 1.105  | N/A    |        |        |        |
| 1.02         | 0.230  | -0.052 | 1.01         | 0.330  | -0.069 | 11.67        | 1.080  | N/A    |        |        |        |
| 2.05         | 0.327  | -0.048 | 2.03         | 0.438  | -0.069 | 10.59        | 1.048  | N/A    |        |        |        |
| 3.04         | 0.429  | -0.045 | 3.09         | 0.542  | -0.068 | Run: BM05024 |        |        |        |        |        |
| 4.11         | 0.564  | -0.047 | 4.12         | 0.646  | -0.067 | Re = 499,698 |        |        |        |        |        |
| 5.12         | 0.719  | -0.057 | 5.15         | 0.743  | -0.065 | $\alpha$     | $C_l$  | $C_m$  |        |        |        |
| 6.14         | 0.869  | -0.066 | 6.14         | 0.831  | -0.060 | -10.20       | -0.697 | -0.080 | -10.27 | -0.781 | -0.069 |
| 7.19         | 0.928  | -0.058 | 7.15         | 0.899  | -0.055 | -9.21        | -0.642 | -0.076 | -9.26  | -0.784 | -0.056 |
| 8.25         | 0.982  | -0.050 | 8.18         | 0.958  | -0.050 | -8.20        | -0.574 | -0.073 | -8.16  | -0.729 | -0.043 |
| 9.24         | 1.019  | -0.043 | 9.23         | 1.001  | -0.043 | -7.21        | -0.485 | -0.070 | -7.20  | -0.660 | -0.036 |
| 10.26        | 1.031  | -0.034 | 10.25        | 1.025  | -0.035 | -6.10        | -0.386 | -0.069 | -6.17  | -0.578 | -0.021 |
| 11.24        | 1.047  | -0.027 | 11.24        | 1.055  | -0.030 | -5.07        | -0.290 | -0.069 | -5.14  | -0.482 | -0.030 |
| 12.29        | 1.062  | -0.022 | 12.26        | 1.081  | -0.026 | -4.16        | -0.202 | -0.068 | -4.10  | -0.382 | -0.041 |
| 13.26        | 1.088  | -0.020 | 13.25        | 1.102  | -0.025 | -3.09        | -0.092 | -0.068 | -3.14  | -0.290 | -0.036 |
| 14.28        | 1.098  | -0.020 | 14.25        | 1.128  | -0.026 | -2.07        | 0.016  | -0.069 | -2.10  | -0.217 | -0.025 |
| 15.25        | 1.100  | -0.022 | 15.28        | 1.125  | -0.029 | -1.06        | 0.117  | -0.069 | -1.04  | -0.160 | -0.015 |
| 16.08        | 0.851  | -0.116 | 16.26        | 1.120  | -0.036 | 0.01         | 0.226  | -0.070 | -0.03  | -0.102 | -0.011 |
| 17.09        | 0.823  | -0.120 | 15.72        | 1.126  | -0.033 |              |        |        | 1.04   | -0.034 | -0.004 |
| 18.04        | 0.814  | -0.124 | 14.76        | 1.130  | -0.028 |              |        |        | 2.08   | 0.035  | 0.001  |
| 19.07        | 0.811  | -0.129 | 13.71        | 1.115  | -0.026 |              |        |        | 3.02   | 0.128  | -0.012 |
|              |        |        |              |        |        |              |        |        | 4.08   | 0.286  | -0.016 |

**S822 (B)**

Fig. 5.18 ( $C_l$  &  $C_m$ )

Run: BM05026

Re = 100,074

| $\alpha$ | $C_l$  | $C_m$  |
|----------|--------|--------|
| -10.27   | -0.781 | -0.069 |
| -9.26    | -0.784 | -0.056 |
| -8.16    | -0.729 | -0.043 |
| -7.20    | -0.660 | -0.036 |
| -6.17    | -0.578 | -0.021 |
| -5.14    | -0.482 | -0.030 |
| -4.10    | -0.382 | -0.041 |
| -3.14    | -0.290 | -0.036 |
| -2.10    | -0.217 | -0.025 |
| -1.04    | -0.160 | -0.015 |
| -0.03    | -0.102 | -0.011 |
| 1.04     | -0.034 | -0.004 |
| 2.08     | 0.035  | 0.001  |
| 3.02     | 0.128  | -0.012 |
| 4.08     | 0.286  | -0.016 |



Run: BM05034  
 $Re = 499,891$

| $\alpha$ | $C_l$  | $C_m$  |
|----------|--------|--------|
| -10.22   | -0.660 | -0.081 |
| -9.19    | -0.614 | -0.077 |
| -8.15    | -0.543 | -0.074 |
| -7.17    | -0.454 | -0.073 |
| -6.16    | -0.355 | -0.072 |
| -5.10    | -0.264 | -0.068 |
| -4.09    | -0.185 | -0.063 |
| -3.07    | -0.100 | -0.060 |
| -2.02    | 0.000  | -0.059 |
| -1.04    | 0.084  | -0.057 |
| -0.05    | 0.177  | -0.056 |
| 1.06     | 0.268  | -0.054 |
| 2.10     | 0.367  | -0.053 |
| 3.06     | 0.459  | -0.052 |
| 4.09     | 0.549  | -0.050 |
| 5.10     | 0.630  | -0.048 |
| 6.14     | 0.713  | -0.045 |
| 7.19     | 0.791  | -0.042 |
| 8.18     | 0.865  | -0.039 |
| 9.15     | 0.928  | -0.035 |
| 10.19    | 0.997  | -0.031 |
| 11.23    | 1.049  | -0.029 |
| 12.24    | 1.083  | -0.027 |
| 13.29    | 1.103  | -0.026 |
| 14.24    | 1.110  | -0.029 |
| 15.22    | 1.122  | -0.036 |
| 16.23    | 1.092  | -0.048 |
| 15.75    | 1.105  | -0.046 |
| 14.71    | 1.111  | -0.034 |
| 13.77    | 1.115  | -0.029 |
| 12.71    | 1.099  | -0.027 |
| 11.75    | 1.071  | -0.028 |
| 10.71    | 1.022  | -0.031 |
| 9.68     | 0.960  | -0.034 |
| 8.66     | 0.896  | -0.038 |
| 7.67     | 0.828  | -0.041 |
| 6.61     | 0.749  | -0.044 |
| 5.57     | 0.671  | -0.047 |
| 4.59     | 0.585  | -0.049 |
| 3.59     | 0.504  | -0.051 |
| 2.51     | 0.411  | -0.053 |
| 1.50     | 0.315  | -0.055 |
| 0.45     | 0.223  | -0.056 |
| -0.52    | 0.132  | -0.057 |
| -1.57    | 0.037  | -0.059 |
| -2.63    | -0.055 | -0.060 |
| -3.56    | -0.143 | -0.062 |
| -4.62    | -0.226 | -0.065 |
| -5.66    | -0.308 | -0.070 |
| -6.69    | -0.408 | -0.073 |
| -7.80    | -0.506 | -0.074 |
| -8.76    | -0.592 | -0.075 |
| -9.77    | -0.643 | -0.080 |

**S834**  
 Fig. 5.22 ( $C_l$  &  $C_m$ )

Run: BM05036  
 $Re = 100,033$

| $\alpha$ | $C_l$  | $C_m$  |
|----------|--------|--------|
| -10.31   | -0.773 | -0.070 |
| -9.20    | -0.769 | -0.054 |
| -8.24    | -0.740 | -0.066 |
| -7.21    | -0.693 | -0.055 |
| -6.18    | -0.610 | -0.051 |
| -5.17    | -0.516 | -0.047 |
| -4.12    | -0.412 | -0.033 |
| -3.10    | -0.332 | -0.022 |
| -2.08    | -0.255 | -0.011 |
| -1.02    | -0.242 | 0.010  |
| 0.01     | -0.136 | -0.000 |
| 0.96     | -0.035 | 0.010  |
| 2.03     | 0.052  | -0.013 |
| 3.07     | 0.153  | -0.008 |
| 4.07     | 0.273  | -0.025 |
| 5.04     | 0.452  | -0.034 |
| 6.13     | 0.771  | -0.045 |
| 7.21     | 0.869  | -0.045 |
| 8.20     | 0.941  | -0.036 |
| 9.24     | 0.996  | -0.033 |
| 10.22    | 1.010  | -0.005 |
| 11.26    | 1.036  | -0.007 |
| 12.26    | 1.058  | 0.002  |
| 13.27    | 1.071  | 0.004  |
| 14.28    | 1.060  | -0.009 |
| 15.12    | 0.851  | -0.101 |
| 16.07    | 0.832  | -0.110 |
| 17.08    | 0.767  | -0.118 |
| 18.10    | 0.792  | -0.136 |
| 19.08    | 0.802  | -0.147 |
| 20.07    | 0.875  | -0.162 |
| 19.60    | 0.848  | -0.161 |
| 18.53    | 0.818  | -0.142 |
| 17.54    | 0.789  | -0.127 |
| 16.59    | 0.809  | -0.125 |
| 15.58    | 0.796  | -0.106 |
| 14.61    | 0.958  | -0.101 |
| 13.79    | 1.079  | -0.000 |
| 12.76    | 1.070  | -0.002 |
| 11.78    | 1.059  | -0.001 |
| 10.74    | 1.031  | -0.013 |
| 9.73     | 1.011  | -0.017 |
| 8.71     | 0.984  | -0.028 |
| 7.68     | 0.917  | -0.045 |
| 6.66     | 0.836  | -0.054 |
| 5.63     | 0.695  | -0.057 |
| 4.57     | 0.364  | -0.013 |
| 3.62     | 0.236  | -0.005 |
| 2.54     | 0.127  | 0.003  |
| 1.49     | 0.035  | 0.004  |
| 0.46     | -0.057 | 0.005  |
| -0.56    | -0.168 | 0.011  |
| -1.57    | -0.237 | -0.001 |
| -2.54    | -0.278 | -0.013 |
| -3.61    | -0.351 | -0.044 |
| -4.65    | -0.440 | -0.034 |
| -5.64    | -0.537 | -0.040 |

|       |        |        |
|-------|--------|--------|
| -6.71 | -0.629 | -0.062 |
| -7.68 | -0.693 | -0.039 |
| -8.73 | -0.740 | -0.079 |
| -9.79 | -0.758 | -0.069 |

|       |        |        |
|-------|--------|--------|
| -6.69 | -0.661 | -0.028 |
| -7.69 | -0.737 | -0.040 |
| -8.74 | -0.795 | -0.039 |
| -9.74 | -0.810 | -0.049 |

Run: BM05038  
 $Re = 150,063$

| $\alpha$ | $C_l$  | $C_m$  |
|----------|--------|--------|
| -10.27   | -0.809 | -0.053 |
| -9.25    | -0.806 | -0.049 |
| -8.22    | -0.773 | -0.040 |
| -7.22    | -0.704 | -0.032 |
| -6.21    | -0.614 | -0.024 |
| -5.15    | -0.500 | -0.029 |
| -4.13    | -0.388 | -0.031 |
| -3.09    | -0.295 | -0.035 |
| -2.07    | -0.197 | -0.037 |
| -1.06    | -0.111 | -0.026 |
| -0.01    | -0.029 | -0.024 |
| 1.00     | 0.064  | -0.020 |
| 2.06     | 0.284  | -0.043 |
| 3.09     | 0.524  | -0.069 |
| 4.14     | 0.676  | -0.075 |
| 5.13     | 0.755  | -0.068 |
| 6.15     | 0.827  | -0.059 |
| 7.17     | 0.886  | -0.053 |
| 8.22     | 0.932  | -0.037 |
| 9.26     | 0.983  | -0.036 |
| 10.25    | 1.011  | -0.024 |
| 11.23    | 1.041  | -0.018 |
| 12.30    | 1.057  | -0.016 |
| 13.29    | 1.065  | -0.016 |
| 14.26    | 1.063  | -0.020 |
| 15.11    | 0.924  | -0.112 |
| 16.10    | 0.862  | -0.118 |
| 17.10    | 0.795  | -0.124 |
| 18.00    | 0.785  | -0.131 |
| 19.08    | 0.805  | -0.138 |
| 20.09    | 0.873  | -0.156 |
| 19.55    | 0.814  | -0.145 |
| 18.56    | 0.788  | -0.136 |
| 17.58    | 0.778  | -0.127 |
| 16.52    | 0.802  | -0.123 |
| 15.57    | 0.875  | -0.115 |
| 14.72    | 1.050  | -0.022 |
| 13.73    | 1.058  | -0.020 |
| 12.77    | 1.057  | -0.014 |
| 11.80    | 1.051  | -0.017 |
| 10.72    | 1.022  | -0.025 |
| 9.75     | 0.996  | -0.029 |
| 8.70     | 0.954  | -0.036 |
| 7.66     | 0.908  | -0.044 |
| 6.66     | 0.863  | -0.056 |
| 5.67     | 0.786  | -0.063 |
| 4.57     | 0.715  | -0.071 |
| 3.57     | 0.608  | -0.079 |
| 2.49     | 0.383  | -0.053 |
| 1.57     | 0.177  | -0.036 |
| 0.47     | 0.006  | -0.018 |
| -0.51    | -0.067 | -0.026 |
| -1.51    | -0.140 | -0.032 |
| -2.57    | -0.246 | -0.035 |
| -3.58    | -0.347 | -0.033 |
| -4.70    | -0.445 | -0.034 |
| -5.66    | -0.557 | -0.030 |

Run: BM05040  
 $Re = 199,991$

| $\alpha$ | $C_l$  | $C_m$  |
|----------|--------|--------|
| -10.31   | -0.838 | -0.057 |
| -9.20    | -0.829 | -0.041 |
| -8.23    | -0.778 | -0.037 |
| -7.20    | -0.698 | -0.036 |
| -6.20    | -0.594 | -0.040 |
| -5.13    | -0.468 | -0.046 |
| -4.12    | -0.353 | -0.048 |
| -3.13    | -0.230 | -0.056 |
| -2.06    | -0.110 | -0.058 |
| -1.09    | 0.003  | -0.058 |
| -0.01    | 0.115  | -0.055 |
| 1.07     | 0.219  | -0.051 |
| 2.05     | 0.310  | -0.045 |
| 3.06     | 0.460  | -0.054 |
| 4.04     | 0.617  | -0.064 |
| 5.16     | 0.766  | -0.073 |
| 6.15     | 0.853  | -0.069 |
| 7.20     | 0.882  | -0.054 |
| 8.19     | 0.927  | -0.043 |
| 9.27     | 0.980  | -0.037 |
| 10.23    | 1.016  | -0.031 |
| 11.22    | 1.047  | -0.024 |
| 12.23    | 1.064  | -0.021 |
| 13.29    | 1.067  | -0.018 |
| 14.27    | 1.073  | -0.021 |
| 15.21    | 1.064  | -0.030 |
| 16.09    | 0.912  | -0.121 |
| 17.09    | 0.819  | -0.125 |
| 18.04    | 0.798  | -0.131 |
| 19.04    | 0.805  | -0.136 |
| 20.06    | 0.857  | -0.149 |
| 19.54    | 0.818  | -0.142 |
| 18.56    | 0.801  | -0.138 |
| 17.58    | 0.812  | -0.131 |
| 16.57    | 0.838  | -0.126 |
| 15.64    | 0.999  | -0.108 |
| 14.70    | 1.066  | -0.029 |
| 13.74    | 1.066  | -0.022 |
| 12.73    | 1.064  | -0.022 |
| 11.73    | 1.055  | -0.027 |
| 10.75    | 1.031  | -0.030 |
| 9.73     | 0.996  | -0.037 |
| 8.70     | 0.950  | -0.042 |
| 7.64     | 0.891  | -0.050 |
| 6.67     | 0.872  | -0.064 |
| 5.60     | 0.810  | -0.074 |
| 4.65     | 0.708  | -0.073 |
| 3.56     | 0.546  | -0.062 |
| 2.57     | 0.380  | -0.050 |
| 1.51     | 0.267  | -0.053 |
| 0.47     | 0.174  | -0.058 |
| -0.56    | 0.067  | -0.060 |
| -1.55    | -0.046 | -0.059 |
| -2.62    | -0.169 | -0.057 |
| -3.62    | -0.290 | -0.053 |
| -4.62    | -0.404 | -0.051 |
| -5.68    | -0.528 | -0.041 |

|                |        |        |                |        |        |                             |        |        |                |        |        |
|----------------|--------|--------|----------------|--------|--------|-----------------------------|--------|--------|----------------|--------|--------|
| -6.70          | -0.646 | -0.035 | Run: BM05129   |        |        | 7.69                        | 0.888  | -0.044 | 1.05           | 0.028  | 0.000  |
| -7.74          | -0.746 | -0.038 | $Re = 349,748$ |        |        | 6.64                        | 0.822  | -0.050 | 2.05           | 0.108  | -0.011 |
| -8.74          | -0.808 | -0.036 | $\alpha$       | $C_l$  | $C_m$  | 5.61                        | 0.761  | -0.059 | 3.08           | 0.241  | -0.002 |
| -9.75          | -0.840 | -0.052 | 10.27          | 1.053  | N/A    | 4.62                        | 0.693  | -0.068 | 4.13           | 0.603  | -0.055 |
| Run: BM05042   |        |        | 11.29          | 1.087  | N/A    | 3.59                        | 0.598  | -0.071 | 5.10           | 0.706  | -0.054 |
| $Re = 350,168$ |        |        | 12.21          | 1.098  | N/A    | 2.56                        | 0.502  | -0.074 | 6.18           | 0.770  | -0.036 |
| $\alpha$       | $C_l$  | $C_m$  | 13.29          | 1.102  | N/A    | 1.56                        | 0.397  | -0.075 | 7.20           | 0.802  | -0.022 |
| -10.27         | -0.879 | -0.048 | 14.22          | 1.100  | N/A    | 0.49                        | 0.288  | -0.076 | 8.18           | 0.838  | -0.020 |
| -9.28          | -0.798 | -0.050 | 15.23          | 1.083  | N/A    | -0.54                       | 0.181  | -0.076 | 9.17           | 0.877  | 0.003  |
| -8.21          | -0.679 | -0.058 | 16.29          | 0.999  | N/A    | -1.55                       | 0.082  | -0.076 | 10.26          | 0.957  | -0.008 |
| -7.18          | -0.551 | -0.067 | 17.08          | 0.855  | N/A    | -2.59                       | -0.027 | -0.077 | 11.24          | 1.010  | -0.015 |
| -6.19          | -0.429 | -0.072 | 18.16          | 0.842  | N/A    | -3.57                       | -0.129 | -0.078 | 12.30          | 1.038  | -0.014 |
| -5.14          | -0.306 | -0.077 | 19.21          | 0.824  | N/A    | -4.64                       | -0.230 | -0.079 | 13.31          | 1.045  | -0.004 |
| -4.11          | -0.190 | -0.078 | 20.20          | 0.855  | N/A    | -5.67                       | -0.325 | -0.081 | 14.24          | 1.036  | -0.010 |
| -3.10          | -0.085 | -0.079 | 19.66          | 0.837  | N/A    | -6.73                       | -0.432 | -0.082 | 15.10          | 0.773  | -0.102 |
| -2.05          | 0.021  | -0.077 | 18.70          | 0.833  | N/A    | -7.72                       | -0.532 | -0.081 | 16.06          | 0.835  | -0.117 |
| -1.02          | 0.122  | -0.077 | 17.70          | 0.850  | N/A    | -8.72                       | -0.645 | -0.076 | 17.11          | 0.774  | -0.126 |
| 0.00           | 0.223  | -0.075 | 16.71          | 0.933  | N/A    | -9.75                       | -0.769 | -0.069 | 18.05          | 0.790  | -0.132 |
| 0.99           | 0.324  | -0.073 | 15.72          | 1.062  | N/A    | Run: BM05130                |        |        | 19.07          | 0.829  | -0.149 |
| 2.00           | 0.424  | -0.071 | 14.76          | 1.093  | N/A    | $Re = 499,966$              |        |        | 20.02          | 0.860  | -0.159 |
| 3.07           | 0.520  | -0.067 | 13.69          | 1.109  | N/A    | $\alpha$                    | $C_l$  | $C_m$  | 19.55          | 0.824  | -0.164 |
| 4.08           | 0.604  | -0.061 | 12.80          | 1.105  | N/A    | 10.28                       | 1.060  | N/A    | 18.50          | 0.791  | -0.150 |
| 5.11           | 0.689  | -0.056 | 11.69          | 1.089  | N/A    | 11.19                       | 1.095  | N/A    | 17.54          | 0.764  | -0.135 |
| 6.16           | 0.786  | -0.056 | 10.74          | 1.075  | N/A    | 12.27                       | 1.125  | N/A    | 16.56          | 0.802  | -0.128 |
| 7.20           | 0.855  | -0.050 | Run: BM05044   |        |        | 13.25                       | 1.136  | N/A    | 15.60          | 0.844  | -0.126 |
| 8.23           | 0.913  | -0.043 | $Re = 499,828$ |        |        | 14.27                       | 1.116  | N/A    | 14.60          | 0.805  | -0.106 |
| 9.19           | 0.978  | -0.040 | $\alpha$       | $C_l$  | $C_m$  | 15.20                       | 1.085  | N/A    | 13.79          | 1.044  | -0.003 |
| 10.23          | 1.031  | -0.035 | -10.24         | -0.820 | -0.066 | 16.38                       | 1.058  | N/A    | 12.75          | 1.036  | -0.001 |
| 11.26          | 1.067  | -0.030 | -9.20          | -0.707 | -0.073 | 17.18                       | 0.894  | N/A    | 11.77          | 1.025  | -0.009 |
| 12.24          | 1.088  | -0.027 | -8.18          | -0.589 | -0.080 | 18.14                       | 0.851  | N/A    | 10.74          | 0.982  | -0.004 |
| 13.33          | 1.088  | -0.026 | -7.21          | -0.483 | -0.082 | 19.21                       | 0.864  | N/A    | 9.70           | 0.916  | -0.004 |
| 14.25          | 1.084  | -0.033 | -6.17          | -0.381 | -0.081 | 20.19                       | 0.882  | N/A    | 8.69           | 0.856  | -0.006 |
| 15.24          | 1.073  | -0.045 | -5.11          | -0.279 | -0.079 | 19.60                       | 0.875  | N/A    | 7.65           | 0.826  | -0.022 |
| 16.22          | 1.053  | -0.059 | -4.13          | -0.182 | -0.078 | 18.74                       | 0.867  | N/A    | 6.67           | 0.791  | -0.029 |
| 15.70          | 1.063  | -0.052 | -3.07          | -0.076 | -0.078 | 17.65                       | 0.877  | N/A    | 5.65           | 0.747  | -0.058 |
| 14.75          | 1.078  | -0.038 | -2.05          | 0.026  | -0.077 | 16.61                       | 0.940  | N/A    | 4.61           | 0.670  | -0.048 |
| 13.77          | 1.091  | -0.027 | -1.01          | 0.134  | -0.077 | 15.90                       | 1.066  | N/A    | 3.57           | 0.368  | -0.023 |
| 12.73          | 1.087  | -0.026 | -0.03          | 0.235  | -0.076 | 14.75                       | 1.099  | N/A    | 2.53           | 0.171  | -0.006 |
| 11.68          | 1.075  | -0.028 | 1.05           | 0.341  | -0.075 | 13.78                       | 1.125  | N/A    | 1.53           | 0.083  | 0.006  |
| 10.75          | 1.050  | -0.032 | 2.06           | 0.449  | -0.074 | 12.77                       | 1.132  | N/A    | 0.51           | 0.003  | 0.008  |
| 9.70           | 1.002  | -0.038 | 3.06           | 0.547  | -0.073 | 11.75                       | 1.120  | N/A    | -0.53          | -0.079 | 0.004  |
| 8.68           | 0.944  | -0.042 | 4.10           | 0.648  | -0.070 | 10.85                       | 1.088  | N/A    | -1.56          | -0.133 | -0.007 |
| 7.69           | 0.880  | -0.046 | 5.08           | 0.734  | -0.065 | <b>S834</b>                 |        |        |                |        |        |
| 6.67           | 0.840  | -0.057 | 6.20           | 0.797  | -0.055 | Fig. 5.24 ( $C_l$ & $C_m$ ) |        |        |                |        |        |
| 5.64           | 0.742  | -0.056 | 7.19           | 0.851  | -0.047 | Run: BM05046                |        |        | Run: BM05048   |        |        |
| 4.63           | 0.648  | -0.060 | 8.26           | 0.923  | -0.042 | $Re = 99,954$               |        |        | $Re = 149,902$ |        |        |
| 3.60           | 0.563  | -0.065 | 9.21           | 0.991  | -0.039 | $\alpha$                    | $C_l$  | $C_m$  | $\alpha$       | $C_l$  | $C_m$  |
| 2.55           | 0.468  | -0.069 | 10.21          | 1.044  | -0.034 | -10.25                      | -0.775 | -0.091 | -10.20         | -0.816 | -0.051 |
| 1.50           | 0.375  | -0.073 | 11.29          | 1.088  | -0.030 | -9.19                       | -0.772 | -0.061 | -9.25          | -0.808 | -0.046 |
| 0.51           | 0.277  | -0.075 | 12.27          | 1.113  | -0.027 | -8.23                       | -0.737 | -0.060 | -8.19          | -0.762 | -0.037 |
| -0.50          | 0.173  | -0.077 | 13.21          | 1.130  | -0.028 | -7.21                       | -0.685 | -0.025 | -7.15          | -0.685 | -0.028 |
| -1.57          | 0.069  | -0.078 | 14.24          | 1.122  | -0.040 | -6.15                       | -0.592 | -0.031 | -6.16          | -0.594 | -0.030 |
| -2.56          | -0.029 | -0.079 | 15.21          | 1.086  | -0.057 | -5.13                       | -0.492 | -0.016 | -5.11          | -0.487 | -0.030 |
| -3.61          | -0.144 | -0.079 | 16.19          | 1.074  | -0.068 | -4.13                       | -0.374 | -0.016 | -4.16          | -0.387 | -0.034 |
| -4.63          | -0.249 | -0.079 | 15.68          | 1.074  | -0.063 | -3.02                       | -0.246 | -0.027 | -3.13          | -0.280 | -0.037 |
| -5.69          | -0.374 | -0.075 | 14.71          | 1.095  | -0.049 | -2.06                       | -0.171 | -0.021 | -2.10          | -0.185 | -0.040 |
| -6.68          | -0.492 | -0.070 | 13.70          | 1.131  | -0.031 | -1.03                       | -0.130 | 0.004  | -1.03          | -0.082 | -0.042 |
| -7.70          | -0.621 | -0.063 | 12.74          | 1.130  | -0.027 | 0.02                        | -0.067 | -0.002 | -0.04          | 0.053  | -0.041 |
| -8.74          | -0.748 | -0.054 | 11.73          | 1.112  | -0.028 |                             |        |        |                |        |        |
| -9.77          | -0.844 | -0.049 | 10.71          | 1.068  | -0.032 |                             |        |        |                |        |        |
|                |        |        | 9.71           | 1.015  | -0.036 |                             |        |        |                |        |        |
|                |        |        | 8.68           | 0.953  | -0.040 |                             |        |        |                |        |        |



| Run: BM05127<br>$Re = 499,789$ |       |       | 20.14 | 0.946  | -0.184 | 20.13 | 0.954  | -0.174 | -3.45 | -0.126 | -0.070 |
|--------------------------------|-------|-------|-------|--------|--------|-------|--------|--------|-------|--------|--------|
| $\alpha$                       | $C_l$ | $C_m$ | 19.65 | 0.954  | -0.188 | 19.71 | 0.924  | -0.166 | -4.54 | -0.259 | -0.062 |
| 10.28                          | 1.020 | N/A   | 18.62 | 0.949  | -0.183 | 18.67 | 0.927  | -0.164 | -5.57 | -0.381 | -0.058 |
| 11.16                          | 1.044 | N/A   | 17.66 | 0.978  | -0.180 | 17.68 | 0.937  | -0.164 |       |        |        |
| 12.29                          | 1.063 | N/A   | 16.62 | 0.924  | -0.172 | 16.69 | 0.974  | -0.168 |       |        |        |
| 13.29                          | 1.071 | N/A   | 15.64 | 0.921  | -0.161 | 15.71 | 0.969  | -0.162 |       |        |        |
| 14.33                          | 1.039 | N/A   | 14.71 | 0.914  | -0.151 | 14.63 | 0.983  | -0.160 |       |        |        |
| 15.37                          | 1.003 | N/A   | 13.70 | 0.970  | -0.142 | 13.68 | 1.043  | -0.148 |       |        |        |
| 16.30                          | 0.993 | N/A   | 12.76 | 1.023  | -0.118 | 12.76 | 1.102  | -0.120 |       |        |        |
| 17.12                          | 0.934 | N/A   | 11.83 | 1.108  | -0.051 | 11.86 | 1.110  | -0.049 |       |        |        |
| 18.26                          | 0.867 | N/A   | 10.83 | 1.071  | -0.031 | 10.89 | 1.110  | -0.036 |       |        |        |
| 19.15                          | 0.899 | N/A   | 9.78  | 1.025  | -0.023 | 9.83  | 1.071  | -0.042 |       |        |        |
| 20.22                          | 0.868 | N/A   | 8.79  | 0.971  | -0.029 | 8.77  | 1.013  | -0.047 |       |        |        |
| 19.65                          | 0.871 | N/A   | 7.80  | 0.912  | -0.033 | 7.81  | 0.958  | -0.053 |       |        |        |
| 18.68                          | 0.860 | N/A   | 6.78  | 0.862  | -0.060 | 6.74  | 0.882  | -0.058 |       |        |        |
| 17.74                          | 0.892 | N/A   | 5.71  | 0.767  | -0.045 | 5.72  | 0.797  | -0.062 |       |        |        |
| 16.85                          | 0.968 | N/A   | 4.72  | 0.675  | -0.057 | 4.74  | 0.718  | -0.068 |       |        |        |
| 15.79                          | 1.002 | N/A   | 3.70  | 0.589  | -0.074 | 3.65  | 0.609  | -0.072 |       |        |        |
| 14.73                          | 1.024 | N/A   | 2.61  | 0.438  | -0.065 | 2.63  | 0.507  | -0.075 |       |        |        |
| 13.75                          | 1.048 | N/A   | 1.63  | 0.281  | -0.058 | 1.58  | 0.405  | -0.078 |       |        |        |
| 12.81                          | 1.071 | N/A   | 0.61  | 0.156  | -0.052 | 0.61  | 0.292  | -0.078 |       |        |        |
| 11.69                          | 1.055 | N/A   | -0.43 | 0.050  | -0.030 | -0.44 | 0.145  | -0.067 |       |        |        |
| 10.70                          | 1.036 | N/A   | -1.45 | -0.047 | -0.040 | -1.45 | 0.033  | -0.064 |       |        |        |
|                                |       |       | -2.50 | -0.125 | -0.060 | -2.49 | -0.089 | -0.057 |       |        |        |
|                                |       |       | -3.52 | -0.222 | -0.062 | -3.50 | -0.207 | -0.050 |       |        |        |
|                                |       |       | -4.54 | -0.309 | -0.045 | -4.55 | -0.316 | -0.049 |       |        |        |
|                                |       |       | -5.55 | -0.385 | -0.073 | -5.55 | -0.416 | -0.051 |       |        |        |
|                                |       |       | -6.56 | -0.482 | -0.052 | -6.54 | -0.511 | -0.031 |       |        |        |
|                                |       |       | -7.58 | -0.550 | -0.022 | -7.57 | -0.561 | -0.006 |       |        |        |
|                                |       |       | -8.56 | -0.571 | -0.005 | -8.56 | -0.583 | 0.014  |       |        |        |
|                                |       |       | -9.56 | -0.585 | -0.002 | -9.50 | -0.591 | 0.030  |       |        |        |

**SD2030 (B)**Fig. 5.28 ( $C_l$  &  $C_m$ )

| Run: BM05094<br>$Re = 99,958$ |        |        | Run: BM05078<br>$Re = 199,941$ |        |        | Run: BM05080<br>$Re = 349,542$ |        |        | Run: BM05082<br>$Re = 500,252$ |        |        |
|-------------------------------|--------|--------|--------------------------------|--------|--------|--------------------------------|--------|--------|--------------------------------|--------|--------|
| $\alpha$                      | $C_l$  | $C_m$  | $\alpha$                       | $C_l$  | $C_m$  | $\alpha$                       | $C_l$  | $C_m$  | $\alpha$                       | $C_l$  | $C_m$  |
| -9.97                         | -0.568 | 0.017  | -9.99                          | -0.589 | 0.037  | -6.03                          | -0.446 | -0.048 | -6.06                          | -0.384 | -0.063 |
| -9.01                         | -0.571 | 0.015  | -8.95                          | -0.586 | 0.028  | -5.02                          | -0.310 | -0.061 | -4.96                          | -0.250 | -0.072 |
| -8.03                         | -0.561 | 0.004  | -8.02                          | -0.590 | 0.010  | -3.97                          | -0.189 | -0.066 | -3.99                          | -0.132 | -0.077 |
| -7.07                         | -0.517 | -0.018 | -7.07                          | -0.554 | -0.015 | -2.99                          | -0.062 | -0.073 | -2.97                          | -0.021 | -0.079 |
| -6.08                         | -0.449 | -0.043 | -6.08                          | -0.479 | -0.041 | -1.94                          | 0.071  | -0.081 | -1.94                          | 0.081  | -0.078 |
| -5.03                         | -0.361 | -0.032 | -5.06                          | -0.374 | -0.052 | -0.90                          | 0.173  | -0.082 | -0.91                          | 0.170  | -0.075 |
| -3.98                         | -0.275 | -0.035 | -3.99                          | -0.272 | -0.046 | 0.11                           | 0.260  | -0.075 | 0.11                           | 0.263  | -0.071 |
| -2.97                         | -0.183 | -0.033 | -2.97                          | -0.157 | -0.053 | 1.12                           | 0.378  | -0.076 | 1.13                           | 0.383  | -0.072 |
| -1.94                         | -0.095 | -0.041 | -1.98                          | -0.037 | -0.058 | 2.19                           | 0.488  | -0.075 | 2.14                           | 0.494  | -0.072 |
| -0.92                         | -0.015 | -0.025 | -0.92                          | 0.076  | -0.062 | 3.17                           | 0.584  | -0.073 | 3.19                           | 0.599  | -0.070 |
| 0.06                          | 0.088  | -0.036 | 0.10                           | 0.214  | -0.069 | 4.18                           | 0.692  | -0.071 | 4.22                           | 0.698  | -0.068 |
| 1.13                          | 0.194  | -0.021 | 1.16                           | 0.350  | -0.077 | 5.23                           | 0.785  | -0.067 | 5.25                           | 0.788  | -0.065 |
| 2.18                          | 0.352  | -0.037 | 2.13                           | 0.453  | -0.075 | 6.29                           | 0.876  | -0.064 | 6.25                           | 0.876  | -0.062 |
| 3.21                          | 0.525  | -0.065 | 3.15                           | 0.546  | -0.070 | 7.26                           | 0.951  | -0.060 | 7.34                           | 0.963  | -0.058 |
| 4.25                          | 0.634  | -0.056 | 4.19                           | 0.658  | -0.068 | 8.29                           | 1.028  | -0.055 | 8.30                           | 1.042  | -0.054 |
| 5.26                          | 0.725  | -0.052 | 5.25                           | 0.753  | -0.063 | 9.33                           | 1.094  | -0.049 | 9.37                           | 1.106  | -0.048 |
| 6.27                          | 0.805  | -0.030 | 6.22                           | 0.835  | -0.059 | 10.37                          | 1.145  | -0.043 | 10.31                          | 1.160  | -0.042 |
| 7.30                          | 0.878  | -0.042 | 7.37                           | 0.917  | -0.054 | 9.85                           | 1.120  | -0.047 | 11.38                          | 1.189  | -0.036 |
| 8.31                          | 0.931  | -0.018 | 8.29                           | 0.985  | -0.049 | 8.78                           | 1.062  | -0.053 | 10.84                          | 1.187  | -0.040 |
| 9.33                          | 0.999  | -0.033 | 9.36                           | 1.043  | -0.043 | 7.82                           | 0.990  | -0.059 | 9.83                           | 1.131  | -0.046 |
| 10.34                         | 1.046  | -0.030 | 10.35                          | 1.095  | -0.037 | 6.76                           | 0.910  | -0.063 | 8.74                           | 1.072  | -0.052 |
| 11.34                         | 1.074  | -0.028 | 11.40                          | 1.127  | -0.031 | 5.75                           | 0.823  | -0.066 | 7.76                           | 1.005  | -0.057 |
| 12.29                         | 1.048  | -0.090 | 12.30                          | 1.148  | -0.087 | 4.70                           | 0.735  | -0.070 | 6.73                           | 0.917  | -0.060 |
| 13.23                         | 0.959  | -0.125 | 13.24                          | 1.079  | -0.135 | 3.69                           | 0.637  | -0.073 | 5.71                           | 0.829  | -0.064 |
| 14.20                         | 0.914  | -0.140 | 14.17                          | 0.991  | -0.156 | 2.64                           | 0.537  | -0.076 | 4.73                           | 0.739  | -0.067 |
| 15.22                         | 0.900  | -0.147 | 15.22                          | 0.969  | -0.159 | 1.67                           | 0.431  | -0.076 | 3.68                           | 0.645  | -0.070 |
| 16.18                         | 0.970  | -0.168 | 16.17                          | 0.979  | -0.163 | 0.62                           | 0.321  | -0.076 | 2.65                           | 0.550  | -0.073 |
| 17.20                         | 0.926  | -0.165 | 17.19                          | 0.949  | -0.162 | -0.41                          | 0.214  | -0.078 | 1.65                           | 0.440  | -0.073 |
| 18.15                         | 0.957  | -0.173 | 18.17                          | 0.931  | -0.161 | -1.47                          | 0.122  | -0.083 | 0.59                           | 0.320  | -0.071 |
| 19.16                         | 0.966  | -0.183 | 19.20                          | 0.939  | -0.169 | -2.47                          | 0.006  | -0.078 | -0.40                          | 0.216  | -0.074 |
|                               |        |        |                                |        |        |                                |        |        | -1.43                          | 0.131  | -0.079 |

|       |        |        |
|-------|--------|--------|
| -2.48 | 0.029  | -0.079 |
| -3.55 | -0.084 | -0.078 |
| -4.52 | -0.194 | -0.074 |
| -5.55 | -0.316 | -0.071 |

|       |        |        |
|-------|--------|--------|
| -2.51 | -0.101 | -0.047 |
| -3.48 | -0.185 | -0.049 |
| -4.56 | -0.265 | -0.057 |
| -5.57 | -0.347 | -0.054 |
| -6.58 | -0.426 | -0.049 |
| -7.53 | -0.484 | -0.016 |
| -8.53 | -0.505 | -0.002 |
| -9.56 | -0.496 | 0.007  |

|       |        |        |
|-------|--------|--------|
| -2.46 | -0.086 | -0.053 |
| -3.47 | -0.205 | -0.054 |
| -4.55 | -0.314 | -0.047 |
| -5.57 | -0.406 | -0.049 |
| -6.56 | -0.500 | -0.029 |
| -7.55 | -0.548 | -0.001 |
| -8.53 | -0.565 | 0.015  |
| -9.50 | -0.571 | 0.029  |

|       |       |     |
|-------|-------|-----|
| 19.73 | 0.985 | N/A |
| 18.85 | 0.950 | N/A |
| 17.82 | 0.963 | N/A |
| 16.72 | 0.981 | N/A |
| 15.89 | 1.014 | N/A |
| 14.76 | 1.073 | N/A |
| 13.96 | 1.118 | N/A |
| 12.89 | 1.153 | N/A |
| 11.91 | 1.181 | N/A |
| 10.85 | 1.166 | N/A |

**SD2030 (B)**

Fig. 5.30 ( $C_l$  &  $C_m$ )

Run: BM05095  
 $Re = 99,923$

| $\alpha$ | $C_l$  | $C_m$  |
|----------|--------|--------|
| -10.01   | -0.509 | 0.015  |
| -9.05    | -0.520 | 0.004  |
| -8.07    | -0.518 | 0.003  |
| -7.03    | -0.478 | -0.020 |
| -6.05    | -0.396 | -0.048 |
| -4.99    | -0.303 | -0.051 |
| -4.01    | -0.234 | -0.053 |
| -2.95    | -0.150 | -0.038 |
| -1.93    | -0.066 | -0.047 |
| -0.89    | 0.001  | -0.039 |
| 0.13     | 0.092  | -0.030 |
| 1.15     | 0.238  | -0.051 |
| 2.18     | 0.428  | -0.057 |
| 3.17     | 0.560  | -0.059 |
| 4.22     | 0.660  | -0.057 |
| 5.24     | 0.732  | -0.033 |
| 6.29     | 0.803  | -0.035 |
| 7.32     | 0.880  | -0.040 |
| 8.29     | 0.960  | -0.037 |
| 9.35     | 1.025  | -0.026 |
| 10.33    | 1.071  | -0.030 |
| 11.36    | 1.097  | -0.028 |
| 12.27    | 1.026  | -0.086 |
| 13.21    | 0.975  | -0.130 |
| 14.21    | 0.939  | -0.135 |
| 15.22    | 0.956  | -0.150 |
| 16.18    | 0.942  | -0.156 |
| 17.20    | 0.964  | -0.160 |
| 18.20    | 0.959  | -0.167 |
| 19.14    | 1.004  | -0.181 |
| 20.18    | 1.022  | -0.194 |
| 19.66    | 0.985  | -0.186 |
| 18.69    | 0.987  | -0.180 |
| 17.64    | 0.960  | -0.171 |
| 16.67    | 0.997  | -0.174 |
| 15.66    | 0.948  | -0.159 |
| 14.65    | 0.940  | -0.148 |
| 13.67    | 0.944  | -0.136 |
| 12.75    | 1.063  | -0.109 |
| 11.79    | 1.086  | -0.046 |
| 10.83    | 1.091  | -0.018 |
| 9.83     | 1.055  | -0.027 |
| 8.83     | 1.000  | -0.025 |
| 7.83     | 0.924  | -0.035 |
| 6.70     | 0.845  | -0.042 |
| 5.79     | 0.790  | -0.055 |
| 4.70     | 0.710  | -0.042 |
| 3.67     | 0.620  | -0.053 |
| 2.72     | 0.528  | -0.069 |
| 1.61     | 0.345  | -0.060 |
| 0.59     | 0.153  | -0.030 |
| -0.42    | 0.049  | -0.025 |
| -1.44    | -0.027 | -0.040 |

Run: BM05086  
 $Re = 199,981$

| $\alpha$ | $C_l$  | $C_m$  |
|----------|--------|--------|
| -10.03   | -0.582 | 0.032  |
| -9.01    | -0.569 | 0.024  |
| -8.03    | -0.560 | 0.007  |
| -7.03    | -0.533 | -0.019 |
| -6.01    | -0.459 | -0.043 |
| -5.05    | -0.360 | -0.052 |
| -3.98    | -0.264 | -0.052 |
| -3.02    | -0.161 | -0.052 |
| -1.94    | -0.004 | -0.065 |
| -0.98    | 0.136  | -0.073 |
| 0.11     | 0.234  | -0.068 |
| 1.18     | 0.316  | -0.060 |
| 2.18     | 0.416  | -0.058 |
| 3.15     | 0.511  | -0.058 |
| 4.22     | 0.613  | -0.057 |
| 5.23     | 0.708  | -0.056 |
| 6.25     | 0.802  | -0.053 |
| 7.27     | 0.895  | -0.052 |
| 8.33     | 0.986  | -0.048 |
| 9.30     | 1.045  | -0.043 |
| 10.32    | 1.097  | -0.038 |
| 11.35    | 1.139  | -0.032 |
| 12.26    | 1.142  | -0.065 |
| 13.26    | 1.077  | -0.132 |
| 14.21    | 1.006  | -0.156 |
| 15.20    | 0.978  | -0.159 |
| 16.17    | 0.977  | -0.161 |
| 17.20    | 0.964  | -0.162 |
| 18.17    | 0.926  | -0.156 |
| 19.16    | 0.944  | -0.164 |
| 20.16    | 0.946  | -0.168 |
| 19.71    | 0.942  | -0.170 |
| 18.63    | 0.936  | -0.165 |
| 17.65    | 0.947  | -0.161 |
| 16.68    | 0.948  | -0.161 |
| 15.66    | 0.970  | -0.160 |
| 14.65    | 0.962  | -0.154 |
| 13.71    | 1.053  | -0.151 |
| 12.75    | 1.091  | -0.124 |
| 11.89    | 1.147  | -0.032 |
| 10.86    | 1.119  | -0.036 |
| 9.81     | 1.070  | -0.042 |
| 8.83     | 1.015  | -0.046 |
| 7.83     | 0.939  | -0.049 |
| 6.79     | 0.848  | -0.052 |
| 5.68     | 0.754  | -0.055 |
| 4.70     | 0.659  | -0.055 |
| 3.68     | 0.565  | -0.056 |
| 2.68     | 0.472  | -0.057 |
| 1.63     | 0.371  | -0.058 |
| 0.65     | 0.280  | -0.061 |
| -0.48    | 0.194  | -0.073 |
| -1.49    | 0.066  | -0.068 |

Run: BM05088  
 $Re = 349,925$

| $\alpha$ | $C_l$  | $C_m$  |
|----------|--------|--------|
| -6.05    | -0.415 | -0.056 |
| -5.07    | -0.280 | -0.067 |
| -3.99    | -0.148 | -0.069 |
| -2.95    | -0.061 | -0.067 |
| -1.92    | 0.043  | -0.067 |
| -0.97    | 0.137  | -0.066 |
| 0.11     | 0.247  | -0.066 |
| 1.10     | 0.347  | -0.066 |
| 2.14     | 0.448  | -0.065 |
| 3.22     | 0.554  | -0.064 |
| 4.20     | 0.660  | -0.063 |
| 5.20     | 0.758  | -0.061 |
| 6.26     | 0.855  | -0.060 |
| 7.30     | 0.948  | -0.057 |
| 8.28     | 1.032  | -0.054 |
| 9.33     | 1.103  | -0.049 |
| 10.36    | 1.145  | -0.041 |
| 11.34    | 1.161  | -0.035 |
| 12.39    | 1.159  | -0.076 |
| 11.86    | 1.169  | -0.034 |
| 10.84    | 1.152  | -0.039 |
| 9.81     | 1.124  | -0.046 |
| 8.78     | 1.070  | -0.053 |
| 7.78     | 0.990  | -0.056 |
| 6.73     | 0.902  | -0.060 |
| 5.74     | 0.805  | -0.062 |
| 4.69     | 0.706  | -0.063 |
| 3.69     | 0.608  | -0.065 |
| 2.68     | 0.504  | -0.066 |
| 1.61     | 0.393  | -0.066 |
| 0.60     | 0.292  | -0.067 |
| -0.44    | 0.189  | -0.067 |
| -1.50    | 0.086  | -0.067 |
| -2.49    | -0.013 | -0.067 |
| -3.46    | -0.104 | -0.068 |
| -4.54    | -0.195 | -0.072 |
| -5.59    | -0.344 | -0.064 |

Run: BM05131  
 $Re = 350,116$

| $\alpha$ | $C_l$ | $C_m$ |
|----------|-------|-------|
| 10.41    | 1.159 | N/A   |
| 11.45    | 1.176 | N/A   |
| 12.32    | 1.188 | N/A   |
| 13.32    | 1.139 | N/A   |
| 14.30    | 1.105 | N/A   |
| 15.31    | 1.029 | N/A   |
| 16.28    | 0.997 | N/A   |
| 17.19    | 0.976 | N/A   |
| 18.42    | 0.944 | N/A   |
| 19.26    | 0.963 | N/A   |
| 20.34    | 0.975 | N/A   |

Run: BM05090  
 $Re = 500,249$

| $\alpha$ | $C_l$  | $C_m$  |
|----------|--------|--------|
| -6.07    | -0.354 | -0.070 |
| -4.98    | -0.250 | -0.069 |
| -4.00    | -0.161 | -0.068 |
| -2.92    | -0.058 | -0.067 |
| -1.91    | 0.039  | -0.067 |
| -0.93    | 0.140  | -0.067 |
| 0.12     | 0.243  | -0.066 |
| 1.13     | 0.355  | -0.065 |
| 2.19     | 0.463  | -0.064 |
| 3.23     | 0.569  | -0.064 |
| 4.19     | 0.665  | -0.063 |
| 5.22     | 0.768  | -0.061 |
| 6.25     | 0.862  | -0.059 |
| 7.29     | 0.962  | -0.057 |
| 8.34     | 1.044  | -0.053 |
| 9.37     | 1.098  | -0.046 |
| 10.34    | 1.141  | -0.040 |
| 11.36    | 1.165  | -0.035 |
| 12.38    | 1.169  | -0.036 |
| 11.87    | 1.175  | -0.033 |
| 10.78    | 1.159  | -0.038 |
| 9.82     | 1.119  | -0.043 |
| 8.81     | 1.072  | -0.051 |
| 7.77     | 0.993  | -0.055 |
| 6.72     | 0.911  | -0.058 |
| 5.74     | 0.810  | -0.060 |
| 4.72     | 0.714  | -0.062 |
| 3.69     | 0.614  | -0.063 |
| 2.65     | 0.507  | -0.065 |
| 1.64     | 0.406  | -0.066 |
| 0.61     | 0.303  | -0.066 |
| -0.42    | 0.188  | -0.066 |
| -1.42    | 0.089  | -0.067 |
| -2.49    | -0.016 | -0.067 |
| -3.52    | -0.119 | -0.068 |
| -4.54    | -0.211 | -0.068 |
| -5.60    | -0.305 | -0.071 |

**SH3055**

Fig. 5.34 ( $C_l$  &  $C_m$ )

Run: BM05056  
 $Re = 99,991$

| $\alpha$ | $C_l$  | $C_m$  |
|----------|--------|--------|
| -10.15   | -0.226 | -0.035 |
| -9.08    | -0.213 | -0.031 |
| -8.08    | -0.279 | -0.016 |
| -7.05    | -0.287 | -0.020 |
| -6.11    | -0.273 | -0.025 |



|       |        |        |       |        |        |       |        |        |       |        |        |
|-------|--------|--------|-------|--------|--------|-------|--------|--------|-------|--------|--------|
| -5.06 | -0.210 | -0.039 | -5.16 | 0.220  | -0.228 | -5.13 | 0.296  | -0.244 | -5.23 | 0.304  | -0.246 |
| -4.05 | -0.120 | -0.066 | -4.17 | 0.376  | -0.237 | -4.13 | 0.409  | -0.247 | -4.11 | 0.436  | -0.247 |
| -3.09 | 0.003  | -0.098 | -3.11 | 0.498  | -0.239 | -3.13 | 0.521  | -0.248 | -3.12 | 0.547  | -0.249 |
| -2.08 | 0.184  | -0.131 | -2.10 | 0.606  | -0.239 | -2.09 | 0.631  | -0.248 | -2.12 | 0.654  | -0.248 |
| -1.05 | 0.344  | -0.148 | -1.07 | 0.705  | -0.235 | -1.08 | 0.737  | -0.247 | -1.04 | 0.767  | -0.247 |
| -0.02 | 0.504  | -0.162 | -0.10 | 0.802  | -0.234 | -0.07 | 0.843  | -0.246 | -0.02 | 0.877  | -0.247 |
| 1.00  | 0.628  | -0.170 | 0.94  | 0.901  | -0.231 | 1.01  | 0.960  | -0.245 | 0.97  | 0.976  | -0.245 |
| 2.01  | 0.740  | -0.160 | 2.06  | 1.008  | -0.228 | 2.02  | 1.057  | -0.242 | 2.06  | 1.092  | -0.244 |
| 3.05  | 0.864  | -0.181 | 3.06  | 1.110  | -0.225 | 3.07  | 1.165  | -0.239 | 3.05  | 1.190  | -0.240 |
| 4.12  | 0.990  | -0.185 | 4.10  | 1.206  | -0.222 | 4.09  | 1.269  | -0.237 | 4.09  | 1.283  | -0.235 |
| 5.11  | 1.093  | -0.180 | 5.10  | 1.303  | -0.218 | 5.08  | 1.366  | -0.233 | 5.16  | 1.395  | -0.233 |
| 6.13  | 1.215  | -0.187 | 6.17  | 1.402  | -0.214 | 6.14  | 1.466  | -0.228 | 6.17  | 1.492  | -0.228 |
| 7.13  | 1.324  | -0.179 | 7.18  | 1.492  | -0.210 | 7.17  | 1.559  | -0.223 | 7.17  | 1.584  | -0.222 |
| 8.20  | 1.436  | -0.176 | 8.18  | 1.581  | -0.206 | 8.22  | 1.645  | -0.216 | 8.29  | 1.680  | -0.215 |
| 9.16  | 1.543  | -0.185 | 9.17  | 1.662  | -0.201 | 9.26  | 1.731  | -0.210 | 9.30  | 1.764  | -0.208 |
| 10.22 | 1.627  | -0.166 | 10.27 | 1.742  | -0.195 | 10.26 | 1.783  | -0.201 | 10.27 | 1.822  | -0.197 |
| 11.26 | 1.718  | -0.169 | 11.29 | 1.809  | -0.188 | 11.24 | 1.838  | -0.191 | 11.30 | 1.859  | -0.184 |
| 12.26 | 1.771  | -0.160 | 12.29 | 1.874  | -0.181 | 12.30 | 1.868  | -0.178 | 12.27 | 1.862  | -0.170 |
| 13.28 | 1.823  | -0.162 | 13.35 | 1.908  | -0.170 | 13.28 | 1.871  | -0.166 | 13.27 | 1.846  | -0.161 |
| 14.35 | 1.846  | -0.155 | 14.32 | 1.891  | -0.157 | 14.29 | 1.842  | -0.163 | 14.30 | 1.830  | -0.160 |
| 15.30 | 1.868  | -0.162 | 15.30 | 1.875  | -0.153 | 15.31 | 1.798  | -0.165 | 15.33 | 1.784  | -0.159 |
| 16.33 | 1.885  | -0.162 | 16.30 | 1.829  | -0.153 | 16.31 | 1.753  | -0.167 | 16.32 | 1.731  | -0.161 |
| 17.25 | 1.824  | -0.165 | 17.26 | 1.786  | -0.159 | 17.27 | 1.720  | -0.169 | 17.27 | 1.712  | -0.168 |
| 18.33 | 1.751  | -0.170 | 18.25 | 1.731  | -0.167 | 18.26 | 1.706  | -0.172 | 18.26 | 1.668  | -0.176 |
| 19.26 | 1.702  | -0.177 | 19.22 | 1.683  | -0.177 | 19.23 | 1.676  | -0.177 | 19.23 | 1.635  | -0.185 |
| 20.24 | 1.645  | -0.191 | 20.19 | 1.643  | -0.190 | 20.17 | 1.649  | -0.193 | 20.16 | 1.600  | -0.197 |
| 19.72 | 1.648  | -0.190 | 19.70 | 1.662  | -0.182 | 19.70 | 1.659  | -0.186 | 19.69 | 1.602  | -0.192 |
| 18.73 | 1.726  | -0.179 | 18.75 | 1.714  | -0.175 | 18.78 | 1.694  | -0.177 | 18.70 | 1.653  | -0.181 |
| 17.81 | 1.785  | -0.171 | 17.73 | 1.760  | -0.166 | 17.74 | 1.713  | -0.170 | 17.70 | 1.701  | -0.173 |
| 16.79 | 1.866  | -0.171 | 16.75 | 1.816  | -0.158 | 16.77 | 1.757  | -0.166 | 16.73 | 1.727  | -0.166 |
| 15.87 | 1.894  | -0.170 | 15.80 | 1.851  | -0.155 | 15.75 | 1.784  | -0.164 | 15.75 | 1.771  | -0.163 |
| 14.80 | 1.855  | -0.155 | 14.80 | 1.883  | -0.156 | 14.82 | 1.822  | -0.160 | 14.73 | 1.811  | -0.159 |
| 13.78 | 1.844  | -0.167 | 13.80 | 1.905  | -0.165 | 13.87 | 1.858  | -0.163 | 13.81 | 1.840  | -0.160 |
| 12.71 | 1.801  | -0.179 | 12.75 | 1.888  | -0.177 | 12.76 | 1.874  | -0.173 | 12.77 | 1.852  | -0.164 |
| 11.78 | 1.750  | -0.178 | 11.83 | 1.847  | -0.186 | 11.78 | 1.866  | -0.185 | 11.74 | 1.859  | -0.175 |
| 10.73 | 1.662  | -0.170 | 10.74 | 1.775  | -0.193 | 10.71 | 1.826  | -0.197 | 10.71 | 1.838  | -0.189 |
| 9.70  | 1.586  | -0.177 | 9.72  | 1.705  | -0.199 | 9.73  | 1.767  | -0.206 | 9.69  | 1.786  | -0.201 |
| 8.71  | 1.481  | -0.175 | 8.71  | 1.623  | -0.204 | 8.70  | 1.695  | -0.214 | 8.70  | 1.720  | -0.211 |
| 7.65  | 1.370  | -0.176 | 7.70  | 1.539  | -0.209 | 7.68  | 1.612  | -0.221 | 7.67  | 1.643  | -0.220 |
| 6.67  | 1.268  | -0.194 | 6.62  | 1.445  | -0.214 | 6.62  | 1.520  | -0.227 | 6.62  | 1.549  | -0.226 |
| 5.63  | 1.146  | -0.190 | 5.65  | 1.361  | -0.218 | 5.59  | 1.417  | -0.230 | 5.65  | 1.459  | -0.231 |
| 4.60  | 1.039  | -0.182 | 4.60  | 1.252  | -0.221 | 4.56  | 1.322  | -0.235 | 4.58  | 1.350  | -0.236 |
| 3.54  | 0.923  | -0.178 | 3.59  | 1.153  | -0.224 | 3.58  | 1.223  | -0.238 | 3.54  | 1.240  | -0.238 |
| 2.50  | 0.804  | -0.172 | 2.52  | 1.054  | -0.227 | 2.55  | 1.117  | -0.241 | 2.56  | 1.143  | -0.240 |
| 1.46  | 0.674  | -0.159 | 1.51  | 0.959  | -0.231 | 1.56  | 1.011  | -0.243 | 1.48  | 1.027  | -0.243 |
| 0.48  | 0.553  | -0.159 | 0.46  | 0.853  | -0.233 | 0.44  | 0.900  | -0.245 | 0.52  | 0.929  | -0.247 |
| -0.53 | 0.452  | -0.156 | -0.60 | 0.756  | -0.238 | -0.58 | 0.797  | -0.247 | -0.51 | 0.827  | -0.247 |
| -1.56 | 0.288  | -0.144 | -1.57 | 0.668  | -0.241 | -1.61 | 0.683  | -0.247 | -1.57 | 0.712  | -0.248 |
| -2.59 | 0.071  | -0.106 | -2.60 | 0.559  | -0.241 | -2.63 | 0.574  | -0.248 | -2.61 | 0.597  | -0.248 |
| -3.61 | -0.080 | -0.080 | -3.64 | 0.446  | -0.241 | -3.66 | 0.466  | -0.248 | -3.61 | 0.492  | -0.249 |
| -4.60 | -0.178 | -0.052 | -4.65 | 0.311  | -0.234 | -4.68 | 0.348  | -0.247 | -4.63 | 0.373  | -0.247 |
| -5.63 | -0.244 | -0.030 | -5.70 | 0.133  | -0.219 | -5.69 | 0.229  | -0.242 | -5.69 | 0.244  | -0.243 |
| -6.61 | -0.247 | -0.026 | -6.71 | -0.050 | -0.199 | -6.68 | 0.100  | -0.235 | -6.71 | 0.120  | -0.238 |
| -7.61 | -0.278 | -0.015 | -7.72 | -0.217 | -0.184 | -7.75 | -0.095 | -0.214 | -7.80 | -0.023 | -0.226 |
| -8.55 | -0.237 | -0.020 | -8.78 | -0.390 | -0.161 | -8.77 | -0.281 | -0.190 | -8.75 | -0.183 | -0.211 |
| -9.61 | -0.238 | -0.027 | -9.79 | -0.558 | -0.127 | -9.76 | -0.477 | -0.158 | -9.76 | -0.396 | -0.173 |

Run: BM05058  
Re = 200,055

| $\alpha$ | $C_l$  | $C_m$  |
|----------|--------|--------|
| -10.10   | -0.255 | -0.007 |
| -9.01    | -0.236 | -0.011 |
| -8.02    | -0.238 | -0.017 |
| -7.10    | -0.183 | -0.032 |
| -6.16    | -0.026 | -0.130 |

Run: BM05060  
Re = 349,917

| $\alpha$ | $C_l$  | $C_m$  |
|----------|--------|--------|
| -10.07   | -0.277 | -0.009 |
| -9.04    | -0.244 | -0.021 |
| -8.09    | -0.180 | -0.051 |
| -7.17    | 0.011  | -0.226 |
| -6.17    | 0.166  | -0.240 |

Run: BM05062  
Re = 500,174

| $\alpha$ | $C_l$  | $C_m$  |
|----------|--------|--------|
| -10.16   | -0.267 | -0.021 |
| -9.17    | -0.226 | -0.047 |
| -8.22    | -0.099 | -0.222 |
| -7.24    | 0.054  | -0.235 |
| -6.20    | 0.188  | -0.241 |

**SH3055**

Fig. 5.36 ( $C_l$  &  $C_m$ )

Run: BM05117  
Re = 99,926

| $\alpha$ | $C_l$  | $C_m$ |
|----------|--------|-------|
| -10.09   | -0.204 | 0.003 |

|       |        |        | Run: BM05066   |        |        | Run: BM05068   |        |        | Run: BM05070   |        |        |
|-------|--------|--------|----------------|--------|--------|----------------|--------|--------|----------------|--------|--------|
|       |        |        | $Re = 200,101$ |        |        | $Re = 349,945$ |        |        | $Re = 500,080$ |        |        |
|       |        |        | $\alpha$       | $C_l$  | $C_m$  | $\alpha$       | $C_l$  | $C_m$  | $\alpha$       | $C_l$  | $C_m$  |
| -9.00 | -0.198 | 0.003  |                |        |        |                |        |        |                |        |        |
| -7.95 | -0.207 | 0.003  |                |        |        |                |        |        |                |        |        |
| -6.98 | -0.224 | 0.004  |                |        |        |                |        |        |                |        |        |
| -5.95 | -0.172 | 0.003  | -10.06         | -0.266 | -0.007 | -10.08         | -0.268 | -0.022 | -10.23         | -0.276 | -0.036 |
| -4.91 | -0.081 | 0.001  | -9.09          | -0.286 | -0.013 | -9.27          | -0.344 | -0.072 | -9.11          | -0.312 | -0.103 |
| -3.99 | 0.116  | -0.002 | -8.13          | -0.297 | -0.066 | -8.21          | -0.238 | -0.117 | -8.21          | -0.217 | -0.160 |
| -2.98 | 0.259  | -0.004 | -7.21          | -0.237 | -0.151 | -7.14          | -0.087 | -0.180 | -7.23          | -0.045 | -0.190 |
| -2.03 | 0.403  | -0.006 | -6.21          | -0.027 | -0.186 | -6.20          | 0.098  | -0.210 | -6.20          | 0.108  | -0.210 |
| -0.90 | 0.571  | -0.009 | -5.12          | 0.173  | -0.211 | -5.23          | 0.240  | -0.223 | -5.13          | 0.255  | -0.225 |
| 0.17  | 0.705  | -0.011 | -4.14          | 0.341  | -0.227 | -4.16          | 0.374  | -0.231 | -4.11          | 0.369  | -0.230 |
| 1.25  | 0.752  | -0.012 | -3.11          | 0.471  | -0.236 | -3.08          | 0.494  | -0.234 | -3.06          | 0.486  | -0.230 |
| 2.22  | 0.826  | -0.013 | -2.09          | 0.588  | -0.238 | -2.11          | 0.597  | -0.234 | -2.08          | 0.598  | -0.232 |
| 3.20  | 0.940  | -0.015 | -1.07          | 0.696  | -0.238 | -1.06          | 0.694  | -0.231 | -1.06          | 0.695  | -0.230 |
| 4.26  | 1.057  | -0.017 | -0.06          | 0.802  | -0.236 | -0.07          | 0.787  | -0.228 | 0.02           | 0.796  | -0.228 |
| 5.21  | 1.161  | -0.019 | 0.96           | 0.904  | -0.232 | 1.03           | 0.894  | -0.228 | 1.00           | 0.889  | -0.226 |
| 6.32  | 1.276  | -0.021 | 2.06           | 0.992  | -0.226 | 2.01           | 0.990  | -0.225 | 2.00           | 0.983  | -0.223 |
| 7.40  | 1.386  | -0.022 | 3.02           | 1.064  | -0.219 | 2.98           | 1.077  | -0.222 | 3.05           | 1.079  | -0.219 |
| 8.50  | 1.484  | -0.024 | 4.06           | 1.144  | -0.211 | 4.06           | 1.167  | -0.217 | 4.10           | 1.172  | -0.214 |
| 9.50  | 1.562  | -0.025 | 5.13           | 1.229  | -0.205 | 5.11           | 1.263  | -0.213 | 5.14           | 1.253  | -0.208 |
| 10.50 | 1.634  | -0.026 | 6.12           | 1.298  | -0.197 | 6.14           | 1.334  | -0.205 | 6.07           | 1.333  | -0.204 |
| 11.37 | 1.686  | -0.027 | 7.16           | 1.361  | -0.190 | 7.14           | 1.400  | -0.197 | 7.15           | 1.404  | -0.195 |
| 12.51 | 1.733  | -0.028 | 8.20           | 1.422  | -0.182 | 8.17           | 1.460  | -0.188 | 8.15           | 1.449  | -0.185 |
| 13.35 | 1.736  | -0.028 | 9.18           | 1.471  | -0.175 | 9.26           | 1.509  | -0.180 | 9.19           | 1.495  | -0.178 |
| 14.44 | 1.692  | -0.027 | 10.24          | 1.504  | -0.168 | 10.24          | 1.533  | -0.173 | 10.24          | 1.520  | -0.174 |
| 15.32 | 1.648  | -0.026 | 11.22          | 1.527  | -0.166 | 11.21          | 1.556  | -0.172 | 11.20          | 1.529  | -0.174 |
| 16.51 | 1.622  | -0.026 | 12.17          | 1.539  | -0.164 | 12.19          | 1.561  | -0.172 | 12.23          | 1.539  | -0.175 |
| 17.40 | 1.645  | -0.026 | 13.22          | 1.537  | -0.165 | 13.23          | 1.565  | -0.171 | 13.20          | 1.534  | -0.175 |
| 18.29 | 1.654  | -0.027 | 14.19          | 1.519  | -0.167 | 14.23          | 1.562  | -0.173 | 14.20          | 1.527  | -0.176 |
| 19.54 | 1.678  | -0.027 | 15.23          | 1.527  | -0.170 | 15.22          | 1.570  | -0.174 | 15.20          | 1.516  | -0.179 |
| 20.40 | 1.677  | -0.027 | 16.22          | 1.524  | -0.173 | 16.15          | 1.547  | -0.177 | 16.21          | 1.530  | -0.182 |
| 19.83 | 1.676  | -0.027 | 17.21          | 1.520  | -0.177 | 17.19          | 1.558  | -0.183 | 17.26          | 1.528  | -0.185 |
| 18.94 | 1.667  | -0.027 | 18.18          | 1.543  | -0.183 | 18.23          | 1.563  | -0.188 | 18.19          | 1.531  | -0.189 |
| 17.92 | 1.650  | -0.026 | 19.21          | 1.561  | -0.187 | 19.20          | 1.568  | -0.192 | 19.15          | 1.531  | -0.203 |
| 16.85 | 1.638  | -0.026 | 20.17          | 1.600  | -0.196 | 20.14          | 1.566  | -0.202 | 20.17          | 1.491  | -0.212 |
| 16.00 | 1.649  | -0.026 | 19.67          | 1.587  | -0.192 | 19.67          | 1.578  | -0.199 | 19.67          | 1.513  | -0.208 |
| 14.90 | 1.663  | -0.027 | 18.71          | 1.532  | -0.185 | 18.68          | 1.563  | -0.192 | 18.60          | 1.528  | -0.197 |
| 13.83 | 1.713  | -0.028 | 17.69          | 1.539  | -0.183 | 17.69          | 1.568  | -0.186 | 17.71          | 1.539  | -0.188 |
| 12.94 | 1.739  | -0.028 | 16.67          | 1.528  | -0.177 | 16.72          | 1.558  | -0.183 | 16.70          | 1.548  | -0.186 |
| 11.81 | 1.714  | -0.028 | 15.72          | 1.531  | -0.174 | 15.72          | 1.561  | -0.179 | 15.73          | 1.531  | -0.182 |
| 10.83 | 1.650  | -0.026 | 14.69          | 1.534  | -0.169 | 14.66          | 1.571  | -0.177 | 14.65          | 1.524  | -0.179 |
| 9.85  | 1.587  | -0.025 | 13.70          | 1.539  | -0.167 | 13.69          | 1.566  | -0.173 | 13.69          | 1.538  | -0.176 |
| 8.82  | 1.504  | -0.024 | 12.70          | 1.530  | -0.165 | 12.68          | 1.562  | -0.173 | 12.65          | 1.538  | -0.176 |
| 7.71  | 1.410  | -0.023 | 11.71          | 1.533  | -0.165 | 11.69          | 1.553  | -0.172 | 11.65          | 1.530  | -0.174 |
| 6.86  | 1.333  | -0.021 | 10.75          | 1.518  | -0.167 | 10.70          | 1.549  | -0.173 | 10.70          | 1.522  | -0.174 |
| 5.81  | 1.223  | -0.020 | 9.68           | 1.487  | -0.172 | 9.69           | 1.521  | -0.177 | 9.67           | 1.509  | -0.175 |
| 4.69  | 1.105  | -0.018 | 8.68           | 1.446  | -0.180 | 8.67           | 1.486  | -0.185 | 8.70           | 1.473  | -0.180 |
| 3.83  | 1.010  | -0.016 | 7.70           | 1.390  | -0.188 | 7.64           | 1.432  | -0.194 | 7.64           | 1.431  | -0.190 |
| 2.76  | 0.886  | -0.014 | 6.62           | 1.335  | -0.196 | 6.62           | 1.372  | -0.203 | 6.66           | 1.372  | -0.198 |
| 1.61  | 0.770  | -0.012 | 5.63           | 1.262  | -0.202 | 5.65           | 1.304  | -0.209 | 5.56           | 1.295  | -0.205 |
| 0.69  | 0.723  | -0.012 | 4.61           | 1.188  | -0.210 | 4.56           | 1.222  | -0.217 | 4.56           | 1.217  | -0.212 |
| -0.42 | 0.641  | -0.010 | 3.58           | 1.105  | -0.215 | 3.55           | 1.133  | -0.221 | 3.58           | 1.127  | -0.216 |
| -1.38 | 0.523  | -0.008 | 2.51           | 1.026  | -0.224 | 2.54           | 1.044  | -0.225 | 2.51           | 1.022  | -0.219 |
| -2.38 | 0.357  | -0.006 | 1.53           | 0.949  | -0.231 | 1.53           | 0.953  | -0.228 | 1.48           | 0.937  | -0.224 |
| -3.39 | 0.204  | -0.003 | 0.46           | 0.850  | -0.234 | 0.43           | 0.843  | -0.230 | 0.44           | 0.843  | -0.227 |
| -4.44 | 0.082  | -0.001 | -0.52          | 0.746  | -0.236 | -0.51          | 0.749  | -0.232 | -0.54          | 0.748  | -0.230 |
| -5.57 | -0.069 | 0.001  | -1.58          | 0.642  | -0.236 | -1.58          | 0.650  | -0.234 | -1.58          | 0.644  | -0.229 |
| -6.46 | -0.190 | 0.003  | -2.62          | 0.532  | -0.239 | -2.58          | 0.552  | -0.237 | -2.66          | 0.532  | -0.230 |
| -7.66 | -0.345 | 0.005  | -3.61          | 0.405  | -0.233 | -3.63          | 0.435  | -0.234 | -3.67          | 0.425  | -0.230 |
| -8.59 | -0.209 | 0.003  | -4.62          | 0.254  | -0.223 | -4.66          | 0.321  | -0.230 | -4.67          | 0.306  | -0.227 |
| -9.57 | -0.189 | 0.003  | -5.68          | 0.061  | -0.199 | -5.68          | 0.175  | -0.219 | -5.72          | 0.182  | -0.219 |
|       |        |        | -6.73          | -0.140 | -0.169 | -6.64          | 0.014  | -0.198 | -6.67          | 0.037  | -0.202 |
|       |        |        | -7.70          | -0.333 | -0.134 | -7.68          | -0.183 | -0.164 | -7.69          | -0.123 | -0.176 |
|       |        |        | -8.72          | -0.495 | -0.107 | -8.70          | -0.362 | -0.129 | -8.70          | -0.297 | -0.141 |
|       |        |        | -9.76          | -0.604 | -0.100 | -9.74          | -0.490 | -0.105 | -9.70          | -0.450 | -0.106 |

# REPORT DOCUMENTATION PAGE

Form Approved  
OMB No. 0704-0188

The public reporting burden for this collection of information is estimated to average 1 hour per response, including the time for reviewing instructions, searching existing data sources, gathering and maintaining the data needed, and completing and reviewing the collection of information. Send comments regarding this burden estimate or any other aspect of this collection of information, including suggestions for reducing the burden, to Department of Defense, Executive Services and Communications Directorate (0704-0188). Respondents should be aware that notwithstanding any other provision of law, no person shall be subject to any penalty for failing to comply with a collection of information if it does not display a currently valid OMB control number.

**PLEASE DO NOT RETURN YOUR FORM TO THE ABOVE ORGANIZATION.**

|   |                                    |                                      |   |  |  |
|---|------------------------------------|--------------------------------------|---|--|--|
| <b>1. REPORT DATE (DD-MM-YYYY)</b><br>October 2004  |                                    | <b>2. REPORT TYPE</b><br>Subcontract |   | <b>3. DATES COVERED (From - To)</b><br>10/31/02-1/31/03                    |  |
| <b>4. TITLE AND SUBTITLE</b><br>Wind Tunnel Aerodynamic Tests of Six Airfoils for Use on Small Wind Turbines: October 31,2002-January 31, 2003 (Revised)  |                                    |                                      |   | <b>5a. CONTRACT NUMBER</b><br>DE-AC36-99-GO10337                           |  |
|   |                                    |                                      |   | <b>5b. GRANT NUMBER</b>  |  |
|   |                                    |                                      |   | <b>5c. PROGRAM ELEMENT NUMBER</b>  |  |
| <b>6. AUTHOR(S)</b><br>Michael S. Selig and Bryan D. McGranahan   |                                    |                                      |   | <b>5d. PROJECT NUMBER</b><br>NREL/SR-500-34515                             |  |
|   |                                    |                                      |   | <b>5e. TASK NUMBER</b><br>WER3.1830  |  |
|   |                                    |                                      |   | <b>5f. WORK UNIT NUMBER</b>  |  |
| <b>7. PERFORMING ORGANIZATION NAME(S) AND ADDRESS(ES)</b><br>University of Illinois at Urbana-Champaign<br>Urbana, Illinois   |                                    |                                      |   | <b>8. PERFORMING ORGANIZATION REPORT NUMBER</b><br>XCX2-32231-01           |  |
| <b>9. SPONSORING/MONITORING AGENCY NAME(S) AND ADDRESS(ES)</b><br>National Renewable Energy Laboratory<br>1617 Cole Blvd.<br>Golden, CO 80401-3393  |                                    |                                      |   | <b>10. SPONSOR/MONITOR'S ACRONYM(S)</b><br>NREL                            |  |
|   |                                    |                                      |   | <b>11. SPONSORING/MONITORING AGENCY REPORT NUMBER</b><br>NREL/SR-500-34515 |  |
| <b>12. DISTRIBUTION AVAILABILITY STATEMENT</b><br>National Technical Information Service<br>U.S. Department of Commerce<br>5285 Port Royal Road<br>Springfield, VA 22161  |                                    |                                      |   |  |  |
| <b>13. SUPPLEMENTARY NOTES</b><br>NREL Technical Monitor: Paul Migliore   |                                    |                                      |   |  |  |
| <b>14. ABSTRACT (Maximum 200 Words)</b><br>Wind Tunnel Aerodynamic Tests of Six Airfoils for Use on Small Wind Turbines represents the fourth installment in a series of volumes documenting the ongoing work of th University of Illinois at Urbana-Champaign Low-Speed Airfoil Tests Program. This particular volume deals with airfoils that are candidates for use on small wind turbines, which operate at low Reynolds numbers. |                                    |                                      |   |  |  |
| <b>15. SUBJECT TERMS</b><br>small wind turbines; airfoils; aerodynamic tests; wind tunnel; University of Illinois   |                                    |                                      |   |  |  |
| <b>16. SECURITY CLASSIFICATION OF:</b>  |                                    |                                      | <b>17. LIMITATION OF ABSTRACT</b><br>UL | <b>18. NUMBER OF PAGES</b>   | <b>19a. NAME OF RESPONSIBLE PERSON</b>           |
| <b>a. REPORT</b><br>Unclassified  | <b>b. ABSTRACT</b><br>Unclassified | <b>c. THIS PAGE</b><br>Unclassified  |   |  | <b>19b. TELEPHONE NUMBER (Include area code)</b> |